

STUDIES IN RADIO ASTRONOMY

Thesis presented  
by  
SHIBAN KRISHEN MATTOO  
to the  
Gujarat University  
for the Ph.D. Degree

043



B5448

DECEMBER 1973

PHYSICAL RESEARCH LABORATORY  
AHMEDABAD - 380009,  
I N D I A.

## S T A T E M E N T

The occurrence of spectral type III bursts (fast drift bursts) was first recognized by Wild (1950) from the frequency-time behaviour of the dynamic spectra at meter wavelengths. They are characterized by their short duration and a rapid drift from high ( $\sim 600$  MHz) to low ( $\sim 20$  KHz) frequencies. It is generally accepted that these bursts are excited by fast streams of particles ejected into the solar corona.

Type III bursts were initially found to be unpolarized (Payne-Scott and Little 1952). Subsequent work showed that type III bursts are partially elliptically polarized. The measurements of polarization characteristics of type III solar radio bursts at meter and decameter wavelengths are important in the understanding of the coronal magnetic fields associated with the generating mechanism and also for the study of the intervening magneto-ionic medium.

An experiment to study the polarization characteristics of solar radio bursts of spectral type III at decameter wavelengths has been conducted by the author at the Physical Research Laboratory, Ahmedabad. The apparatus consists of a time-sharing radio polarimeter which measures the four Stokes parameters that completely define the state of polarization of the incoming radiation.

The polarization observations, relating to type III radio bursts, taken during the period from 1969 to 1973 can be divided into three distinct parts. The first part of the work, reported in this thesis, deals with the measurements of polarization characteristics of type III burst radiation at 25 MHz with 20 KHz bandwidth. The second part refers to the polarization measurements made simultaneously at two closely-spaced frequencies, namely, 34.993 and 34.997 MHz. At both these frequencies, the bandwidth used was 800 Hz. The last part includes measurements of the polarization parameters of type III burst radiation at 35 MHz simultaneously in two bandwidths, namely, 7.5 and 12.5 KHz, in order to compute the total Faraday rotation suffered by the radiation in passing through the intervening magneto-ionic medium.

Theoretical considerations suggest that the total Faraday rotation suffered by the type III burst radiation at 35 MHz should at least be of the order of  $10^5$  radians after passing through the solar corona and the earth's ionosphere. If such a large value of Faraday rotation at 35 MHz can really turn out, then it would be impossible to explain the occurrence of linearly or highly elliptically polarized solar radio bursts in the presence of coronal scattering and finite source thickness. Thus it is important to make an experimental determination of the

total amount of Faraday rotation suffered by the type III burst radiation.

Our observations indicate that the total Faraday rotation at 35 MHz is of the order of  $10^3$  radians which is two orders of magnitude less than the theoretical value. An attempt has been made by the author to find out if the magneto-ionic mode coupling can explain this discrepancy. It has been found that the mode coupling alone is not sufficient to explain the difference between the experimentally observed and the theoretical values of the Faraday rotation. An alternative explanation based on the idea that the type III radiation is generated at the second harmonic of the local plasma frequency, rather than the fundamental appears to resolve this difference. Our explanation is consistent with the theory of generation of type III solar radio bursts developed by the Russian workers.

It has been suggested in literature that a partially elliptically polarized radiation can be represented in terms of superposition of two fully polarized but mutually incoherent signals, one circularly polarized and the other linearly polarized signal. We made an attempt to test for the validity of this representation for type III burst emission and the results are incorporated in this thesis.



The data processing was carried out by the author on the IBM 1620 and 360-44 computers at the Physical Research Laboratory, Ahmedabad.

The thesis is divided into six chapters as follows:

In the first chapter we have reviewed our present state of knowledge of solar type III bursts. Since this thesis is mainly related to the polarization characteristics of type III solar radio bursts, it may appear that the first chapter does not have direct relevance, to the main subject matter of the thesis. Still, we felt that a review of the current knowledge about type III solar radio bursts may serve as a useful introduction to the type III burst radiation in general.

The second chapter contains a brief review of the present knowledge of the polarization characteristics of type III solar radio bursts. The effect of the Faraday rotation on polarization measurements and its significance in relation to the source region and the intervening magnetospheric medium are discussed.

The third chapter gives the experimental details of a two-bandwidth (7.5 and 12.5 KHz) time-sharing radio polarimeter at 35 MHz. Various electronic circuits are discussed in detail. The operational procedure and the effects of ground reflections on the measurement of the Stokes parameters are also dealt with.

The fourth chapter gives the single bandwidth polarization measurements at 25 and 35 MHz. For the sake of comparison, the polarization data obtained at the National Research Council, Canada at 74 MHz in 1963 are also incorporated. The main results reported here are the comparison of various polarization parameters obtained at 25 and 35 MHz with that obtained at other frequencies by different workers. A type III event which occurred on July 14, 1969 has been discussed in detail. Also included in this chapter is the comparison of polarization parameters obtained at two closely spaced frequencies, namely, 34.993 and 34.997 MHz.

The measurements of the Faraday rotation suffered by type III burst radiation at 35 MHz have been described in the fifth chapter. The interpretation of the results of the Faraday rotation is also included in this chapter. Finally, the problems, of the occurrence of linearly polarized type III bursts in terms of two mutually incoherent signals (100 per cent circularly and linearly polarized radiation) are also discussed.

The sixth chapter summarizes the conclusions drawn from the present investigation, and some suggestions for future work.

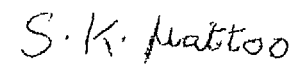
In this thesis we have presented new results on the Faraday rotation measurements of type III burst

radiation and the polarization parameters at two closely-spaced frequencies. This has proved quite useful for understanding the nature of the source of type III bursts and the propagation characteristics of the intervening magneto-ionic medium. This work has also been accepted for publication (Bhonsle and Mattoo, 1973).

In addition, the author has also worked on radio star scintillations during his tenure as a Ph. D. student. We have not included this work in this thesis. This work is published and can be found in the following references:

1. Bhonsle, R.V., Alurkar, S.K., Narayanan, K., and Mattoo, S.K. 1970, J. Tel. Comm. Engrs., 17, 217.
2. Mattoo, S.K., and Bhonsle, R.V. 1971, Indian Journal of Pure and Applied Physics, 9, 601.

  
(R.V. BHONSLE)

  
(S.K. MATTOO)

POLARIZATION STUDIES OF TYPE III SOLAR  
RADIO BURSTS AT DECAMETRIC WAVELENGTHS

D E D I C A T I O N

TO MY UNCLE  
PANDIT NIRANJAN NATH MATTU

## A C K N O W L E D G E M E N T S

It would be impossible to acknowledge adequately all the persons who have helped me directly or indirectly during my tenure as a Ph. D. student. Nevertheless, certain persons have given generously their time and efforts and deserve at least my explicit thanks.

First of all the author thanks his thesis adviser, Professor R.V. Bhonsle, who at various stages of the work presented here kindly offered constructive guidance. Countless discussions with him were invaluable. I also had the benefit of stimulating and close interaction which he has given me in the preparation of this thesis.

I express my sincere thanks to Prof. D. Lal and Prof. K.R. Ramanathan for their keen interest in the solar radio astronomy programme at Physical Research Laboratory, Ahmedabad.

For the operation and construction of the radio polarimeter, the work of Sohanlal is gratefully acknowledged. Without his help and cooperation much of the work presented here could not have been done. K. Narayanan provided a useful technical expertise at the initial stage of the instrumentation and R. Sharma designed and fabricated the antenna systems used. The author acknowledges his debt for their efforts, advice and comments. For the maintenance of the radio polarimeter, the efforts of M.V. Dalal are highly appreciated.

I have the pleasant duty of recording my indebtedness to Dr. S.K. Alurkar, who has read the whole of the manuscript with the greatest care and removed many blemishes which might have escaped less vigilant eyes. Discussions with him were useful.

My thanks are due to A.H. Desai who was always available to render me assistance. He helped me in the reduction of the data. I am also appreciative of him as a decorator of my thesis.

The author wishes to express his special appreciation to V. Badarinadh, A.D. Bobra, N.S. Nirman, H.S. Sawant and P. Venat for their enthusiastic cooperation and careful voluntary work.

Dr. (Miss) Anna Mani of India. Meteorological Department provided me with balloons for carrying out the antenna and ground reflection measurements. I express my gratitude to her.

I thank the personnel of the Computing center, Workshop and the Draughting and Photography section for their cooperation. Mr. K.S. Dholakia has put in his best to make photographs presentable. R.M. Panchal and J.A. Panchal have helped in hardware developments.

The financial support was received from the Ministry of Education and Department of Atomic Energy, Government of

India and for the last two years from Department of Space, Government of India.

I thank D. Stephen for his beautiful and speedy typing of several versions of this thesis from my illegible original manuscripts.

I have received praiseworthy help and moral support from D.K. Wali of Nuclear Fuel Complex, Hyderabad and R.K. Kaul and Iqbal Kaul of High Altitude Research Laboratory, Gulmarg. The author expresses his sincere thanks to all of them.

It is a pleasure to acknowledge that I undertook the Ph. D. course at the suggestion of Prof. H. Razdan of Nuclear Research Laboratory, Srinagar. He has watched the progress of the work presented here with keen interest. I am indebted to him for helpful advice he used to give whenever occasion demanded.

Whatever value this work may have, however, must be attributed in large part to my mother and sisters, who consistently encouraged and consoled in my efforts, and often turned despair into renewed hope.

S. K. Mattoo  
(S.K. MATTOO)



# C O N T E N T S

	<u>Page</u>
<u>STATEMENT</u>	i - vi
<u>ACKNOWLEDGEMENTS</u>	i - iii
<u>CHAPTER I</u> <u>A REVIEW OF SPECTRAL TYPE III</u> <u>SOLAR RADIO BURSTS</u>	1 - 46
1.1    INTRODUCTION	1
1.2    CHARACTERISTICS OF TYPE III BURSTS	2
1.21    DYNAMIC SPECTRA	2
1.22    FREQUENCY RANGE	6
1.23    HARMONICS	6
1.24    FINE STRUCTURE	9
1.25    INTENSITY OF TYPE III BURSTS	12
1.26    POLARIZATION	13
1.3    ASSOCIATION OF TYPE III BURSTS WITH $H_{\alpha}$ SOLAR ACTIVITY	14
1.31    ASSOCIATION OF TYPE III BURSTS WITH TYPE V AND TYPE U BURSTS	15
1.32    ASSOCIATION OF TYPE III WITH MICROWAVE AND X-RAY BURSTS	17
1.33    ASSOCIATION OF TYPE III BURSTS WITH STREAMS OF PARTICLES IN THE INTERPLANETARY MEDIUM	19
1.4    POSITION MEASUREMENTS OF TYPE III BURSTS AND EFFECTS OF SCATTERING	21
1.5    THE SOURCE SPEED AND THE INTERPLANET- ARY OBSERVATIONS OF HECTOMETER AND KILOMETER WAVELENGTH TYPE III BURSTS	23
1.6    GENERATING MECHANISM	28
1.61    TWO-STREAM INSTABILITY	29

	<u>Page</u>
1.62 NON-LINEAR INTERACTION FOR SUPPRESSION OF TWO- STREAM INSTABILITY	30
1.63 CONVERSION OF PLASMA WAVES	33
1.64 THEORIES OF POLARIZED TYPE III BURST EMISSION FROM SOLAR CORONA	35
1.641 THEORY OF FOMICHEV AND CHERTOK	35
1.642 YIP'S THEORY OF POLAR- IZATION	44
1.7 CONCLUSION	45
<u>CHAPTER II</u> <u>A REVIEW OF POLARIZATION CHARACTER-</u> <u>ISTICS OF TYPE III BURSTS</u>	47 - 67
2.1 INTRODUCTION	47
2.2 SUMMARY OF POLARIZATION OBSERVA- TIONS	47
2.3 CAUSES OF DEPOLARIZATION OF TYPE III RADIO BURSTS	50
2.31 FARADAY DISPERSION AS A CAUSE OF DEPOLARIZATION	51
2.32 DEPOLARIZATION DUE TO SOURCE THICKNESS	54
2.33 DEPOLARIZATION DUE TO SCATTER- ING EFFECTS	56
2.4 MEASUREMENT OF FARADAY ROTATION	58
2.41 EXPERIMENTAL DETERMINATION OF FARADAY ROTATION OF TYPE III BURSTS	59
2.5 THE CONSTANCY OF ORIENTATION ANGLES OF POLARIZATION ELLIPSES OF TYPE III BURSTS	60
2.6 LINEAR POLARIZATION	61

	<u>Page</u>
2.7 SYSTEMATIC VARIATION OF POLARIZATION CHARACTERISTICS	63
2.8 PROBLEM WITH THE OBSERVATION OF ELLIPTICAL POLARIZATION	64
2.9 STATEMENT OF THE PROBLEM	65
<u>CHAPTER III</u> <u>EXPERIMENTAL SET-UP:</u>	68 - 113
<u>A TIME-SHARING TWO-BANDWIDTH</u>	
<u>RADIO POLARIMETER AT 35 MHz</u>	
3.1 INTRODUCTION	68
3.11 SPECIFICATION OF POLARIZATION IN TERMS OF STOKES PARAMETERS	68
3.12 POLARIZATION WORK AT AHMEDABAD	72
3.2 PRINCIPLE OF OPERATION OF A TIME-SHARING POLARIMETER	72
3.3 DESCRIPTION OF A TWO-BANDWIDTH POLARIMETER AT 35 MHz	76
3.31 ANTENNAS	78
3.32 RECEIVER	80
3.321 35 MHz PREAMPLIFIERS	80
3.322 3-WAY POWER DIVIDER, SWITCHING SCHEME AND MODULATOR	80
3.323 MIXER, LOCAL OSCILLATOR AND I.F. AMPLIFIER	84
3.324 HYBRID POWER DIVIDER AND BANDPASS FILTERS	87
3.325 SQUARE-LAW DETECTORS	88
3.326 TIME-DEMODULATORS	88
3.327 OPERATIONAL AMPLIFIERS	91
3.328 CHART RECORDERS	94

	<u>Page</u>
3.33 CONTROL CIRCUITS.	94
3.331 PULSE GENERATOR	95
3.332 RING COUNTER	95
3.333 " OR " GATES	97
3.4 CALIBRATION PROCEDURE	99
3.41 PHASE AND GAIN ADJUSTMENTS	99
3.42 DAILY CALIBRATIONS	100
3.5 POTENTIAL SOURCES OF ERROR	101
3.51 ERROR DUE TO RELATIVE PHASE DIFFERENCE BETWEEN THE TWO ORTHOGONAL COMPONENTS	101
3.52 NONZERO CROSSTALK	103
3.53 REFLECTIONS FROM LOCAL OBJECTS, ESPECIALLY THE GROUND	108
3.54 STATISTICAL ERRORS	112
<u>CHAPTER IV</u>	114 - 162
<u>POLARIZATION MEASUREMENTS OF</u> <u>TYPE III BURSTS AT 25 AND</u> <u>35 MHz AT AHMEDABAD</u>	
4.1 INTRODUCTION	114
4.2 TYPICAL POLARIMETER RECORDINGS OF TYPE III BURSTS	115
4.3 POLARIZATION MEASUREMENTS WITH SINGLE BANDWIDTH	118
4.31 POLARIZATION PERCENTAGE $m$	119
4.32 AXIAL RATIO $r$	128
4.33 ORIENTATION ANGLE $\chi$	138
4.4 POLARIZATION CHARACTERISTICS OF THE SOLAR EVENT ON JULY 14, 1969	140
4.41 INTENSITY	141

	<u>Page</u>
4.42 DEGREE OF POLARIZATION	144
4.43 AXIAL RATIO AND ORIENTATION ANGLE	145
4.5 POLARIZATION CHARACTERISTICS OF TYPE III BURSTS AT 34.993 AND 34.997 MHz	150
4.51 INTENSITY	152
4.52 POLARIZATION DEGREE	152
4.53 AXIAL RATIO	155
4.54 ORIENTATION ANGLE	155
4.55 POLARIZATION OF TYPE IIIb BURSTS RECORDED ON ONE CHANNEL ONLY	160
4.6 CONCLUSIONS	161
<u>CHAPTER V</u> <u>MEASUREMENTS OF FARADAY ROTATION OF TYPE III BURSTS AT 35 MHz</u>	163 - 216
5.1 INTRODUCTION	163
5.2 PRINCIPLE OF TWO-BANDWIDTH MEASUREMENT OF THE FARADAY ROTATION	164
5.3 TYPICAL POLARIMETER RECORDINGS	167
5.4 RESULTS OF TWO-BANDWIDTH POLARIZA- TION MEASUREMENTS	171
5.41 DEGREE OF POLARIZATION	172
5.42 CALCULATION OF FARADAY ROTA- TION AT 35 MHz	175
5.43 AXIAL RATIO	180
5.44 ORIENTATION ANGLE	182
5.5 REPRESENTATION OF PARTIAL ELLIPTICAL POLARIZATION	182

	<u>Page</u>
5.6 INTERPRETATION OF RESULTS OF FARADAY ROTATION MEASUREMENTS	188
5.61 DIFFERENTIAL ABSORPTION	190
5.62 MODE COUPLING	191
5.63 MODE COUPLING IN THE EARTH'S IONOSPHERE	193
5.64 ESTIMATE OF THE CORONAL MAGNETIC FIELD	194
5.65 MODE COUPLING IN THE SOLAR CORONA	197
5.66 THE EXTENT AND/OR POSITION OF THE MODE COUPLING REGIONS	202
5.67 DIFFICULTIES WITH THE MODE COUPLING AS AN EXPLANATION FOR THE OBSERVED LOW VALUES OF THE FARADAY ROTATION	207
5.68 EXPLANATION IN TERMS OF SECOND HARMONICS	213
5.7 FARADAY ROTATION AT 35 MHz AND THE EXISTENCE OF LINEAR POLARIZATION	214
CHAPTER VI <u>CONCLUSIONS AND SUGGESTIONS FOR FURTHER STUDY</u>	217 - 224
6.1 CONCLUSIONS	217
6.2 SUGGESTIONS FOR FURTHER STUDY	221
<u>REFERENCES</u>	225 - 237

## CHAPTER - I

### A REVIEW OF SPECTRAL TYPE III SOLAR RADIO BURSTS

#### 1.1 INTRODUCTION

Wild (1950) was the first to recognize the existence of fast-drift bursts on the dynamic spectrum records at meter and decameter wavelengths. Since then these bursts are referred to as spectral type III bursts and have been extensively studied by both ground-based and satellite-borne receivers.

Type III bursts are characterized by their short duration and rapid drift from high to low frequencies, covering all or part of the range from about 600 MHz to 20 KHz (Malville 1962b, Slysh 1967a, Hartz 1969, Dunckel et al. 1972, Alexander et al. 1969, Fainberg and Stone 1970a, b; Haddock and Alvarez 1973). They can be observed either in isolation or, in groups of 10 - 100 bursts or they can occur in persistent storms (Fainberg and Stone 1970a, Dunckel et al. 1972).

Wild et al. (1950) originally suggested that the fast-drift bursts originate due to the excitation of plasma waves at the respective plasma levels of the solar corona as a result of the exciter moving outward through it at high velocities of about .2 to .8c. The particle streams (electrons or protons), believed to be an exciting agency, are generated during solar flares, although not all type III bursts are associated with flares.

A review of observations, their interpretations, origin, and associations of the type III solar radio emissions with  $H\alpha$  flares, X-ray bursts, etc. is found in papers by Wild et al. (1963), Maxwell (1965), Kundu (1965, 70), Smith (1970b), Boischot (1970), Newkirk (1971), and Wild and Smerd (1972).

In this chapter, we present a brief description of the observed characteristics of type III bursts, their interpretations and generating mechanisms.

## 1.2 CHARACTERISTICS OF TYPE III BURSTS

### 1.21 DYNAMIC SPECTRA

Figure 1.1 shows a group of type III bursts recorded by means of the dynamic spectrum analyzer at the Physical Research Laboratory, Ahmedabad operating over a frequency range of 40-240 MHz (Bhonsle and Alurkar 1968). Frequency profiles of type III bursts are smooth curves with no sudden variations within frequency interval of a few MHz. The bandwidth is usually greater than 10 to 15 MHz, in many cases extending over more than 100 MHz. The frequency of maximum intensity drifts rapidly with time in the direction of decreasing frequency at an average rate of  $30 \text{ MHz S}^{-1}$  around 100 MHz and  $0.01 \text{ MHz S}^{-1}$  around 1 MHz (Maxwell 1965, Hartz 1969).

The time profiles show a rapid rise to maximum intensity and an exponential decay to pre-burst level. The bursts are of short duration, of the order of .18 to .25 S



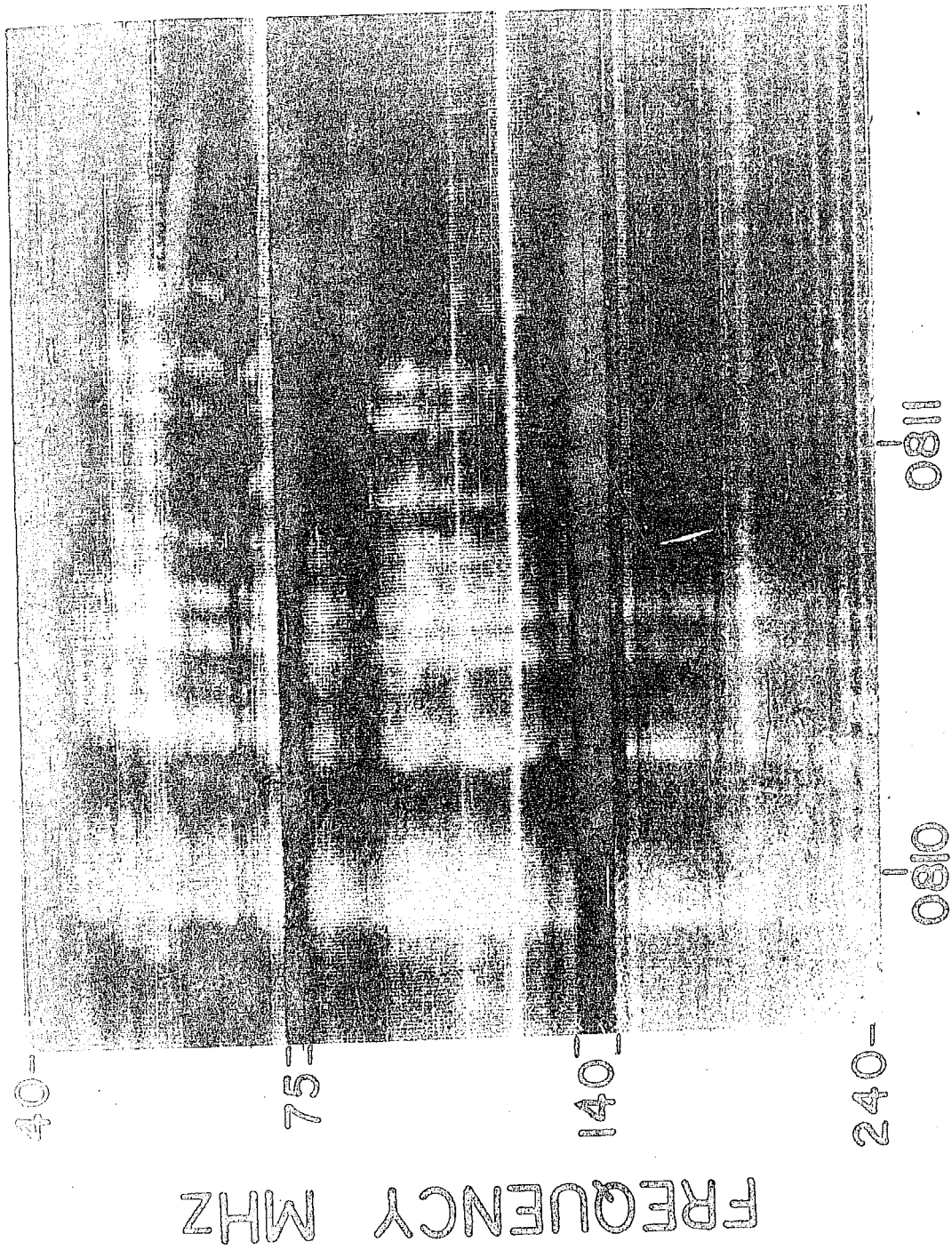


Figure 1.1 A group of type III bursts recorded by Ahmedabad radio spectroscopy in the frequency range 40-240 MHz on December 12, 1970 at 0810 U.T.

between 200 to 400 MHz (de Groot 1959, Elgaroy 1961), which increases with decreasing frequency. The duration increases to about 30 S at 3 MHz and to 150 S at .45 MHz (Slysh 1967b, Alexander et al. 1969). Hughes and Harkness (1963) found in a sample of 16 type III bursts the durations of the fundamentals and the second harmonics were same, but on the average the fundamental was of longer duration. Main source of error in determining the duration can be due to the confusion with possible type V continuum emission which is sometimes so short that it is not easily recognized on ordinary spectrum records (Elgaroy 1961, Wild et al. 1963, Wild 1969a, Kundu 1965).

The time profile of the burst results from two effects: the excitation of plasma waves and their damping. The excitation is determined by the finite length of the stream of particles and/or by the finite bandwidth of the emission at each level in the corona. The exponential decay of the burst is generally due to the collision damping at meter-waves and Landau damping at longer wavelengths (Aubier and Boischot 1972, Zaitsev et al. 1972). The propagation effects like scattering due to inhomogeneities, can lead to a retardation and quasi-exponential decay for an impulsive emission (Fokker 1965b, Steinberg et al. 1971).

The time profile of type III bursts can be used for the determination of coronal temperature if it is assumed that the decay of emission is due to the damping of plasma waves. The temperatures derived in the metric

wavelengths are larger than those generally derived from the emission of the quiet sun and slowly varying component. It is about  $2 \times 10^6$  °K (Boischot et al. 1960, Malville 1961, Elgaroy 1961). The temperatures at decametric wavelengths (Aubier and Boischot 1972) are on the average similar or slightly larger than those derived within a streamer from optical observations (Newkirk et al. 1970, Fort et al. 1972, Koutchmy 1971). The temperature determined at hectometer wavelengths are systematically too small for the curve to be smoothly related to the temperature observed in situ at 1 A.U. The values range from more than  $5 \times 10^4$  °K (Hartz 1969) to  $1.7 \times 10^5$  °K (Slysh 1967b) which are smaller than the value at the orbit of the earth of the order of  $10^5$  °K (Noble and Scarf 1963, Neugebauer and Snyder 1966). It seems that the temperatures are probably underestimated when we use lower frequencies. This can possibly be due to the existence of Landau damping of plasma waves at lower frequencies, which is more efficient than collisional damping.

Wild (1963b) pointed out that the time distribution of individual bursts within a type III group is not always random, sometimes they show a quasi-periodicity. Similar type of periodicities has been observed as the "pinch effect" in the laboratory plasma experiments.

The average time-integrated spectrum of type III bursts can be approximated by the power function  $\nu^{-\alpha}$ , where  $\alpha$  has a value between 2.8 and 3.6 and  $\nu$  is the frequency (Wild 1950).

## 1.22 FREQUENCY RANGE

The distribution of starting frequencies of type III burst groups appears to have a bimodal character (Malville 1962a). The low frequency peak occurs during high solar activity period. During such periods, the number of type III bursts increases, their starting frequency decreases, and the noise storm activity, usually restricted to frequencies above 100 MHz, appears below 100 MHz. Malville (1962a) and Elgaroy (1961) pointed out similarity of behaviour of type III and noise storm bursts. The burst component of noise storms occasionally has the appearance and drift rate typical of type III bursts of restricted bandwidth (30 to 50 MHz). The noise storm activity appears, in general, to occur at the upper frequency limit of type III activity. The noise storm bursts seem to be narrow bandwidth extension of type III bursts.

## 1.23 HARMONICS

The dynamic spectra of type III bursts sometimes show two similar formations in which the features of one are duplicated at about double the frequency as shown in Figure 1.2. The harmonics occur in about 60 per cent of the bursts observed in the 40 - 240 MHz range (Wild et al. 1954b). However, the findings of Smerd et al. (1962) revealed that from a large number of type III bursts recorded during 2.5 years of observations, only 6 events had a well-defined harmonic structure. It should be recognized that a reliable

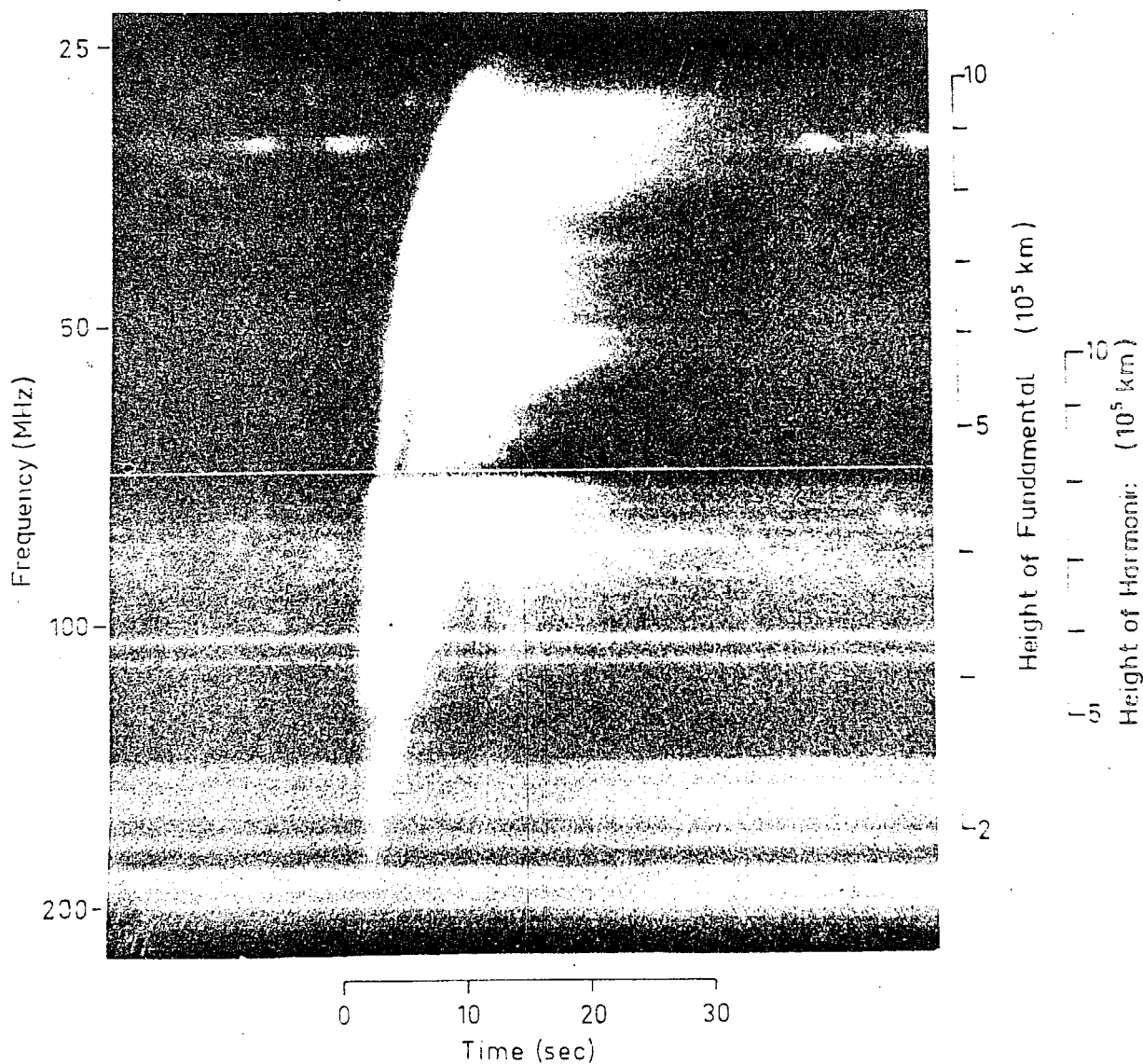


Figure 1.2 A type III burst, showing fundamental and second harmonic structure. It is followed by brief type V continuum. Recorded at Culgoora Observatory on July 26, 1970 01<sup>h</sup>00<sup>m</sup>.5 (After Wild and Smerd 1972).

identification of the fundamental and second harmonic in type III radiation is hindered by the fact that type III bursts very often occur in groups. The average ratio of the second harmonic frequency to the fundamental frequency decreases from 2 at the centre of the disk to 1.6 at the limb and the second harmonic arrives 1.5 to 2 S before the fundamental (Stewart 1962). The number of events showing both fundamental and second harmonic increases from centre to limb and possibly declines suddenly beyond the limb (Wild et al. 1959a). The "swamping effect" is invoked to explain this observation (Smith 1970b). The observed ratio of fundamental to second harmonic brightness temperature decreases from the centre of the solar disk to the limb (Wild et al. 1959a). The fundamental band shows a sharp low frequency cut-off. These observations can be interpreted as due to the increase in the differential optical depth between the second harmonic and the fundamental as the source approaches the limb. At the limb the fundamental is largely absorbed and cannot escape in a perfectly homogeneous corona. Roberts (1959) pointed out that the fundamental at the limb can escape only if the scattering due to small-scale irregularities is effective. The fact that type III bursts appear to occur in locally dense regions of the corona also makes the escape of radiation possible (Shain and Higgins 1959).

From the observations of the Culgoora radio heliograph at 80 MHz, Stewart (1972) found that the radial distance of fundamental and harmonic sources is almost equal but displaced in the transverse direction. This transverse displacement was treated as an evidence for that the source emitted predominantly in the backward direction at second harmonic so that it is seen in reflection. However, Riddle (1972) showed that the combined effects of spherical refraction and random scattering on radiation emitted isotropically from a source can produce this transverse shift.

#### 1.24 FINE-STRUCTURE

According to Elgaroy (1961) type III bursts show a fine structure that may take the form of blobs or irregular features such as small elements of reverse frequency drift and " U " bursts. Type III bursts sometimes occur intermittently, that is, the radiation stops at some frequency and starts later as a direct continuation of its initial trace. Less frequently, the radiation stops abruptly without re-starting. In the decameter range, a great variety of solar bursts is observed, which does not appear on higher frequencies (Ellis 1969). The narrow-band bursts appear on the spectrograph as sharp lines of almost constant frequency and lasts for 1 to 2 S (Ellis and McCulloch 1966, 1967). High resolution spectrographs show that individual bursts are generally made up of two components separated slightly in frequency. They are known as "split pairs".

The split pair bursts are often observed in chains which drift from high to low frequencies, in a manner similar to the type III bursts. The lower frequency element arrives about 0.1 s before the other (Ellis and McCulloch 1967). Single bursts, identical to one isolated element of a split pair and triple bursts have been observed (Ellis and McCulloch 1966, 1967; de la Noë and Boischot 1972). The single elements are known as "stria bursts" as shown in Figure 1.3. The stria bursts have a narrow bandwidth of about 15 to 100 KHz and appear generally much more polarized than the type III bursts (sometimes  $\sim 100\%$  circularly polarized). In split pairs or doublets the low frequency element has a bandwidth of the order of 50 KHz in the frequency range of 24-28 MHz. In the upper frequency element, on the other hand, the bandwidth varies between 40 to 300 KHz (Ellis and McCulloch 1967). In a given chain of narrow-band bursts (Type IIIb), the degree of polarization differs from one stria burst to another and are always polarized in the same sense (Ellis and McCulloch 1967, de la Noë and Boischot 1972, Sastry 1972).

Ellis and McCulloch (1967) noted harmonic relation between a type IIIb and type III or between two type IIIb bursts. However de la Noë and Boischot (1972) pointed out that type IIIb burst appears as a precursor of type III burst, and not its fundamental emission because there is generally no time gap between a type IIIb and type III



### The Type IIIb Burst: A Precursor of Decametre Type III Radio-Burst

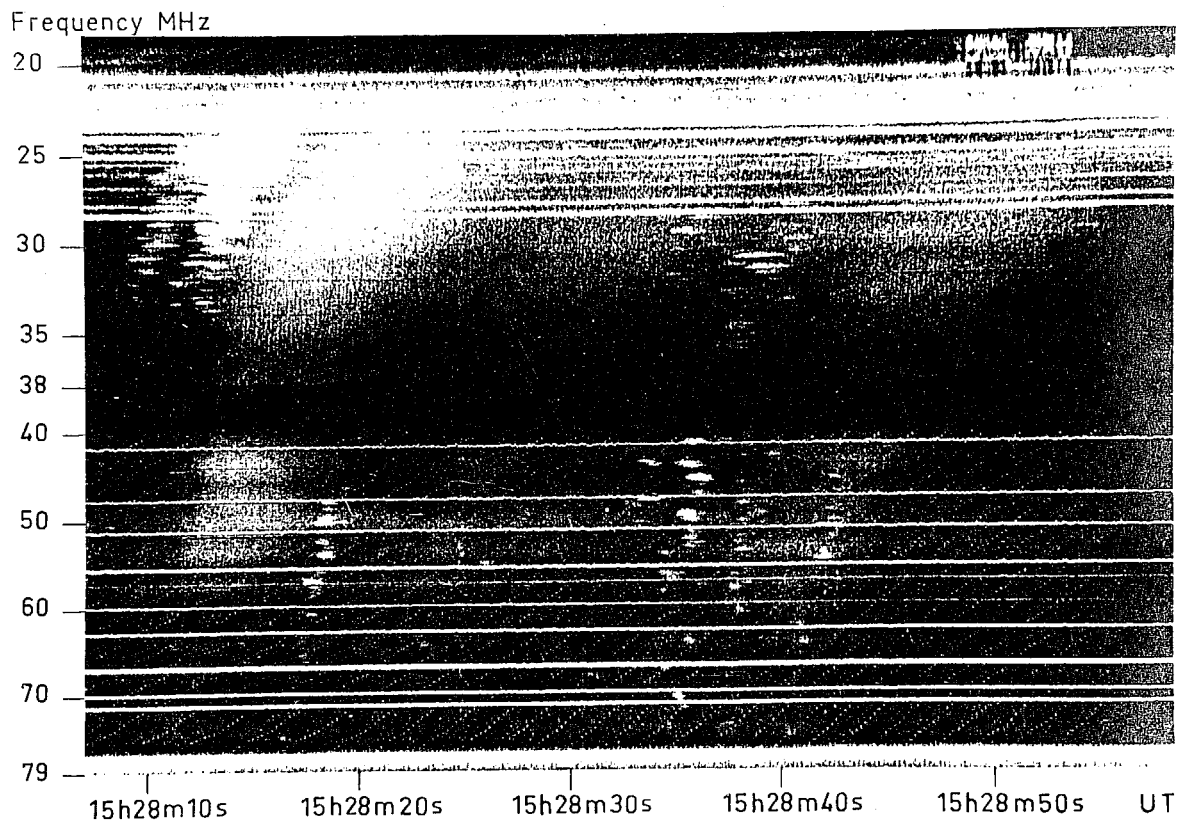


Figure 1.3 A group of type III bursts and stria-bursts occurring on August 13, 1970. Some stria-bursts are isolated but the majority is grouped to form type IIIb bursts (After de la Noë and Boischot 1972).

as would be expected if they were harmonically related. An important thing to note is that type IIIb and stria bursts are observed at only decameter wavelengths and only when there is a noise storm in progress at meter (type I bursts) and decameter (type III burst storms) wavelengths.

Ellis and McCulloch (1967) concluded that type IIIb bursts are excited by streams of electrons moving at 0.3 - 0.5 c, similar to those which excite the usual type III bursts. In type IIIb, the stream of electrons excites only sporadic and short lived emission (Stria-bursts) in groups which can be reduced to a single unit. It is then very likely that some similar streams can exist which move out through the corona without giving rise to any electromagnetic emission.

Ellis and McCulloch (1967) favour the idea that an exciter excites electrostatic resonances such that the two elements of split pairs of bursts may be identified with radiation near the plasma frequency and the upper hybrid frequency. They identified triplets with the resonance and combination frequencies of plasma frequency and gyro-frequency of electrons and ions. Smith (1972) takes precursor to a type III burst as an indication of a large amplitude oscillation at the head of the exciting stream.

#### 1.25 INTENSITY OF TYPE III BURSTS

The maximum flux density (Wild 1950, Wild and Smerd 1972) is  $\lesssim 32 \times 10^{-20} \text{ W m}^{-2} \text{ Hz}^{-1}$  which is mostly

due to emission near the fundamental. The flux density corresponds to a brightness temperature  $\sim 10^{11}$  °K for fundamental radiation, which appears to be emitted into a solid angle of  $\pi$  radians, and a brightness temperature of  $10^{9.4}$  °K for second harmonic radiation, which appears to be emitted into a solid angle of  $2\pi$  radians.

Since the angular size of type III sources depends on coronal scattering (Riddle 1972; Fokker 1965b), the true brightness temperature of type III bursts at meter wavelengths may be considerably greater than the measured values ( $\sim 10^{11}$  °K, Wild and Smerd 1972).

#### 1.26 POLARIZATION

Type III bursts were initially found to be predominantly unpolarized at 97 MHz (Payne-Scott and Little, 1952) but linear polarization was detected in some cases. Subsequently, different workers measured polarization characteristics of type III bursts at different frequencies (Bhonsle and McNarry 1964b, Cohen 1959, Cohen and Fokker 1959, Akabane and Cohen 1961, Bhonsle et al. 1967, Chin et al. 1971 and Dodge 1973). Briefly, the values of axial ratio have been found to vary from 0 to  $\pm 0.7$ . Occasionally circular polarization with both senses of rotation has been reported. In majority of type III bursts, the degree of polarization has been found to be partially elliptical. These polarizations and the effect of Faraday

rotation due to intervening magneto-ionic medium will be discussed in greater detail in Chapter II.

### 1.3 ASSOCIATION OF TYPE III BURSTS WITH H $\alpha$ SOLAR ACTIVITY

The H $\alpha$  solar activity manifests itself both in emission as well as absorption. Solar flares are observed in H $\alpha$  line as sudden brightening of a small region in the chromosphere while surges, filaments and other small features associated with active centers are observed in absorption against the bright solar disk (Martres et al. 1972, Tlamicha and Takakura 1963, Kuiper 1973). Many type III bursts have been found to be associated with solar flares but they have been observed with flares of all importances; when associated with large flares they coincide with the explosive phase which marks the time of sudden expansion of the flare area (Wild et al. 1954a, Tandenberg-Hansen 1967). It is quite likely that some type III bursts have no optical activity associated with them (Swarup et al. 1960, Malville 1961, 1962a, Kuiper 1973). The occurrence of a surge with a flare increases the likelihood of an associated type III event. Loughhead et al. (1957) and Graedel (1970) noted that the association of flares with type III bursts depends in some way on the development of the active region in which flares occur. Malville (1961) and Simon (1962) found that the association of flares with type III bursts rises significantly when a noise storm overlies the active region producing flares or when a type IV burst is associated with the region. Recent

careful analysis of high resolution H $\alpha$  pictures of solar activity by Axisa et al. (1973) and Kuiper (1973) have shown that almost all type III bursts have some H $\alpha$  activity associated with them. Dulk (Kuiper 1973) has found from radioheliograph studies at 80 MHz, that type III bursts occur in regions of open field, with or without a coronal streamer nearby. Kuiper (1973), from his studies of one-dimensional positions of type III bursts in the frequency range of 20 to 60 MHz found that these bursts occurred over active regions whose calculated coronal fields were characteristically diverging and generally open. This diverging magnetic-field is not characteristic of streamers. Kuiper, therefore, concluded that type III bursts need not occur preferentially in streamers as was first suggested by Wild et al. (1959a).

1.31 ASSOCIATION OF TYPE III WITH TYPE V AND TYPE U BURSTS

Type III bursts are generally interpreted as radio emissions due to plasma oscillations excited by fast electrons suddenly ejected with an average velocity of 0.37 c at the time of the flare explosion, sometimes in repeated bursts of  $\sim 1$  S duration. They travel out along open-field lines through the corona into the interplanetary medium. Some electrons are trapped in closed-loop structures, giving rise to type V and type U bursts. Wild (1970) has proposed a model for the magnetic field configuration, shown in Figure 1.4, on the basis of radioheliograph studies

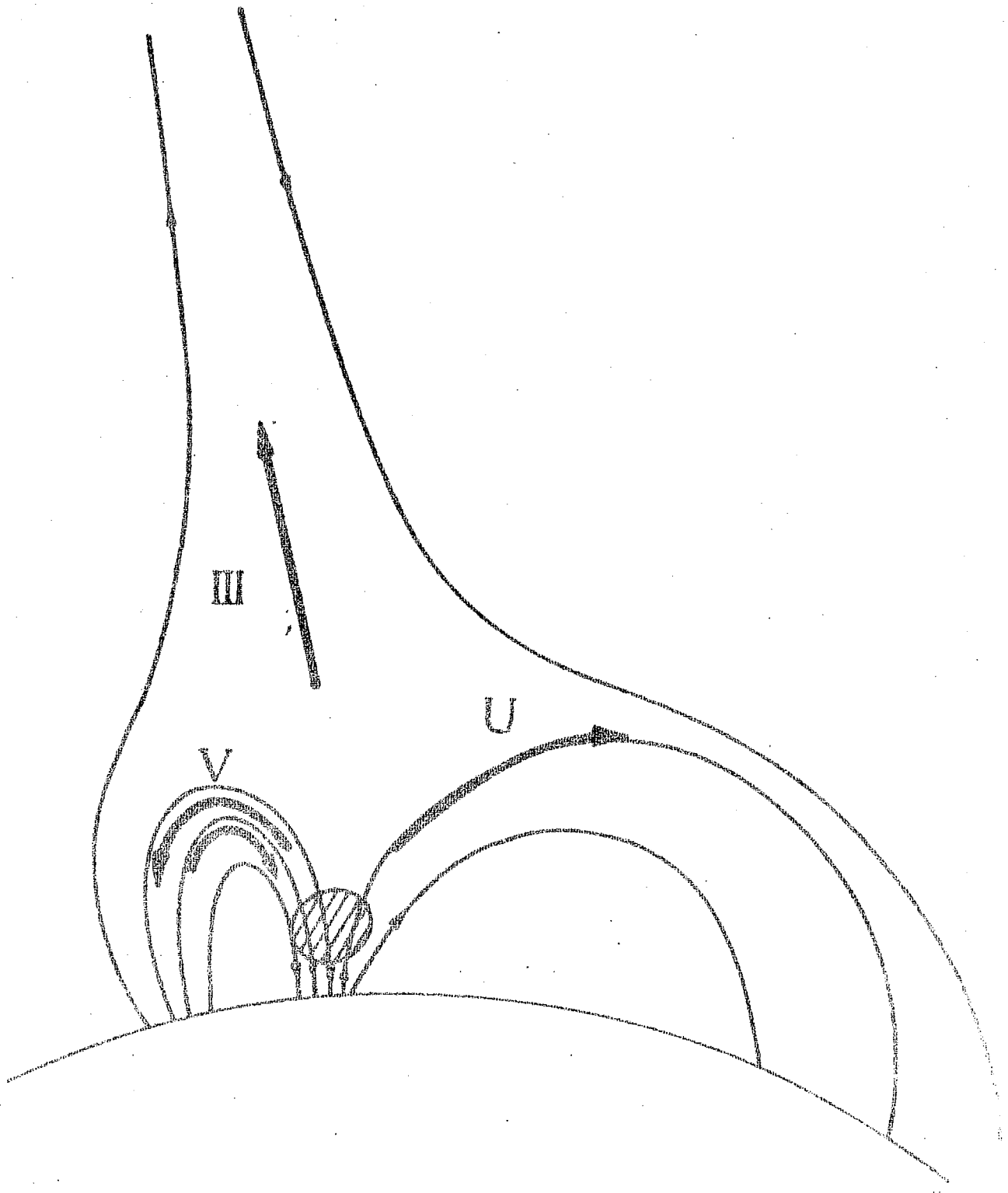


Figure 1.4 Schematic magnetic field configuration to illustrate the possible different paths taken by electrons ejected in the Flash-phase explosion (hatched region) in classical type III, type V and inverted U bursts (From Wild and Smerd 1972).

of the relative positions of type III, U and V bursts.

The percentage of definitely identified type III with associated type V events at 4-2 MHz is 1.8 (Haddock and Graedel 1970), in close agreement with the corresponding value of 2 per cent, given by Thompson and Maxwell (1962) for higher frequency observations. The type III events associated with type V are characteristically observed near the limb (Wild et al. 1959b).

Type U bursts were first reported by Maxwell and Swarup (1958) and Haddock (1958). Their occurrence at longer wavelengths does seem to be rare, although one with a reversing frequency of 35 MHz (Sheridan et al. 1959) and the other with a reversing frequency of 0.7 MHz corresponding to a height of about  $35 R_{\odot}$  from the sun (Stone and Fainberg 1971) have been reported. Observation of Faraday rotation by Schatten (1970) of microwave telemetry signals from Pioneer VI satellite, when it was occulted by the sun, also showed an evidence that the line of sight was intruded by the "magnetic bottle" following a solar flare. These rare instances might be taken as an indication that apparently closed magnetic loops do not, in general, occur sufficiently high in the corona where type U-bursts at low frequencies originate (Fokker 1970).

### 1.32 ASSOCIATION OF TYPE III WITH MICROWAVE AND X-RAY BURSTS

It is now generally accepted that flare-time electron

acceleration and its interaction with the ambient solar atmosphere can explain the occurrence of type III bursts at meter wavelengths as well as that of bursts at centimeter wavelengths and X-rays. It has been suggested by de Jager and Kundu (1963) that for simultaneous occurrence of all these three types of bursts would require expulsion of electrons both in the upward and downward direction from the seat of the flare. The electrons ejected in the upward direction travel through the corona without being "braked" thus producing type III bursts at meter wavelengths, while those electrons accelerated in the downward direction would enter the denser regions and produce centimeter wavelength bursts by synchrotron process and later the same electrons might produce hard X-rays. This idea is supported from the evidence that the time-structures of centimeter bursts and hard X-rays often agree in detail.

The association of type III bursts with microwave bursts is only about 15% and increases to 40% when type III burst is associated with type V (Kundu 1962). Like type III burst, the microwave burst occurs near the start of the optical flare (Covington and Harvey 1961). The majority of type III bursts occur earlier than, but very close to, the maximum of microwave bursts (Kundu 1965).

High energy X-ray bursts are associated with microwave bursts in 100% cases, whereas the association with type III bursts is only about 20% (Kundu 1965).



1.33 ASSOCIATION OF TYPE III BURSTS WITH STREAMS  
OF PARTICLES IN THE INTERPLANETARY MEDIUM

The electron events observed in interplanetary space have been shown to be closely correlated with solar optical flares (Van Allen and Krimigis 1965, Anderson and Lin 1966, Lin and Anderson 1967). The prompt events begin approximately 30 min. to 60 min. after the maximum development phase of the solar flare. The associated flare may be of importance as small as 1-. For delayed solar electron events, the electrons appear at the earth 20 to 40 hours following a large (importance  $\geq 2$ ) solar flare. Low energy proton fluxes also appear in association with these electron fluxes. The emission of 40 KeV electrons by small solar flares seems to be a distinct phenomenon from the emission of energetic protons and relativistic electrons (Lin 1970a).

Pure electron events, produced primarily by sub-flares and importance 1 flares, are closely related to energetic ( $\sim 20$  KeV) X-ray bursts, impulsive microwave bursts and type III radio bursts, while proton events characterized by large flares are related to type II and type IV radio bursts, intense X-ray bursts, and sometimes relativistic energy electrons. Lin (1970a) found lower limits on the percentage association of type III bursts with proton and electron events as 77% and 82% respectively. The small flares associated with low energy electron events make this correlation very significant.

Smith (1970a) has examined the possibilities of a proton stream as an exciter for type III bursts. He has suggested that modest proton streams could be accelerated by much less significant flares and would miss detection at the earth because of high transverse diffusion in the interplanetary space. So very high correlation of subflares (producing low energy electrons only) cannot be treated as an evidence against the proton stream exciters. However, the abandonment of the electron stream hypothesis may seem pre-mature in the absence of new evidence to the contrary. Observations at very low frequencies can provide useful information to decide in favour of either electron or proton stream.

Lin (1970a) observed that some small flares were not accompanied by energetic phenomenon in particles, X-ray or radio emission. Giovanelli (1958) noted that the explosive phase ( a sudden rapid and bright expansion) initiated many solar phenomena such as type III radio bursts, X-ray bursts and microwave bursts. It is likely that the acceleration of 10 - 100 KeV electrons is the basic mechanism of the explosive phase as suggested by Wild (1963a). The energy range of electron stream is in agreement with that deduced from the speed of type III exciters and energies of X-ray bursts.

Lin and Anderson (1967) and Lin (1970a, b) found that electron fluxes for a typical type III storm range from  $10 - 10^3$  electrons  $\text{cm}^{-2} \text{ s}^{-1}$ . Van Allen (1971) indicates that for a large burst, fluxes upto  $10^5$  electrons  $\text{cm}^{-2} \text{ s}^{-1}$  have been recorded.

1.4 POSITION MEASUREMENTS OF TYPE III BURSTS  
AND EFFECTS OF SCATTERING

Using sweep-frequency interferometer measurements over a frequency range 40 - 70 MHz, Wild et al. (1959a) determined one dimensional positions of type III bursts associated unambiguously with flares near the limb. These observations strongly support the hypothesis that radiation at different frequencies originate at the local plasma frequencies from different levels as their exciting agencies travel outward through the solar corona. Morimoto and Kai (1961) found that the heights of type III bursts at 200 MHz varied from 0.2 to 0.3 solar radius which was considerably higher than the height of 200 MHz plasma level for the normal corona. These results were consistent with the interpretation that the type III bursts originate in coronal streamers. Kuiper (1973) determined the radial distance of type III sources at 60 MHz to be about  $1.6 R_{\odot}$ , which agrees with the height determination by Wild et al. (1959a) to within an experimental error. In the absence of definite evidence as to whether type III burst is due to fundamental or second harmonic radiation, it was not possible to confirm from Kuiper's observations whether type III burst occurred in coronal streamers or in the quiet corona.

Smerd et al. (1962) found that the position of harmonic radiation was inside that of the fundamental. The observations of Labrum (1971) indicate that the harmonic may be received either along a direct path or after

reflection from the corona. This means that the harmonic source can be double. Heliograph observations at 80 MHz, however, indicate that the fundamental and harmonic arrive from very nearly the same direction (Stewart 1972).

McLean (1971) and Stewart (1972) observed a transverse shift of the harmonic source relative to that of the fundamental. This was thought to be an evidence that the second harmonic source emits predominantly in the backward direction and received by the observer after reflection from the lower level in the corona. This idea has been given theoretical support by Zheleznyakov and Zaitsev (1970b), especially for events with electron stream velocity greater than .5 c. However, the work of Riddle (1972) shows that the combined effects of spherical refraction and scattering on radiation emitted isotropically from a point source can produce extended harmonic and fundamental sources in nearly the same position. When the stream velocity is  $\sim 0.3$  c, the size of the forward lobes for harmonic radiation remains greater than the size of back lobes (Zheleznyakov and Zaitsev 1970b). The scattering analysis of Riddle (1972) shows that the polar diagrams of radiation for a source velocity  $\sim 0.3$  c are similar to the source emitting isotropically.

It was found that the length and lateral dimensions of the burst source increase with decreasing frequency. The increase in the lateral size may be due to both a

"fanning out" of the electron stream and to the scattering and refraction of radio waves in the corona (Hughes and Harkness, 1963). The first systematic studies of scattering due to small-scale irregularities in the corona were made by Fokker (1965b), who showed that scattering could cause an increase in the angular size of the source and a shift in its apparent position. In the scattering theory the effects of refraction due to large-scale features of the solar corona and absorption have been included by Steinberg et al. (1971), Steinberg (1972) and Riddle (1972). Angular size of type III bursts measured by Wild and Sheridan (1958) at 45 and 60 MHz were 10' arc and 6' arc respectively. Goldstein (1959) found the dimension of type III bursts in the 105 to 140 MHz range to be about 3.2' arc or greater. Weiss and Sheridan (1962) found that the brightness distribution of type III source could be represented by a "core-halo" model. At 26.3 MHz Erickson (1962) obtained an average brightness distribution of a type III burst source showing a core ( $< 10'$  arc) and a halo (38' arc). The power in the core at 26.3 MHz was only about 8 per cent of the total power, as compared to 58 per cent at 60 MHz. This is to be expected since scattering should be greater at low frequencies.

1.5     THE SOURCE SPEED AND INTERPLANETARY OBSERVATIONS  
OF HECTOMETER AND KILOMETER WAVELENGTH TYPE III  
BURSTS

The derived velocities of type III sources range from 0.2 c to greater than 0.6 c corresponding to electron

energies of 20 - 100 KeV (Wild et al. 1959a). It is sometimes suggested that the source particles may be protons rather than electrons (Smith and Fung 1971), in which case the particle energy would be 40 - 200 MeV rather than 20 - 100 KeV. Sturrock (1963) attributed the cause for the source velocity, being so well defined, to the transmission properties of the chromosphere and energy distribution of electrons. The source speed is calculated from the dynamic spectra and depends critically on what electron density model is assumed for the lower corona and the interplanetary medium. Stewart (1965) showed that outward velocity remained constant from the lower solar atmosphere out to 2 solar radii. Using an extrapolated model of a coronal streamer Hartz's (1964) analysis suggested a trend of deceleration for the exciter at greater heights. The average drift velocities were found to be .35 c only if modified streamer electron density, derived from pressure equilibrium across the streamer boundary, is used (Hartz 1969, Alexander et al. 1969). Haddock and Alvarez (1973) determined a mean velocity of  $\sim 0.32$  c for the exciter. These velocities were derived by using a model of coronal electron density distribution within the solar wind values.

There was an obvious need to determine the source velocity independent of the assumed model for electron density. Slysh (1967a) found that type III burst radiation at 0.2 MHz, detected by a satellite orbiting the moon,

appeared to be arriving from a distance of 1 A.U. instead of 35 solar radii as expected. This indicated that the streamer density decreases less slowly than the modified electron density model used by Hartz (1964).

The earth satellite observations at very low frequencies revealed that several hundred thousand ( $\sim 10^5$ ) bursts can be emitted from an active region during one complete solar rotation. They are distinct from individual or groups of type III bursts because of their long duration. They are known as "Type III storms" (Fainberg and Stone 1970a). The rate of occurrence of individual drifting bursts in a storm shows a strong dependence on the heliographic longitude, 1 burst per 10 S near the central meridian passage (CMP). Near the CMP the apparent drift rate is maximum and as an active region approaches the limb, the average drift rate decreases. The apparent drift rate dependence on the heliographic longitude is caused by the modification introduced by the "light-time" correction for propagation between the source and the observer. The drift time from one frequency to another is a function of the velocity of the stream, the altitudinal difference in positions of the sources where the radiation originates, and the "light-time" correction which is dependent upon the heliographic longitude. Assuming that at large distances from the sun the path of the outward moving agency is essentially constant, Fainberg and Stone (1970b) derived

for the outward moving source a velocity of the order of .37 c in the height range of 10 to 40 solar radii by applying the method of least-squares to a large number of bursts. In conclusion, one is inclined to think that type III exciters travel out to large distances without any deceleration. An important thing to note is that Fainberg and Stone's (1970b) method of calculating the speed of the exciter is independent of the streamer electron density models.

Warwick (1965) distinguished between decametric type IV emission and decametric continuum. The decametric continuum is characterized by a continuum background upon which are superimposed a massive number of type III bursts. The observations have shown that the decametric continuum is related to the type III storms at very low frequencies. Warwick (1965), therefore, proposed that it is the decametric continuum which degenerates into the massive number of type III storm bursts. Further, he has suggested that the presence of decametric continuum indicates the existence of conditions suitable for the production and escape of super-thermal electrons into the interplanetary medium. Boischot et al. (1970) have pointed out that the noise storm at meter wavelengths, which consists of very fast and narrow banded type I bursts superimposed upon an intense continuum degenerates into a series of type III bursts at decameter wavelengths, even if it lasts for hours or days. Fainberg and Stone (1970a) proposed that meter, decameter, and



hectometer storms are all produced by the same outward streaming electrons, and that under suitable conditions are measured by space probes beyond the magnetosphere. However, meter and decameter storms consist of both bursts and background continuum. The detection of background continuum by Fainberg and Stone (1971a) at hectometer and kilometer wavelengths strengthens Warwick's idea. One implication of the continuum is that it may represent the constant streaming of superthermal electrons ( $\sim 40$  KeV) for an extended period of time along channelled paths through the interplanetary medium.

Fainberg and Stone (1971b) arrived at a streamer electron density model by assuming that 2.8 MHz plasma level occurs at 11.6 solar radii. They obtained a streamer density enhancement of 16 times the quiet corona at sunspot minimum. It should be noted that the most favourable conditions for the generation and escape of type III bursts are found in the densest region of the streamers. Making use of this fact, Graedel (1970) has used the study of hectometer bursts as a means to derive the properties of the coronal streamer structures which show definite extension and shape upto 5 solar radii above the photosphere. However, Newkirk (Graedel 1970) has pointed out that the use of radio bursts (to explore coronal streamers) may be premature because of limited number of observations made which support the assumption that type III radio bursts originate in streamers. Zaitsev et al. (1972) have proposed

that bursts are generated at the second harmonic of the plasma frequency. This is supported by the satellite observations of Haddock and Alvarez (1973). This should reduce the enhancement of electron density calculated by Fainberg and Stone (1971b) by a factor of 4, and perhaps still further if effects of scattering are taken into account (Steinberg et al. 1972).

Fainberg and Stone (1971b) found that the time of CMP as determined by the maximum drift rate is a function of frequency; it occurs later in time at the lower frequencies. They associated this progressive delay with the curvature of the path (garden-hose curvature) and calculated the average bulk velocity (solar wind speed) at distances between 14 and 36 solar radii. The inferred solar wind speed is of the order of  $380 \text{ km s}^{-1}$  in this region.

#### 1.6 GENERATING MECHANISM

In the elementary theory of type III solar radio bursts developed by Ginzburg and Zheleznyakov (1958, 1961), the source of radio emission consists of plasma waves which are excited by the passage through the corona of a bunch of fast electrons ejected during the explosive phase of a solar flare or a flare-like event. Evidences in favour of bunches of electrons acting as the exciter relate to the onset of type III bursts and X-ray burst emission occurring within a second or so of the flash

phase of the flare and the interplanetary observations of electron events associated with type III bursts. The electrons are thought to be accelerated during the development of the instability associated with a flare (Parker 1963, Carmichael 1964, Sturrock and Coppi 1966, de Jager 1967, Sweet 1969, Sturrock 1972). While protons are also often present at the time of type III bursts (McDonald 1973), their flux is too low to excite plasma waves to explain the observed bursts (Lin 1973).

#### 1.61 TWO-STREAM INSTABILITY

Cerenkov plasma waves are set up by the passage through a medium of a charged particle at a speed greater than the phase velocity of the medium. However, Ginzburg and Zheleznyakov (1961) pointed out that collective effects of electrons in the stream must be considered. These coherent waves tend to "trap" the stream electrons in the potential "wells" of the waves by electrostatic forces. This gives rise to the two-stream instability or Landau damping depending upon whether the particle velocity is respectively greater or less than the phase velocity in the medium. The plasma waves can grow (by the two-stream instability) only when the velocity distribution has a positive gradient at the phase velocity of the medium (Bohm and Gross 1949a, b). The energy of the plasma waves is mainly concentrated near the plasma frequency. Sturrock (1963) pointed out that

the two-stream instability would cause plasma waves to grow at a rate that far exceeds the decay rate due to collisional damping. He showed that this growth rate would produce tremendous beam deceleration in only a few meters. This would cause flattening of the peak of the velocity distribution function of the stream before the collisional damping would become strong enough to inhibit the instability. Because type III bursts are detected at hectometer and kilometer wavelengths, the bunches of electrons must rise to very high coronal levels (Fainberg and Stone 1970a, b). Further, as indicated earlier that the stream travels out in the corona without any deceleration, it would appear that the electron beam must be stabilized, that is, the two stream instability may not occur in a gross way.

#### 1.62 NON-LINEAR INTERACTIONS FOR SUPPRESSION OF TWO-STREAM INSTABILITY

A number of processes based upon induced scattering of plasma waves (Tsytovich 1966, Kaplan and Tsytovich 1967, Tsytovich 1970, Smith and Fung 1971, Smith 1970b), wave-wave interaction (Sturrock 1965), and geometrical factors (Smith 1970b) have been invoked to suppress the instability. The wave-wave interaction requires the nonthermal level of ion-acoustic waves. Radar back-scatter experiments of the sun can be interpreted as evidence for non-thermal level of ion-acoustic waves (Gordon 1968) above active regions. These acoustic waves can be set up as a

consequence of reverse current of thermal electron streams at a velocity exceeding the sound speed (Melrose 1970b) or in the current sheets in the active region streamers and by the mode coupling of large amplitude Alfvén waves (Smith 1972). The basic purpose of the suppression processes mentioned above is to withdraw the plasma waves from the resonance of the beam and therefore cut-off the formation of a plateau. Maintaining that no process has been found effective enough to stabilize the electron stream, Smith and Fung (1971) favour the proton streamer as an exciting agency. However, as pointed out already, a definite new evidence is required before electron hypothesis can be abandoned.

Baldwin (1964), Zheleznyakov and Zaitsev (1970a) and Zaitsev et al. (1972) have shown that conditions for the growth of plasma waves exist and are continually maintained near the leading edge of the stream where faster particles outnumber the slower ones. It was pointed out that the process of fast electron beam formation within a short time of flare explosion, results in a spatially bounded stream of electrons and inhomogeneities in density in its front and back. The faster particles tend to move towards the head of the train and the slower ones to the rear; but

because faster particles tend to become decelerated by the plasma wave and the slower ones accelerated, a process of dynamic recycling can occur. It is important to note that, according to this theory, stabilization of the stream is found unnecessary and, therefore, quasi-linear relaxation should occur. Further, Zaitsev et al. (1972) have pointed out that the necessity of stream stabilization, a conclusion derived from the observation that a particle stream travels out in the corona undecelerated, is an illusion. They have shown that it is the energy density maximum in the plasma wave packets which travels in the corona with a constant velocity as determined from the dynamic spectrum and position measurements of type III bursts and not the electron stream. This velocity is determined by the mean fast electron energy at the moment of their formation in the flare region. The time evolution of the plasma instability in the theory worked out by Zheleznyakov (1970a, b) and extended by Zaitsev (1972) becomes a function of the stream parameters (Landau damping) and collisional frequency. In the meterwave range, the collisional damping is more important whereas in the longer wavelengths and decameter wavelengths Landau damping becomes important. This theory has an encouraging support from the controlled experiments of Hendrickson et al. (1971). They found that radio emission occurs from the leading edge of the pulses of 35-45 KeV electrons that were injected into the ionosphere plasma.

Also Lin (1973) has shown evidence which supports the interpretation in terms of the leading edge of pulses. He found that when a beam of electrons reached the satellite, the energy spectrum was unstable. However, as the beam density increased, the velocity distribution became more and more stable. It would appear, therefore, that the unstable configuration needed to generate coherent plasma waves occurs only at the leading edge of the beam and, consequently, that only this part of the beam is responsible for type III bursts.

The satellite observations both of radio waves and particle fluxes have provided a means of comparing different theories. Evans et al. (1971) find a close agreement between the Smith's (1970a, b) theory for electron streams and the observations of electron fluxes of Lin and Anderson (1967) and Lin (1970a, b). They also find that Zheleznyakov and Zaitsev's (1970a, b) quasi-linear theory is a close second in showing a reasonable agreement. It seems then that the Zheleznyakov and Zaitsev's theory shows much promise and is amply supported by observations.

#### 1.63 CONVERSION OF PLASMA WAVES

It has generally been accepted, according to the theory of Ginzburg and Zheleznyakov (1958), that plasma waves become partially transformed into electromagnetic waves through scattering on thermal fluctuations in the

plasma. The Rayleigh scattering, which does not involve any substantial frequency change, yields emission in the fundamental mode of type III bursts, while combination scattering leads to the appearance of second harmonic. In case of combination scattering, the nonlinear coupling has been accepted as a better alternative (Sturrock 1961, Melrose 1970a). The combination scattering appears to radiate the second harmonic in the backward direction, so that radiation is observed only after reflection near plasma level. In some instances, however, harmonic radiation does propagate directly to the earth (Labrum 1971). These observations and Riddle's (1972) analysis on scattering indicate that some rethinking about the generation of second harmonic is needed. It is worth emphasizing that according to Zheleznyakov and Zaitsev (1970b) a simultaneous observation of the first and second harmonic will be quite a rare event and, therefore, type III bursts would be recorded primarily in the second harmonic of the local plasma frequency. This is because the regular refraction will cause the fundamental harmonic radiation to emerge from the corona within a small solid angle compared to the second harmonic radiation. These ideas appear to agree with the experimental findings of Smerd et al. (1962) who, from a large number of type III bursts recorded during 2.5 years of observation, could identify



only six events having a well-defined harmonic structure. Zaitsev et al. (1972) find a good agreement between this theory and observations at hectometer wavelengths. In addition, recent satellite observations of type III bursts by Haddock and Alvarez (1973) at hectometer and kilometer wavelengths show that although fundamental and second harmonic radiations may occur at the same time, the latter lasts for much longer time as compared to the former.

The synchrotron theory proposed by Kuckes and Sudan (1969, 1971) requires very much stronger magnetic field, a point that counts against this theory.

1.64     THEORIES OF POLARIZED TYPE III BURST  
          EMISSION FROM SOLAR CORONA

The polarization of type III bursts can be the result of the emission process and/or due to the conditions for escape and propagation of radio emission from the magneto-active solar coronal regions. Fomichev and Chertok (1968a) have argued in favour of the latter processes. These two influencing factors, giving rise to the observed polarization characteristics of type III bursts, are discussed separately.

1.641    THEORY OF FOMICHEV AND CHERTOK

In the magneto-active coronal plasma, the levels of escape of ordinary and extraordinary waves, where the corresponding refractive indices become equal to zero,

occur at different heights. The level of escape for extraordinary waves is situated above that for ordinary waves. The radio emission generated between these levels is completely polarized because only an ordinary wave can escape from this region. Also during the propagation in the corona, extraordinary waves experience greater absorption than ordinary waves. The mode coupling, which also affects the polarization characteristics, is not taken into consideration by Fomichev and Chertok (1968a). A specific analysis of the influence of conditions of escape and propagation of radio emission requires a knowledge of the altitudinal extent of the emission region and its position relative to the levels of reflection for ordinary and extraordinary waves. For type III bursts, Fomichev and Chertok (1968a) have put the level of reflection for extraordinary waves within the emission region (Figure 1.5a). Knowing the altitudinal extent of the emission region and of corpuscular stream, exciting a type III burst, one can trace the time history of polarization characteristics of type III bursts. Taking escape conditions only into account, it has been shown that a type III burst is initially fully polarized and decreases to a constant value for some part of the duration of the burst before becoming finally completely unpolarized (Figure 1.6). The duration during which the radiation remains fully polarized is of the order of .04 S at 60 MHz and requires a polarimeter which should have a time

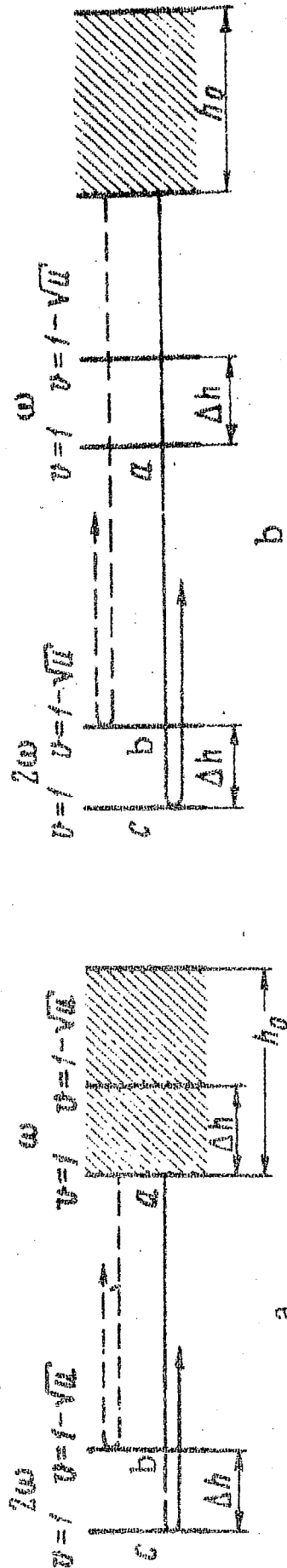


Figure 1.5 The schematic representation of the relative positions of the emission region (hatched region) and the levels of escape corresponding to ordinary and extraordinary waves represented by  $\psi = 1$  and  $\psi = 1 - \sqrt{U}$  respectively both at fundamental  $(\omega)$  and second harmonic  $(2\omega)$ , where  $\psi = \omega_0^2/\omega^2$  and  $U = \omega_0^2/\omega^2$ .  $\omega_0$  = Langmuir frequency,  $\omega_0 =$  gyrofrequency, and  $\omega =$  radiation frequency. (a) If the level of escape corresponding to extraordinary wave falls within the emission region then type III burst is either fully or partially polarized, (b) if it falls far below the emission region, the type III burst is unpolarized (After Pomichev and Chertok 1968a).

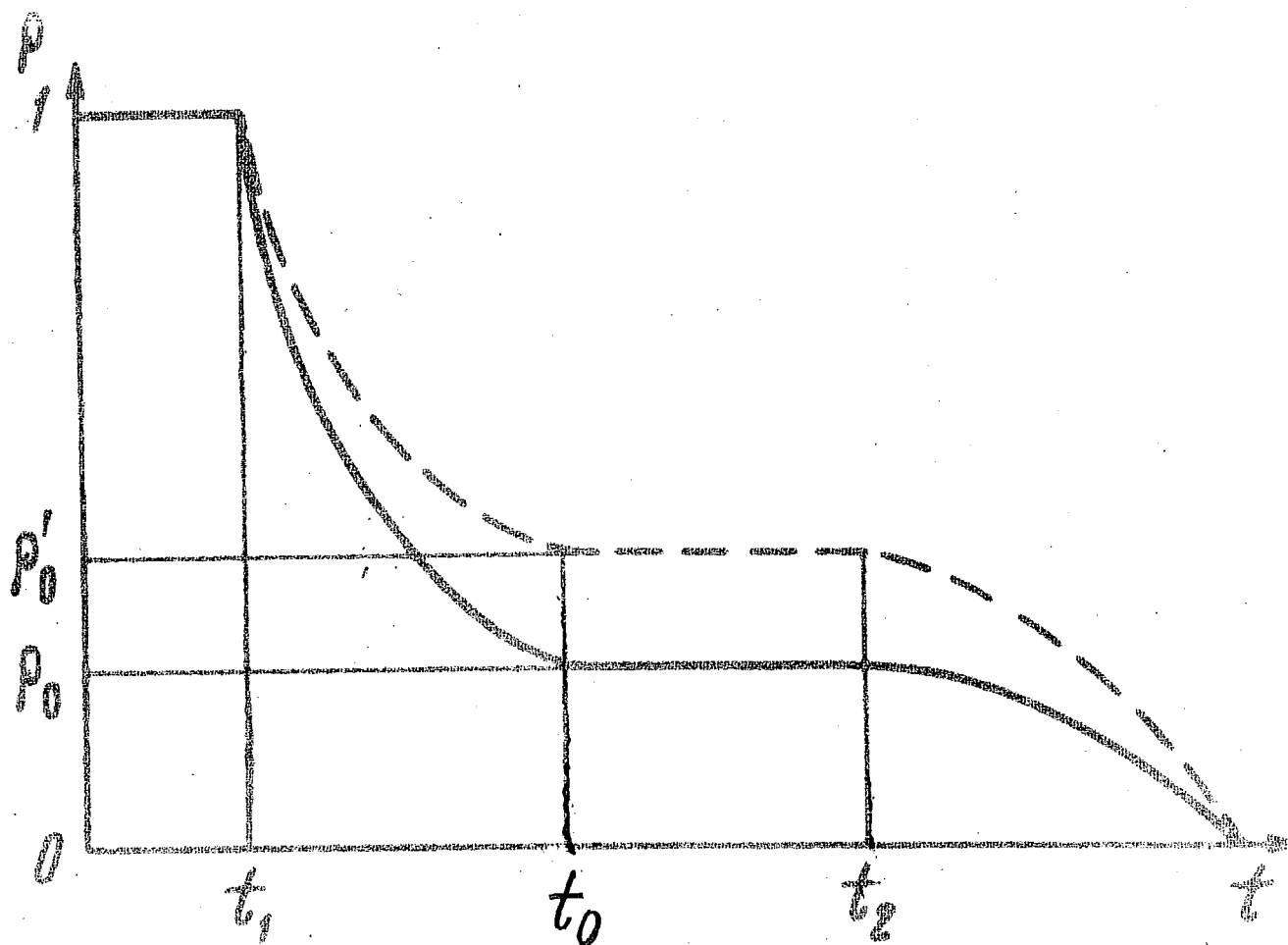


Figure 1.6 The time dependence of the degree of polarization ( $P_t$ ) taking into account escape conditions only (solid curve) and even when conditions for propagation of ordinary and extraordinary waves are also included (dashed curve). At 60 MHz,  $t_1 = 0.04$  S,  $t_0 = .3$  S,  $t_2 = .7$  S,  $P_0 = 6\%$  and  $P'_0 = 13\%$ . (After Fomichev and Chertok 1968a).

resolution of 0.01 S to detect such quick changes in polarization. The time dependence of polarization characteristics does not change much even when taking into account simultaneously both the escape conditions and the differential absorption for propagation of ordinary and extraordinary waves. The polarization appears in the ordinary mode.

The polarization of second harmonic can be explained by taking into account that we observe emission of the harmonic for the most part after reflection from a lower level in the corona, whereas the emission of the fundamental arrives at the earth directly from the generation region (Smerd et al. 1962, Stewart 1972). Because of the displacement of reflection levels for the ordinary and extraordinary waves at the second harmonic and the relative position of the emission region above the level of reflection corresponding to extraordinary wave, the differential absorption for the reflected emission can be appreciable and thus giving rise to polarized second harmonic (Figure 1.5b). The radio emission after reflection may have quite high polarization corresponding to waves of both ordinary and extraordinary type. The sign of polarization depends upon the heliographic longitude and reverses around  $40^{\circ}$  -  $60^{\circ}$  (Fomichev and Chertok 1970).

The degree of polarization is a function of the source extent  $h(\theta)$  and the altitudinal displacement

$\Delta h(\theta)$  of the level of escape for the extraordinary wave relative to the ordinary wave ( $\theta$  is the heliographic longitude) (Figure 1.7). The latter has strong dependence on the magnetic field. It follows then that an appreciable polarization occurs only when the corona contains sufficiently strong magnetic fields and for such bursts the radio emission of the harmonic must also reveal a high degree of polarization (Fomichev & Chertok 1968a). However, as already mentioned earlier, the work of Riddle (1972) shows that the combined effects of spherical refraction and random scattering on radiation emitted isotropically from a point source can produce an extended harmonic and fundamental sources giving the impression as if the source emitted second harmonic predominantly in the backward direction. This analysis, which explains the transverse shift in the relative position of the second harmonic of type III burst, challenges the validity of the assumption of Fomichev and Chertok, namely, that the second harmonic radiation is predominantly emitted in the backward direction. Another difficulty is that this explanation by Fomichev and Chertok requires fractional emission bandwidth  $(\Delta\nu/\nu) \sim 0.15$ , which seems to be rather large (Smith 1970b).

The predicted characteristic temporal change in the degree of polarization at a fixed frequency is in qualitative agreement with the investigations of polarization measurements at 40 and 60 MHz (Gopala Rao 1965);

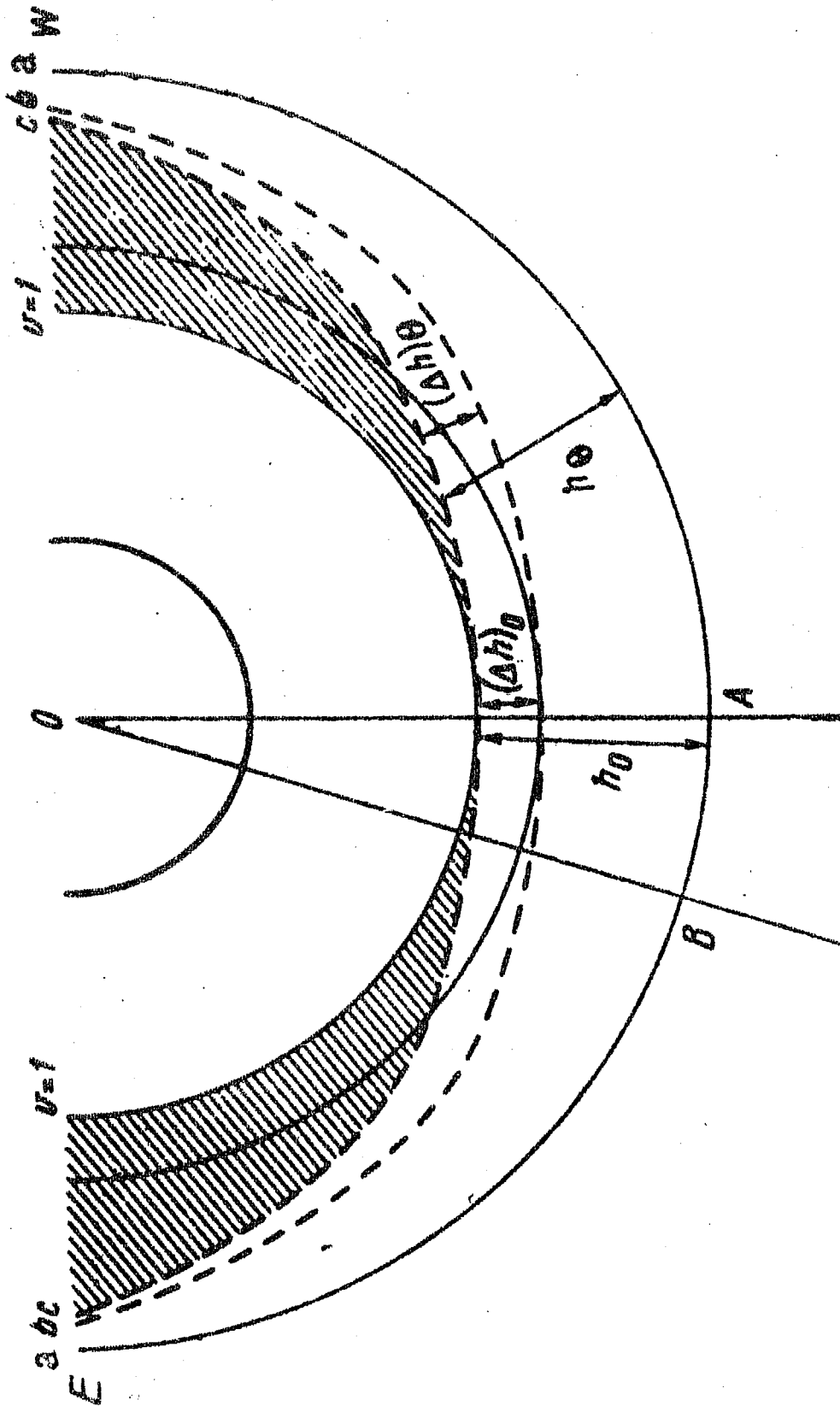


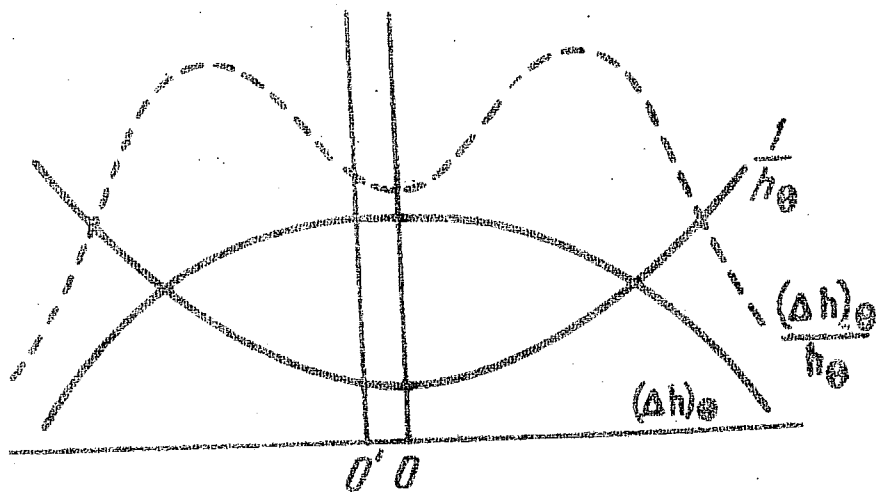
Figure 1.7 illustrates that as the angular distance of the source or type III burst from central meridian passage (OA) increases, the level of emergence of ordinary and extraordinary waves (curves b and c) rise slightly above the levels of  $u = 1$  and  $u = 1 - \sqrt{u}$ , while the distance  $\Delta h(\theta)$  between them decreases (After Pomichnev and Chertok 1968b).

it appears that type III bursts possess a double structure: the sharp, intense, drifting feature with relatively strong polarization, and a diffuse background of longer duration with relatively weak or zero polarization. Gopala Rao (1965) also noted an inverse relationship between the degree of polarization and the duration of type III bursts.

As the angular distance from the central meridian increases, the levels of emergence of the ordinary and extraordinary waves rise slightly above the corresponding levels at the centre of the sun's disk. It is because of refraction effect. This results in the reduction in the source extent  $h(\theta)$  because the radiation will not reach the earth from below the level bounded by the level of emergence for ordinary wave which rises with longitude. Also the altitudinal displacement  $\Delta h(\theta)$ , as shown in Figure 1.7, decreases as the heliographic longitude increases (Fomichev and Chertok 1968b). The degree of polarization is determined by  $\Delta h(\theta)/h(\theta)$  (Fomichev and Chertok 1968a). This function is double-humped for intermediate heliographic longitudes (Figure 1.8).

The results of the polarization observations carried out at the Potsdam Astrophysical Observatory at 23.5 MHz (Bandwidth 1.5 KHz, years 1961-63) showed that the increase in the mean degree of polarization at intermediate heliographic longitudes in the western and eastern





LONGITUDE

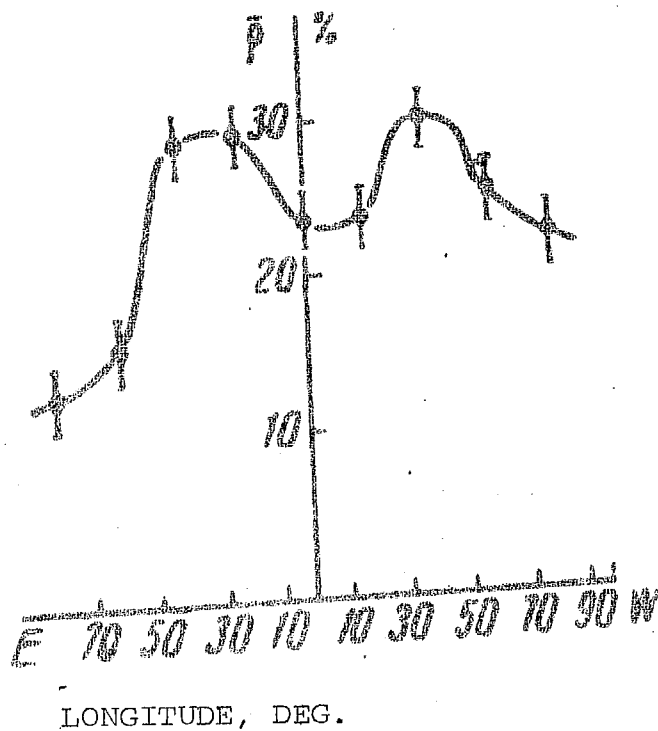


Figure 1.8 illustrates qualitative dependence of  $h(\Theta)$  and  $\Delta h(\Theta)$  on heliographic longitude. The dashed curve shows the longitude dependence of  $\Delta h(\Theta) / h(\Theta)$ . The lower portion of the figure shows the longitude dependence of the measured mean degree of polarization ( $\bar{P}$ ) of type III bursts at 23.5 MHz (After Fomichev and Chertok 1968b).

part of the disk is due mainly to the enhanced proportion of strongly polarized bursts as shown in Figure 1.8 (Fomichev and Chertok 1968b). This is in agreement with the interpretation of polarized type III bursts by Fomichev and Chertok (1968a). However, Chin et al. (1969) did not find double hump in the distribution of mean degree of polarization at 25.3 MHz with respect to heliographic longitude. Instead, they found a behaviour of axial ratio of polarization ellipse similar to the behaviour of mean degree of polarization estimated by Fomichev and Chertok (1968b). It seems some more observations need to be made to resolve this difference.

#### 1.642 YIP'S THEORY OF POLARIZATION

Yip (1970) considered the effect of the sunspot magnetic field on the following: (1) process of generation of weakly damped plasma waves with frequencies near the plasma resonance frequencies through Cerenkov and cyclotron processes; (2) transformation of plasma waves into electromagnetic waves by the thermal fluctuations in the ambient solar coronal plasma; and (3) propagation of electromagnetic waves in the solar coronal active regions. He has shown that the excited Cerenkov plasma waves can only be transformed into an ordinary wave at the fundamental frequency and into both ordinary and extraordinary waves at the second harmonic. The transformed electromagnetic

radiation at the second harmonic maximizes in different directions for the ordinary and extraordinary waves. This results in polarization characteristics at second harmonic to become a function of the wave normal angle with respect to the magnetic field. Because the main power of second harmonic components is emitted at larger wave normal angles, it is possible that some of the second harmonic components pass through the polarization limiting region where the bipolar sunspot magnetic field direction is opposite to that in the source region. Then, referring to the leading spot hypothesis, the sense of polarization of the second harmonic component reverses on passing through the polarization limiting region and a fraction of the type III bursts will be right-handed polarized. This is in agreement with the observations of Komesaroff (1958) and Bhonsle and McNarry (1964b). Yip has explained many other features of polarization characteristics of type III bursts. The combined effects of spherical refraction and random scattering should exercise some influence on the conclusions reached by Yip (1970).

#### 1.7 CONCLUSION

In conclusion, it is worth emphasizing that the observations and interpretations of type III bursts, reviewed in this chapter, have been more often than not used as a means for determining the conditions in the

solar corona and some aspects of the solar activity. For instance, type III bursts have been used to evaluate the temperature of the inner and outer corona (Boischot et al. 1960, Malville 1961, Elgaroy 1961, Hartz 1969, Aubier and Boischot 1972) and the electron density for the corona and the interplanetary medium (Wild et al. 1959a, Shain and Higgins 1959, Weiss 1963, Newkirk 1959, 1967; Zaitsev et al. 1972, Kuiper 1973, Haddock and Alvarez 1973). The hectometer and kilometer wavelength observations of type III bursts have been used to determine the solar wind velocity (Fainberg and Stone 1971b). Further, the very occurrence of type III bursts and their association with X-ray and microwave bursts have been treated as an evidence for acceleration of energetic particles, their escape from active regions along open field lines, and their confinement in closed magnetic loops. Finally, type III burst positions have been used to identify the flares or the  $H_{\alpha}$  active regions (Kuiper 1973, Axisa et al. 1973) and their relative positions with respect to other types of solar radio bursts in delineating the topology of the coronal magnetic fields (reviewed by Wild and Smerd 1972).

## C H A P T E R - I I

### A REVIEW OF POLARIZATION CHARACTERISTICS OF TYPE III BURSTS

#### 2.1 INTRODUCTION

Measurement of the Stokes parameters with narrow-band receivers constitutes a powerful method to study the polarization properties of solar radio bursts, if one is careful about the problems like ground reflection, antenna cross-talk, etc. The polarization characteristics of type III bursts have been studied by analogue as well as digital techniques by many workers using polarimeters with bandwidths ranging from few hundred kilohertz to as low as five Hertz. For complete specification of polarization, the quantities of interest are the total intensity, degree of polarization axial ratio and orientation of the major axis of the polarization ellipse. Since the solar radio waves must propagate through the magneto-ionic medium between the source and the receiver, it is impossible to observe the original state of polarization of bursts. However, the propagation effects on the state of polarization due to Faraday rotation, mode-coupling, scattering due to small-scale irregularities, etc. can be investigated with multi-frequency polarization observations of type III radio bursts.

#### 2.2 SUMMARY OF POLARIZATION OBSERVATIONS

Type III bursts, as a result of earlier work, were thought to be unpolarized (Payne - Scott 1949, Wild and

McCready 1950, Payne - Scott and Little 1951, Little and Payne - Scott 1952). Komesaroff (1958) made polarization measurements of type III bursts by using a suitably modified solar radio spectrometer in the frequency range of 40 - 240 MHz. It was clear from his investigations that many type III bursts were circularly polarized. A large number of type III bursts showed no evidence of polarization. The polarization of type III bursts occurring on the same day showed the same sense of rotation; furthermore, this was the same as that of any type I radiation occurring within a period of one or two days. Several type III bursts were observed at harmonic frequencies; and of these some were polarized, though not all. In each case it was found that the fundamental was more polarized than the harmonic. Subsequent observations by Cohen (1959), Cohen and Fokker (1959), Akabane and Cohen (1961), Bhonsle and McNarry (1964b), Bhonsle et al. (1967), Chin et al. (1971) and Dodge (1972) indicated that some type III bursts were partially elliptically polarized. Measurements of the degree of polarization of type III bursts at 40 and 60 MHz by Gopal Rao (1965) showed that the source might consist of two components; a narrow, intense and polarized burst component superimposed on a diffuse background of longer duration with relatively weak or no polarization. Recent narrow-band (4.8 Hz) measurements of polarization within an overall bandwidth of 3 KHz at 34 MHz by Dodge (1972)

indicated that there was a scatter of circular and elliptical polarizations within the total bandwidth of 3 KHz near the commencement of the burst. This changed to a uniform spectral distribution of near-linear polarization during the more intense portions of the burst. The degree of polarization also increased with the total intensity of the burst. Clustering of orientation angles of polarization ellipses within  $\pm 10^\circ$  around the mean orientation has been reported by several workers. Observational evidence has been accumulating over many years, obtained by means of narrow-band receivers at different frequencies, in support of the occurrence of linearly polarized type III bursts, at least, occasionally. Fokker (1971) considers this paradoxical in the presence of scattering effects. Grogard and McLean (1973) attempted a search for the existence of linear polarization in type III bursts at 80 MHz but without success. Their failure to detect linear polarization might be due to the limitation of their equipment which could not have measured the small amount of differential Faraday group delay, if the Faraday rotation were as low as  $10^3$  radians. Such low values of Faraday rotation have been measured by Bhonsle and Mattoo (1973) at 35 MHz by means of a two-bandwidth polarimeter, described in Chapter III of this thesis. An upper limit to the Faraday rotation at 34 MHz has been determined by Dodge (1972) to be of the order of  $1.75 \times 10^3$  radians, which is in good agreement with our values.

### 2.3 CAUSES OF DEPOLARIZATION OF TYPE III RADIO BURSTS

The amount of depolarization that radiation suffers depends on the bandwidth of the polarimeter; a narrow bandwidth polarimeter is more suited to detect weakly polarized bursts. Typically, at meter wavelengths, bandwidths of the order of a few kilohertz or more have been used in the past. Only recently digital techniques (Bhonsle et al. 1967; Chin et al. 1971) are being adopted for polarization work that permit substantial reduction in the effective receiver bandwidth using fast Fourier transform methods (Dodge 1972). Use of a finite receiver bandwidth has immediate repercussions on the observed polarization properties of bursts, which can ultimately affect polarization measurements through dispersion of orientation angles of polarization ellipses. Further, the source thickness and multiple propagation paths from source to the receiver in the presence of scattering on irregularities in the intervening medium, can affect the polarization measurements because the total Faraday rotation is also an integral function of the propagation path. Of the three processes, the first two can produce comparable effects so far as depolarization due to the finite receiver bandwidth is concerned. The effect of propagation along multiple paths due to scattering, though relatively small, can be unfavourable for the observation of linear polarization.



### 2.31 FARADAY DISPERSION AS A CAUSE OF DEPOLARIZATION

Using the time-sharing polarimeter at 200 MHz (Suzuki and Tsuchiya 1958) at the Tokyo Astronomical Observatory, Hatanaka et al. (1955) found that the radiation is, in general, a mixture of a randomly polarized and an elliptically polarized component. Further, the observations made with the Cornell polarimeter (Cohen 1958a), with a 10 KHz bandwidth at 200 MHz, revealed that some type III bursts were weakly linearly or highly elliptically polarized (Cohen 1959, Cohen and Fokker 1959). It was suggested that large amount of Faraday rotation,  $\sim 10^5$  radians, could occur in the corona. As a consequence, position angles of polarization ellipses would be uniformly spread at different frequencies within the receiver bandwidth, and any elliptically polarized radiation would tend to be reduced to circular plus random polarization. It seemed then, that the Cornell polarimeter detected linear polarization because of the narrow bandwidth of the receiving system.

Hatanaka (1956) found that ellipticity was correlated with the position of the source on the sun's disk, but the degree of polarization was less correlated, and the orientation angle of the polarization ellipse showed no correlation at all. It was further suggested that due to a very large Faraday rotation suffered by the radiation in passing through the solar corona and the earth's ionosphere, the

axis of the polarization ellipse might have been rotated by some amount and that unless the electron density and the magnetic field along the path of the radiation were known, the original orientation angle of this axis could not be obtained.

Hatanaka (1956) discussed Faraday rotation suffered by the radiation in passing through the corona and the earth's ionosphere. When a polarized electromagnetic wave enters a homogeneous magnetized medium, it splits into two characteristic modes (ordinary and extraordinary), which have different phase velocities; and, when the frequency is sufficiently high, the two modes are circularly polarized with opposite sense of rotation (except for the case where the magnetic field is almost exactly transverse). The axial ratio and the sense of rotation of the emergent wave do not change, but the plane of polarization does.

In calculating the effect of Faraday rotation (Akabane and Cohen 1961) the basic assumption is that at some point in the solar atmosphere (the source) the polarization of the radio wave is independent of frequency, at least, over the receiver bandwidth. At the source the position angle of the polarization is  $\chi_0$ . The ray propagates to the earth, where its position angle  $\chi$  is different because of the Faraday rotation, so that

$$\chi = \chi_0 + \phi = \chi_0 + b \nu^{-2} \quad \dots(1)$$

where  $\phi$  = the Faraday rotation in radians,  $\nu$  is the frequency in Hz and  $b$  is constant. The Faraday rotation for the quasi-longitudinal regime of the magneto-ionic theory (Ratcliffe 1959) is given approximately by

$$\phi = 2.36 \times 10^4 \nu^{-2} \int N(z) H_{||}(z) dz \quad \dots(2)$$

where  $\phi$  is in radians;  $\nu$  is in Hz;  $N(z)$  is the number of electrons in  $\text{cm}^{-3}$ ;  $H_{||}$  is the longitudinal component of magnetic field in Gauss;  $z$  is in cm.

Hatanaka (1956) estimated that at 200 MHz, the Faraday rotation might be of the order of  $10^4$  to  $10^6$  radians, because of a general dipole-type magnetic field of the sun. Since  $\phi$  is a function of frequency, an elliptically polarized signal containing a spectrum of frequencies is dispersed into a continuum of ellipses with a spread of orientations. The angular dispersion rate is, from (2)

$$\frac{d\phi}{d\nu} = -2 \phi / \nu_0 \quad \text{radians/Hz.}$$

$$\text{If } \Delta\nu / \nu_0 = (\nu_2 - \nu_1) / \nu_0 = B / \nu_0 \ll 1$$

$$\text{then } \Theta = 2 \phi B \nu_0^{-1} \quad \dots(3)$$

where  $\Theta$  is the dispersion angle corresponding to the

frequency band B limited by  $\nu_1$  and  $\nu_2$  and  $\nu_0$  is the center frequency in Hz.

Because of the dispersion in position angles, the measured polarization would differ from that at the source. This situation was first discussed by Hatanaka (1956), who analyzed the response for a polarimeter with a square pass band. Figure 2.1 depicts the results of analysis by Akabane and Cohen (1961) of dispersion effects on polarization parameters within a Gaussian pass band of the receiver. It can be seen that the dispersion partially depolarizes the wave, and the simplest way to express this, would be, following Akabane and Cohen (1961), in terms of the cross-correlation function of the two circular modes given by:

$$\mu_{RL} = \mu_0 \exp(-\theta^2/4)$$

where  $\mu_0$  is the initial value of  $\mu_{RL}$ . The other effect of the dispersion is the change in the shape of the polarization ellipse, with the result, that an elliptical polarization would tend to be random plus circular polarization (Cohen 1960, Akabane and Cohen 1961).

## 2.32 DEPOLARIZATION DUE TO SOURCE THICKNESS

The type III radiation at a fixed frequency does not originate within an infinitesimal layer in the solar corona. It is because a range of frequencies is emitted at any one level in the solar corona. This is known as the emission



bandwidth. An emission bandwidth of as small as 10 KHz corresponds to 300 km of the source thickness at 35 MHz plasma level in the solar corona. Typically, for a normal type III burst, the emission bandwidth at 35 MHz is of the order of 1 MHz. This corresponds to the source thickness of 3000 km at 35 MHz source region. If it is assumed that type III bursts at 35 MHz are primarily generated at the fundamental plasma frequency, then the Faraday rotation suffered by the radiation at 35 MHz due to the source thickness alone can be of the order of  $10^4 - 10^5$  radians corresponding to the source thickness of 3000 km and a magnetic field of .1 to 1 Gauss. Because the radiation at a fixed frequency is emitted at a range of heights in the solar corona and that the Faraday rotation which is a function of propagation path is large near the plasma level, the observable polarization, at a given frequency even with a monochromatic receiver, will appear to be depolarized relative to the original polarization imposed by the emission mechanism.

## 2.33 DEPOLARIZATION DUE TO SCATTERING EFFECTS

Under quasi-longitudinal approximation, the total Faraday rotation suffered by the radiation in addition to its frequency dependence, is also dependent on the integrated product of the electron density and the longitudinal component of the magnetic field along the propagation path.

Therefore, if the radiation is scattered by irregularities in the propagation medium, it will reach the observer along many paths of different lengths. The effect of scattering was dealt with in detail first by Fokker (1965b) and subsequently by Steinberg et al. (1971) and Riddle (1972). The scattering analysis by Steinberg et al. (1971) indicated that scattered rays reach the observer with a wide spread of differential time delays, between the direct and scattered rays, of the order of 0.05 S. Thus, the total Faraday rotation along different paths would obviously be widely different. Fokker (1971) argued that a relatively small scatter, of the order of  $10^{-4}$  of the mean value in the Faraday rotation along individual rays, would suffice to obliterate the position angle of any linear polarization originally present. If the mean value of Faraday rotation is indeed  $10^5$  radians, as was assumed by Fokker (1971), then the Faraday dispersion angle turns out to be of the order of 10 radians, which should wipe out any linear polarization originally present. But the fact remains that the occurrence of linear polarization has been reported from time to time by many authors (Akabane and Cohen 1961, Bhonsle and McNarry 1964b, Chin et al. 1971, Dodge 1972). Our own observations of polarization of type III bursts carried out at 25 and 35 MHz, presented in detail in Chapters IV and V, confirm the occurrence of linear polarization. We have recently measured the total

Faraday rotation at 35 MHz, which is of the order of  $10^3$  radians only. Such a low value of Faraday rotation would reduce the Faraday dispersion angle due to scattering to something of the order of 0.1 radian. This indicates that the conditions for the occurrence of linear polarization are not all that unfavourable. Grogard and McLean (1973) attempted to detect the existence of linear polarization at the source at 80 MHz. Their failure to detect linear polarization is due to the instrumental limitation in measuring the small values of the differential Faraday group delays corresponding to Faraday rotation of the order of  $10^3$  radians.

#### 2.4 MEASUREMENT OF FARADAY ROTATION

It has been recognized that proper estimates of Faraday rotation provides a valuable information on the joint influence of electron density and the longitudinal component of the magnetic field along the path of propagation. The Faraday rotation measurements relate to the entire propagation path from the source to the observer, if the quasi-longitudinal condition holds for the mode of propagation in the magneto-ionic medium. If it so happens that somewhere along the propagation path the quasi-transverse approximation holds, then ordinary and extraordinary modes do not travel independently which leads to mode-coupling. The region of mode-coupling produces



" limiting polarization " (Budden 1952) and thus, the observer will measure only the Faraday rotation occurring between the polarization limiting region and the receiver. It is possible to make an order of magnitude estimate of the contributions to the total Faraday rotation by the earth's ionosphere, magnetosphere and the interplanetary medium, under the assumption that the QL-approximation is valid.

#### 2.41 EXPERIMENTAL DETERMINATION OF FARADAY ROTATION OF TYPE III BURSTS

Under the assumptions that the source produces a fully polarized radiation and the propagation is quasi-longitudinal, a measurement of polarization gives an upper limit to Faraday rotation. From measured values of  $\mu_{RL}$ , the complex cross-correlation factor, for type III bursts at 200 MHz within a bandwidth of 10 KHz, Cohen (1959) found that the Faraday dispersion angle  $\theta \leq 2$  radians, with the corresponding values of the Faraday rotation  $\phi \leq 2 \times 10^4$  radians. In order to test for the existence of the Faraday rotation in the solar corona, Akabane and Cohen (1961) made polarization measurements of type III bursts at 200 MHz simultaneously within two bandwidths (10 and 22 KHz) and computed the Faraday rotation unambiguously. They observed that many type III bursts had a Faraday rotation of the order of  $10^4$  radians. The complex correlation factor  $\mu_{RL}$  decreased with increasing

bandwidth and at 300 KHz bandwidth the bursts were either unpolarized or weakly circularly polarized. The number of bursts decreased rapidly as  $\mu_0$  increased. The maximum value of  $\mu_0$  was about 0.3 with a bandwidth of 10 KHz. Our measurements of the Faraday rotation, at 35 MHz made with bandwidths of 7.5 and 12.5 KHz, which form the subject matter of this thesis, indicate that it is of the order of  $1.8 \times 10^3$  radians. This is in excellent agreement with the upper limit of  $1.75 \times 10^3$  radians found by Dodge (1972) at 34 MHz in an overall bandwidth of 3 KHz.

## 2.5 THE CONSTANCY OF ORIENTATION ANGLES OF POLARIZATION ELLIPSES OF TYPE III BURSTS

Cohen and Fokker (1959), Cohen (1959a), Bhonsle et al. (1967), and Dodge (1972) noted that in case of some type III groups of bursts the orientations were within few degrees (clustering) for all the bursts in a group. Since the source has a finite depth near the plasma level, the Faraday rotation of the radiation generated within the source at different depths makes it difficult to attribute the constancy of the orientation angles to the source region. Dodge (1972) also has put forth a similar argument to explain his observations at 34 MHz. Our observations at 25 and 35 MHz presented in Chapter IV of this thesis, also indicate that in certain groups of type III bursts the orientation angles had a spread within  $\pm 10^\circ$ . Cohen (1959) explained the constancy in the orientation angles of

type III bursts at 200 MHz by invoking the existence of a quasi-transverse region, high in the corona, that was responsible for " limiting polarization ". The constancy of orientation angles can be explained in terms of the constancy of the integrated product of the electron density and the longitudinal component of the magnetic field at least over a time interval ( $\sim$  a few minutes) for which the group of type III bursts lasts.

## 2.6 LINEAR POLARIZATION

As already mentioned in section 2.1, many authors (Cohen 1959, Akabane and Cohen 1961, Bhonsle and McNarry 1964b, Chin et al. 1971, and Dodge 1972), in addition to our observations at 25 and 35 MHz reported in this thesis, have confirmed the occurrence of linearly polarized type III bursts. The linear polarization cannot be attributed to the source because the large Faraday rotation, within the source of finite depth would " wash out " any linear polarization originally present.

Cohen (1960) showed that a circularly polarized wave at a frequency greater than a " transitional " frequency maintains its sense of rotation across the QT region, but at frequencies less than the " transitional " frequency, it is reversed. This process must be continuous with frequency, and therefore linear polarization must emerge at an appropriate frequency. The linear polarization is

obtained by allowing a single magneto-ionic mode to proceed from a region of weak coupling to one of strong coupling, and then again to a region of weak coupling. As the wave proceeds from a region of weak coupling, the axial ratio of the polarization ellipse gets smaller and stops changing in the region of strong coupling. The wave persists in this particular ellipse until the second region of weak coupling is encountered. From there onwards, the ellipse tightens up again, and it ultimately just becomes linear. A QT transitional frequency of 200 MHz can, in fact, be obtained with reasonable values of electron density and magnetic field, at a height of 0.5 solar radius above the photosphere. With this model, however, the polarization is frequency-sensitive and thus exceptional geometric circumstances would be required to explain the occurrence of linear polarization. However, the occurrence of bursts with linear polarization is not exceptional. Cohen (1959) and Akabane and Cohen (1961) found that strong circular polarization was rare; on the contrary they found that many of the type III bursts were weakly elliptically and linearly polarized. Similar results were obtained by Bhonsle and McNarry (1964b), Harvey and McNarry (1970), Chin et al. (1971), and Dodge (1972). It was found that axial ratios of the polarization ellipses were mostly less than 0.2, but occasionally values as great as 0.7 were observed. Fomichev and Chertok (1969a) have reported that the

degree of linear polarization at 23.5 MHz at all heliographic longitudes exceeds the degree of circular polarization. This implies extremely limited manifestation of Faraday rotation and hence absence of Faraday effect over the greater part of the wave path in the corona. If the component of linear polarization of type III bursts is explained on the basis of mode coupling (Cohen 1960, Zheleznyakov and Zlotnik 1964), then it admits the possibility of the emission emanating from the source corresponding to a wave of single mode (ordinary/extraordinary) and that the QT region for mode coupling is situated high in the corona.

## 2.7 SYSTEMATIC VARIATION OF POLARIZATION CHARACTERISTICS

Chin et al. (1971) have reported a striking difference in the distribution of degree of polarization and the axial ratio of the polarization ellipse at 25.3 MHz (bandwidth 100 Hz) between the year 1966 on the one hand and each of the years 1968 and 1969 on the other hand. In 1966 the range of axial ratio was considerably larger than in 1968 and 1969. But the degree of polarization was systematically smaller in 1966 than in the other two years. Fokker (1971) explained this year to year difference in terms of the effects of Faraday rotation on 100 per cent polarized emission. His explanation requires radiation to suffer the total Faraday rotation of the order of  $10^5$  radians.

Since our value of the total Faraday rotation at 35 MHz is only of the order of  $10^3$  radians, it is doubtful whether Fokker's assumption of 100 per cent polarization at the source is justified.

## 2.8 PROBLEM WITH THE OBSERVATION OF ELLIPTICAL POLARIZATION

Fokker (1971) has pointed out that the existence of partially elliptically polarized radiation at the source does not necessarily mean that there should exist a single radiation mechanism that produces elliptically polarized radiation. A superposition of two fully polarized but mutually incoherent signals, one circularly polarized and the other linearly polarized, results in a partially elliptically polarized signal. The degree of polarization and the axial ratio of resulting ellipse depend upon the relative proportion of two incoherent components. Also such a superposition results in a polarization ellipse with the axial ratio that is related to the degree of polarization. However, it is necessary to correct for the depolarization due to Faraday dispersion within the receiver bandwidth before one can really test Fokker's suggestion regarding the representation of elliptically polarized radiation as a mixture of linear and circular polarization. Our analysis of 35 MHz polarization data does not favour Fokker's representation of elliptically polarized radiation.

## 2.9 STATEMENT OF THE PROBLEM

We have reviewed the present state of knowledge of type III bursts in Chapters I and II. We now propose to define the problems of current interest in polarization studies of type III solar radio bursts at decameter wavelengths. In particular, as mentioned in Section 1.5, there are good reasons to believe that the physics of the solar corona changes beyond 2 solar radii from the center of the sun. They are: (1) the decametric continuum radiation degenerates into a massive number of bursts. That means conditions are favourable for the production and escape of super-thermal electrons ( $\sim 40$  KeV) into the interplanetary medium (Warwick 1965), and (2) a great variety of solar bursts, like stria bursts, are observed at decameter wavelengths (Ellis and McCulloch 1966, 1967; Ellis 1969, de la Noe and Boischot 1972). Very little was known about the polarization behaviour of decametric type III bursts when we initiated a systematic study of polarization characteristics of these bursts. In the first phase of this work, we made a series of observations at 25 MHz with a bandwidth of 20 KHz. Later we carried out measurements of polarization at two closely spaced frequencies, separated by 4 KHz near 35 MHz, each with a bandwidth of the order of 800 Hz.

Since it was rather difficult to understand the occurrence of linear polarization in the presence of large amount <sup>of</sup> Faraday rotation suffered by type III burst radiation ( $\sim 10^5 - 10^7$  radians), we felt that this problem could be resolved by a direct determination of the total Faraday rotation along the entire propagation path. There are some direct measurements (Akabane and Cohen 1961, Kai 1963), but, to our knowledge none at decameter wavelengths. We have measured the total Faraday rotation suffered by type III burst radiation at 35 MHz by means of a two-bandwidth (7.5 and 12.5 KHz) time-sharing polarimeter. It is  $\sim 10^3$  radians.

Our observations indicate that the conditions for the occurrence of linearly polarized type III bursts are not all that unfavourable. But it is desirable to explain such a low value of the observed Faraday rotation  $\sim 10^3$  radians at 35 MHz because even if we disregard the sunspot magnetic field and take into account only the dipole field of 1 Gauss at the poles of the sun, we should have obtained a value of  $\sim 10^5$  radians. An analytical attempt has been made to see whether the mode coupling at regions of transverse magnetic fields can explain such a low value of the observed Faraday rotation. Further, we have suggested the possibility that type III burst radiation might be generated predominantly, in the second harmonic of the local



plasma frequency at the decameter wavelengths, which could qualitatively explain such a low observed value of the Faraday rotation ( $\sim 10^3$  radians).

## C H A P T E R - III

### EXPERIMENTAL SET UP; A TIME-SHARING TWO-BANDWIDTH RADIO POLARIMETER AT 35 MHz

#### 3.1 INTRODUCTION

#### 3.11 SPECIFICATION OF POLARIZATION IN TERMS OF STOKES PARAMETERS

The subject of Stokes polarization parameters and the instrumental techniques for their measurement has been reviewed by Cohen (1958a). Here, we propose to recapitulate briefly some aspects of polarization measurements. The four parameters that specify the state of polarization of a partially polarized radiation are the total intensity  $I$ , degree of polarization  $m$ , axial ratio  $r$ , and orientation angle of the polarization ellipse  $\chi$ ;  $r > 0$  means left-handed sense of polarization and  $r < 0$  means right-handed (Figure 3.1). In general, partially polarized radiation can be uniquely resolved into unpolarized part  $I_u$  and completely polarized part  $I_e$  (Chandrasekhar 1955). The Stokes Parameters are a set of four numbers  $I$ ,  $Q$ ,  $U$  and  $V$ ;  $I$  refers to the total intensity, and  $Q$ ,  $U$  and  $V$  specify the polarized part of the radiation. They all have dimensions of intensity and, therefore, have an advantage of being closely related to the antenna measurements. They are defined by the following relationships:

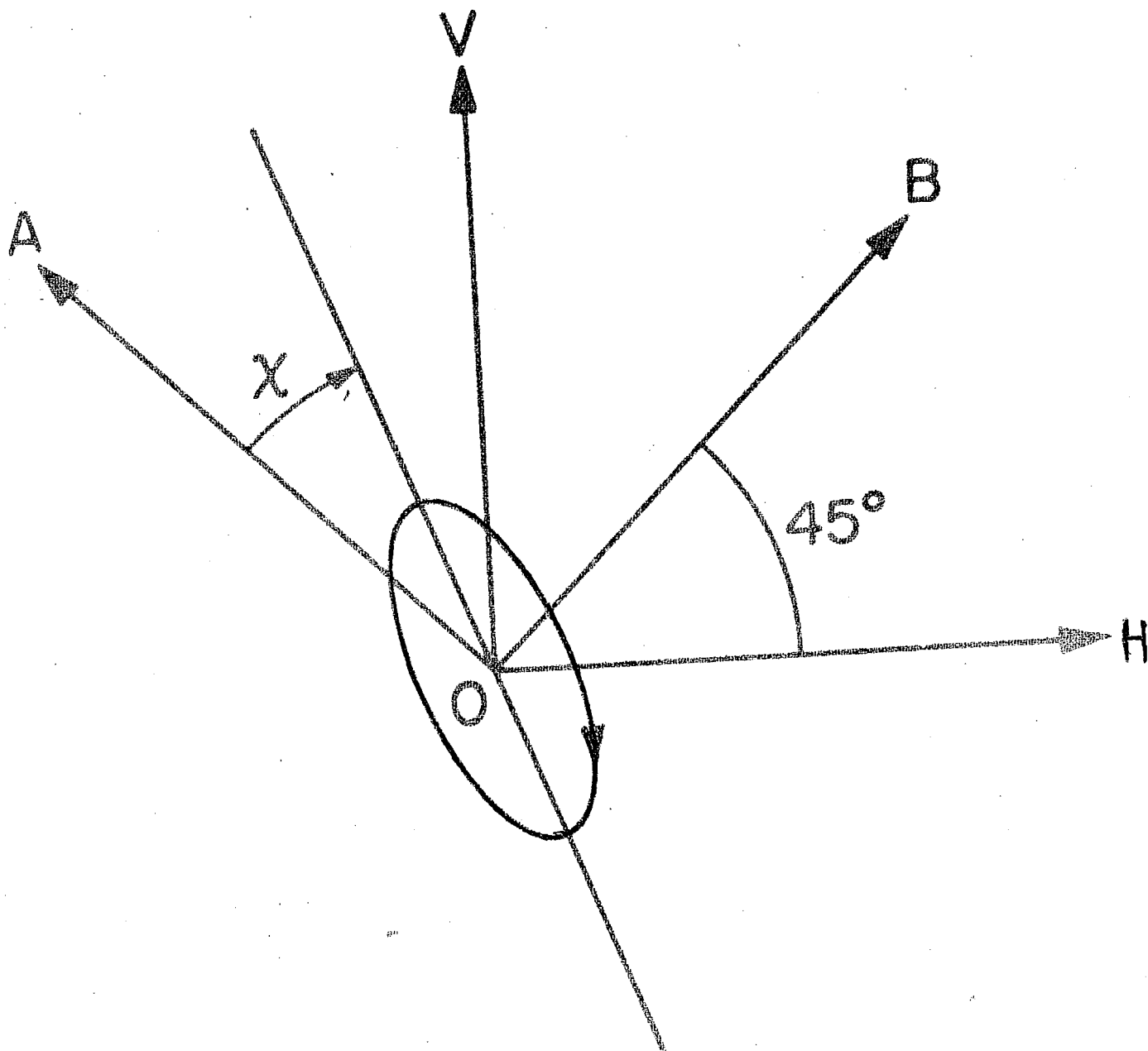


Figure 3.1 Coordinate system

$$I = I_e + I_u \quad \dots(1)$$

$$Q = I_e \cos 2\beta \cos 2\chi, \quad \dots(2)$$

$$U = I_e \cos 2\beta \sin 2\chi, \quad \dots(3)$$

$$\text{and } V = I_e \sin 2\beta. \quad \dots(4)$$

where

$$\beta = \tan^{-1} r. \quad \dots(5)$$

The quantities  $m$ ,  $r$ , and  $\chi$  are given by

$$m = \frac{I_e}{I} = (Q^2 + U^2 + V^2)^{1/2}/I, \quad \dots(6)$$

$$\sin 2\beta = V/I_e \quad \dots(7)$$

$$\text{and } \tan 2\chi = U/Q. \quad \dots(8)$$

The values of  $\chi$  depend upon the sign of  $U$  and  $Q$ .

Figure 3.2 shows how  $\chi$  can be measured from  $-90^\circ$  to  $+90^\circ$ . Some of the known techniques involve measurement of Stokes parameters in terms of quantities of different nature like intensity, cross-correlation product and phase angle between the two orthogonal components of radiation. With the progress in digital data processing techniques by computers, digital radio polarimeters have been developed first at Stanford (Bhonsle et al. 1967 and Chin et al. 1971), and later at Boulder (Dodge 1972). Such polarimeters have been used to study the high time and frequency resolution polarization characteristics of type III solar radio bursts. There would be a distinct advantage if all the Stokes parameters would be measured only in terms of

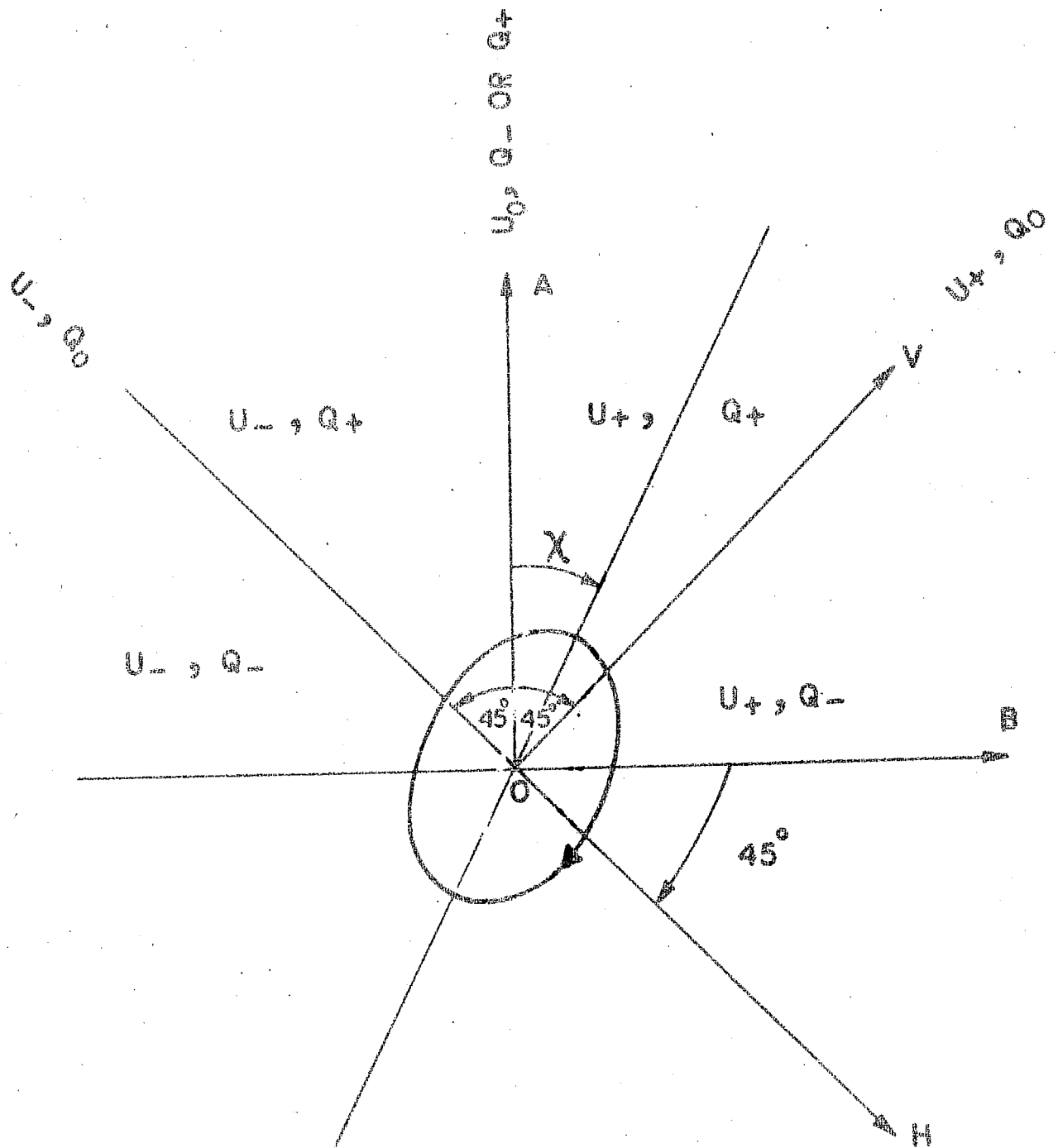


Figure 3.2 Dependence of the orientation angle  $\chi$  on the sign of  $U$  and  $Q$ .

$U_0, Q_0$  mean  $U, Q = 0$

$U_-, Q_-$  mean  $U, Q < 0$

$U_+, Q_+$  mean  $U, Q > 0$

intensities so that the same receiver can be shared for their measurements.

### 3.12 POLARIZATION WORK AT AHMEDABAD

The radio polarimeter set up at Ahmedabad has been designed to operate on the so-called "time-sharing principle". The principle of operation of this polarimeter will be described in detail in section 3.2 of this chapter. Important specifications of this polarimeter are given in Table 3.1. The polarimeter has undergone a development in three distinct stages as mentioned below:

- Operation of the polarimeter (i) at 25 MHz with a bandwidth of  $\pm 10$  KHz from July, 1969 to June, 1970;
- (ii) near 35 MHz at two frequencies separated by 4 KHz with bandwidth of 800 Hz at each frequency, from January to March, 1972, and
- (iii) two bandwidth (7.5 and 12.5 KHz) polarimeter at 35 MHz from July, 1972 to this date.

### 3.2 PRINCIPLE OF OPERATION OF A TIME-SHARING POLARIMETER

In this section, we explain the principle of operation of a particular combination of a pair of cross-polarized linear antennas and the fast electronic-switching of the appropriate relative phase delays between them to simulate different polarizations. This fast-switching

TABLE 3.1

SPECIFICATIONS OF THE TWO-BANDWIDTH TIME-  
SHARING 35 MHz RADIO POLARIMETER

Antenna:

Cross-polarized Yagi

Cross talk : - 32 db

Gain :  $6 \pm 1$  db (expected)

Beam width :  $40^{\circ} \times 40^{\circ}$

R.F. pre amplifiers:

	<u>Channel A</u>	<u>Channel B</u>
Centre frequency	: 35 MHz	35 MHz
Gain (Maximum)	: 40 db	40 db
Bandwidth	: 1 MHz	1 MHz
Gain control (Manual)	: 12 db	12 db
Noise figure	: 2.7 db	2.5 db

Receiver:

Local oscillator frequency	: 45.7 MHz
Mixer	: balanced
Conversion gain	: 12 db
I.F.	: 10.7 MHz
I.F. gain	: 80 db
I.F. bandwidth	: 50 KHz
I.F. band pass filter	: 7.5 and 12.5 KHz
bandwidths	
Detector type	: Square-law

Loss in square law detector	:	3 db
Pen recorder time constant	:	1 sec.
D.C. amplifier gain	:	17 db
Integration loss	:	20 db.
Operational amplifiers		
gain	:	Unity
Audio amplifier gain	:	40 db
Audio amplifier bandwidth	:	50 KHz
Power combiner isolation	:	35 db
Two-way power divider isolation:		30 db
ON/OFF Ratio of modulator	:	48 db
ON/OFF ratio of time demodulator:		30 db



of antennas becomes absolutely necessary because solar burst durations can be very small. All the Stokes parameters which specify the burst radiation must be sampled in a time short compared to the growth-time of the burst.

In order to measure the Stokes parameters,  $I$ ,  $Q$ ,  $U$  and  $V$ , we use the following relationship (Chandrasekhar 1955).

$$I(\Psi, \epsilon) = \frac{1}{2} [I + Q \cos 2\Psi + (U \cos \epsilon - V \sin \epsilon) \sin 2\Psi] \quad \dots(9)$$

where  $\Psi$  is the angle between the plane of vibration and the  $V$  direction (Figure 3.1) and  $\epsilon$  is the relative phase delay introduced between the cross-polarized antennas. If

$\Psi = \pm 45^\circ$  then equation (9) simplifies to

$$I(\epsilon) = I + U \cos \epsilon - V \sin \epsilon \quad \dots(10)$$

$$\text{and } Q = I_A - I_B \text{ and } I = I_A + I_B \quad \dots(11)$$

where  $I_A$  and  $I_B$  are the orthogonal intensities of radiation.

We can obtain two linear polarizations in vertical and horizontal directions, and two circular polarizations with right and left handed sense, by putting relative phase delays; between signals induced in the antenna A and B, of  $0$ ,  $\pi$ ,  $+\pi/2$  and  $-\pi/2$ , respectively. If we denote the powers received with these connections by  $I_V$ ,  $I_H$ ,  $I_R$ , and  $I_L$ , we can write by (10),

$$I_V = I ( 0 ) = I + U \quad \dots(12)$$

$$I_H = I ( \pi ) = I - U \quad \dots(13)$$

$$I_R = I ( \pi/2 ) = I - V \quad \dots(14)$$

$$I_L = I ( -\pi/2 ) = I + V \quad \dots(15)$$

on combining equations (12) and (13) and (14) and (15) we get

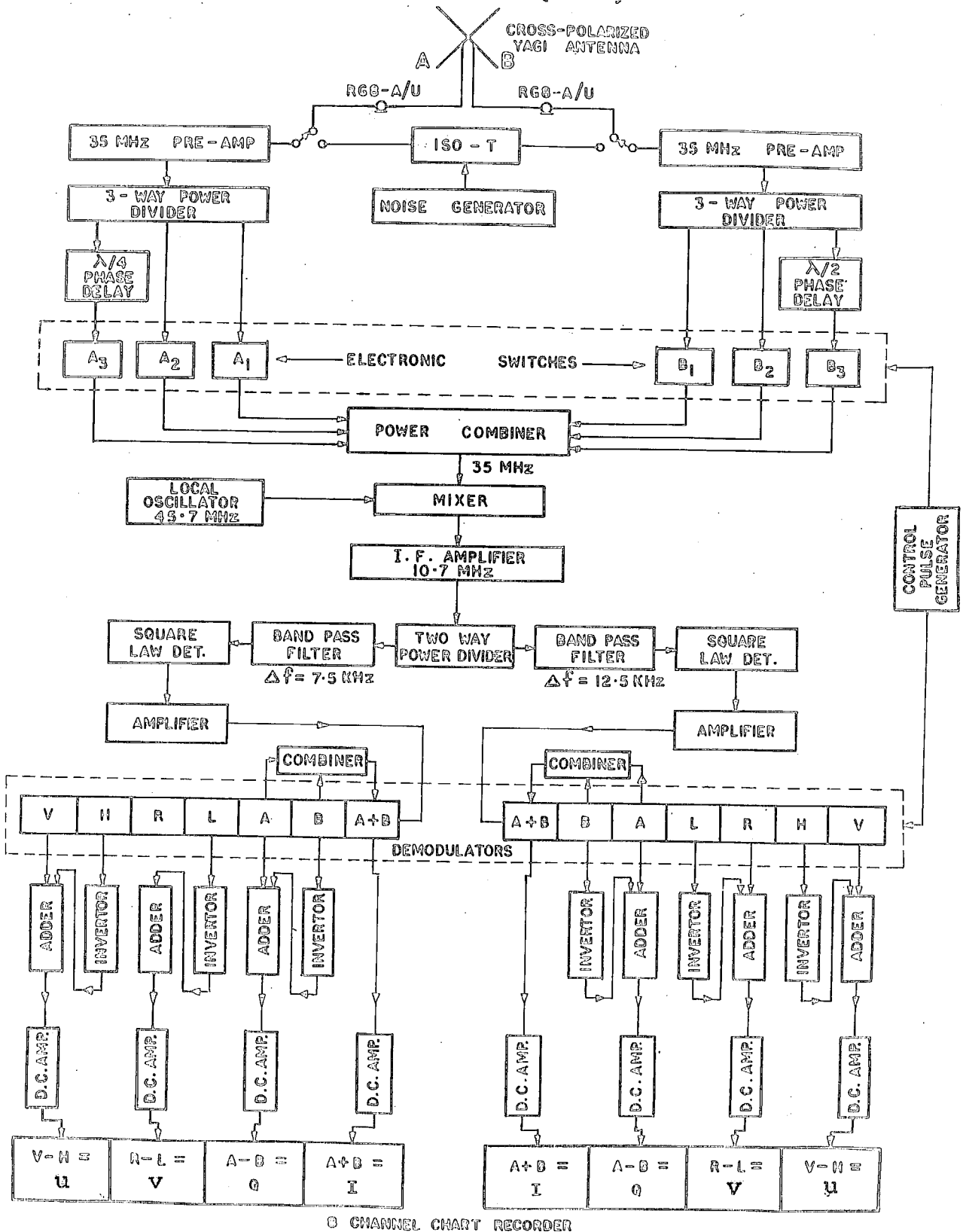
$$U = ( I_V - I_H )/2 \quad \dots(16)$$

$$V = ( I_L - I_R )/2 \quad \dots(17)$$

Thus, the Stokes parameters are obtained by adopting the above-mentioned procedure and the polarization degree, the axial ratio, and the direction of polarization ellipse can be calculated by making use of equations (5) to (8).

### 3.3 DESCRIPTION OF A TWO-BANDWIDTH POLARIMETER AT 35 MHz

A functional diagram of a time-sharing two-bandwidth polarimeter at 35 MHz is given in Figure 3.3. A pair of equatorially mounted cross-polarized Yagi antennas is oriented at  $\pm 45^\circ$  angle with the North-South meridian at the local noon in the celestial sphere. The two antenna outputs at 35 MHz, after suitable amplification, are combined in sequence introducing appropriate relative phase delays to generate different polarizations as discussed in Section 3.2. The orthogonal intensities,  $I_A$  and  $I_B$ , of radiation are also measured separately. After the amplification of the signal in the I.F. amplifier the signal is



CHANNEL CHART RECORDER

I, Q, U, V → STOKES POLARIZATION PARAMETERS

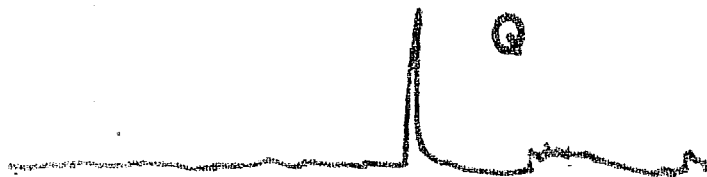
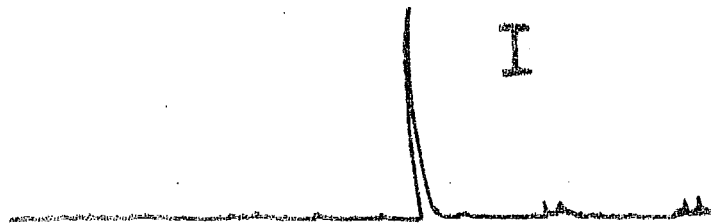
Figure 3.3 Block diagram of Two bandwidth (7.5 and 12.5 KHz) polarimeter at 35 MHz.

divided into two channels by a power divider. The two I.F. signals are filtered separately by means of band-pass filters of 7.5 and 12.5 KHz. This enables us to make simultaneous measurement of the Stokes parameters in the two bandwidths. Thus, we have, after the square law detection, a sequence of six outputs namely,  $I_V$ ,  $I_H$ ,  $I_R$ ,  $I_L$ ,  $I_A$  and  $I_B$  for each bandwidth for every switching cycle. These intensities are time-demodulated into six separate channels by time-demodulators which are operated synchronously with the modulators. Finally, using operational amplifiers to perform additions and subtractions of various channels we record the Stokes parameters I, Q, U and V in each bandwidth on two 4-channel chart recorders, as shown in Figure 3.4. We present more details of the various sub-systems of the polarimeter in the following subsections.

### 3.31 ANTENNAS

A pair of cross-polarized Yagi antennas, each with a folded dipole, two directors and a reflector are equatorially mounted and mechanically driven to track the Sun. Each antenna has been adjusted for the feed point impedance of 50 ohms resistive. The receiver is connected to the antennas through two pieces of RG8/U cables of equal length. The antenna parameters are listed in Table 3.1. The measured cross-talk was - 32 db. The calculated half power beam width of each antenna was about  $40^\circ \times 40^\circ$  and a front to back

FREQ. = 35 MHz  
BANDWIDTH = 75 KHZ  
MAY 3, 1973



TYPE III BURST

0656.5                      0659.5  
U.T. (HOURS)

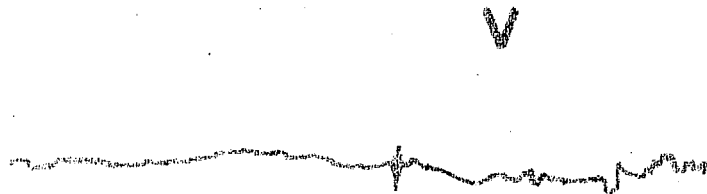
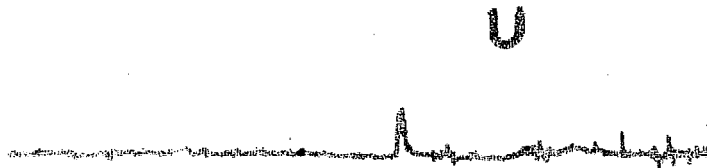


Figure 3.4 Recorded Stokes parameters I, Q, U and V of type III bursts at 35 MHz.

ratio of at least 22 db. The first side lobe was at an angle of  $80^{\circ}$  and at least 16 db down with respect to the main beam.

### 3.32 RECEIVER

#### 3.321 35 MHz PREAMPLIFIERS

The two antenna outputs at 35 MHz are amplified by a preamplifier in each channel. The circuit for a preamplifier shown in Figure 3.5 is a 5-stage amplifier, consisting of one stage of a low noise figure transistor (2N3571) followed by four stages of CIL 911. A noise figure of 2.5 db and a gain of 40 db have been achieved. The parameters for both the preamplifiers are listed in Table 3.1. The 3-db bandwidth of each preamplifier is about 1 MHz. The bandwidths of the preamplifiers are purposely kept little more than what is necessary so as to minimize the relative phase difference suffered by the signals after amplification. Further, phase shifters have been provided in each preamplifier to balance out any residual phase difference before the signal passes on to the modulators.

#### 3.322 3-WAY POWER DIVIDER, SWITCHING SCHEME AND MODULATOR

The outputs of each 35 MHz preamplifier are divided equally in four parts by means of two four way power dividers. Since we need only three outputs per

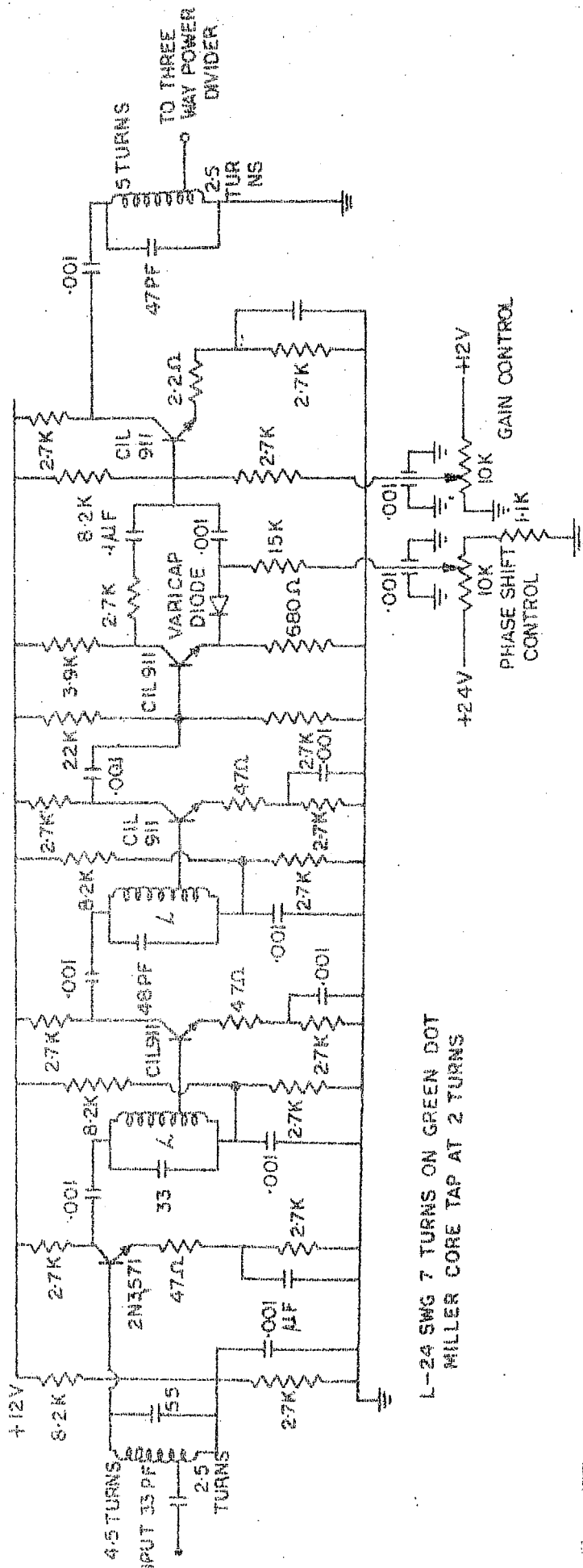


Figure 3.5 35 MHz preamplifier circuit

channel, one output port of each power divider is terminated with a 50 ohm resistor. Power dividers with isolation between any two output ports of better than - 30 db and phase equality of  $\pm 1^\circ$  were commercially available. The isolation among the output ports of the power dividers is important from the point of view of reducing the interaction among different electronic switches which introduce various phase delays by using appropriate lengths of coaxial cables.

An electronic switching system is incorporated to measure polarization parameters of rapidly varying phenomenon, such as bursts. It is assumed that polarization characteristics of the short duration bursts do not vary appreciably within the sampling period.

Figure 3.6 represents the time relationship between the modulators and demodulators in a given switching sequence that yields six pieces of information. They are controlled by common gate pulses each with duration of 4 milliseconds. In the first 4 milliseconds the modulators  $A_1$  and  $B_1$  and the demodulator V are "on". The voltages at 35 MHz obtained from two antennas are combined to give V component of the polarization at the output of the demodulator V. In the next 4 millisecond interval  $A_1$ ,  $B_3$  and H are "on", and the H component is measured, and so on. Thus a set of six pieces of information is



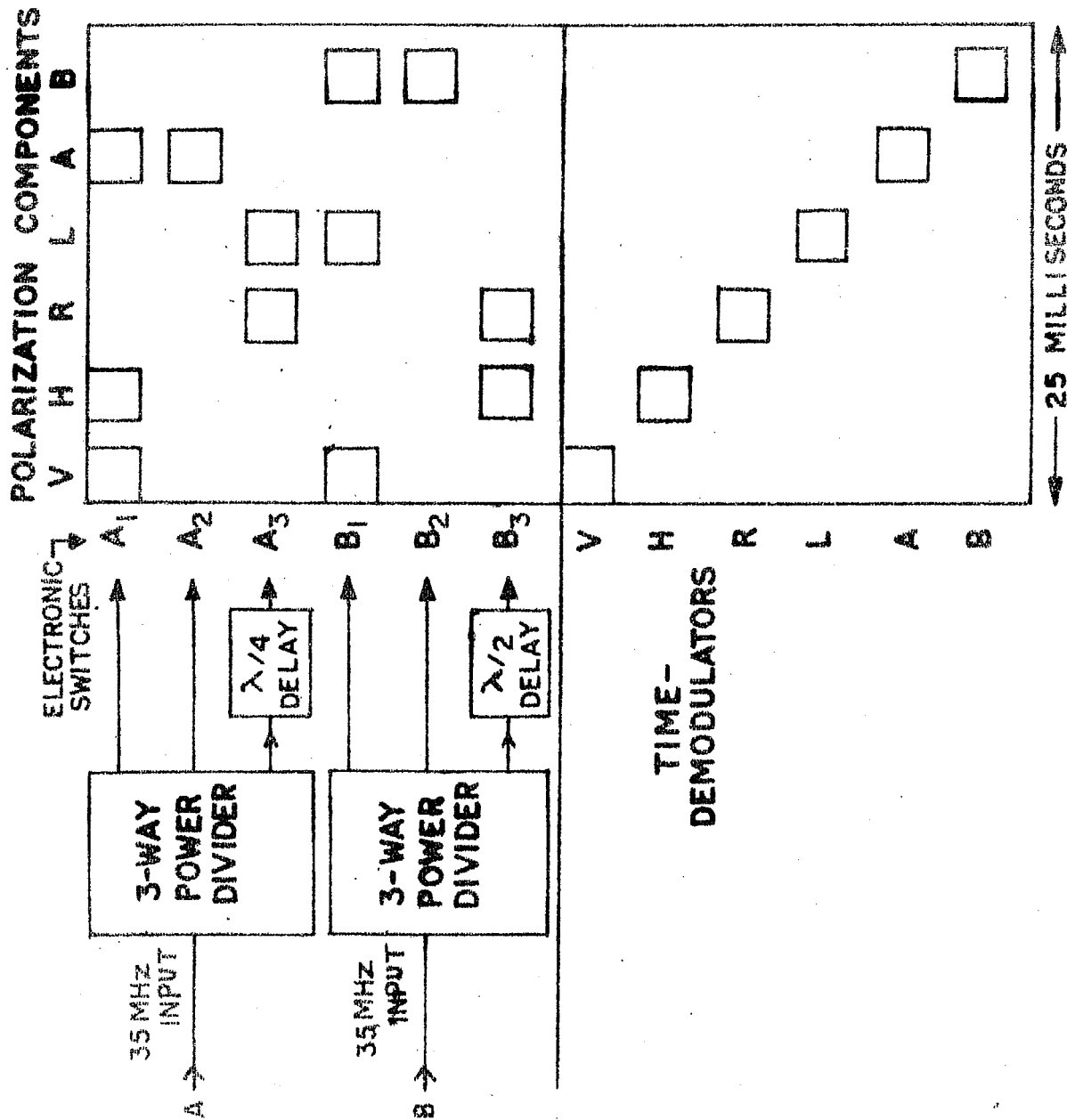


Figure 3.6 Switching sequence used in time-sharing radio polarimeter at 35 MHz at Ahmedabad.

picked up in about 24 milliseconds and the cycle repeats.

The circuit of the r.f. modulator used for introducing phase delays is shown in the Figure 3.7. It uses 1N34 diodes and serves as a solid state SPDT-type switch. This arrangement gives ON-OFF ratio of 46 db. The switches are followed by an amplifier stage to compensate for the insertion loss due to the modulators. The voltage gains of  $A_2$  and  $B_2$  are adjusted to  $(\sqrt{2} - 1)$  times that of the other four so as to equalize overall gains of all the six channels. Thus, the outputs of the six components are all equal when the incident radiation is randomly polarized. After the signal is detected by a square-law detector, the equations (12) to (17), representing relationships between the four Stokes parameters and six intensity measurements, become

$$I = I_A + I_B \quad \dots(18)$$

$$Q = I_A - I_B \quad \dots(19)$$

$$U = I_V - I_H \quad \dots(20)$$

$$V = I_L - I_R \quad \dots(21)$$

The modulator outputs are combined by a power combiner and fed to a mixer as a sequence of pulses at 35 MHz.

### 3.323 MIXER, LOCAL OSCILLATOR AND I.F. AMPLIFIER

Figure 3.8 shows how the 35 MHz output from the combiner is converted to 10.7 MHz intermediate frequency by means of a mixer. A Clapp-type local oscillator at

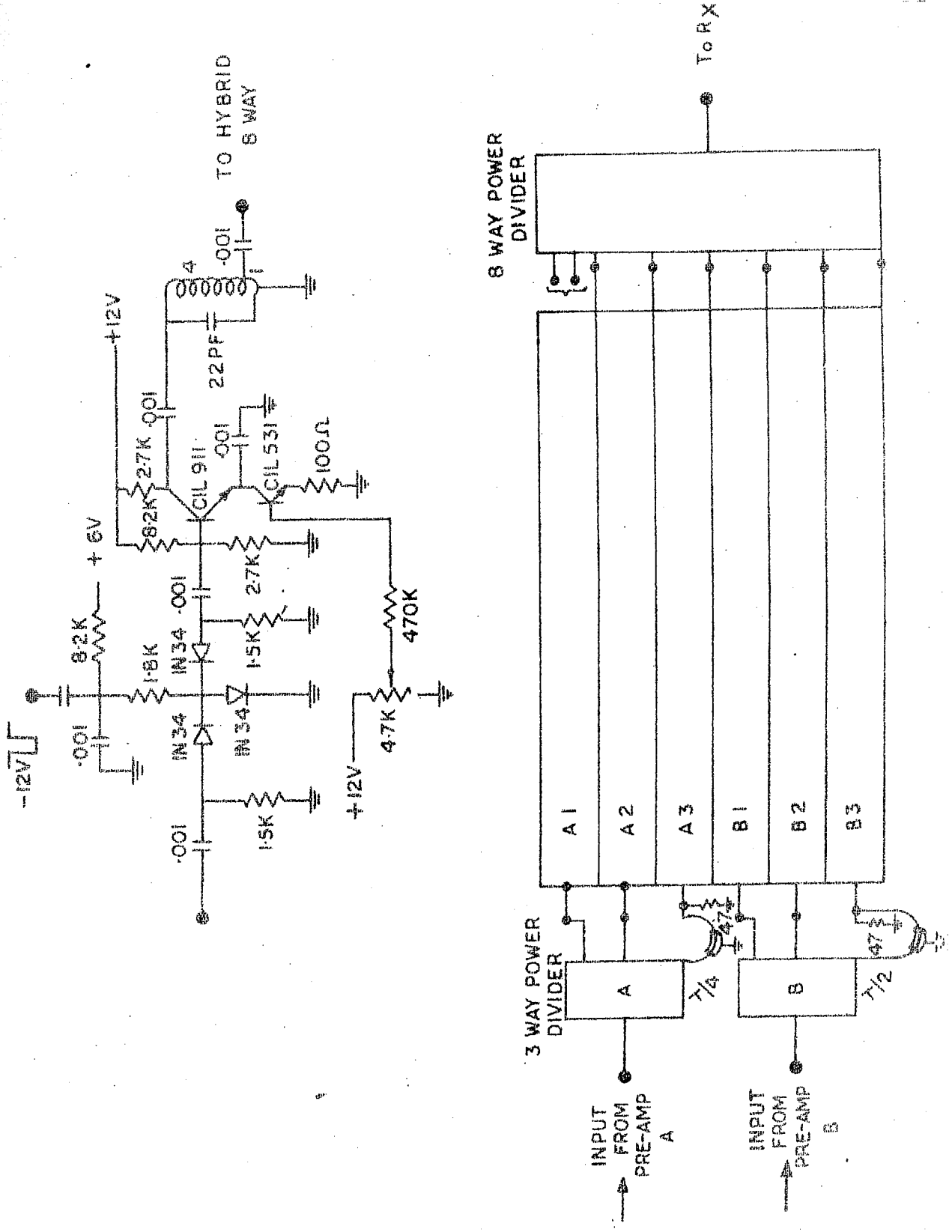


Figure 3.7 Modulator circuit

Figure 3.8 Circuit diagram of oscillator, mixer, I.F. amplifier, Hybrid power divider and square law detector.

45.7 MHz has been used to generate 10.7 MHz I.F. signal. For the sake of frequency stability, a buffer stage has been incorporated between the local oscillator and mixer.

### 3.324 HYBRID POWER DIVIDER AND BANDPASS FILTERS

Measurement of Stokes parameters in two bandwidths can be done by incorporating two band-pass filters of the desired bandwidths (7.5 and 12.5 KHz) at the two outputs of the two-way power divider which is fed by the signal coming from the I.F. amplifier. A lumped-circuit hybrid (Kurzok 1962) used as a two-way power divider is shown in Figure 3.8b. The lumped-circuit hybrid used in 35 MHz radio polarimeter was preferred to its distributed-circuit equivalent because of the intolerable lengths of transmission lines needed at 35 MHz, and also because the achieved isolation between the two outputs is greater. The isolation of the lumped-circuit hybrid used is frequency sensitive and is about - 30 db at 35 MHz. Since both the bandwidths used are very narrow the frequency sensitivity of the isolation did not pose a problem. Each coil was adjusted to resonate at 35 MHz and were laid out physically at right angles to prevent undesirable electro-magnetic coupling. The outputs are tapped from the output coils and fed to two crystal band-pass filters. Merimac PD-30-55 (Type 6347, MA) and PD-80-55 (Type 6347, MB) crystal band-pass filters and follow-up amplifiers yielded 3 db-bandwidths of 7.5 and

12.5 KHz respectively at 10.7 MHz central frequency. The frequency response as seen at the output of the square-law detectors for each channel is shown in Figure 3.9.

### 3.325 SQUARE-LAW DETECTORS

Since the Stokes parameters are measured in terms of intensity of the radio waves incident upon the antenna system, a detector with square-law characteristics is desirable in order to maintain a linear input/output relationship of the polarimeter. A solid-state low-output level square-law detector (Ohm and Snell 1963) shown in Figure 3.8b is a network of series and parallel 1N34A diodes. The overall square-law characteristics of the 35 MHz polarimeter (I-channel) is shown in Figure 3.10. It is seen that the output voltage is linearly proportional to the input power until the output at the square-law detector exceeds 8 m.v. So the quantum of post-detector gain required for satisfactory recording on chart is decided by the square-law characteristics of the detector. We operate the radio polarimeter at about 3 m.v. noise level at the output of the square-law detector.

### 3.326 TIME-DEMODULATORS

The outputs of the square-law detector are first amplified before they are time-demodulated. Two sets of time demodulators are used, one for 7.5 KHz bandwidth channel and the other 12.5 KHz channel. Two 2N995

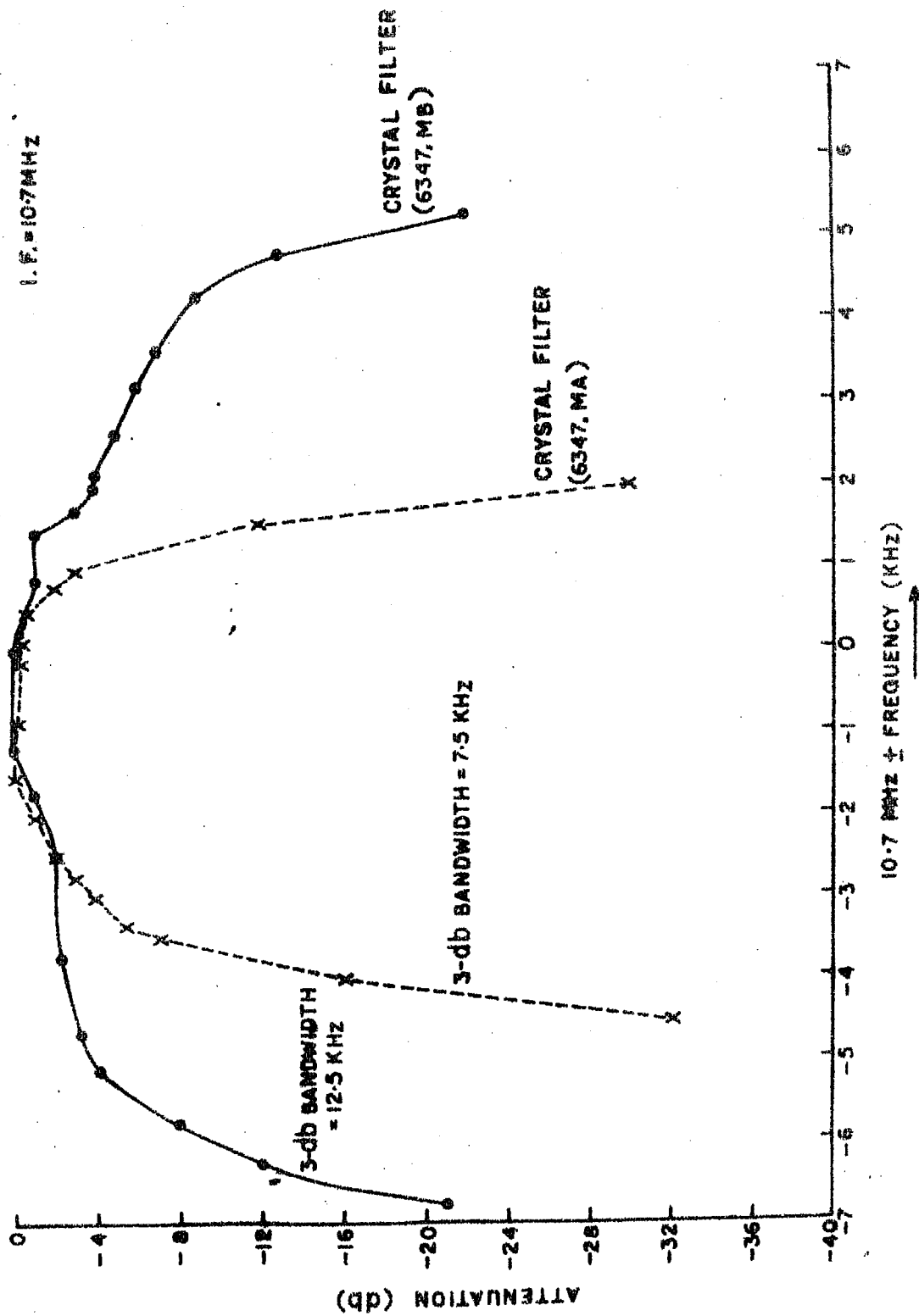


Figure 3.9 I.F. Bandpass characteristics of receiver.

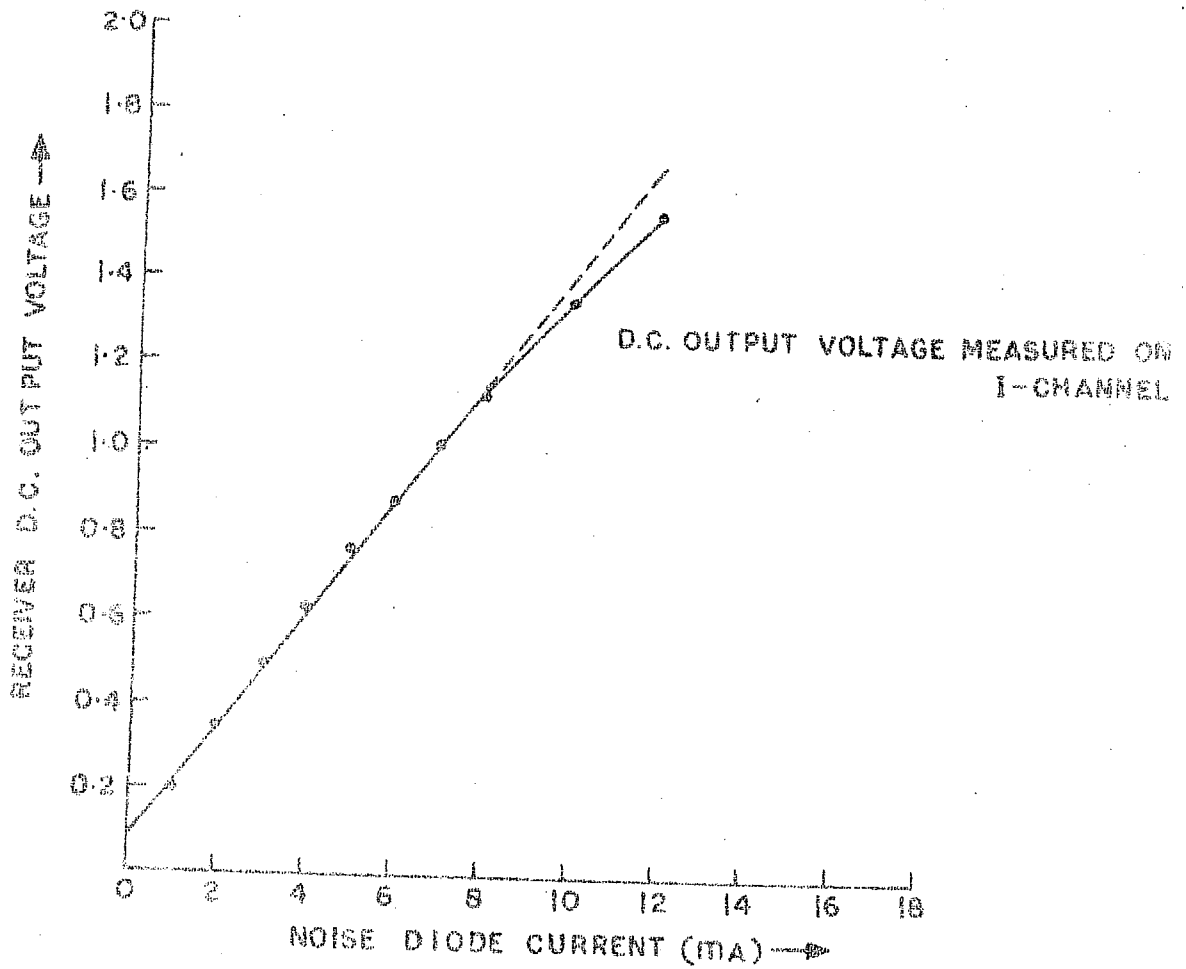


Figure 3.10 INPUT/OUTPUT response of 35 MHz receiver



transistors in an arrangement shown in Figure 3.11 are used to time-demodulate the signal. The synchronous pulses from the control pulse generator are fed inductively at the base of the transistors to operate the demodulators.

### 3.327 OPERATIONAL AMPLIFIERS

A direct-coupled amplifier, with a large open loop gain and bandwidth, used as an operational amplifier is shown in Figure 3.12. This consists of an emitter follower, two cascaded difference amplifiers which include a constant current generator and common feed back arrangement. The open loop gain was calculated to be about 2400. The frequency response with a resistive feed back was found to be reasonably flat upto 50 KHz. The measured drift per degree centigrade over a 15-minute period was about  $20 \mu\text{V}$  referred to the input. This is quite good for a direct-coupled amplifier without a chopper. The gain can be adjusted by the ratio of the value of the feed back resistor  $R_2$  to that of the input resistor  $R_1$ . The same circuit can be used as an integrator by using a resistor and a capacitor in parallel in the feed back loop. Analogue operations, involving additions and subtractions, to get  $A - B$ ,  $R - L$ , and  $V - H$  intensities are carried out by the operational amplifiers.

A d.c. amplifier, in which the gain is unity and negative, has been used as an inverter. This is achieved

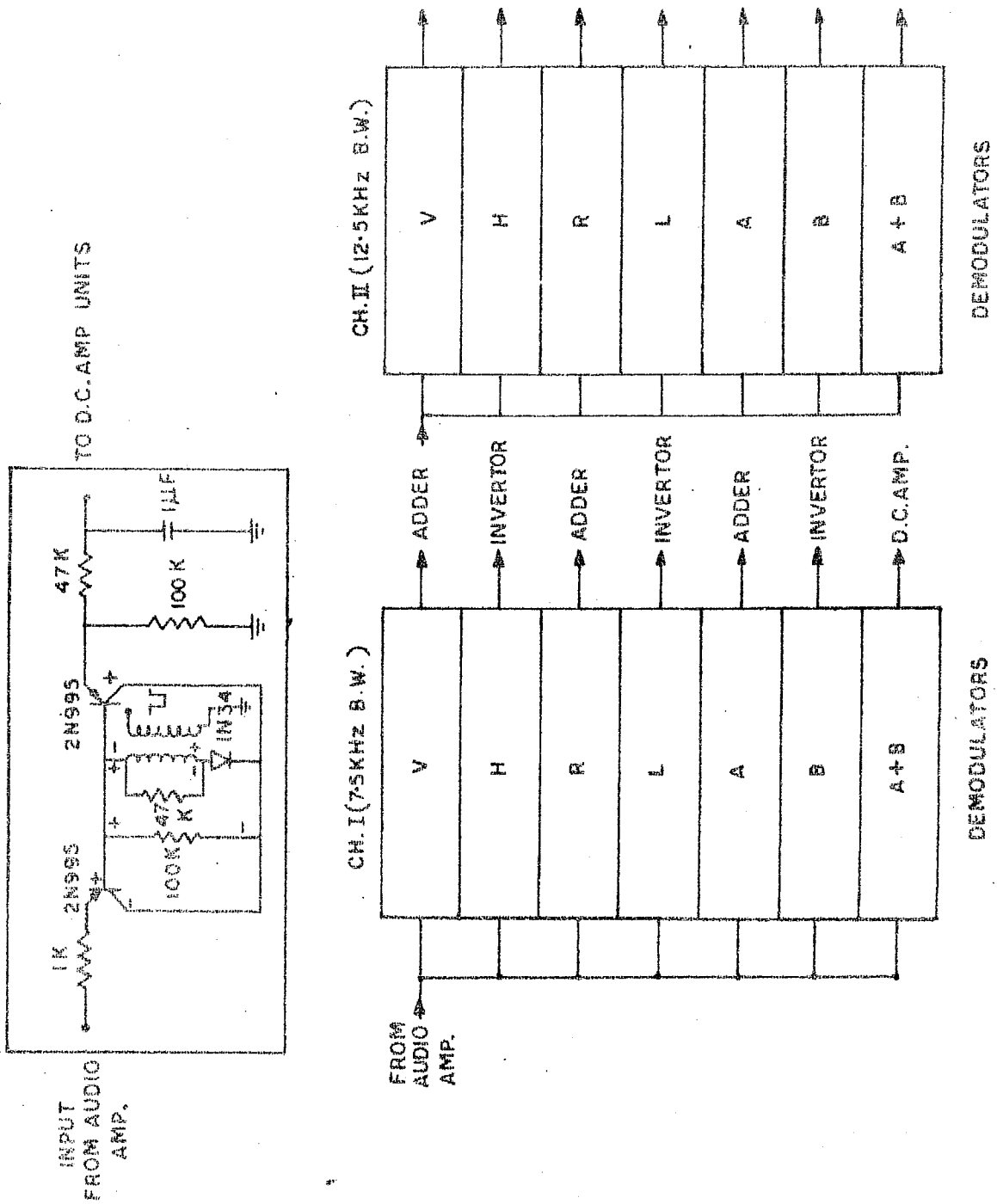
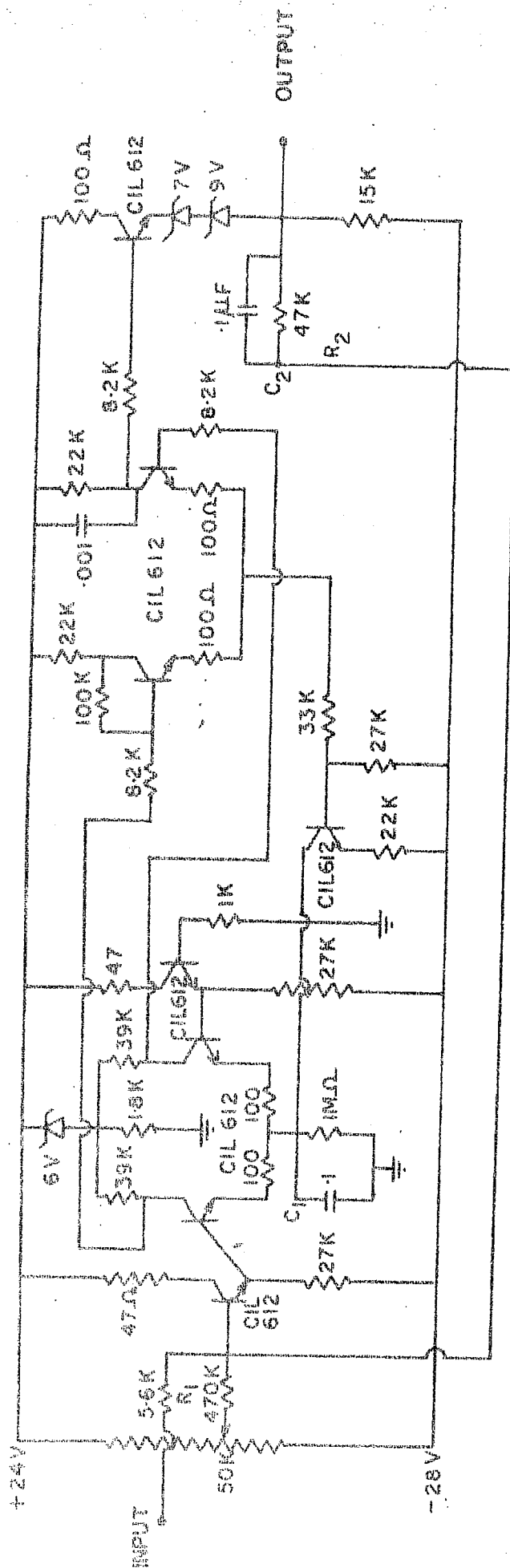


Figure 3.11 Demodulator circuit.



O. C. App.  $R_1 = 5.6 \text{ K.}$   $R_2 = 470 \text{ K.}$

FOR AUDIO AMP. COUPLE INPUT & OUTPUT THROUGH CAPACITOR

[illegible]

2  
Q  
H  
E  
T  
Q  
  
Q  
W  
Q  
Q  
Q  
  
Q  
Q  
L.

[illegible]

by making  $R_1 = R_2$ , where  $R_1$  and  $R_2$  are input and feedback resistors respectively. An arrangement, in which two inputs to a d.c. amplifier are fed through two resistors each equal to  $R_1$  such that the resistance in the feed back loop  $R_2 = R_1 + R_1$ , is used to obtain an output which is a linear combination of the two inputs. All these operations can be carried out with better than 1 per cent accuracy and are operated at unity gain.

The desired outputs, I, Q, U and V (see Figure 3.4) obtained from various time-demodulated signals, after going through the process of electronic analogue operations, are integrated with a time constant of 0.5 S before they are finally recorded on two 4-channel chart recorders, as shown in Figure 3.3.

### 3.328 CHART RECORDERS

Two 4-channel recorders mechanically coupled are used to record the four Stokes parameters in each bandwidth. On one chart recorder time marks at every minute are also recorded. The chart recorder speed is maintained at 60 cms an hour but can be increased when required.

### 3.33 CONTROL CIRCUITS

The modulators and demodulators in the polarimeter are controlled by a square wave generator which feeds them the same enabling pulse simultaneously so as to simulate

various polarizations and separate them into six channels as shown in Figure 3.6. Pulse generator, ring counter and OR gates involved in these operations are described in the following subsections.

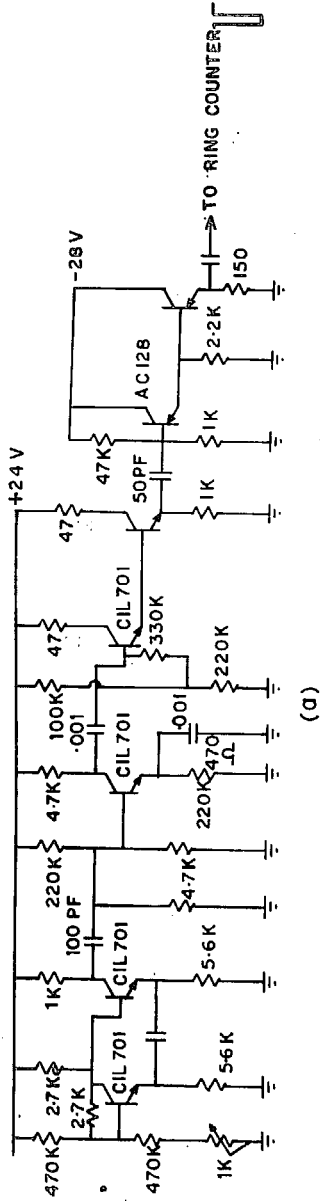
### 3.331 PULSE GENERATOR

A free-running emitter-coupled multivibrator has been used as a pulse generator, whose circuit diagram is given in the Figure 3.13. The frequency of the multivibrator is adjusted to 250 Hz. The output is taken from the collector of the second transistor. After differentiation and suitable amplification, the output of the multivibrator is fed to a Darlington pair before being clamped by a P-N-P transistor (AC 128) for getting a negative going pulse of -12 volts pulse height. A Darlington pair is used so that the clamping circuit does not load the free running multivibrator. The output from the pulse generator is taken through an emitter follower.

### 3.332 RING COUNTER

A chain of binaries in which the output of the first binary is coupled to the second and that of the second to the third, and so on, with the output of the last binary coupled back to the input of the first binary, is called a Ring Counter. In such a counter, each binary device receives its triggering signal directly from the source. This is done so that only one binary responds to the

# PULSE GENERATOR



# RING COUNTER

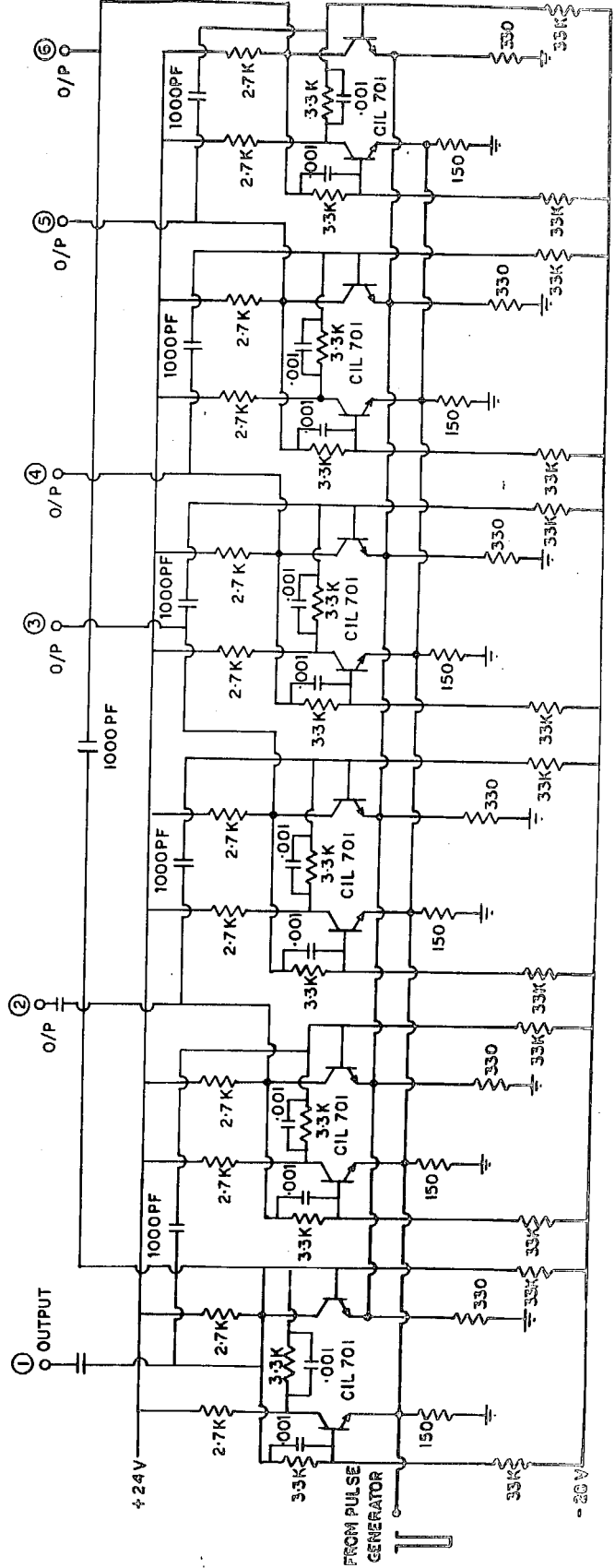


Figure 3.13 Circuit diagrams of pulse generator and ring counter.

triggering signal. With each successive triggering the response of the binary system shifts from one to the other. This way sequential gating waveforms are obtained. In the system adopted by us, six binaries are used as shown in Figure 3.13 to generate a sequence of six gating waveforms in a period of 25 milliseconds. The last gating waveform obtained from the last binary device also resets the first binary device to make the system ready for the next cycle. The six outputs shown in Figure 3.13 are followed by emitter-coupled monostable multivibrators, shown in Figure 3.14, in which the feed back has been provided through a common resistor. The d.c. voltage derived from a potentiometer controls the collector current which, in turn, controls the gate width of the wave forms. We have adjusted a pulse width of 2 milliseconds and a gap of 2 milliseconds is provided to avoid the cross-talk between different channels.

### 3.333 " OR " GATES

" OR " gates using 1N66 diodes are incorporated in the control pulse generator to generate sequential gate waveforms for the modulators and time-demodulators. Arrangement of OR gates to work out appropriate relationship between the modulators and time-demodulators is shown in Figure 3.14. The sequence of the gate waveforms in a period of 25 milliseconds, available for different

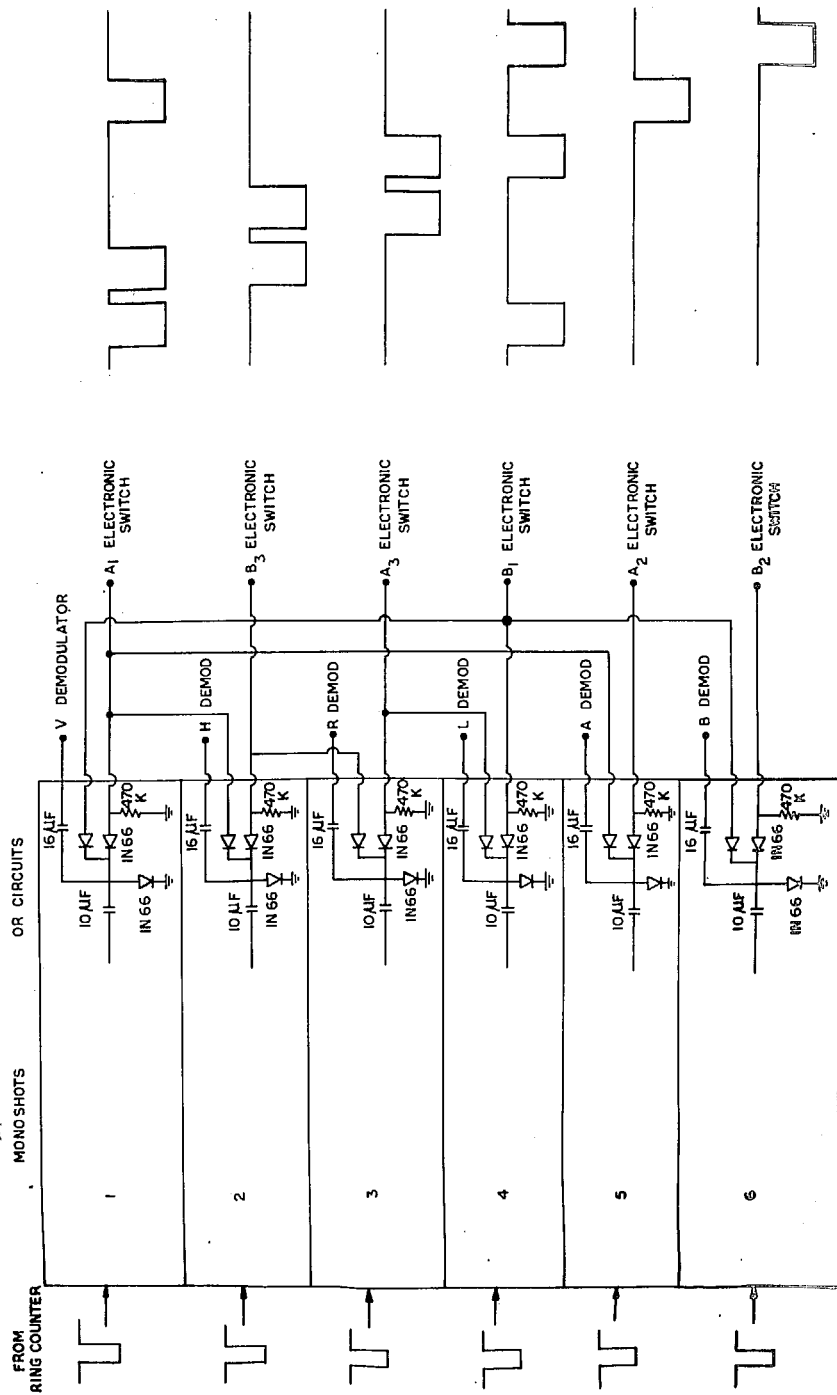
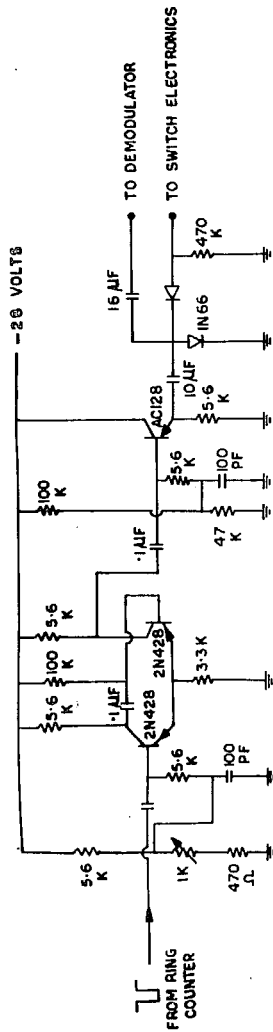


Figure 3.14 Circuit diagrams of monoshots and "OR" gates.



modulators, is also shown in Figure 3.14. The interaction between the different channels is low because of high reverse-to-forward resistance ratio of 1N66 diodes.

### 3.4 CALIBRATION PROCEDURE

#### 3.41 PHASE AND GAIN ADJUSTMENTS

The relative phase difference between the two orthogonal components of the incident radiation must remain unchanged at the outputs of the preamplifiers. The phase controls provided in the two preamplifiers were adjusted to equalize the intensities on the R and L channels when the two inputs of the polarimeter are fed from the two outputs of an ISOT connected to a diode noise generator. This arrangement simulates linear polarization in the vertical direction. The same test was repeated after feeding the noise through two equal lengths of co-axial cables which are used to connect the antenna feed points to the inputs of the polarimeter. Further, linear polarization was tested by radiating a c.w. signal at 35 MHz from a  $\lambda/8$  test dipole and orienting the Yagi antennas such that the antenna elements are oriented at an angle of  $\pm 45^\circ$  to the test dipole (Bhonsle and McNarry 1964a). This test was repeated by radiating a linear polarization from about 300 ft overhead the antenna with the help of a tethered balloon. Any phase inequality between the two channels can be measured by a R.F. vector voltmeter and adjusted

to  $\pm 1^\circ$  by the phase shifters. Also the bandwidth of both the preamplifiers is sufficiently wide so that the phase inequality between the two channels does not become a sensitive function of the frequency. The phase adjustment was done first and then the gains of the two preamplifiers were equalized. Two similar noise diode generators are available at the inputs of the two preamplifiers for gain calibration. To match the gains of the two preamplifiers, equal amounts of noise powers are fed to the inputs of the preamplifiers and the gain controls provided in each preamplifier are adjusted to produce equal outputs. The post detector gain of the 7.5 KHz bandwidth channel is greater than that of the 12.5 KHz channel by a factor of 1.6 (  $12.5 / 7.5$  ) so as to obtain equal deflections on both the channel.

### 3.42 DAILY CALIBRATIONS

The polarimeter recordings are calibrated daily against the output of two similar temperature-limited diode noise generators. Since we are directly measuring the Stokes parameters we simulate some typical polarizations to calibrate the four channels, that is, I, Q, U and V in the two bandwidths. By introducing different phase delays between the noise generators and the inputs of the radio polarimeter we simulate the conditions of completely unpolarized and 100 per cent linearly and circularly polarized

radiation. The phase adjustments are carried out once in a week.

### 3.5 POTENTIAL SOURCES OF ERROR

The five main sources of errors are: (1) the phase inequality impressed by the instrument between the two orthogonal components of the radiation, (2) the antenna nonzero cross-talk, (3) the nonzero cross-talk as a result of the interaction between the various subsystems of the receiver, (4) the reflections from the local objects and the ground, and (5) the statistical nature. These sources of errors are discussed separately.

#### 3.51 ERROR DUE TO RELATIVE PHASE DIFFERENCE BETWEEN THE TWO ORTHOGONAL COMPONENTS

Errors resulting in the relative phase difference between the two channels can arise mainly because of possible non-resistive impedance of antennas and unequal phase shifts introduced by the two preamplifiers and the coaxial cables connecting the antenna feed points to the inputs of the polarimeter. We consider this error under the assumptions of complete isolation between the two antenna outputs and between the various subsystems of the receiver.

Let  $\Delta$  be the error in the relative phase difference between the two orthogonal components. Using relation (10) we obtain the expressions for  $I_V$ ,  $I_H$ ,  $I_R$  and  $I_L$  as

$$I_V = I + U \cos \Delta + V \sin \Delta \quad \dots(22)$$

$$I_H = I - U \cos \Delta \pm V \sin \Delta \quad \dots(23)$$

$$I_R = I + U \sin \Delta - V \cos \Delta \quad \dots(24)$$

$$I_L = I \pm U \sin \Delta + V \cos \Delta \quad \dots(25)$$

Let the apparent Stokes parameters and other polarization parameters in the presence of  $\Delta (\neq 0)$  be represented by primes. From the equations (22) to (25) we obtain

$$U' = U \cos \Delta + V \sin \Delta \quad \dots(26)$$

$$V' = V \cos \Delta \pm U \sin \Delta \quad \dots(27)$$

The apparent values of  $I$  and  $Q$  are not in error because any error introduced in the relative phase difference between the two orthogonal components does not change the intensity of two orthogonal components thus

$$Q' = Q \quad \dots(28)$$

$$I' = I \quad \dots(29)$$

Equations (26) to (28) are used to compute apparent polarized component of the intensity  $I_e$ , as

$$I_e' = (Q'^2 + U'^2 + V'^2)^{1/2} = I_e \quad \dots(30)$$

$$\text{so } m' = m \quad \dots(31)$$

where in  $m'$  = degree of polarization when  $\Delta \neq 0$

As long as the antennas are oppositely polarized, the polarization degree is correctly found and this conclusion does not depend upon the magnitude of  $\Delta$ .

The apparent value of the axial ratio  $r'$  is calculated from the expressions (27) and (30). For  $\Delta \ll 1$

$$\begin{aligned} \sin 2\beta' &= V'/I_e \\ &= \frac{V \cos \Delta + U \sin \Delta}{I_e} \\ &= \sin 2\beta (1 - \Delta^2/2) + \cos 2\beta \sin 2\chi \dots (32) \end{aligned}$$

when the wave is not circular, that is  $r \neq 1$ , we have

$$\delta r \approx 1/2 (1+r^2) \sin 2\chi \dots (33)$$

and when the wave is circular ( $r=1$ )

$$\delta r \approx \Delta \dots (34)$$

For noncircular wave  $\delta r = 0$  for certain orientations. If  $\delta r$  has to be less than .01 then  $\Delta$  should in no case exceed .02 radians. The phase controls provided in the preamplifiers are adjusted to equalize the phase in the two channels so that this error is negligible.

### 3.52 NONZERO CROSSTALK

The crosstalk between the different subsystems of the receiver can be a major source of error. The crosstalk between the two preamplifiers, mainly through the power combiner, is better than -30 db. The crosstalk caused by the leakage at the modulators and demodulators is better than -46 db. The interaction between the two bandwidth channels through a two-way power divider is better than -30 db. Most of the antenna crosstalk is

because of the incidental nonorthogonality of the two crossed dipoles.

Let the crosstalk be a factor of  $k$ ; that is, when one volt is applied to terminal A of Figure 3.1,  $k$  volts appear at terminal B. The voltages induced on the two antennas can be written in terms of instantaneous voltages in the presence of the crosstalk as

$$\begin{aligned} E_1' &= E_1 \sin(\omega t) + k E_2 \sin(\omega t - \delta) \\ E_2' &= k E_1 \sin(\omega t) + E_2 \sin(\omega t - \delta) \end{aligned} \quad \dots(35)$$

Introducing a phase delay  $\zeta$  in the second component of the equation (35) we get

$$E_1' = a \sin(\omega t - \theta_1) \quad \dots(36)$$

$$E_2'(\zeta) = b \sin(\omega t - \theta_2 - \zeta) \quad \dots(37)$$

where

$$a \cos \theta_1 = E_1 + k E_2 \cos \delta$$

$$a \sin \theta_1 = k E_2 \sin \delta$$

$$b \cos \theta_2 = k E_1 + E_2 \cos \delta$$

$$\text{and } b \sin \theta_2 = E_2 \sin \delta$$

On combining the two voltages of equations (36) and (37) we get the apparent intensity  $I'(\zeta)$  after taking the mean of the expression obtained for the intensity of radiation for a period longer than the time period of the

wave. Thus

$$\begin{aligned} I'(\xi) &= a^2 + b^2 + 2ab \cos(\theta_2 - \theta_1 + \xi) \\ &= (1 + k^2) I + 2kU + [2kI + (1 + k^2)U] \\ &\quad \cos\xi - (1 - k^2)V \sin\xi \quad \dots(39) \end{aligned}$$

After going through the procedure of introducing different phase delays we obtain the apparent values of the Stokes parameter denoted by primes as

$$I' = I \quad \dots(40)$$

$$U' = 2kI + (1 + k^2)U \quad \dots(41)$$

$$V' = (1 - k^2)V \quad \dots(42)$$

$$Q' = (1 - k^2)Q \quad \dots(43)$$

These give

$$I_e'^2 = 4k^2 I^2 + 4k^2 U^2 + 4k(1 + k^2)IU + (1 - k^2)^2 I_e \quad \dots(44)$$

or in terms of polarization degree

$$m'^2 = 4k^2 + 4k^2 U^2 / I^2 + 4k(1 + k^2)U/I + (1 - k^2)^2 m \quad \dots(45)$$

or

$$\begin{aligned} m'^2 &= 4k^2 + 4k^2 m^2 \cos^2 2\beta \sin^2 2\chi + 4mk(1 + k^2) \cos 2\beta \\ &\quad \sin 2\beta + (1 - k^2)^2 m^2 \quad \dots(46) \end{aligned}$$

These equations can be interpreted by treating some special cases:

- (a) For completely unpolarized wave  $m = 0$ , equation (46) reduces to  $m' = 2k$  ... (47)

In case of the antennas used in the radio polarimeter the measured value of crosstalk between the antennas was better than -30 db ( $k=.03$ ) and this gives

$$m' = .06 \quad \dots(48)$$

Thus 6 per cent polarization will be read for an unpolarized wave, when the crosstalk is -30 db.

(b) For a completely polarized wave, that is,  $m = 1$ , assuming  $k \ll 1$ , equation (46) reduces to

$$m' - m = \Delta m = \frac{2k(1-r^2)}{(1+r^2)} \sin^2 \chi \quad \dots(49)$$

where  $\Delta m = m' - m$ .

For a circular wave and certain orientations

$$\Delta m = 0.$$

For  $r \ll 1$ , that is, a highly elliptically polarized radiation excluding certain orientations,  $\Delta m \ll .06$ . Thus, the maximum error introduced in the measurement of the polarization degree and crosstalk is less than 6 per cent for a polarized radiation and 6 per cent for an unpolarized radiation.

From equations (42) and (44) we obtain the expression for the apparent value of the axial ratio,  $r'$  as

$$\sin^2 \beta' = \left[ m(1-k^2) \sin^2 \beta \right] / \left[ 4k^2 + 4k^2 \cos^2 2\beta \sin^2 \chi + 4k(1+k^2) \cos 2\beta \sin^2 \chi + (1-k^2)m^2 \right]^{1/2} \quad \dots(50)$$



Again, some special cases are treated.

- a) For  $m = 0$ , that is, for a completely unpolarized wave, equation (50) reduces to  $r' = 0$ .

Therefore a completely unpolarized wave is read as 6 per cent linearly polarized radiation (Instrumental polarization). The apparent orientation angle dependent on the intensity of the incident radiation is  $(\tan^2 \chi' = 2kI)$ .

- b) For  $m \simeq 1$ , that is, a a completely polarized radiation, assuming  $k \ll 1$ , equation (50) reduces to  $\sin^2 \beta' = \sin^2 \beta / [1 + 4k \cos^2 \beta \sin^2 \chi]^{\frac{1}{2}}$  or

$$\delta r = |2kr \sin \chi| \quad \dots (51)$$

where  $\delta r = r' - r$ .

The error introduced in the measurement of the axial ratio depends upon orientations. For a nearly circular wave  $\delta r \simeq .06$ , and a for highly elliptical polarization,  $\delta r \simeq .001$ , and  $\delta r$  becomes zero for a linearly polarized radiation. So the antenna errors, either due to nonzero crosstalk or due to the relative phase difference between the two orthogonal components, may not exceed 6 per cent in the measurement of polarization degree and .06 in the axial ratio.

3.53     REFLECTIONS FROM LOCAL OBJECTS, ESPECIALLY  
THE GROUND

Errors due to reflections from local objects, especially the ground, can be quite serious with the antenna systems having a broad beam-width. Thus, this needs proper assessment in order to understand and correct, if necessary, for an undesirable effect due to ground reflection.

The ground can be treated as a semiconductor having a dielectric constant as well as conductivity. The electric properties of the ground depend upon the nature of the terrain and particularly its humidity and slightly on the frequency. The moisture content in the soil drastically changes the electrical properties of the ground. For instance, for wavelengths  $> 3$  m, the dielectric constant changes from a value of 30 (with respect to vacuum) for a humid soil to a value of 4 when the soil is very dry. Similarly, the soil conductivity may change by a factor of 10. When the soil is very humid, it becomes a very good conductor electrically ( $\sim 0.01$  mho/m, David and Voge 1969). This implies that the error due to ground reflections has a seasonal dependence. For longer wavelengths, the conduction current is predominant i.e. the ground can be treated as a good conductor.

For a perfectly plane conducting reflecting surface, the boundary conditions which decide the

characteristics of the reflected wave are simple, that is, the vertical polarization is reflected without any phase change, while the horizontal polarization is totally reflected but with a  $180^{\circ}$  phase change. In general, the phase change is dependent upon the dielectric constant and electrical conductivity. Thus the effective field with its characteristic polarization as seen by the antennas is the sum of the incident field and the reflected field. For specular reflection from the ground, there is always a phase path difference between the directly received incident radiation and the reflected radiation. This phase path difference is a function of the effective antenna height from the ground and the elevation angle of the source. The phenomenon becomes much more complicated if the reflecting surface exhibits irregularities. The specular reflection will disappear if the dimensions of the irregularities are large compared with the wavelength, giving rise to a series of elementary reflections, more or less random in all directions; in other words, to scattering. In addition, obstacles can prove to be nuisance as they may produce undesirable effects like phase changes, attenuation and diffraction.

From the above description it is amply clear that it is very difficult to calculate the exact contribution from the ground. One can do some theoretical iterative

computations and thus make some estimate of the errors (Dodge 1972). But then such estimates very rarely correspond to the real situation. What one can do is to minimize such errors by being very choosy about the site where antennas are to be installed and keep the back and side lobe responses facing the ground at the minimum possible level. We have taken due care in the selection of the site. Further, we restricted our observation period to 2-3 hours before and after the local noon so that the undesirable effects, due to nearby objects and large beam-width of the antennas, are minimized. Also the elevation angle of the sun can reach a minimum of  $54^{\circ}$  at the meridian transit at our station. This minimizes the errors due to a low elevation angle of the source. The measured front-to-back ratio of the antenna gain is  $\sim 20$  db. This implies that the reflected wave will be attenuated by  $\sim 20$  db when the antenna is looking at the zenith.

We estimated a limit on the error due to ground reflections by observing the flux from galactic background. Since the antenna beam-width is about  $40^{\circ} \times 40^{\circ}$ , the flux coming from the galactic background, which is an extended source, can be assumed to be randomly polarized. This extended source due to the galactic background encounters varying reflecting conditions at the ground. For recording the galactic background the system is to be operated at a

higher gain. It is seen that the error in the polarization degree and the axial ratio does not exceed 10%. The  $\chi$  - values were found to be randomly distributed. But it should be noted that the  $\chi$  - values of the radiation coming from a narrow source on the sun may not be randomly distributed by the ground reflection because the solar radiation from sources of angular dimension  $10'$  arc (core) at 35 MHz effectively reduces the antenna beam-width to the dimension of the radio sources as viewed from the earth (Dodge 1972). This implies that an antenna will receive the reflected radiation from a smaller reflection area and thereby experience a more uniform ground reflection. Thus, this may sometimes give rise to a clustering of the orientation angles (Chapters IV and V). However, we do not feel that this effect is operative because our two-frequency observations reveal that there is at least one large group of type III bursts which showed far lesser fluctuations in the orientation angles at one frequency than in the other and the ground effects, if operative, are essentially broad-band and thus would not selectively fluctuate position angles only at one frequency.

Further, we made an estimate of the errors due to ground reflection by radiating a linearly polarized radiation at a height of  $\sim 300$  ft. (by floating a tethered balloon) above the boom of the antenna system when the

antenna system was looking at the zenith. We could measure the error in the degree of polarization and axial ratio caused by the coupling due to reflection from the surrounding objects and the ground. It did not exceed the 10 per cent limit fixed by calculating the error in measurements using galactic background. Thus, we feel that the errors due to ground reflection can be serious but in our case it turns out that the total error is less than 10 per cent and, therefore, should not affect the conclusions reached in Chapters IV and V.

### 3.54 STATISTICAL ERRORS

Because of the depolarization considerations the I.F. bandwidth  $B$  is kept small. The integration time  $T$  does not exceed 1 S. The receiver output fluctuates because both the burst radiation and the receiver noise have statistical nature. The relative fluctuations in power are  $\sim (BT)^{-1/2}$ . With  $B = 7.5$  KHz and  $T = 1$  S, the relative fluctuations in power does not exceed 1 per cent. The error of this kind increases only if any attempt is made to measure the polarization parameters of the radio bursts with intensity smaller than receiver noise (Cohen 1958b). We did not make any attempt to analyze the bursts which have a low flux. So we consider these errors to be very small.

While scaling the data the errors can creep in, particularly in case of those bursts which have produced amplitudes less than 5 mm on the intensity channel. We have scaled our data at the peaks of the bursts and we have not analyzed those bursts which had caused amplitudes less than 5 mm.

## C H A P T E R - I V

### POLARIZATION MEASUREMENTS OF TYPE III BURSTS AT 25 AND 35 MHz AT AHMEDABAD

#### 4.1 INTRODUCTION

The present chapter describes polarization measurements of type III bursts observed at 25 and 35 MHz. The measurements of Faraday rotation at 35 MHz with the two-bandwidth (7.5 and 12.5 KHz) polarimeter (described in Chapter V) enabled us to correct the polarization parameters ( $m$  and  $r$ ) of type III bursts at 25 and 74 MHz which were recorded with bandwidths of 20 and 10 KHz respectively by the method suggested by Akabane and Cohen (1961). Polarization data at 74 MHz were those obtained by Bhonsle and McNarry (1964b) in Canada. Initially polarization measurements at 35 MHz were made in a bandwidth of 800 Hz only, and since it was found that the measured Faraday rotation was of the order of  $10^3$  radians only, we did not correct the narrow bandwidth (800 Hz) measurements of polarization parameters at 35 MHz for the Faraday rotation. To identify type III events recorded by the 25 MHz polarimeter, we made use of the film recordings of the radio spectroscop operating in the frequency range of 40 - 240 MHz at the Physical Research Laboratory, Ahmedabad. Further, some type III events, confirmed by the spectroscopes operating at the Weissenau Radio Astronomy Station, Astronomical Institute of Tübingen University, (West Germany) in the



frequency range of 30 - 1000 MHz and at the Culgoora Solar Observatory, Australia in the frequency range of 10 - 220 MHz, were recorded by our polarimeter. The actual number of type III groups of bursts recorded in the period from July, 1969 through June, 1970 was 35.

#### 4.2 TYPICAL POLARIMETER RECORDINGS OF TYPE III BURSTS

Direct recording of the Stokes parameters I, Q, U and V makes it possible to recognize, at least qualitatively, the type of polarization by inspection of the polarimeter recordings. Some typical radio polarimeter recordings made at 25 and 35 MHz with a post-detection time constant of 1S are shown in Figures 4.1a and 4.1b.

Figure 4.1a shows a complex group of type III bursts at 35 MHz which lasted for about 3 minutes. The degree of polarization varied from 10 to 30 per cent. The axial ratio was variable, that is, the ellipticity was varying from one burst to another. The sense of rotation was left-handed and is indicated by the sign of V, which, in this case, is positive.

Figure 4.1b shows a group of type III bursts having a duration of 2 minutes. In this case both the polarization degree and the axial ratio were variable. The axial ratio changed in sign as well as in magnitude. It may be noted that the axial ratio changed sign twice

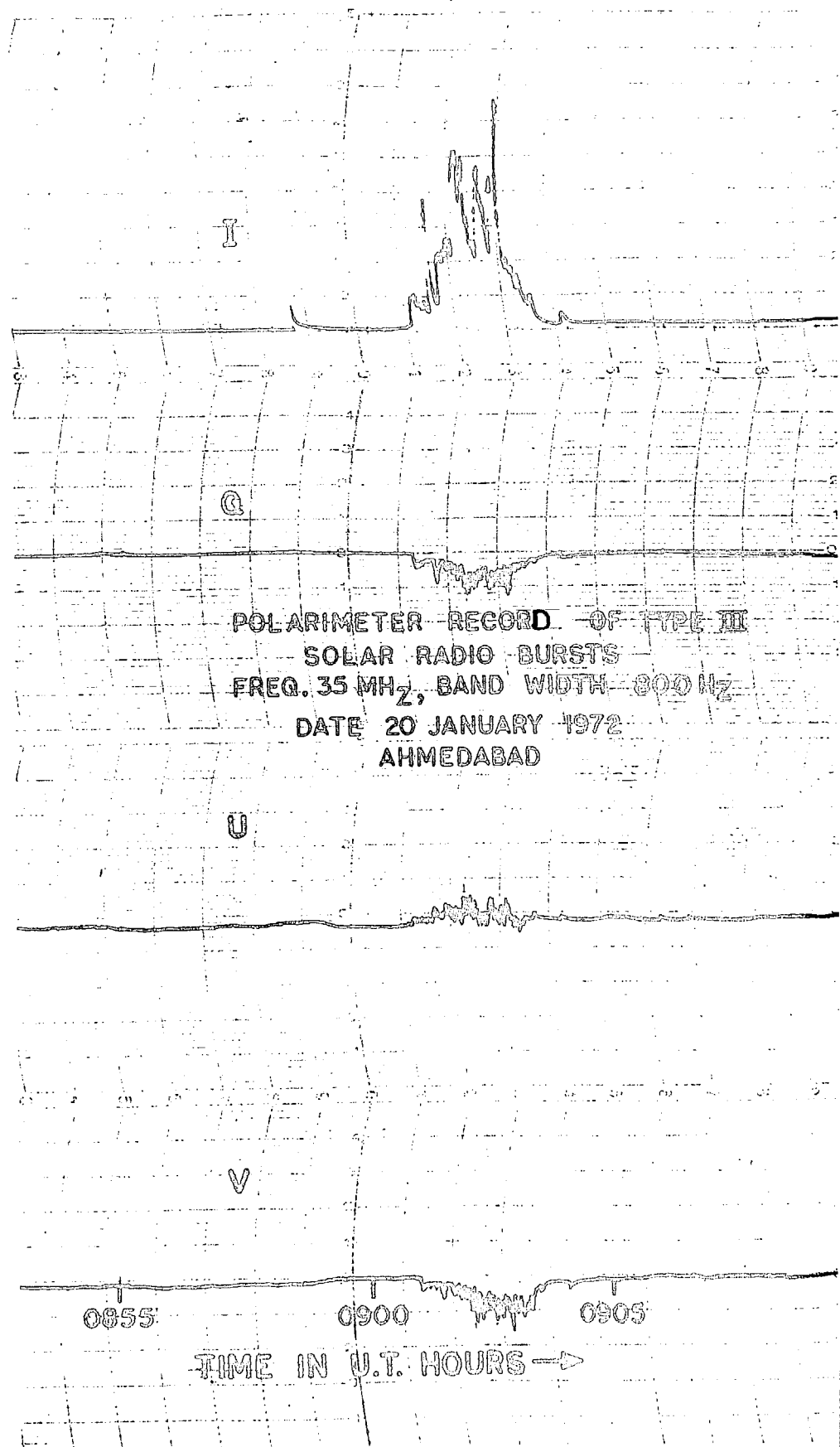


Figure 4.1a Narrow-band polarimeter record at 35 MHz.

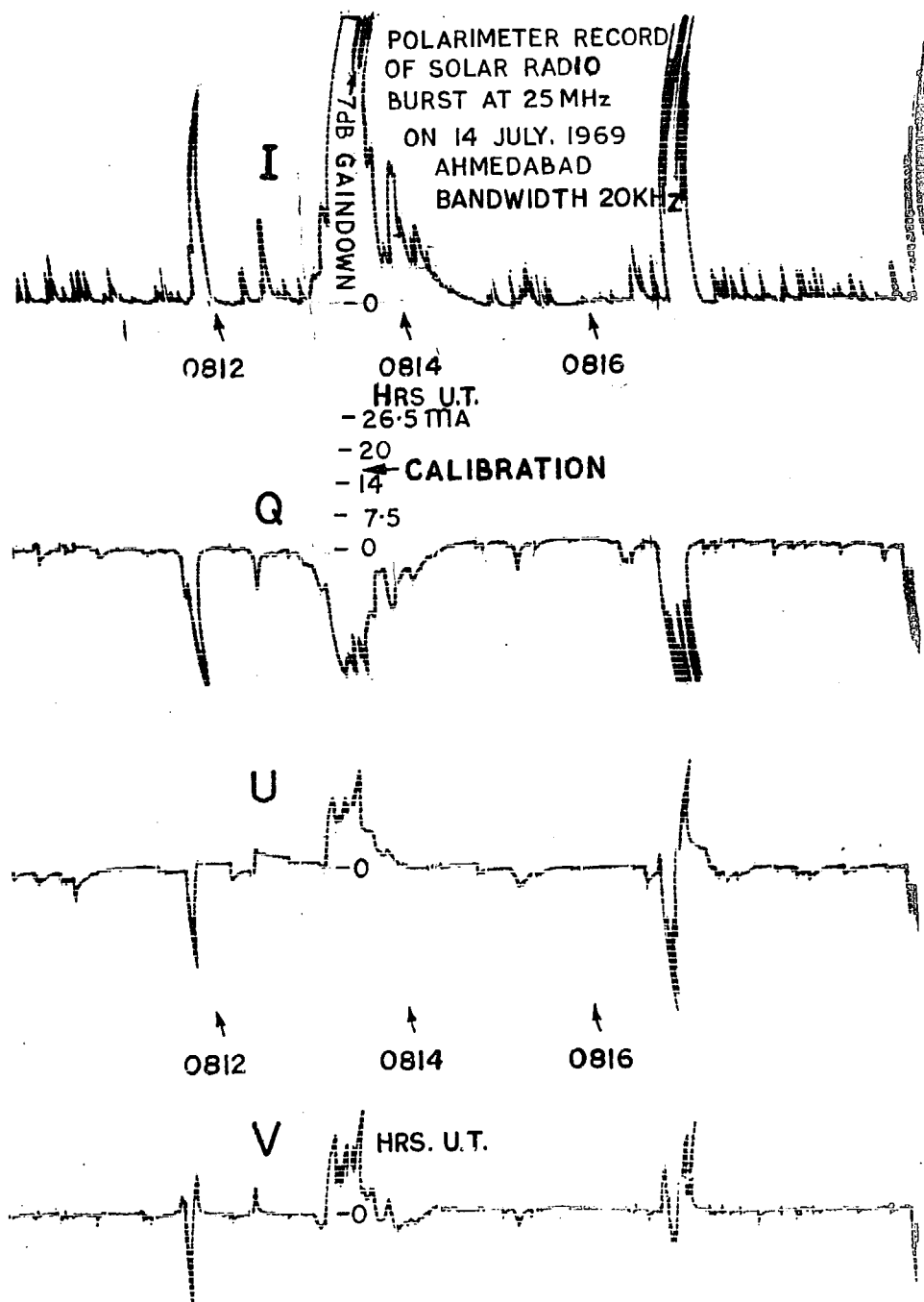


Figure 4.1b Polarimeter record at 25 MHz.

during the period of the burst activity, once at the beginning when the burst amplitude suddenly increased later when the burst activity subsided. We shall discuss this event later in more details.

#### 4.3 POLARIZATION MEASUREMENTS WITH SINGLE BANDWIDTH

We describe single bandwidth polarization measurements of type III bursts at 25 and 35 MHz in three parts as follows:

(1) The polarization parameters of type III bursts and their statistical distribution observed at 25 and 35 MHz are presented and compared with the polarization parameters of type III bursts measured at 200 MHz by Akabane and Cohen (1961) and at 25 MHz reported by Chin et al. (1971). For statistical comparison we have also included polarization data at 74 MHz which was recorded at the National Research Council (N.R.C.) of Canada in 1963 by Bhonsle and McNarry.

(2) Polarization characteristics of a group of spectral type III bursts at 25 MHz associated with the solar event recorded on July 14, 1969 at 0813 U.T. are discussed in detail, and possible interpretation given.

(3) From January through April, 1972 a radio polarimeter was operated to measure the Stokes parameters simultaneously at two frequencies, 4 KHz apart near 35 MHz. The polarization parameters and the intensity

of type III bursts at the two closely spaced frequencies (34.993 and 34.997 MHz) are compared and discussed.

#### 4.31 POLARIZATION PERCENTAGE m

Out of the observed 35 groups of type III bursts at 25 MHz which appeared in the period from July, 1969 through June, 1970, we have selected only 18 groups of bursts for analysis. The remaining 17 groups were quite weak in intensity. Similarly only 126 bursts were selected out of the observed 341 type III bursts at 74 MHz which occurred either singly or in groups during the observing period May to June, 1963.

Figures 4.2a and 4.3a represent the distribution of the percentage of polarization m at 25 MHz with a bandwidth of 20 KHz and at 74 MHz with a bandwidth of 10 KHz. Although the receiving bandwidth at 25 MHz was wider than the receiving bandwidth at 74 MHz, it can be seen from Figures 4.2a and 4.3a that there were only 5 bursts at 25 MHz which showed a polarization degree less than 10 per cent whereas at 74 MHz there were as many as 20 bursts, excluding completely unpolarized bursts, which showed polarization less than 10 per cent. The fact that at 25 MHz, there were very few bursts having a polarization degree less than 10 per cent, seems to be in good agreement with the observations of Chin et al. (1971) at 25 MHz with a bandwidth of 100Hz only. The latter

25 MHz ,  $\Delta f = \pm 10$  KHz

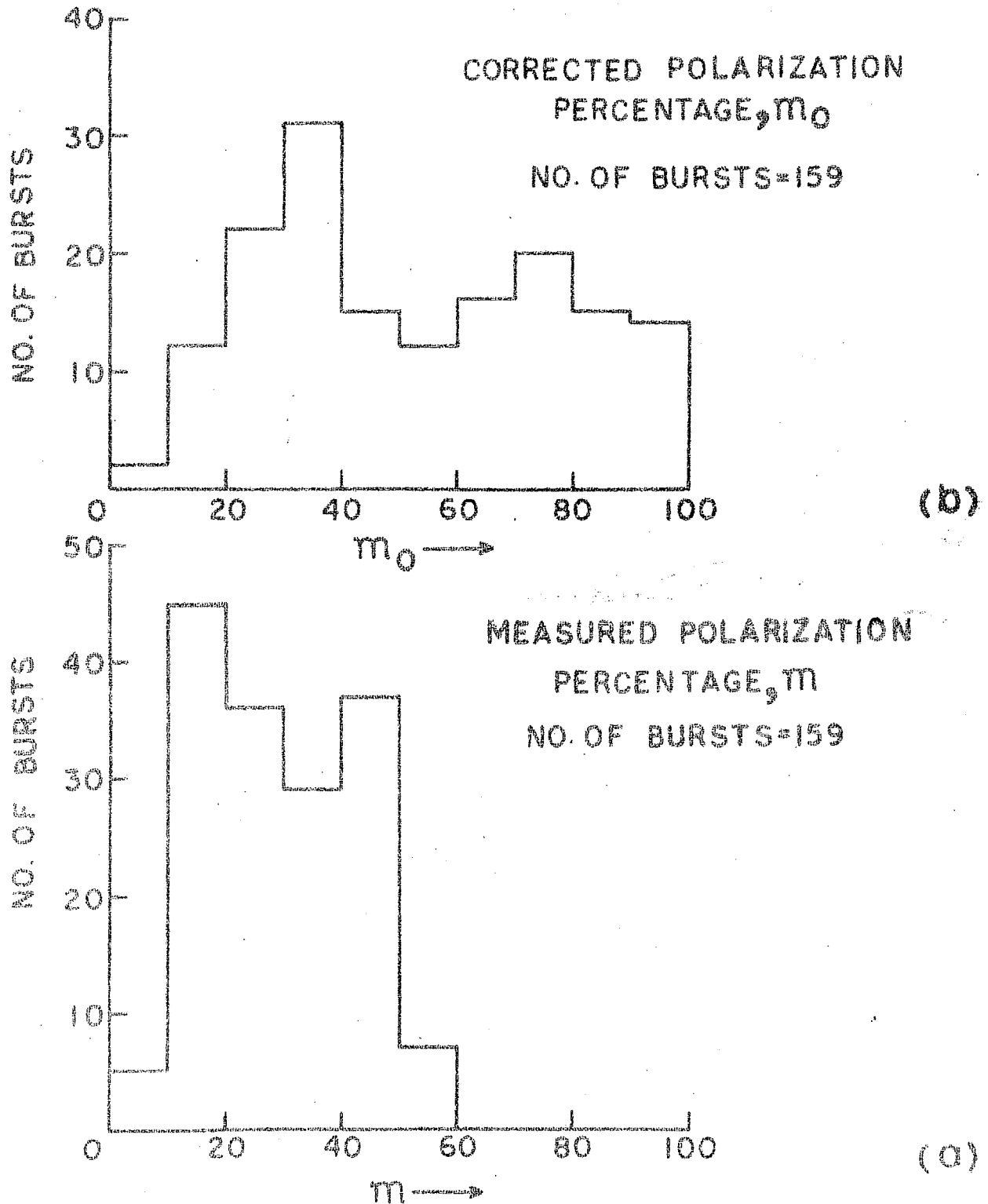


Figure 4.2 Polarization percentage at 25 MHz.

74 MHz ,  $\Delta f = \pm 5 \text{ KHz}$

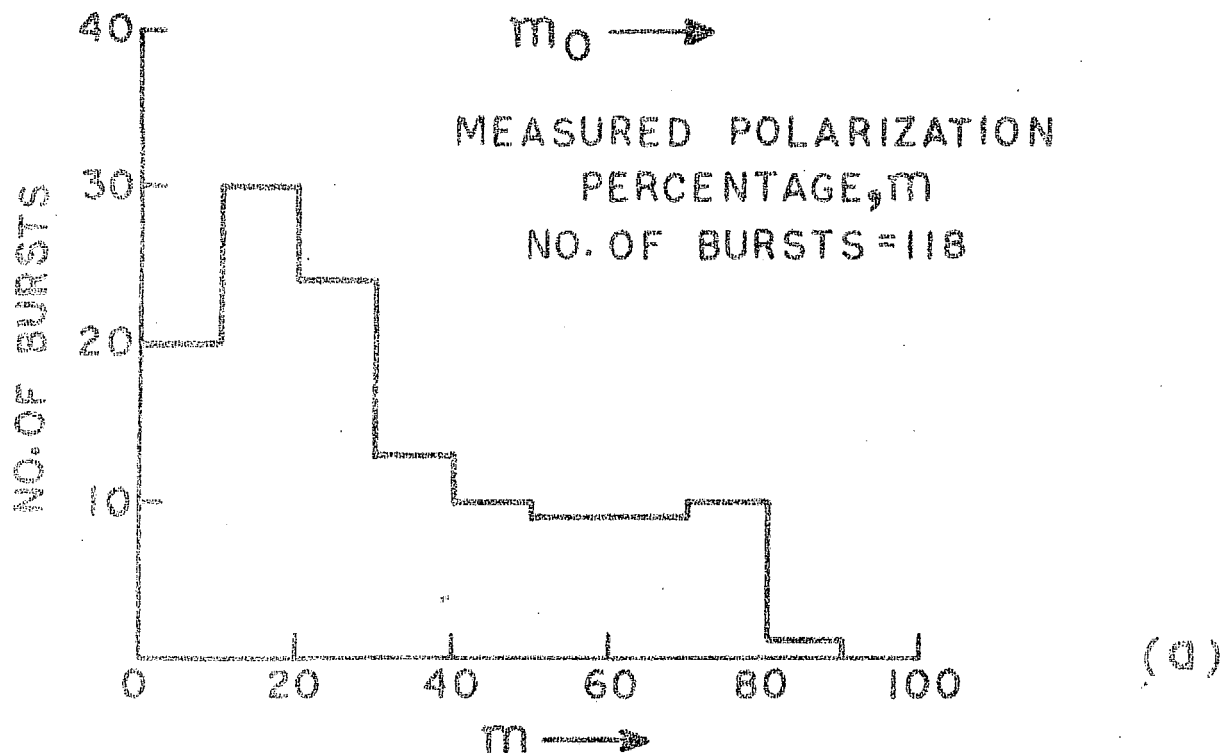
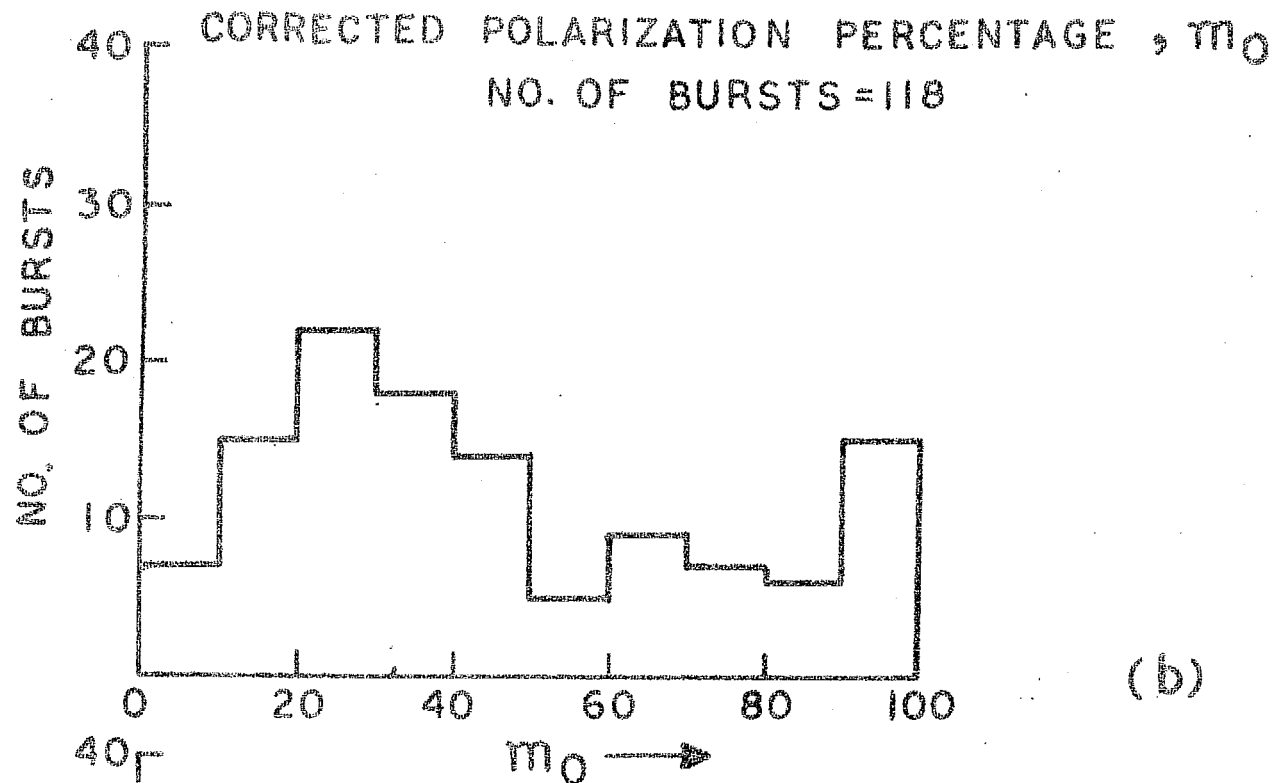


Figure 4.3 Polarization percentage at 74 MHz.

observations made in 1966 and 1969, did not contain a single burst observed with polarization degree less than 10 and 20 per cent respectively and in 1968 there was only one burst which had polarization degree less than 30 per cent.

There were as many as 82 bursts out of 159 bursts at 25 MHz and 64 bursts out of 126 bursts at 74 MHz which had polarization degree less than 30 per cent. In Table 4.1 the summary of polarization percentage observed at 25 and 35 MHz at Ahmedabad, at 74 MHz at N.R.C. Canada and at 25 MHz at the Stanford University, U.S.A. is given. The highest degree of polarization observed at 25 MHz (Ahmedabad) did not exceed 60 per cent whereas at 74 MHz it was as high as 85 per cent. It should be noted that at 25 MHz we have not recorded any unpolarized burst whereas at 74 MHz at N.R.C., there were as many as 44 completely unpolarized bursts of intensity greater than 5 times that of the galactic background and 10 of intensity greater than 20 times that of the galactic background. The average degree of polarization both at 25 and 74 MHz was 30 per cent. At 35 MHz with a bandwidth of 800 Hz only, the average degree of polarization was 54 per cent and the highest was 90 per cent.

From the analysis of the type III bursts observed at 35 MHz (reported in the Chapter V of this thesis) the



T A B L E - 4.1

## SUMMARY OF RESULTS OF POLARIZATION PERCENTAGE AND AXIAL RATIO OF TYPE III BURSTS

Place	Frequency in MHz	Bandwidth in KHz	Polarization percentage			Axial Ratio		
			Highest	Lowest	Average	Highest	Lowest	Average
A.R.O. Ottawa (1963)	74	10	85 97*	0 0*	30 45*	.78 .55*	.05 .0	.28 .19*
P.R.L. Ahmedabad (1969-1970)	25	20	57 95*	5 5*	29 52*	.68 .49*	0 0	.20 .12*
P.R.L. Ahmedabad (1972)	35	0.8	90	16	54	.76	0	.30
Stanford University 1966			60	15	30	.8	< .05	.3
1968	25	0.1	90	15	56	.2	< .05	.05
1969			90	25	60	.7	< .05	.10

\* Corrected for Faraday rotation.

\*\* Values for this station were derived from the histograms reported by Chin et al. (1971).

computed Faraday rotation is of the order of  $10^3$  radians. We assumed the same value of Faraday rotation at 25 MHz to correct for its effects on the polarization parameters, namely, the polarization percentage  $m$  and the axial ratio  $r$  of polarization ellipse of type III bursts recorded by our radio polarimeter at 25 MHz with a bandwidth of 20 KHz. For 74 MHz polarization data we computed an upper limit on the Faraday rotation by adopting the following procedure:

The correlation factor (between the right and left circularly polarized components of the radiation) and the polarization degree  $m$  (Akabane and Cohen 1961) are related by the following equation

$$\mu = \frac{m \cos 2\beta}{(1 - m^2 \sin^2 2\beta)^{1/2}} \quad \dots (1)$$

Knowing the value of  $m$  and the axial ratio  $r = \tan^{-1}\beta$  for each burst we have computed the corresponding value of the correlation factor  $\mu$ . Figure 4.4 shows the distribution of the correlation factor at 74 MHz. The number of bursts decreases as the correlation factor increases.

There were as many as 72 bursts out of 126 bursts which had a correlation factor less than 0.3. It should be noted that there were only 13 bursts which had a correlation factor less than 0.1. The correlation factor did not exceed 0.8.

74 MHz ,  $\Delta f = \pm 5 \text{ KHz}$   
NO. OF BURSTS = 126

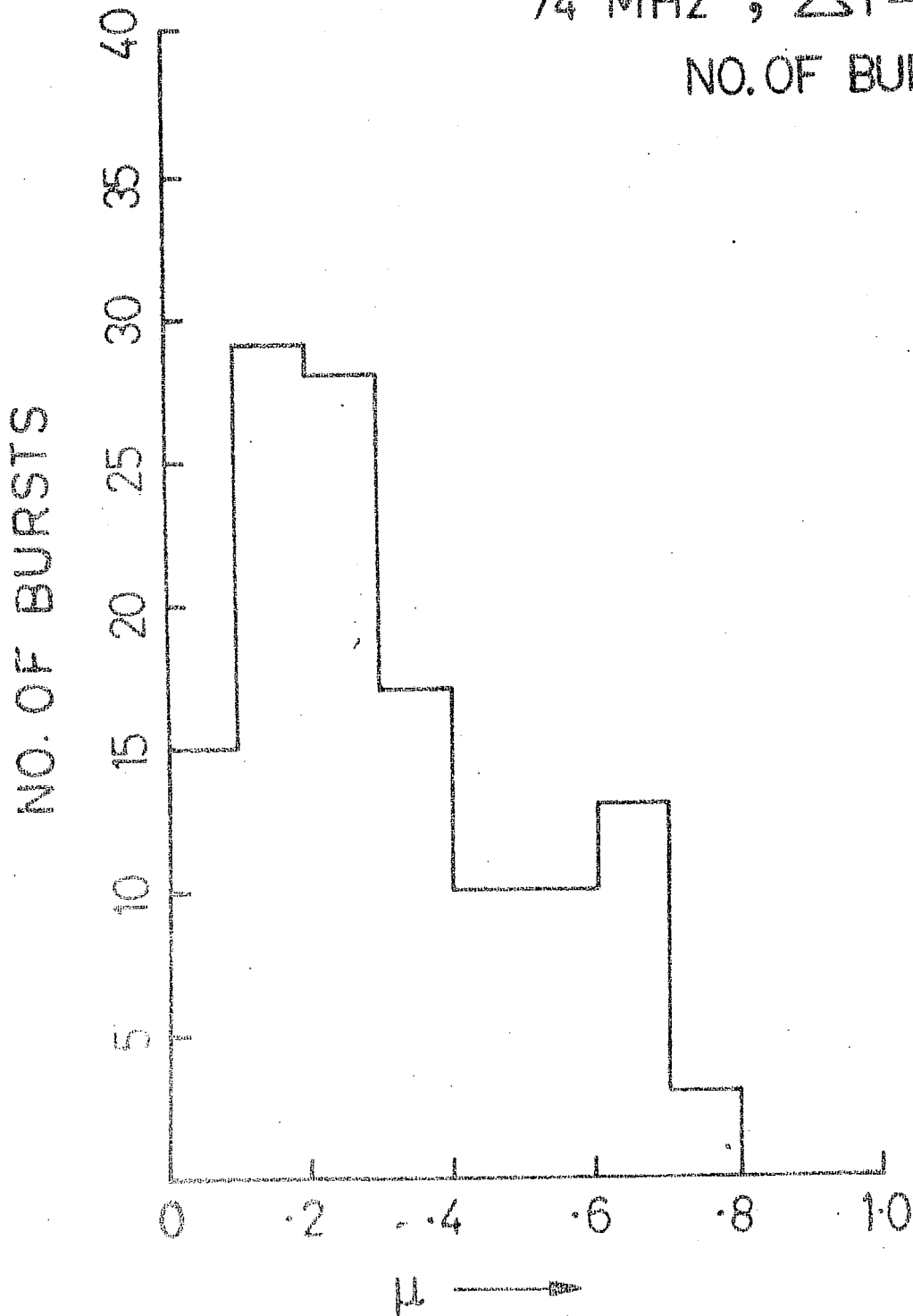


Figure 4.4 Computed correlation factor at 74 MHz

We assume that the solar corona is a magnetized plasma and that the radio wave propagates in the quasi-longitudinal mode of the magneto-ionic theory. The dispersion in polarization angles  $\theta$ , produced as a result of the spread in the orientation angle  $\chi$  which in turn is due to the Faraday rotation  $\Phi$  suffered by radiation coming from the solar corona, is given as

$$\theta = 2B \Phi / \nu \text{ radians} \quad \dots(2)$$

where  $\nu$  = frequency in Hz; B = bandwidth in Hz.

The dispersion in position angles depolarizes the wave and the simplest way to express this is in terms of the cross-correlation function between the two circular modes:

$$\mu = \mu_0 \exp(-\theta^2/4) \quad \dots(3)$$

where  $\mu_0$  is the correlation factor between the two circular modes at the source.

Under the assumptions mentioned above and the one that at the source  $\mu_0$  is unity, that is, the radiation emitted by the source region is hundred per cent polarized, we computed the upper limit on Faraday rotation at 74 MHz by using the equations (2) and (3).

It was found that 72 bursts at 74 MHz had the cross-correlation factor  $\mu$ , less than 0.3 and that the highest value was  $\approx 0.8$ . Using relation (3), we thus get  $\theta \leq 2.2$  radians for  $\mu = 0.3$  and  $\theta \leq 1.2$  radians for  $\mu = 0.7$ .

Making use of relation (2) and the computed value of  $\theta$ , we get an upper limit on Faraday rotation  $\Phi$  at 74 MHz as  $7.4 \times 10^3$  radians for  $\mu = 0.3$  and  $10^3$  radians for  $\mu = 0.7$ . This shows that the value of Faraday rotation may vary between  $10^3$  and  $7.4 \times 10^3$  radians. Thus, we find an excellent agreement between the upper limit on the total Faraday rotation at 74 MHz and the experimentally measured value of Faraday rotation at 35 MHz, which is of the order of  $10^3$  radians. Thus we have used a value of  $5 \times 10^3$  radians to correct the polarization parameters at 74 MHz. The upper limit on the Faraday rotation at 74 MHz is calculated only to justify the value ( $5 \times 10^3$  radians) of the Faraday rotation used for correcting the polarization parameters at 74 MHz.

Figures 4.2b and 4.3b represent the distribution of polarization percentage at 25 and 74 MHz respectively corrected for the effect of Faraday rotation. Assuming that the depolarization is caused due to the Faraday rotation suffered by the radiation while passing through the intervening magneto-ionic medium, that is, the solar corona and the earth's ionosphere, it is shown in Table 4.1 that the highest degree of polarization increases from 57 to 95 per cent at 25 MHz and 85 to 97 per cent at 74 MHz. This corrected average degree of polarization increases from 30 to 52 per cent at 25 MHz and at 74 MHz it increases from 30 to 45 per cent.

4.32 AXIAL RATIO  $r$

The histograms shown in Figures 4.5a and 4.6a relate to the distributions of axial ratio  $r$  at 25 and 74 MHz respectively. At 25 MHz the number of bursts decreases as the axial ratio increases. This does not seem to be the case with type III bursts observed at 74 MHz. At both the frequencies the range of axial ratio is quite large but in the case of 74 MHz the distribution seems to be more or less uniform between  $r = 0$  and  $r = 0.45$ . The spread in the distribution of axial ratio observed by Chin et al. (1971) at 25 MHz is explained by Fokker (1971) as a result of possible systematic difference in the amount of Faraday rotation from year to year within the receiver bandwidth. Considering the fact that the two histograms relate to two different periods, namely, 1963 (74 MHz) and 1969 - 1970 (25 MHz) and that Fokker's explanation needs Faraday rotation of the order of  $10^5$  radians, which may not be the case, we feel that the spread in axial ratio should be explained on different lines. If an assumption is made that the observed polarization properties of type III bursts are not associated with the mechanism of generation of the bursts but are imposed entirely due to the effects of propagation through the solar corona, then the axial ratio is dependent upon the angle that the magnetic field makes with the direction of

25 MHz ,  $\Delta f = \pm 10$  KHz

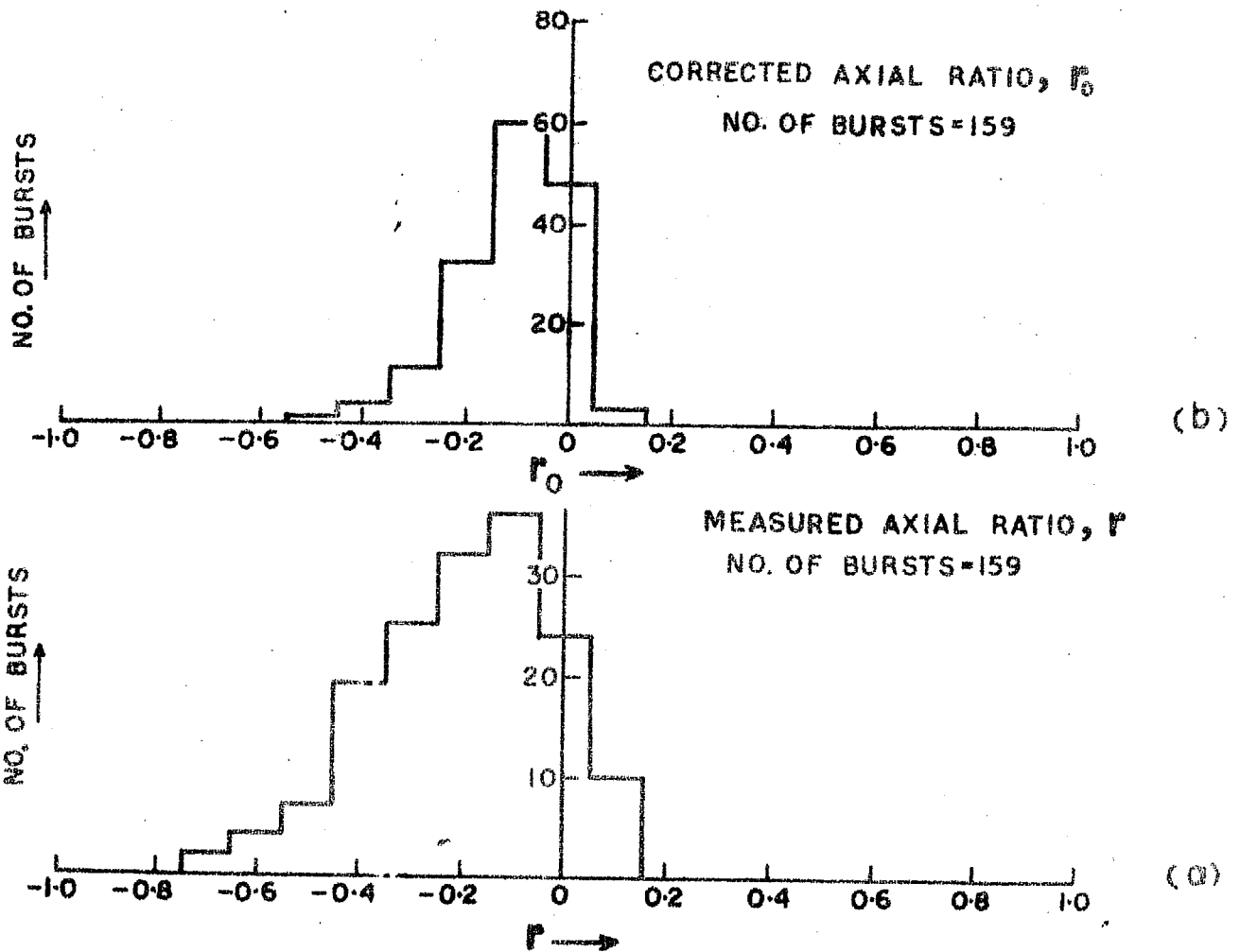


Figure 1.5 Axial ratio at 25 MHz.

74 MHz ,  $\Delta f = \pm 5 \text{ KHz}$

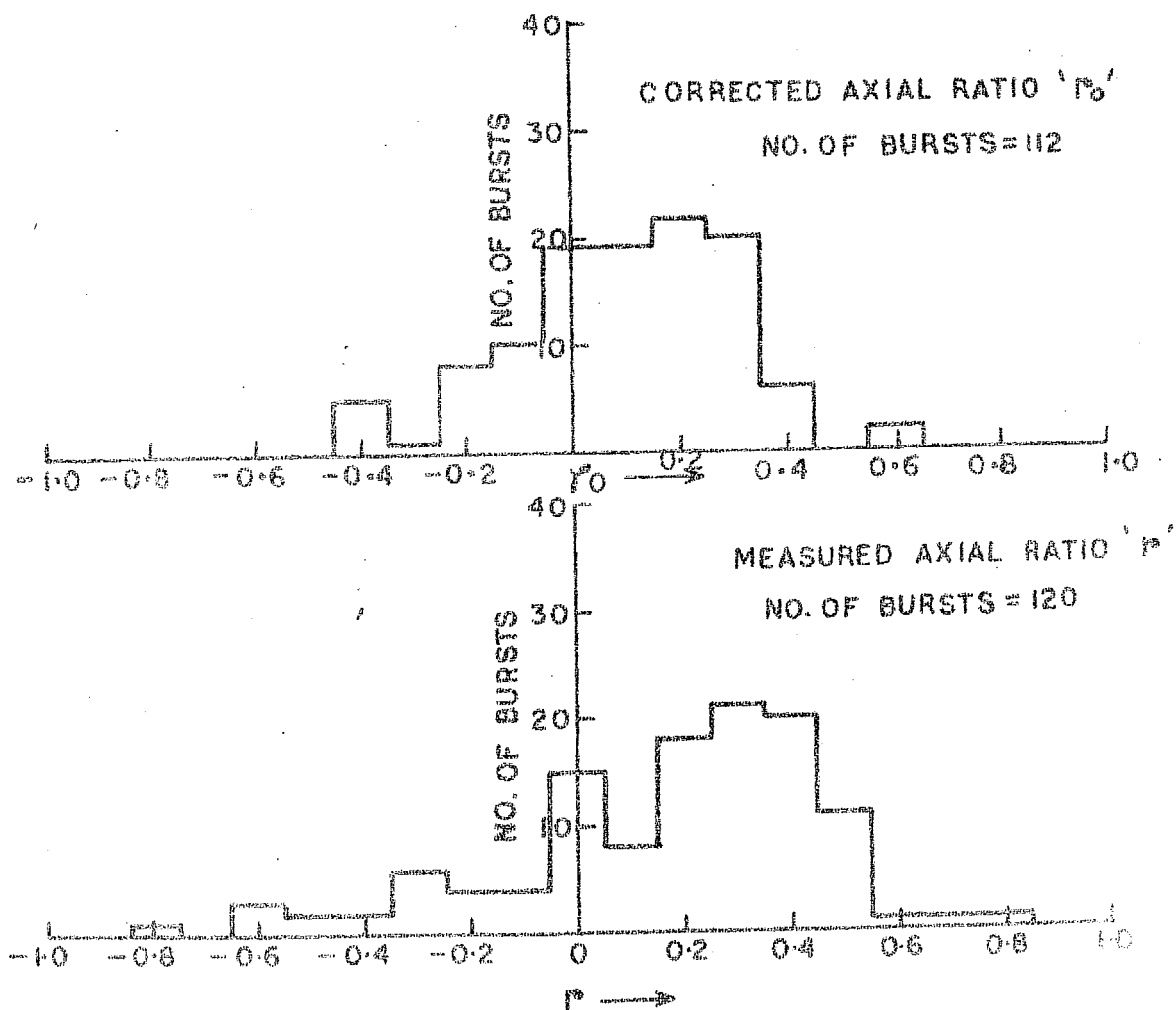


Figure 4.5 Axial ratio at 74 MHz.



propagation (Cohen 1959). The large variation in the axial ratio of different bursts within a group could be explained as a result of different directions of propagation for different bursts within a group.

At 25 MHz there are 33 groups of bursts which showed right handed sense of rotation for all the bursts within a group and 2 groups with left handed sense of rotation. Similarly, at 74 MHz 28 groups of bursts showed left handed and 8 right handed sense of rotation. There were two groups of bursts at 25 MHz and 8 at 74 MHz which changed the sense of rotation during the period of burst activity. Assuming that the sense of rotation to be dependent upon the polarity of the magnetic field associated with the source of radiation, the bursts having right handed sense of rotation should be associated with the south polarity of the magnetic field and vice versa. The change in the sense of rotation within a group of bursts could then be explained to be due either to more than one source emitting the radiation within a group, but situated in regions with opposite magnetic fields or, according to Suzuki (1961), the source is of sufficiently large size so as to occupy regions of opposite polarities above a centre of activity. Yip (1970) has pointed out that it could be due to the situation that in such cases the second harmonic components pass through the polarization limiting region where the magnetic field is

in the direction opposite to that in the source region.

At 25 MHz we have not observed any completely circularly polarized isolated burst or a burst within a group. However, at 74 MHz, there were 6 bursts, which had intensity greater than 20 times the galactic background intensity, with axial ratio unity and right handed sense of rotation. The polarization degree did not exceed 16 per cent for any of the completely circularly polarized bursts.

Table 4.1 summarizes the results of the axial ratio of polarization ellipse of type III bursts observed at 25 and 74 MHz. The largest value of the axial ratio did not exceed 0.7 at 25 MHz and 0.8 at 74 MHz. The lowest value of the axial ratio remained quite close to zero, that is, highly elliptically polarized bursts were observed both at 25 and 74 MHz. The mean value of the axial ratio at 25 MHz was 0.2 which is less than the mean value of 0.28 at 74 MHz. It should be noted that the receiving bandwidth of the 25 MHz radio polarimeter was twice that of the 74 MHz radio polarimeter at N.R.C. The lower value of the mean axial ratio observed at 25 MHz seems to be consistent with the fact that the Faraday rotation decreases as the frequency of radiation decreases (Akabane and Cohen 1961, Bhonsle and Mattoo 1973). 15 per cent of the type III bursts at 25 MHz and 12 per cent at 74 MHz had axial ratios less than 0.05,

(highly elliptical or linearly polarized bursts). Figures 4.5b and 4.6b represent the distribution of the axial ratio corrected for the effect of Faraday rotation at 25 and 74 MHz respectively. After the correction it is found that the range of the axial ratio decreases considerably. This decrease in the range of the axial ratio may not be true at the source region; and could be verified either with very narrow band radio polarimeters (small thickness of the source region and a negligible spread in the Faraday rotation angles) or by correcting the polarization parameters of each burst with the corresponding experimentally measured value of the Faraday rotation. In Table 4.1 we have indicated the values of the highest, lowest and mean axial ratio corrected for the Faraday rotation both at 25 and 74 MHz. It is seen that the corrected mean value of the axial ratio at 25 MHz comes on the order of the mean value obtained for the observations at 25 MHz reported by Chin et al. (1971).

In Table 4.2 we have compared the fraction of type III bursts having axial ratio less than 0.2 (highly elliptical) with and without correction for the Faraday rotation effects. It is seen that the uncorrected fraction of type III bursts increases from 0.3 at 200 (Akabane and Cohen 1961) and 74 MHz to 0.54 at 25 MHz (PRL, Ahmedabad). The corrected fraction of type III bursts increases from

## SUMMARY OF AXIAL RATIO DATA OF HIGHLY ELLIPTICALLY POLARIZED TYPE III BURSTS

Place	Fre- quency in MHz	Band- width in KHz	Year and period	No. of bursts used for anal- ysis	No. of bursts having axial ratio less than .2			$y = \frac{(\omega)_H}{(\omega)}$	Expected probabi- lity of occurrence under ran- dom magne- tic field conditions	
					Fraction					
					Uncor- rected	Cor- rected	Aver- aged			
Cornell Uni- versity Ithaca	200	10	March- Sept. (1959)	64	21	.3	.014 (1 Gauss)	.0028		
N.R.C. Ottawa	74	10	May-June (1963)	120	38	60	.3	.018 (.5 Gauss)	.0038	
Stanford Uni- versity	25	.1	1966 1968 1969	45 41 130	17 40 100	.4 .97 .77	.5			
P.R.L. Ahmedabad	25	20	(July 69 to June 70)	159	86	127	.54	.011 (.1 Gauss)	.0022	
P.R.L. Ahmedabad	35	.8	Jan-March (1972)	26	11	.4				

\* Total number of bursts analysed in the years 1966, 1968 and 1969 at Stanford University

0.5 at 74 MHz to 0.8 at 25 MHz. The latter value compares well with the observations at the same frequency with a very narrow bandwidth (100 Hz) radio polarimeter (Chin et al. 1971). In the same table we have indicated values of  $Y$ , which is equal to the ratio of the gyro-frequency  $(\omega_H)$  to the radiation frequency  $(\omega)$ , at the coronal emission levels of different frequencies assuming the magnetic field values of 1, 0.5 and 0.1 Gauss at the coronal levels of emission of 200, 74 and 25 MHz respectively. The value of  $Y$  is required to calculate the expected probability of observing linear polarization under the assumption of randomly oriented magnetic fields. The expected probability can be found out as follows:

In the case of a magneto-ionic medium which has magneto-ionic parameters  $X, Y$  ( $X = \omega_o^2 / \omega^2$ ,  $\omega_o$  being the plasma frequency, Ratcliffe 1959) both much less than 1 and also negligible collisions, the axial ratio  $r$  of the magneto-ionic modes is given as (Cohen 1959)

$$r = \alpha / Y \quad \dots (4)$$

where  $\alpha$  is the angle that the magnetic field makes with the perpendicular to the propagation direction. For a fixed direction of propagation and randomly oriented magnetic fields, the probability  $P(r_o)$  that the axial ratio is less than the specified value  $r_o$  is given by finding the probability  $P(\alpha_o)$  of  $\alpha_o$  obtained from the

relation (4) under the assumption of randomly oriented magnetic fields. The following relation can be used to find out the probability  $P(r_o)$  at different frequencies:

$$\begin{aligned} |P(r_o)|_{\substack{r_o \\ -r_o}}^{\substack{r_o \\ -r_o}} &= |P(\alpha)|_{\substack{\alpha_o \\ -\alpha_o}}^{\substack{\alpha_o \\ -\alpha_o}} \\ &= \int_0^{2\pi} \int_{90-\alpha_o}^{90+\alpha_o} \sin\theta \, d\theta \, d\phi / 4\pi \\ &= \sin \alpha_o \end{aligned} \quad \dots(5)$$

$\sin\alpha_o \simeq \alpha_o$  for small values of  $\alpha_o$ , where  $\theta$  and  $\phi$  have usual meanings as referred to the coordinate system used. Table 4.2 shows the probability of observing the axial ratio  $r$  of less than 0.2 at various frequencies. It should be noted that the indicated values of the probability  $P(r_o)$  at various frequencies are the same as that of a ray, starting from the source-region meets the transverse field configuration on its outward passage through the solar corona. It follows from Table 4.2 that:

- (1) the probability of finding the axial ratio of less than 0.2 under the assumptions of randomly oriented magnetic fields is on the same order at all the frequencies.
- (2) the observed fraction of bursts having the axial ratio of less than 0.2 at all the frequencies is much greater than the expected probability under the assumption of randomly oriented magnetic field conditions. This shows that the magnetic field is ordered at all these coronal

levels so as to cause the high occurrence of highly elliptical polarization.

(3) the experimentally observed probability of finding linear polarization seems to increase as the frequency decreases. As mentioned in section 2.33, Fokker (1971) pointed out that it is difficult to explain the existence of linearly polarized bursts if the Faraday rotation suffered by type III bursts is as large as  $10^5$  radians. Grogard and McLean (1973) attempted to detect the linear polarization at 80 MHz by making use of a technique which completely eliminates the effect of ground reflections. They claimed non-existence of linearly polarized type III bursts. However, their method of detection of linearly polarized bursts has a limitation if the Faraday rotation is of the order of  $10^3$  radians (Bhonsle and Mattoo 1973). Thus, the possibility of the existence of linear polarization for type III bursts cannot be entirely ruled out.

(4) the observed fraction of bursts having uncorrected axial ratio of less than 0.2 at 25 MHz is greater than the same at 74 MHz despite the fact that the receiving bandwidth at 25 MHz is twice as large as that at 74 MHz. This seems to be consistent with the trend that measured Faraday rotation decreases as the frequency decreases (Akabane and Cohen 1961, Bhonsle and Mattoo 1973).

The last two conclusions are not completely unambiguous because the observations refer to two different periods. Again, the observations of Chin et al. (1971) at 25 MHz show that the fraction of type III bursts having axial ratio less than 0.2 at 25 MHz varies from 0.4 in 1966 (though number of bursts analyzed is small) to 0.97 in 1968. It would be interesting to observe polarization properties of type III bursts simultaneously at different frequencies.

#### 4.33 ORIENTATION ANGLE $\chi$

Figure 4.7a and 4.7b show the distribution of the orientation angle  $\chi$  of type III bursts observed at 25 and 74 MHz, respectively. It is seen that the orientation angles of the major axis of the polarization ellipses of the type III bursts, both at 25 and 74 MHz, are not evenly distributed with respect to the given antenna reference system as would be expected, because the orientation data cannot be extended to the source in the presence of large amount of Faraday rotation suffered by the radiation while passing through the solar corona and the earth's ionosphere. At 25 MHz, the  $\chi$  values are grouped in the range  $-10^\circ$  to  $20^\circ$ . Similarly at 74 MHz the  $\chi$  values are grouped between  $-50^\circ$  and  $-30^\circ$ . This is quite interesting particularly because the observations at 25 and 74 MHz refer to two different periods and also that the observations sites



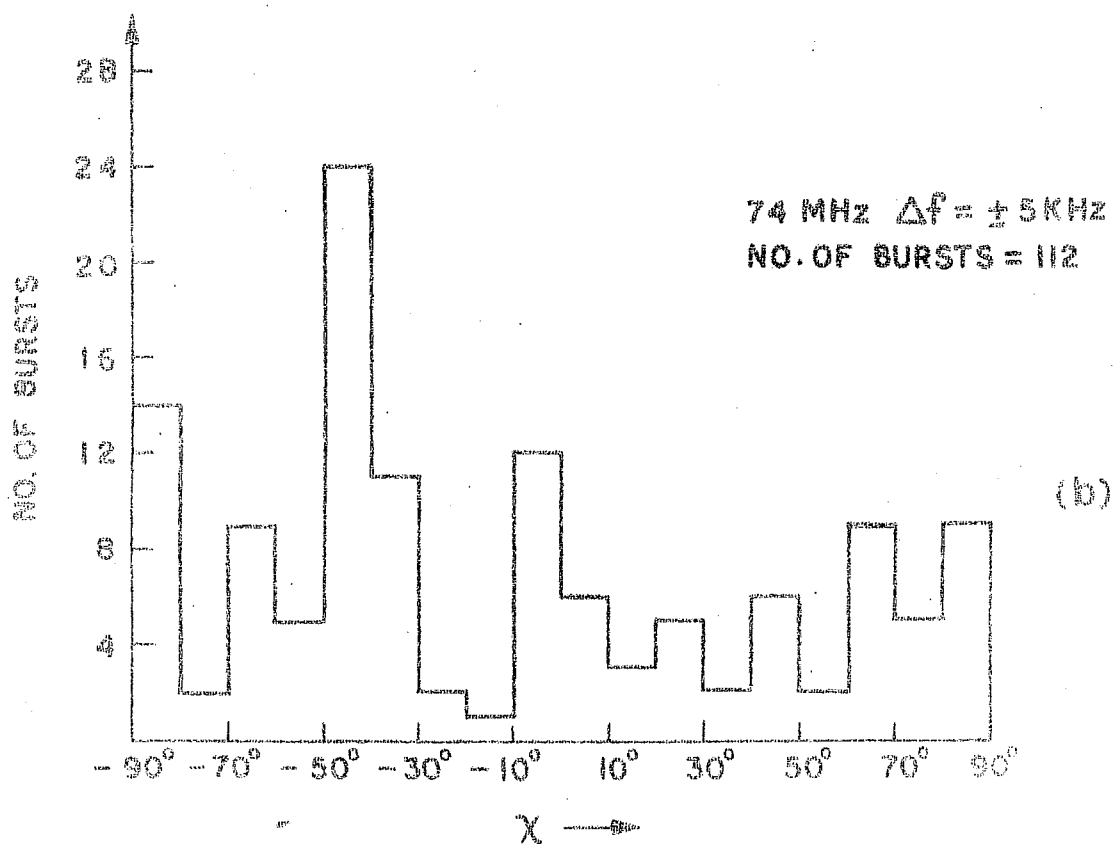
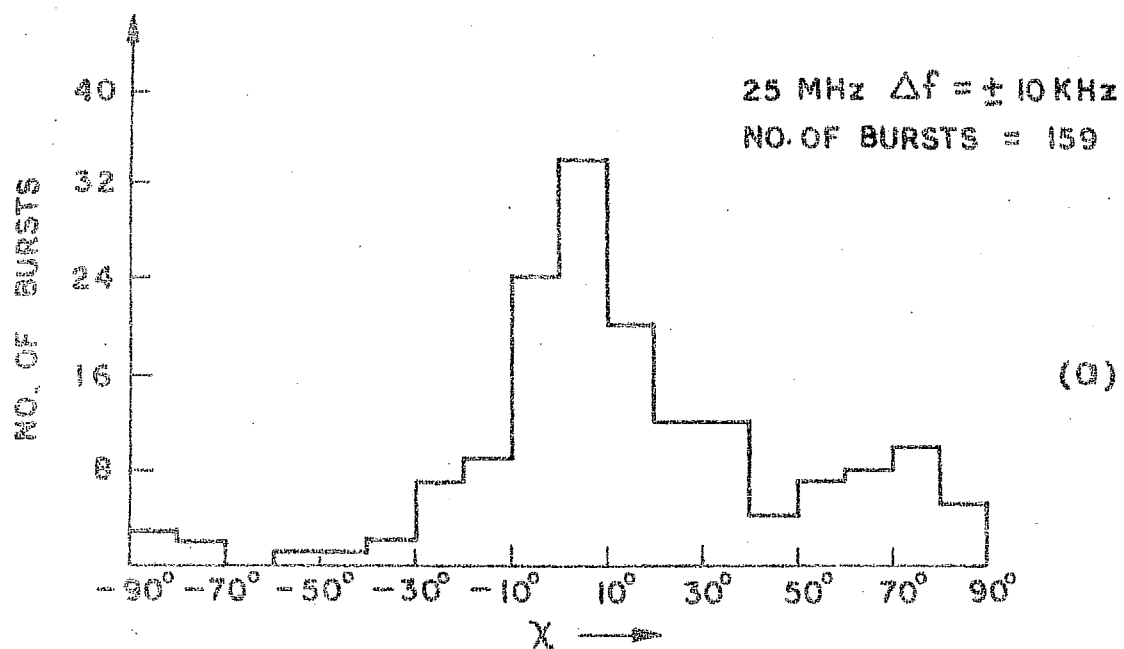


Figure 4.7 Orientation angle at 25 and 74 MHz.

are different. In a group of bursts the orientation angles of different bursts were within  $\pm 10^\circ$  about the mean value. Similar tendency for clustering of orientation angles was reported by Cohen (1959) at 200 MHz and recently by Dodge (1972) at 34 MHz.

In view of the clustering of orientation angles presented in Figure 4.7, the following conclusions can be drawn:

- (1) The magnitude of the total electron content and magnetic field in the path of radiation must remain essentially constant for the duration of the group of bursts. This also implies that the scattering effects, so far as their effect on orientation is concerned, are not that excessive so as to randomize the orientation angles.
- (2) For linear polarizations to be intrinsic to the source, the occurrence of constant position angle requires an extreme stability of the source position, if the Faraday rotation is large near the source (Cohen 1959).

#### 4.4 POLARIZATION CHARACTERISTICS OF THE SOLAR EVENT ON JULY 14, 1969

Figure 4.1b shows the four-channel polarimeter recording of a group of solar radio bursts of spectral type III observed between 0813 and 0815 U.T. One can distinguish 10 different peaks on the I-channel. It may be noted that the intensity of radiation does not drop to

zero between the two successive peaks. This could either be due to a possibility that the bursts occurred in quick succession or that there might be a simultaneous emission of a background component with a longer duration. The average duration of individual type III bursts at 25 MHz has been estimated to be about 10 seconds and since the polarimeter output time constant is about 1 second the time-profile of the intensity of type III bursts will not be affected. We favour the latter possibility, that is, the simultaneous emission of background and burst components, in view of the fact that the dynamic spectrum of the same group of bursts shown in Figure 4.8 shows the presence of individual bursts superimposed upon a diffuse background radiation. Further, it may be noted that all the individual bursts in this group do not have the same drift speed.

#### 4.41 INTENSITY

Figures 4.9a - d show the variation in intensity, degree of polarization, axial ratio, and the orientation angle of the major axis of the polarization ellipse as a function of time. The values of I, Q, U and V have been scaled manually from the polarimeter recording at the peaks and troughs of the intensity of radiation. For comparison the total radiation I and the computed polarized component of radiation  $I_e$  are plotted on the same scale. It can be seen that  $I_e$  is less than I throughout the

DYNAMIC SPECTRUM OF SOLAR RADIO BURSTS  
AT METER WAVELENGTHS  
ON 14<sup>th</sup> JULY, 1969 AHMEDABAD

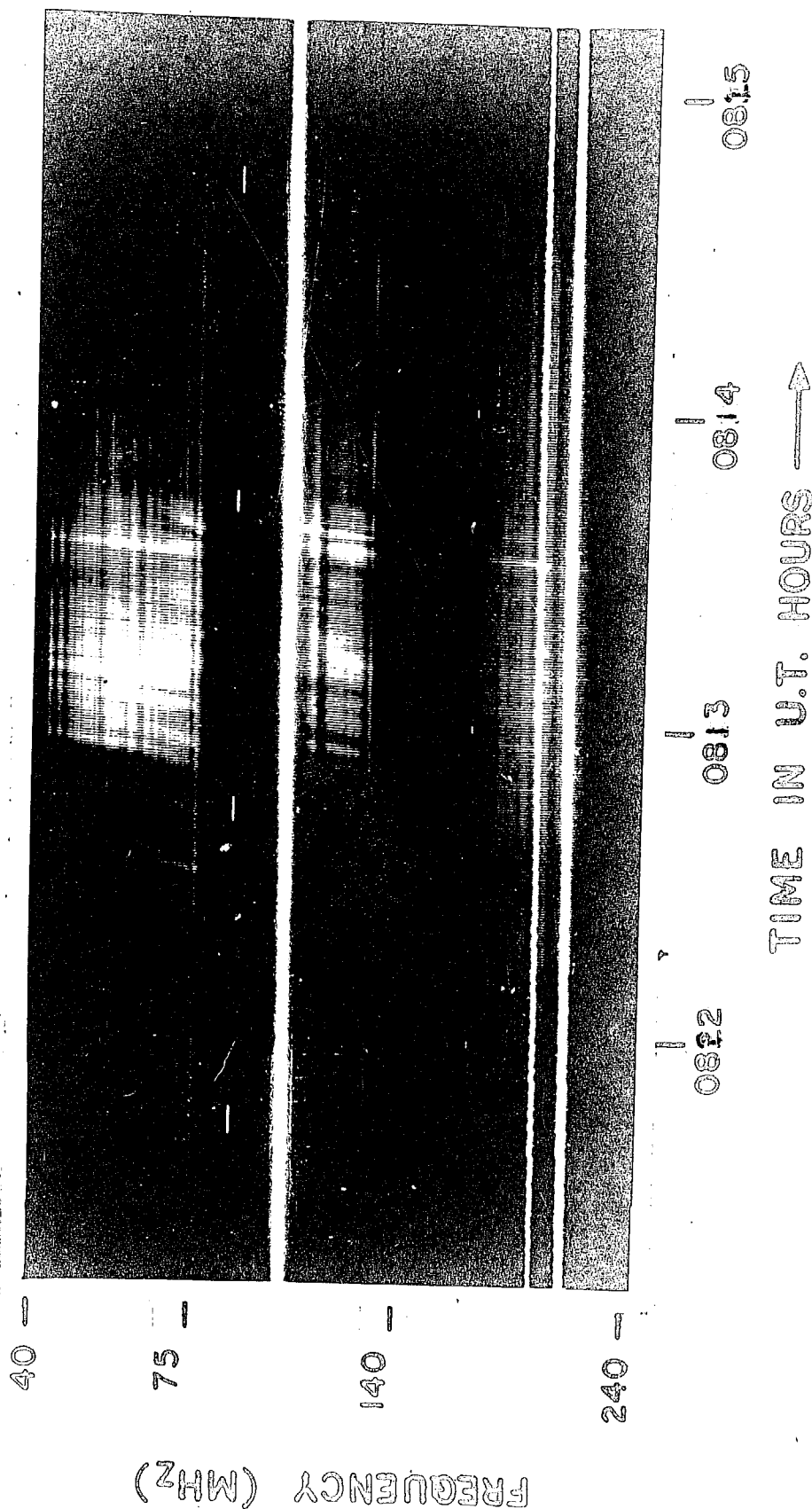


Figure 4.8 A group of type III bursts along with a continuum recorded on July 14, 1969. Recorded by Ahmedabad radio spectroscopist at 0813 U.T.

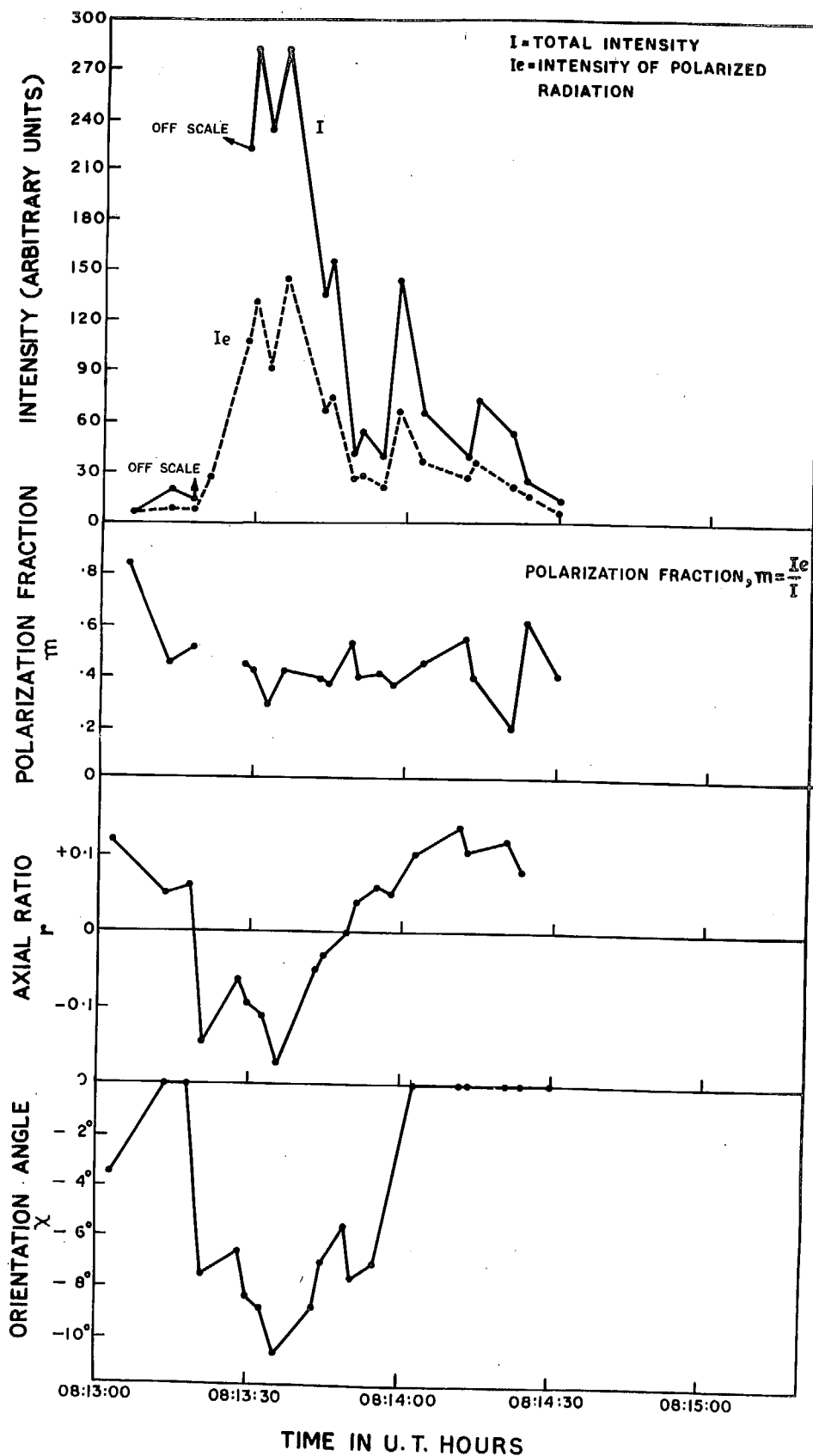


Figure 4.9 Various polarization parameter of the solar event recorded on July 14, 1969.

duration of the event except at one or two points where  $I_e$  is comparable to  $I$ . Thus it can be concluded that the radiation was partially polarized.

#### 4.42 DEGREE OF POLARIZATION

The variation of the degree of polarization  $m$  during this event may be seen from the plot in Figure 4.9b. It can be noticed that  $m$  varied between about 30 per cent to 85 per cent during the event. Making point to point comparison, the general trend in the time variation of  $m$  is to increase when the total intensity  $I$  decreases and vice versa. This means that the radiation is relatively weakly polarized in the presence of bursts. This can be explained if the burst component of radiation is either unpolarized or weakly polarized as compared to the polarization of the background component of radiation or, if polarized, it must be incoherent with the background component. Since the polarization percentage drops down during the life time of the burst, it is logical to conclude that the burst component of radiation is to a large extent unpolarized (or weakly polarized). In other words, it can be concluded that this solar event consisted of two components of emission occurring simultaneously, the burst component that is unpolarized or weakly polarized and the background component that is strongly polarized. The dissimilarity in the degree of polarization of the

burst and that of the background component of the radiation suggests (a) that they must originate in the coronal regions pervaded by weak and strong magnetic fields, respectively and (b) that their mechanisms of generation may also be different. One can visualize this as a situation in which bunches of energetic electrons are ejected in different directions from the source. The burst component may be resulting from the plasma oscillations excited by those electrons, which escape more or less along the neutral plane in the magnetic field configuration of a coronal streamer, whereas the background component may be caused by those electrons which are injected in the strong field regions. Further evidence that the type III bursts are generated in weak field regions comes from the absence or low degree of circular polarization of bursts. The interpretation suggested above is consistent with the model of burst source given by Wild and Smerd (1972) for type III, V and U from their radioheliograph observations at 80 MHz. This model has already been described in detail in section 1.31 (see also Figure 1.4).

#### 4.43 AXIAL RATIO AND ORIENTATION ANGLE

Figure 4.9c shows the variation of the axial ratio with time. It can be noticed that the axial ratio varied

between - 0.18 to 0.13. The sequence of variation of the axial ratio was as follows: Initially the axial ratio remained positive, when the burst activity became intense the axial ratio changed its sign from positive to negative and when the burst activity subsided the axial ratio again returned to its positive value. Thus we conclude that the change of sign is due to the appearance of burst component. This argument seems to give us evidence for that there were two generating mechanisms simultaneously operative, one giving rise to fast drifting type III bursts and the other background and/or that the two components originated in two dissimilar magnetic field regions. The suggestion that these two components came from different regions can be appreciated by referring to Figure 4.9d in which the orientation angle of the major axis of the polarization ellipse with respect to the antenna system is plotted as a function of time. Although the orientation data cannot be directly related to the source owing to the large amount of Faraday rotation suffered by the radiation in the intervening magneto-ionic medium, it seems that the observed relative changes in the instantaneous values of the orientation angles can be attributed to the source in this case. It is seen that when the axial ratio changed from left-handed to right-handed the value of  $\chi$  changed by  $17^\circ$  and remained more or less steady around this value until the burst activity subsided after which the orientation angle returned



to the initial value. It should be pointed out here that after the burst activity subsided the original sense of rotation was restored simultaneously with the return of the orientation angle to its original value.

The variation in the magnitude of the axial ratio can be appreciated from the plot shown in Figure 4.10 in which the unpolarized radiation,  $I_u = I - I_e$ , is plotted against the axial ratio  $r$ . It is seen that for a large unpolarized radiation the axial ratio has remained negative and it is during this time that the burst component contributed largely to the total radiation. When the burst activity seemed to be subsided, the background and the burst component either contributed equally to the total radiation or else it is the background component which contributed largely to the total radiation. The axial ratio changed sign when the burst activity subsided and remained positive till the end of the event. This point of view can be appreciated from the point 'A' in the plot in Figure 4.10. At this point there was a burst which thus raised the level of the unpolarized radiation and  $r$  tends to be negative.

The changes in the sense of rotation of the polarization ellipse is expected to occur if the radiation encounters a quasi-transverse magnetic field configuration on its passage out from the source region to the observation point. The QT conditions could exist either in the

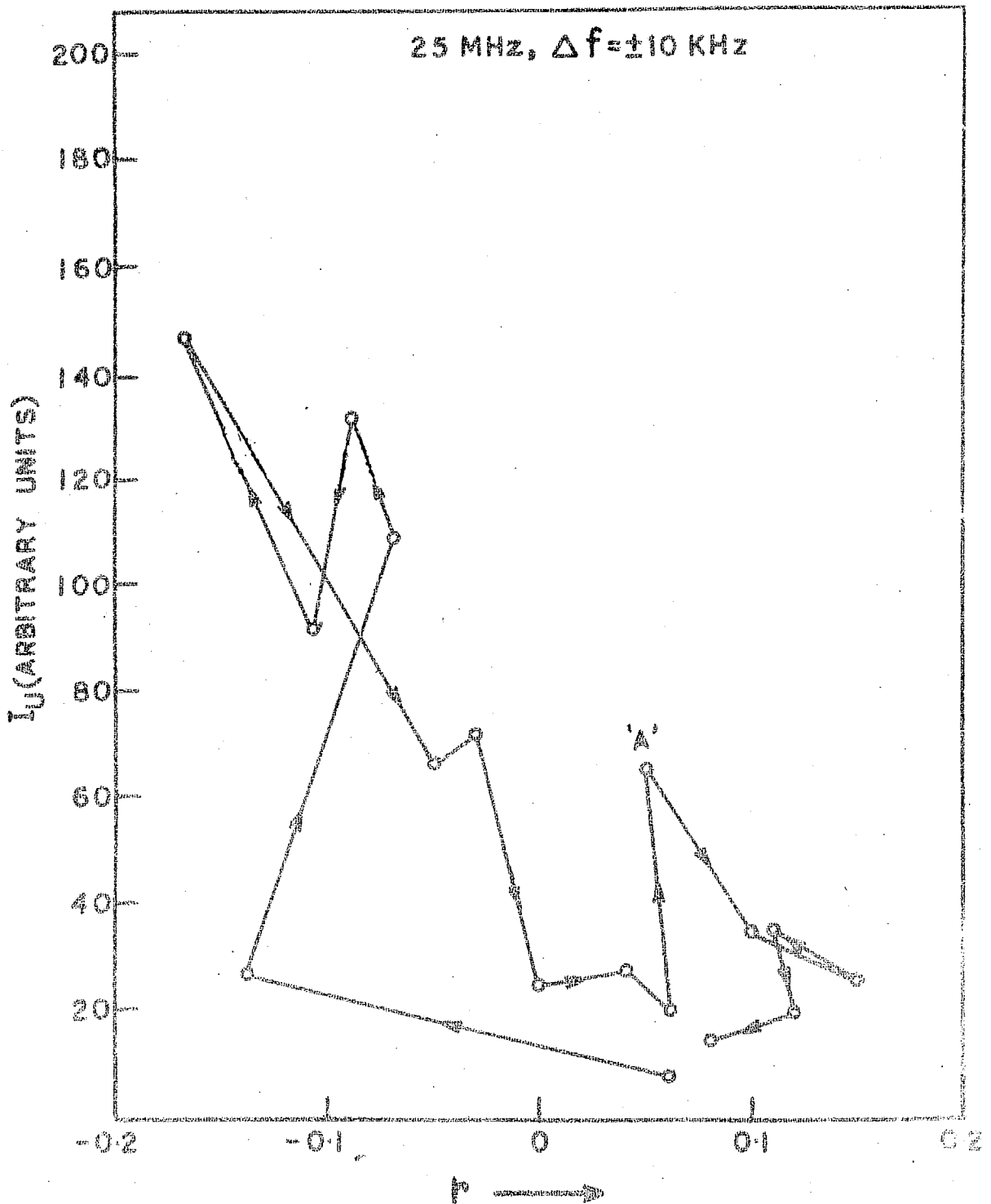


Figure 4.10 shows the relation between the unpolarized intensity and the axial ratio for type III burst recorded on July 14, 1969. Arrows indicate the direction of increasing time.

corona or in the earth's ionosphere when the angle between the direction of the ray propagation and the magnetic field is close to 90 degrees. As will be discussed later (Chapter V) for the solar event observed around local noon the mode of radio propagation in the earth's ionosphere should be quasi-longitudinal. Under these circumstances we expect that the effect of the earth's magnetic field and electrons in the ionosphere is to cause the Faraday rotation of the plane of polarization unaccompanied by any changes in the axial ratio. The observed changes in the axial ratio must, therefore, be attributed to the region close to the source of radiation in the solar corona.

Since the sense of rotation for the background radiation and for the polarized part of the burst component of the radiation were opposite, the two components cannot originate in the same source region with the similar polarity of the magnetic field. Assuming that the state of polarization was entirely due to the effects of propagation of the radiation through the corona, the mixed polarizations R and L may result either from the burst component and the background component coming from two different centers of activity, or from one and the same center of activity (Fokker 1965). In both the cases, however, it is necessary that the rays coming either from the sources of burst component or from the background

component, do not meet QT regions in their path of propagation. Transverse propagation of the observed radiation in the solar corona is more likely to occur when the source is near the limb (Fokker 1965) than when it is in the central part of the disk. A solar flare on July 14, 1969 has been reported to have occurred at a position S13, W 21 between 0813 and 0832 hours U.T. Thus, it is unlikely that the QT regions in the solar corona could have changed the sense of rotation. We, therefore, conclude that the flare-produced background and type III burst radiation originated in two different regions of the centre of activity. An observational evidence for such multiple sources has now become available from two-dimensional position determinations of bursts and storms made with the Culgoora radio-heliograph (Wild and Smerd 1972).

#### 4.5 POLARIZATION CHARACTERISTICS OF TYPE III BURSTS AT 34.993 AND 34.997 MHz

Having completed the series of observations at 25 MHz with a single bandwidth, we planned another series of observations at two closely spaced (4 KHz apart) frequencies near 35 MHz. The exact frequencies at which the the polarimeter was operated during January - March, 1972 were 34.993 and 34.997 MHz. The overall bandwidth for these two channels was 800 Hz each. During this period we have recorded 50 type III bursts which occurred either

singly or in groups. All these 50 events were confirmed by the solar radio spectrometers operating at Ahmedabad (India), Weissenau (West Germany) and Culgoora (Australia). Of these 50 events, only 37 high intensity bursts were used for detailed analysis to minimize scaling errors.

In addition, we recorded 3 intense type III bursts by our radio spectrometer ( frequency range: 40 - 240 MHz) but did not record them on the polarimeter on either channel, although the polarimeter was in normal operating condition. This may be explained if the type III burst did not extend very much below 40 MHz and had a cut-off in emission between 35 and 40 MHz. Such abrupt cut-offs in emission at decameter wavelengths have been reported in the case of type IIIb bursts (Ellis and McCulloch 1966, 1967 and de la Noe and Boischot 1972). It should also be mentioned that there were 3 events which were recorded as type III bursts on our radio spectrometer but they were evident on the polarimeter recordings on only one channel but not on the other. This suggests that there may be a considerable fine structure in frequency on the scale of a few kilohertz. Thus, it is possible that we may have recorded type IIIb bursts instead of the conventional type III bursts in the case of these 3 events.

We shall now describe the polarization properties of the 37 type III bursts at their peak intensities at

34.993 and 34.997 MHz. The quantities  $I$ ,  $m$ ,  $r$  and  $\chi$  have their usual meaning at 34.997 MHz while the same are primed for 34.993 MHz channel. The number of bursts included in the histograms shown in Figures 4.11 to 4.14 is not the same since it was sometimes difficult to obtain all the information simultaneously on both the channels.

#### 4.51 INTENSITY

Figure 4.11a represents the distribution of  $I'/I$ , which indicates that not all bursts have the expected ratio of unity. The ratio  $I'/I$  should have been near unity if all the bursts were much broader than the frequency separation (4 KHz) between the two channels. Many bursts have intensity ratios as high as 1.8 or 1.9 and only 2 bursts have intensity ratio less than 0.7. It was observed that the intensity ratio  $I'/I$  of different bursts in a given group does not always remain constant. This analysis thus shows that normally the intensity of a burst may vary by a factor of 2 in a frequency band of 4 KHz near 35 MHz.

#### 4.52 POLARIZATION DEGREE

Figures 4.12a - b represent the distribution of polarization degree at 34.997 and 34.993 MHz, respectively. The degree of polarization varies between 10 and 90 per cent in both the channels and the distribution at 34.997 MHz seems to be more uniform than that at 34.993 MHz. This indicates that the polarization degree at 34.997 MHz, is

I, m, r AND  $\chi$   $\rightarrow$  34.997 MHz,  $\Delta f = 800$  Hz  
 $I', m', r'$  AND  $\chi'$   $\rightarrow$  34.993 MHz,  $\Delta f = 800$  Hz

RATIO OF INTENSITY  
 AT 34.993 AND 34.997 MHz

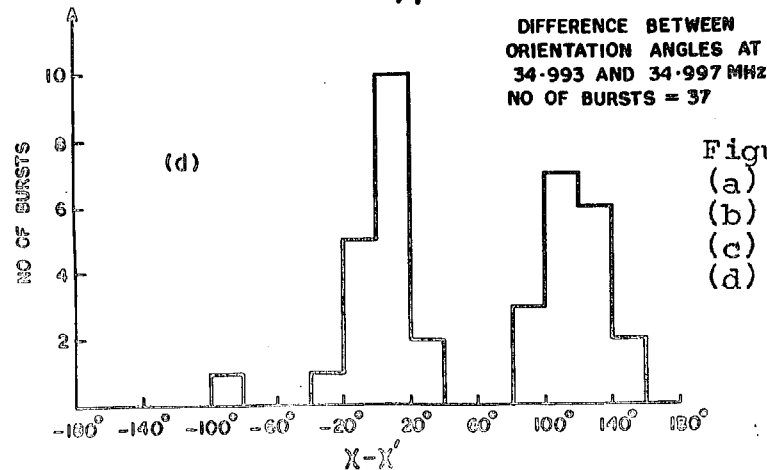
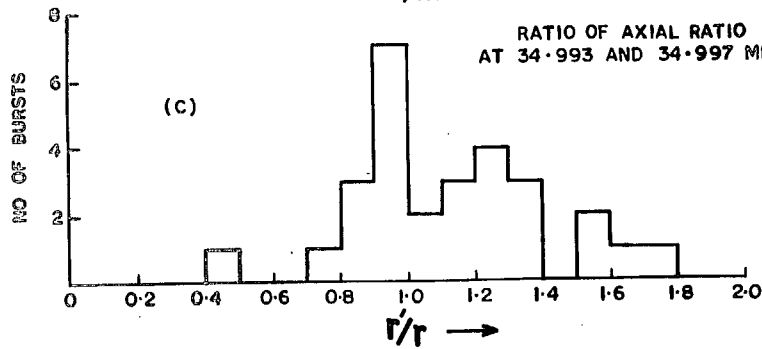
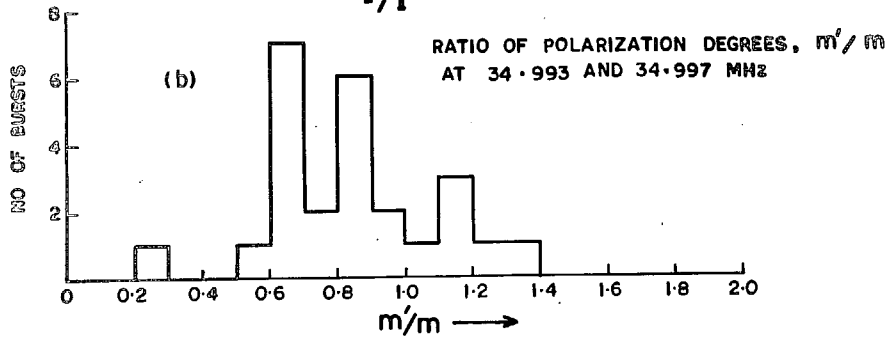
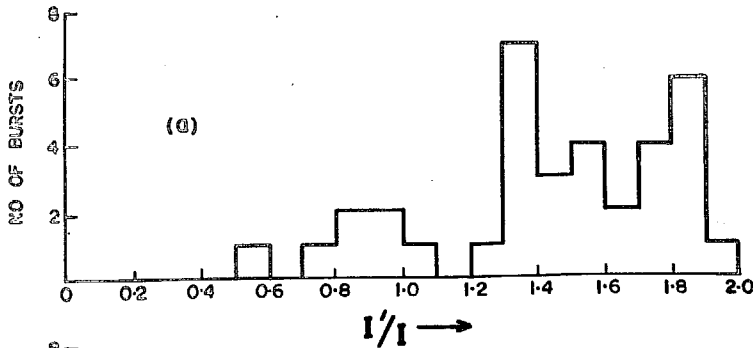


Figure 4.11 Distribution of  
 (a) intensity ratios,  
 (b) ratio of polarization degree,  
 (c) ratio of axial ratio and  
 (d) difference between the  
 orientation angles of  
 type III bursts at 34.997 and  
 34.993 MHz.

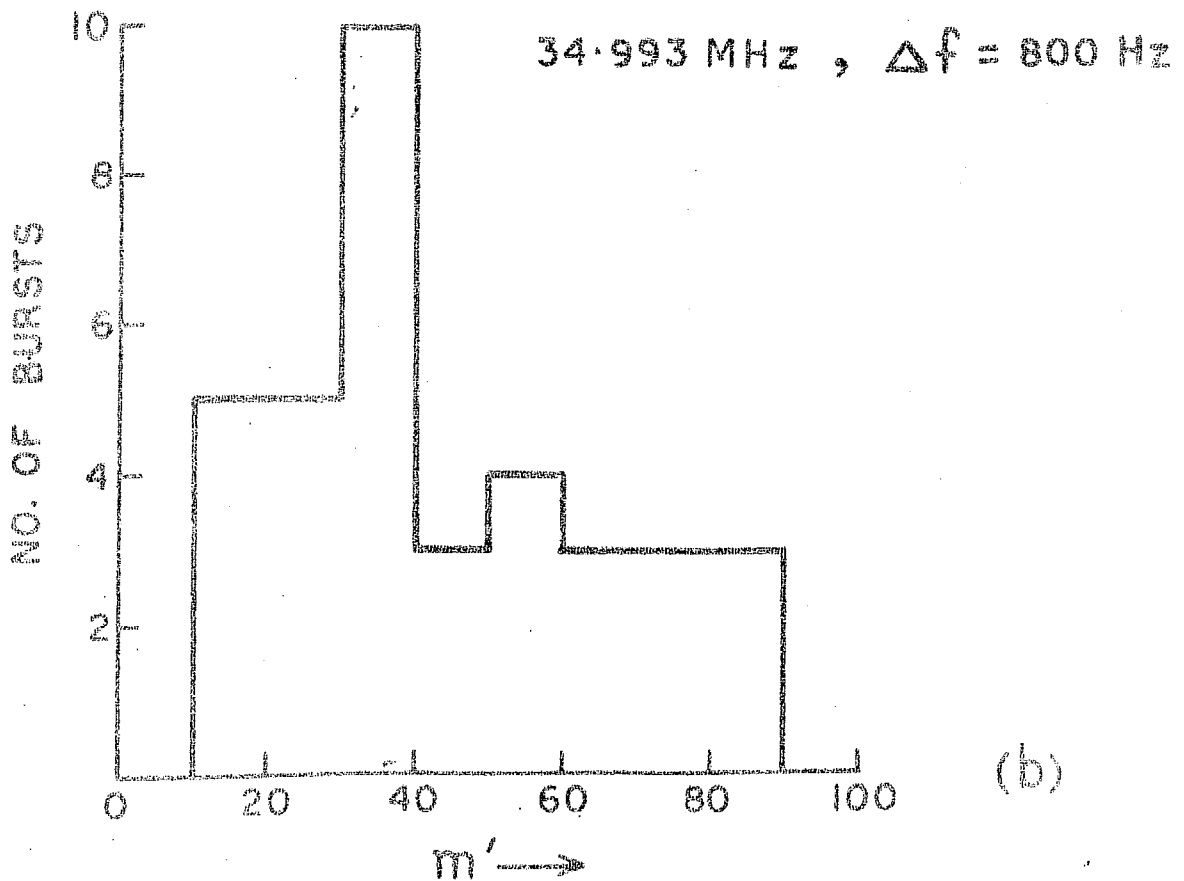
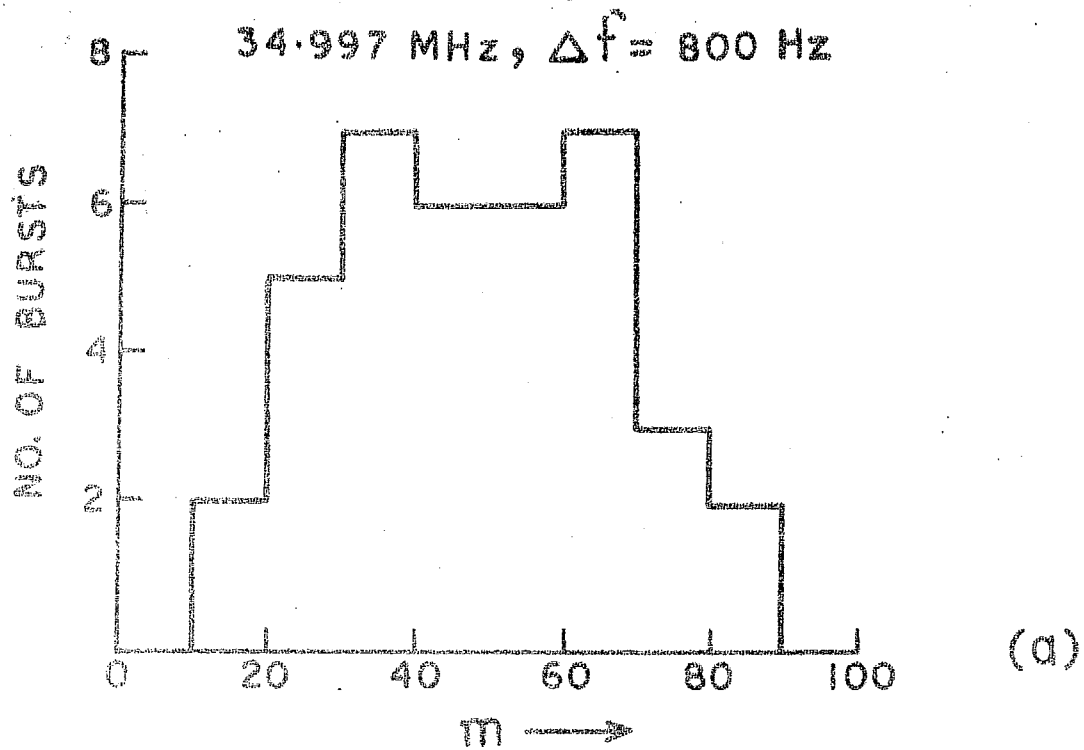


Figure 4.12 Polarization percentages at two closely spaced frequencies (34.993 and 34.997 MHz).



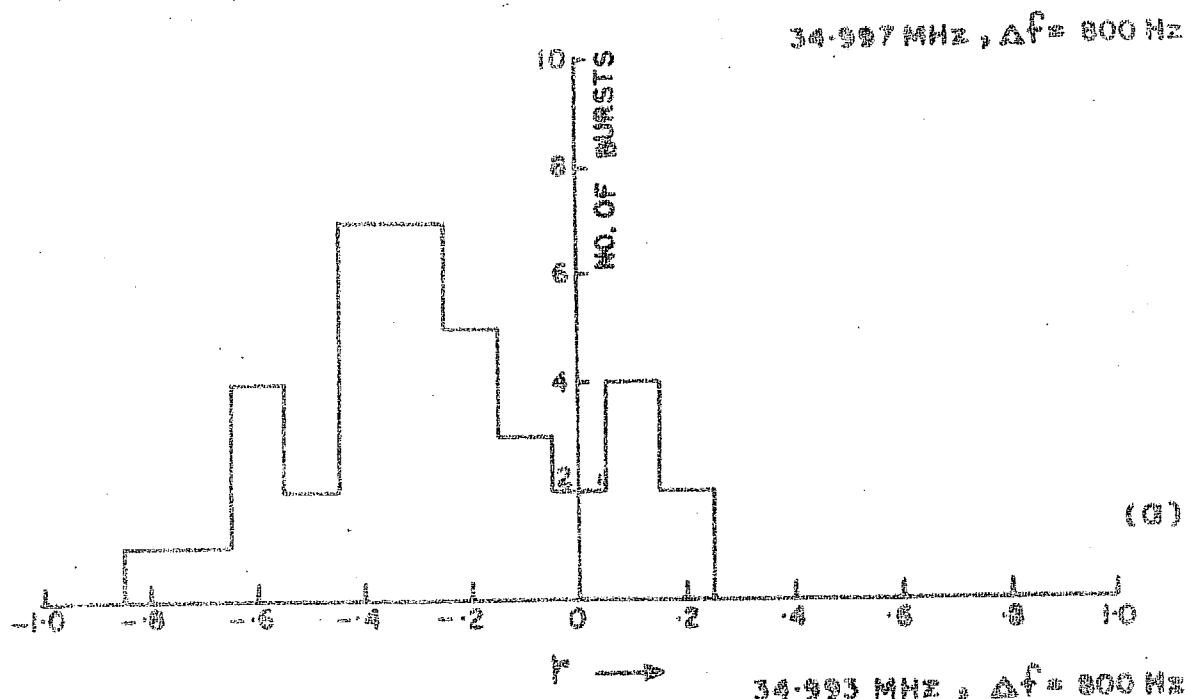
in general greater than that at 34.993 MHz. This is clearly borne out by Figure 4.11b which represents the distribution of the ratios of polarization degree  $m'$  at 34.993 MHz to the polarization degree  $m$  at 34.997 MHz for each burst. It is seen that there are as many as 18 bursts which had  $m'/m$  ratio less than unity. It should be noted that the lowest value of  $m'/m$  is 0.25 and the highest 1.4.

#### 4.53 AXIAL RATIO

Figures 4.13a - b represent distribution of axial ratios  $r$  and  $r'$ , respectively. The occurrence of right handed polarity is more frequent than left handed one at both the frequencies during the period January - March, 1972. Not a single burst was observed which had opposite sense of rotation at two frequencies. The range of the axial ratio is quite large at both the frequencies. In Figure 4.11c we have plotted the distribution of the ratio of axial ratios  $r'$  to  $r$  for each burst. As many as 12 bursts had  $r'/r$  less than 1 and 16 bursts had  $r'/r$  greater than 1.

#### 4.54 ORIENTATION ANGLE

Figures 4.14a - b correspond to the distributions of the orientation angle of the polarization ellipse of type III bursts observed at 34.997 and 34.993 MHz, respectively. At both the frequencies there seems to be



34.993 MHz,  $\Delta f = 800$  Hz

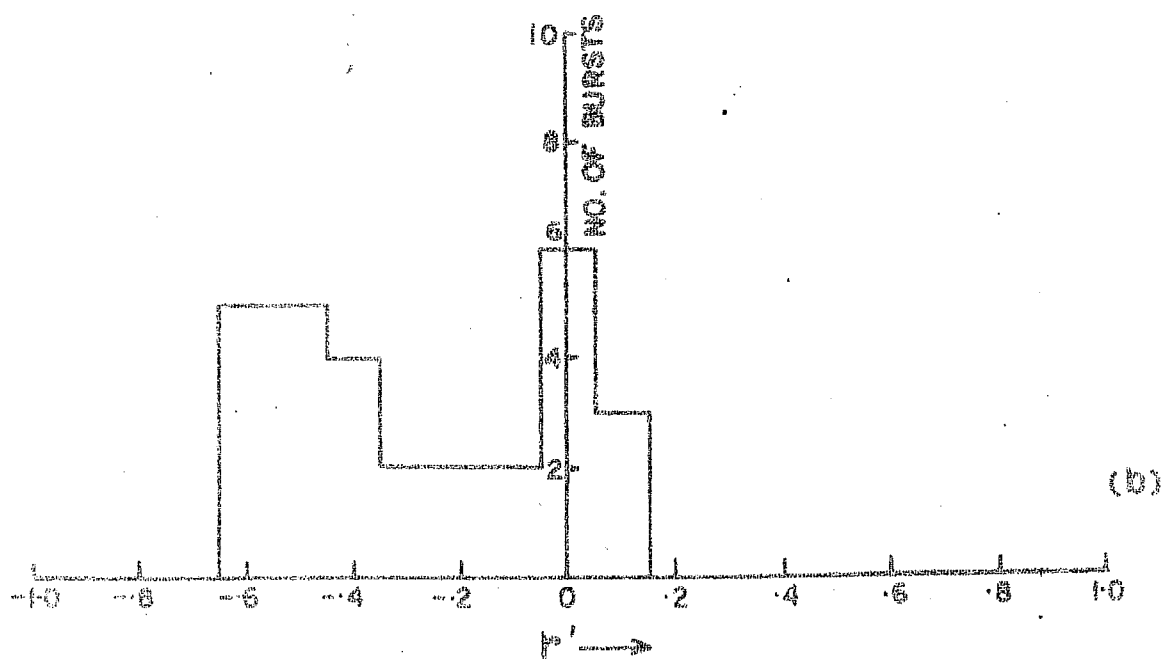
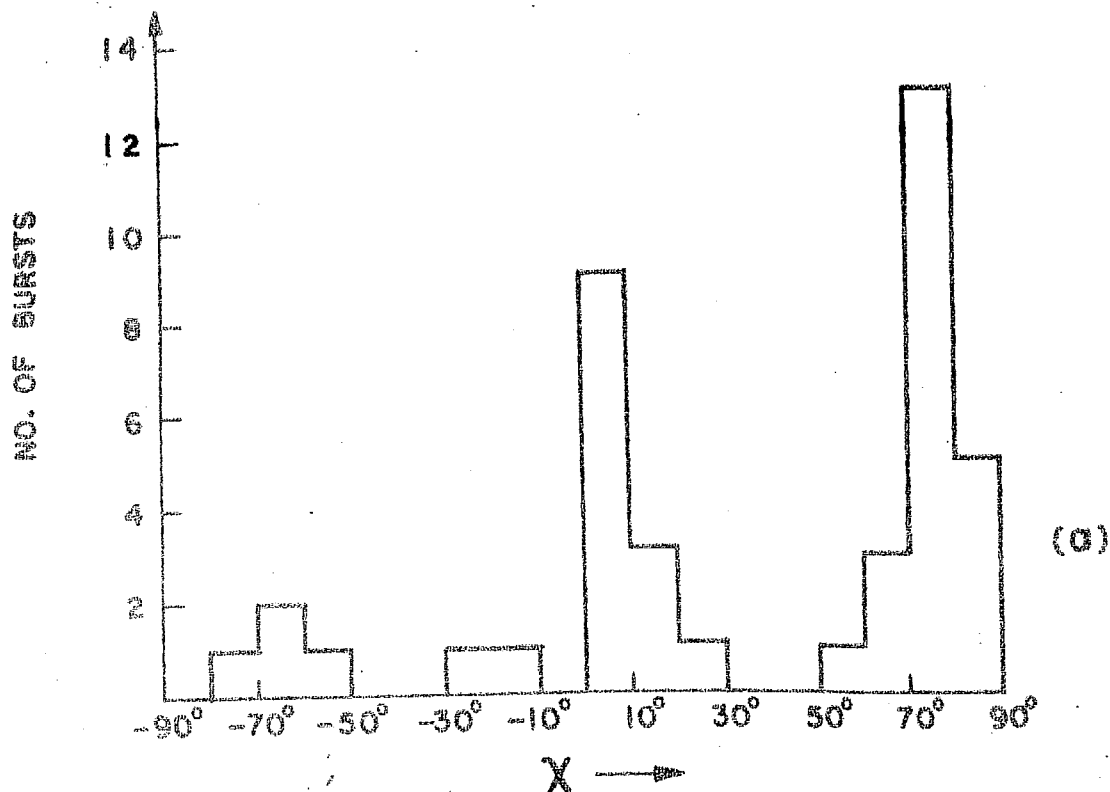


Figure 4.13 Axial ratio at two closely spaced frequencies (34.993 and 34.997 MHz).

34.997 MHz,  $\Delta f = 800$  Hz  
NO. OF BURSTS = 42



34.993 MHz,  $\Delta f = 800$  Hz  
NO. OF BURSTS = 53

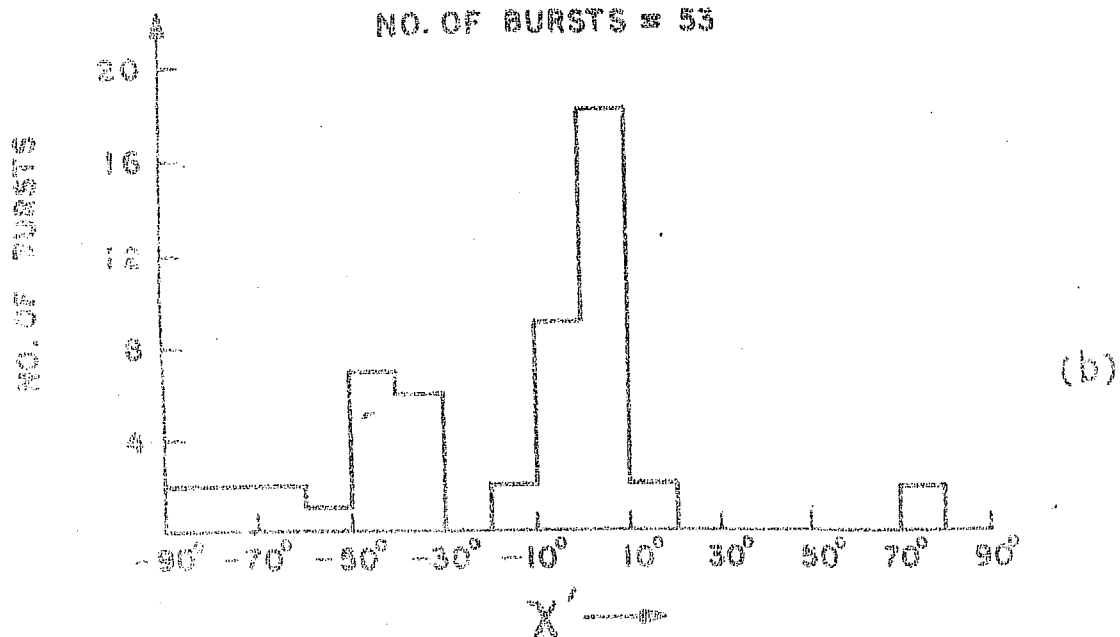


Figure 4.14 Orientation angle at closely spaced frequencies (34.993 and 34.997 MHz).

some preference for orientation angles within  $\pm 20^\circ$ , that is, clustering of orientation angles. Similar clustering tendency of orientation angles has been reported earlier by many workers (Cohen and Fokker 1959, Cohen 1959a, Bhonsle and McNarry 1964b, Bhonsle et al. 1967, Dodge 1972). Figure 4.11d represents the distribution of the difference of orientation angles  $(\chi - \chi')$  at the two frequencies. For 15 bursts the position angles of polarization ellipses do not differ by more than  $\pm 20^\circ$ . For the other 18 bursts the difference in the position angles is in the range  $80^\circ$  to  $160^\circ$ . The observed small difference in the orientation angles at the two frequencies can be explained from the following simple calculation of the Faraday rotation at 35 MHz:

The amount of Faraday rotation  $\phi$  may be expressed as

$$\phi = \frac{2.36 \times 10^4}{\nu^2} \int N \cdot H_{||} dz \quad \dots(5)$$

where  $N$  is the electron density,

$H_{||}$  in Gauss is the component of the magnetic field parallel to the propagation direction and  $\nu$  = frequency in Hz.

If  $\phi_1$  and  $\phi_2$  refer to the Faraday rotations at two closely spaced frequencies  $\nu_1$  and  $\nu_2$ , respectively, then from relation (5) we have

$$\frac{\phi_1 - \phi_2}{\phi} = \frac{\nu_1^{-2} - \nu_2^{-2}}{\nu^{-2}} \quad \dots(6)$$

if  $\nu_1 - \nu_2 \simeq \nu$ , then, to a first approximation

$$\frac{\phi_1 - \phi_2}{\phi} = 2 \frac{(\nu_2 - \nu_1)}{\nu} \quad \dots(7)$$

For our observations  $\nu_2 - \nu_1 \simeq 4 \times 10^3$  Hz

and  $\nu = 35 \times 10^6$  Hz

Substituting the values for  $(\nu_2 - \nu_1)$  and  $\nu$  gives

$$\frac{\phi_1 - \phi_2}{\phi} \simeq 2 \times 10^{-4} \quad \dots(8)$$

If the Faraday rotation suffered by the radiation while passing through the solar corona and the earth's ionosphere were as high as  $10^5$  radians, then  $\phi_1 - \phi_2 \simeq 20$  radians. This should have been sufficient to randomize the distribution of  $(\chi - \chi')$ , particularly when scattering effects cannot be ignored. Although the Faraday rotation at 35 MHz may be as low as  $10^3$  radians, still it is not possible to extend the orientation data to the source but it seems reasonable that the scattering effects should be rather less severe in randomizing the  $(\chi - \chi')$  distribution. These results are in good agreement with those of Dodge (1972) who measured the spread in orientation angles at 34 MHz within an overall bandwidth of 3 KHz. He derived an upper limit on the Faraday rotation to be of the order of  $1.75 \times 10^3$  radians

in order to explain the lack of measurable effect of Faraday rotation on the orientation angles at different frequencies within the 3 KHz bandwidth.

4.55 POLARIZATION OF TYPE IIIb BURSTS RECORDED  
ON ONE CHANNEL ONLY

In course of this analysis, we came across 3 interesting bursts, mentioned earlier in the Section 4.5, which were recorded only on the 34.993 MHz polarimeter channel. Two of these events did not have their counterpart on the 34.997 MHz channel, while the third one had a few very small spikes during the event. This lack of correspondence between the two channels could be attributed to a fine-structure in frequency, as is obtained in the case of type IIIb bursts.

Two bursts were strongly ( 95 per cent ) linearly polarized and remained constant at all the peaks of the bursts in the group. The third burst showed polarization degree varying from 30 to 50 per cent and the axial ratio varied from 0.05 to 0.62 and had left-handed sense of rotation throughout the duration of the burst. In all the three cases the orientation angle of the major axis of the polarization ellipse remained constant throughout the period of the burst activity.

## 5.6 CONCLUSIONS

The main conclusions of this chapter are summarized below:

- 1) Average degree of polarization of type III bursts at 25 and 74 MHz was of the order of 30 per cent with bandwidths of 20 and 10 KHz respectively and 54 per cent at 35 MHz with a bandwidth of 800 Hz.
- 2) More than 30 per cent of the total number of type III bursts were highly elliptically polarized (axial ratios  $> 0.2$ ) at all the frequencies. Axial ratios  $< 0.05$  (almost linear polarization) have been observed in about 15 per cent of the total number of bursts.
- 3) Clustering of orientation angles within  $\pm 20^\circ$  have been observed in certain groups of type III bursts at all the frequencies.
- 4) Changes in the polarization behaviour of the solar event of July 14, 1969, suggested the existence of more than one radio source with different polarization characteristics; a highly polarized background radiation and relatively weakly polarized burst component.
- 5) Polarization characteristics on two closely spaced (4 KHz apart) frequencies near 35 MHz show appreciable differences between them.

- 6) Difference in orientation angles at 34.993 and 34.997 MHz was about  $20^\circ$  for the same bursts. This implies that the total Faraday rotation may not have been more than about  $10^3$  radians.
- 7) The existence of a fine-frequency structure similar to that observed in the case of type IIIb bursts was indicated by the absence of three bursts on one of the two closely spaced frequencies.



## C H A P T E R - V

### MEASUREMENTS OF FARADAY ROTATION OF TYPE III BURSTS AT 35 MHz

#### 5.1 INTRODUCTION

The measurement of Faraday rotation at decameter wavelengths assumes great importance in explaining many experimental results such as (1) the existence of linear polarization or otherwise in some type III bursts (2) clustering of orientation angles of bursts within a group and (3) small difference in the orientation angles of a given burst when observed at two closely spaced frequencies. The items (1) and (2) have already been discussed in Chapters II and IV, while item (3) has been dealt with in Chapter IV. Moreover, Faraday rotation measurements of type III bursts are not available at any frequency except at 200 MHz (Akabane and Cohen 1961). Even the most recent work (Dodge 1972) reports only an upper limit on the Faraday rotation at 34 MHz. Hence, the necessity for an experimental determination of the Faraday rotation of type III bursts at decameter wavelengths cannot be overemphasized.

In this chapter we discuss the Faraday rotation measurements of type III bursts carried out by means of a two bandwidth time-sharing polarimeter at 35 MHz. The two bandwidths used are 7.5 and 12.5 KHz. The Faraday rotations were calculated by following the method used by Akabane and Cohen (1961).

## 5.2 PRINCIPLE OF TWO-BANDWIDTH MEASUREMENT OF THE FARADAY ROTATION

Akabane and Cohen (1961) showed that the Faraday rotation could be calculated unambiguously by measuring the polarization at 200 MHz simultaneously in two bandwidths, 10 and 22 KHz, under the assumption that the observed depolarization was due to Faraday dispersion within the finite receiver bandwidth. It was shown that, if the effective bandwidth is B, then the dispersion angle  $\theta$ , in radians is related to the Faraday rotation as

$$\theta = 2B \Phi \nu_o^{-1} \quad \dots(1)$$

$$\text{where } \Phi = 2.36 \times 10^4 \nu_o^{-2} \int N(z) H_{||}(z) dz \quad \dots(2)$$

= the Faraday rotation, radians,

$\nu_o$  = the receiver center frequency, Hz,

B = effective bandwidth, Hz,

$N(z)$  = electron density,  $\text{cm}^{-3}$

$H_{||}(z)$  = the longitudinal component of the magnetic field, Gauss;

and  $z$  = the path length, cm.

Because of the dispersion in position angles, the measured polarization will differ from that at the source. The result would be that a wide bandwidth receiver would observe less linear polarization than a narrow - band receiver. For a Gaussian band, it can be shown that

$$\mu = \mu_o e^{-\theta^2/4} \quad \dots(3)$$

where  $\mu$  = the observed degree of coherence between the right and left circular components, and  $\mu_o$  = the degree of coherence between the two circular components at the source.

The complex correlation factor between the right and left circularly polarized components (R and L) of the radiation is related to the measured degree of polarization and the axial ratio by

$$\mu = m \cos 2\beta \cdot e^{i\gamma} / (1 - m^2 \sin^2 2\beta)^{1/2} \quad \dots(4)$$

where  $m$  = polarization fraction,

$\tan \beta = r$  = the axial ratio of the polarization ellipse,

$\gamma$  = phase angle between the R and L components of the radiation =  $2\chi(\nu_o)$

and  $\chi(\nu_o)$  = the orientation angle of the major axis of the polarization ellipse at the center frequency.

Since the time-sharing polarimeter at 35 MHz has been designed to record the Stokes parameters (I, Q, U and V) separately for each bandwidth, it is convenient to reduce polarization data in terms of the degree of polarization  $m$ , the axial ratio  $r$ , and the orientation angle  $\chi$ , of the polarization ellipse. Therefore, before applying Akabane and Cohen's theory for the determination of the Faraday rotation  $\odot$ , we calculate from equation (4), the

values of  $\mu_n$  and  $\mu_w$  using the experimentally measured values of  $m$  and  $r$  from the narrow and wide bandwidth polarization measurements respectively. If both the receiver passbands have a Gaussian shape, then it can be shown that

$$\mu_n / \mu_w = \exp \left[ -\frac{1}{4} (\theta_n^2 - \theta_w^2) \right] \quad \dots(5)$$

where 'n' and 'w' mean narrow and wide band respectively.

In terms of bandwidths, equation (5) can be written as

$$\mu_n / \mu_w = \exp \left[ -\theta_n^2 / 4 (1 - B_w^2 / B_n^2) \right] \quad \dots(6)$$

In this equation  $B_w$  and  $B_n$  are known and  $\mu_w$  and  $\mu_n$  are calculated. This allows  $\theta_n$  to be calculated from equation (6) and  $\Phi$  to be calculated from equation (1).

The other effect of the dispersion is the change in the shape of the polarization ellipse; an elliptically polarized wave tends to be reduced to circular plus random polarization. It can be shown that

$$\operatorname{cosec}^2 2\beta = 1 + (\mu / \mu_0)^2 \cot^2 2\beta_0 \quad \dots(7)$$

where  $r_0 = \tan \beta_0$  = the axial ratio at the source.

Substituting  $\mu_n$  or  $\mu_w$  for  $\mu$ , and correspondingly  $r_n$  or  $r_w$  for  $\tan \beta$ , one can calculate  $r_0$  from equation (7).

The degree of polarization at the source is related to the measured degree of polarization, the Faraday dispersion angle  $\theta$  and the axial ratio of the polarization ellipse at the source by the relation

$$m = m_0 \left[ e^{-\theta^2/2} + (1 - e^{-\theta^2/2}) \sin^2 2\beta_0 \right]^{1/2} \quad \dots(8)$$

Since  $r_o$  can be calculated from equation (7) and  $\theta$  is known,  $m_o$  can be computed from equation (8).

### 5.3 TYPICAL POLARIMETER RECORDINGS

Figure 5.1a shows a group of type III solar bursts which was observed at 35 MHz, between 0837 and 0842 U.T. on August 1, 1972, with a receiver bandwidth of 12.5 KHz. Figure 5.1b represents the same event but with a receiver bandwidth of 7.5 KHz. Prior to the onset of the bursts, there are three types of noise calibrations of the polarimeter. The calibration marked 'B' is due to the noise level corresponding to 10 mA current, in the diode noise generator, injected to the input of channel 'B' of the polarimeter (Figure 3.3), when channel 'A' is terminated by a 50 ohms resistor. Similarly, the calibration 'A' is carried out when channel 'B' is terminated by a 50 ohms resistor. The calibration "ISO-T" is carried out by feeding the same level of noise simultaneously to both the channels, so as to simulate "vertical linear polarization". It can be easily seen from the response of all the four channels I, Q, U and V that, the polarimeter displays appropriate deflections in case of all the three calibrations. Table 5.1 summarizes the Faraday rotation values for the bursts belonging to this group. It may be noted that the mean value of the Faraday rotation for this event is  $3.35 \times 10^3$  radians, the extreme values being  $2.9 \times 10^3$  and  $3.8 \times 10^3$  radians.

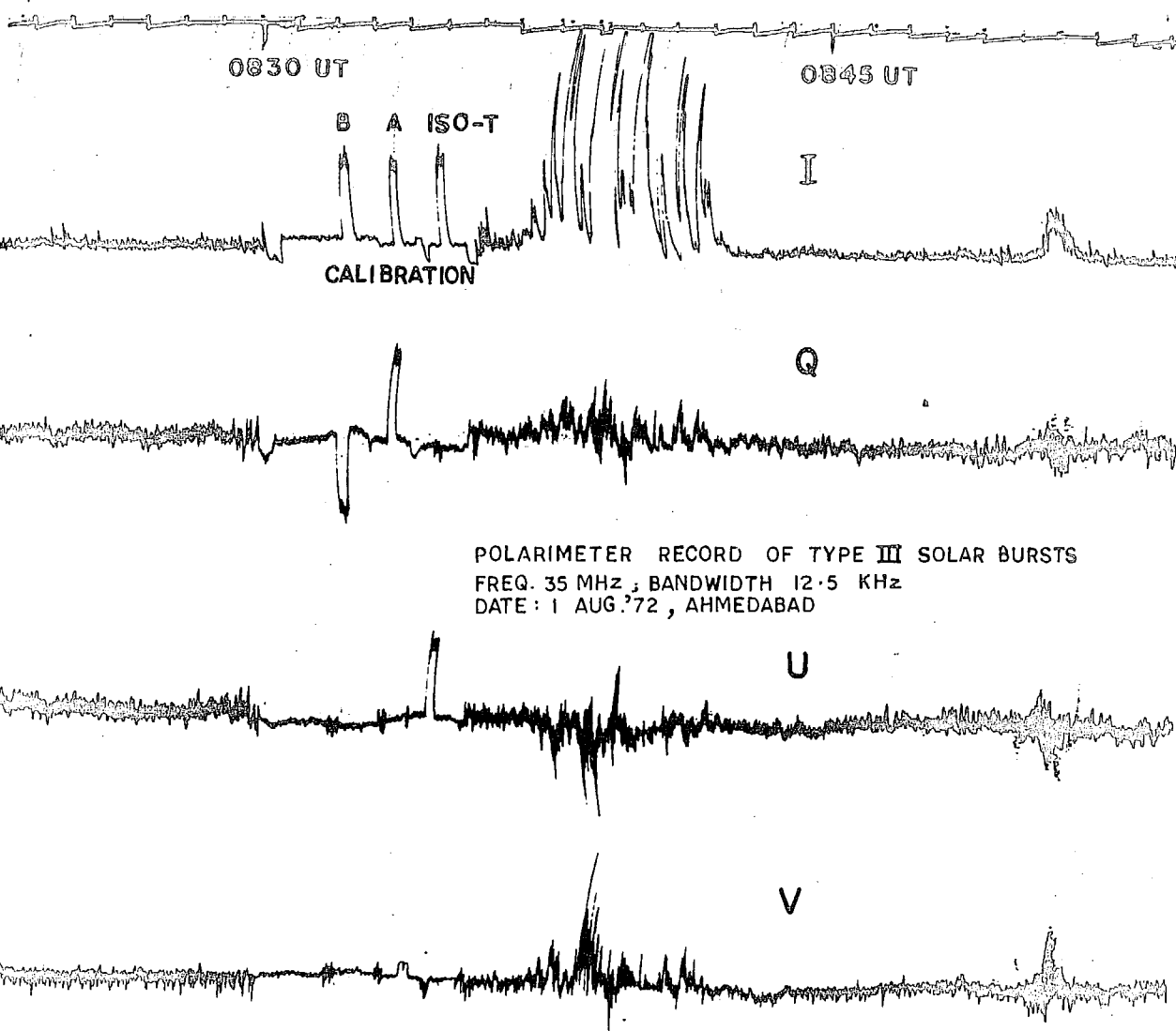


Figure 5.1a Polarimeter record on August 1, 1972 of a group of type III solar radio bursts at 35 MHz in a bandwidth of 12.5 KHz.

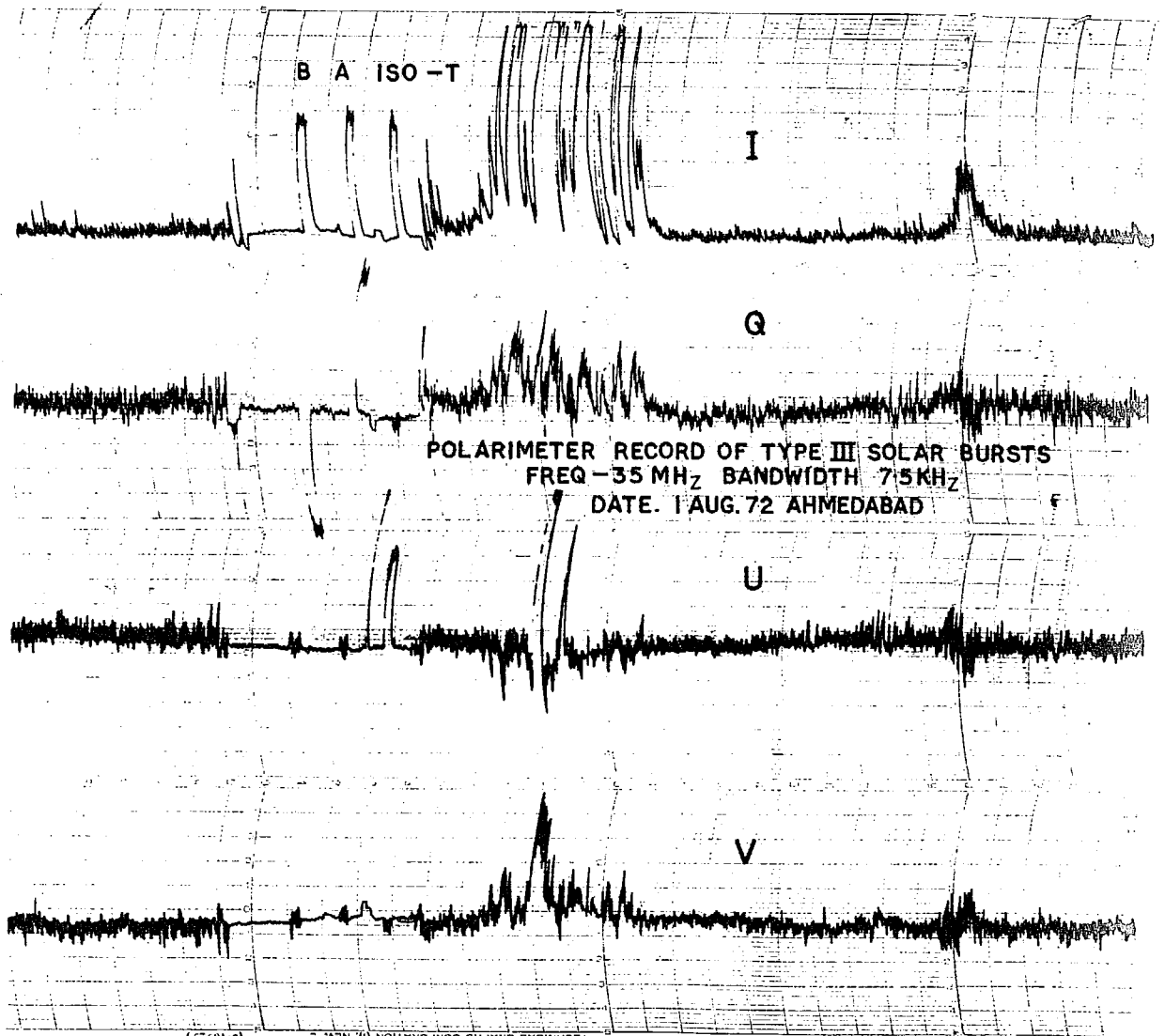


Figure 5.1b Polarimeter record on August 1, 1972  
of a group of type III solar radio bursts  
at 35 MHz in a bandwidth of 7.5 KHz,

T A B L E - 5.1 \*

SUMMARY OF THE FARADAY ROTATION DATA ( 1ST AUGUST, 1972)

Time (U.T.)	$m_n$	$r_n$	$m_w$	$r_w$	$\mu_n$	$\mu_w$	$\theta_n$ (radians)	$\phi$ ( $\times 10^3$ radians)
0837 30.0	0.63	0.12	0.30	0.19	0.45		1.34	3.1
0838 0.0	0.48	0.13	0.20	0.35	0.34		1.56	3.6
15.0	0.37	0.24	0.16	0.45	0.32		1.61	3.8
0839 0.0	0.53	0.22	0.20	0.35	0.32		1.60	3.7
0841 30.0	OFF SCALE		0.21	0.39				
37.0			0.18	0.52				
0842 0.0	0.41	0.36	0.25	0.50	0.47		1.31	3.0
15.0	0.45	0.30	0.30	0.47	0.51		1.23	2.9
22.0	0.36	0.18	0.22	0.41	0.46		1.32	3.1

\* Symbols used

- U.T. = Universal time
- $m_n, m_w$  = degree of polarization at 7.5 and 12.5 KHz respectively
- $r_n, r_w$  = axial ratio at 7.5 and 12.5 KHz respectively
- $\mu_n, \mu_w$  = degree of coherence between R & L components at 7.5 and 12.5 KHz respectively
- $\theta_n$  = the Faraday dispersion angle in 7.5 KHz bandwidth, radians
- $\phi$  = the Faraday rotation, radians



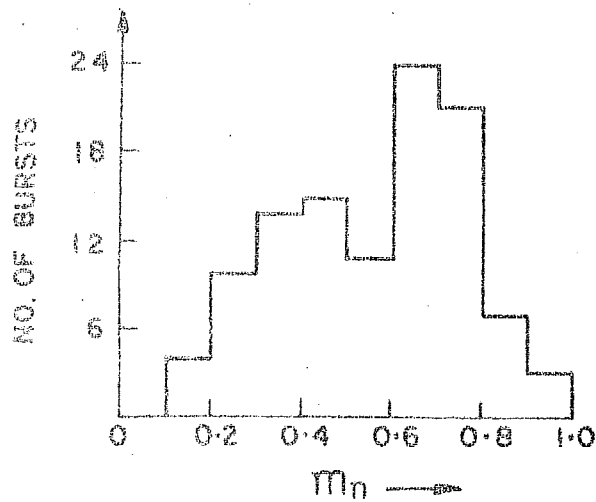
#### 5.4 RESULTS OF TWO-BANDWIDTH POLARIZATION MEASUREMENTS

Two-bandwidth polarization observations of solar bursts at 35 MHz started from July, 1972. We have analyzed data of type III bursts recorded during the period July, 1972 to April, 1973. During this period 73 bursts were identified by the Ahmedabad dynamic Radio spectroscopy as being type III's, which occurred either singly or in groups. Of the 73 type III events, only 44 were used for analysis; of these 13 were isolated type III bursts. Calculations were limited to those bursts, which had produced a deflection in the I-channel of more than 5 divisions, in order to minimize the scaling errors. All the bursts used for further analysis had a degree of polarization in either channel greater than 10 per cent. Polarization parameters of type III bursts were calculated only at peaks of the bursts on all the 8 channels. They were checked against noise generator calibrations by a procedure described in Chapter III. Various polarization parameters at the peaks of type III bursts could be evaluated for 106 bursts in both the wide and the narrow bandwidths, 109 bursts in narrow bandwidth and 121 bursts in wide bandwidth channels. In the following Sections we present the statistical distribution of various polarization parameters.

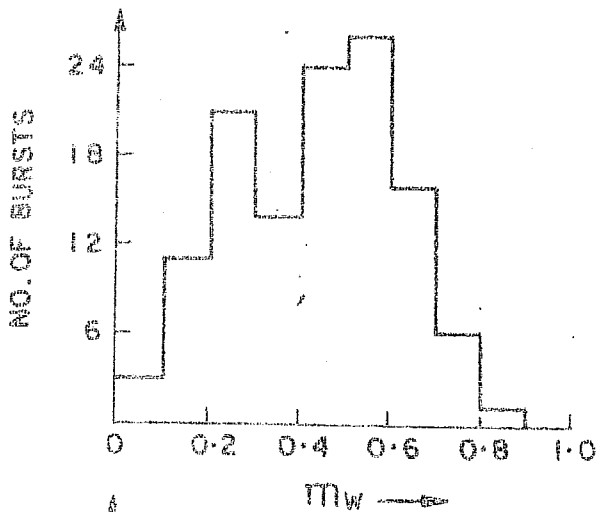
#### 5.41 DEGREE OF POLARIZATION

The distribution of  $m_n$  and  $m_w$ , the degrees of polarization in narrow (7.5 KHz) and wide (12.5 KHz) bandwidths are shown as histograms in Figure 5.2a - b respectively. In Table 5.2 we have shown the various statistical parameters together with their highest, lowest and average values. The degree of polarization in the narrow bandwidth ranges from 14 to 95 per cent whereas the average value is nearly 55 per cent. In the wide bandwidth, the degree of polarization varies from 5 to 87 per cent and the average value is 47 per cent. From Figure 5.2a - b, it is amply clear that the maximum number of type III bursts have polarization degree lying in the range of 60 to 80 per cent in the narrow bandwidth channel and 40 to 60 per cent in the wide bandwidth channel. Thus, the depolarization of the order of 20 per cent due to the larger bandwidth of the receiver is observed.

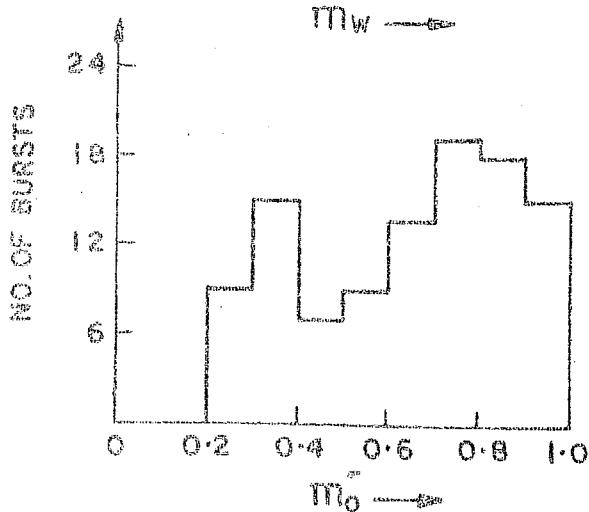
Having obtained the Faraday dispersion angle (as explained in Section 5.2), we calculated the polarization degree  $m_o$  at the source. Its statistical distribution is shown in Figure 5.2c. In Table 5.2 we have shown that the highest and the lowest polarization degree increased to 100 and 20 per cent respectively whereas the average value increased to 66 per cent. Referring to Figures 5.2a and b, a bimodal characteristics of the distribution of polarization



(a)



(b)



(c)

Figure 5.2 Polarization percentage at 35 MHz in two bandwidths (7.5 and 12.5 KHz) and at the source.

T A B L E - 5.2\*

HIGHEST, AVERAGE AND LOWEST VALUES  
OF VARIOUS POLARIZATION PARAMETERS

Polarization parameter	No. of bursts used for analysis	Highest	Average	Lowest
$m_n$	109	.94	.55	.14
$m_w$	119	.87	.47	<.05
$m_o$	98	1.0	.66	.20
$\mu_w / \mu_n$	"	0.97	.62	.27
$\theta_n$	"	1.73	.83	.35
$\phi$	"	$4.0 \times 10^3$	$1.9 \times 10^3$	$.9 \times 10^3$
$r_n$	109	.52	.18	<.05
$r_w$	121	.55	.24	<.05
$r_o$	106	.51	.13	<.05

\* Symbols are defined in Table 5.1

degree appears to be marginally significant. This bimodal character becomes more pronounced in the distribution of  $m_o$ , the polarization degree at the source. If this bimodal characteristics has any significance at all, then it implies that there may be two kinds of type III bursts, highly polarized and weakly polarized ones. This would require different physical conditions at the region where polarization is imposed on the type III burst radiation.

#### 5.42 CALCULATION OF FARADAY ROTATION AT 35 MHz

We have seen in the last section, that the polarization degree as measured with a wider bandwidth receiver has been less than that with a narrow bandwidth receiver. The same is true for the correlation factors  $\mu_w$  and  $\mu_n$  which can be calculated from  $m_w$ ,  $m_n$ ,  $r_w$  and  $r_n$  using equation (4). Our aim is to measure the Faraday dispersion angle  $\Theta$ , which requires the knowledge of the ratio  $\mu_w/\mu_n$  (equation (6)). This ratio is a measure of the depolarization caused by the receiver bandwidths. The values of  $\mu_w/\mu_n$  are plotted as a histogram in Figure 5.3. The average value of  $\mu_w/\mu_n$  is  $\approx 0.84$ . Only 32 bursts had  $\mu_w/\mu_n$  less than 0.7. The distribution curve of  $\mu_w/\mu_n$  at 200 MHz (Akabane and Cohen 1961) is somewhat similar to the one shown in Figure 5.3 for 35 MHz.

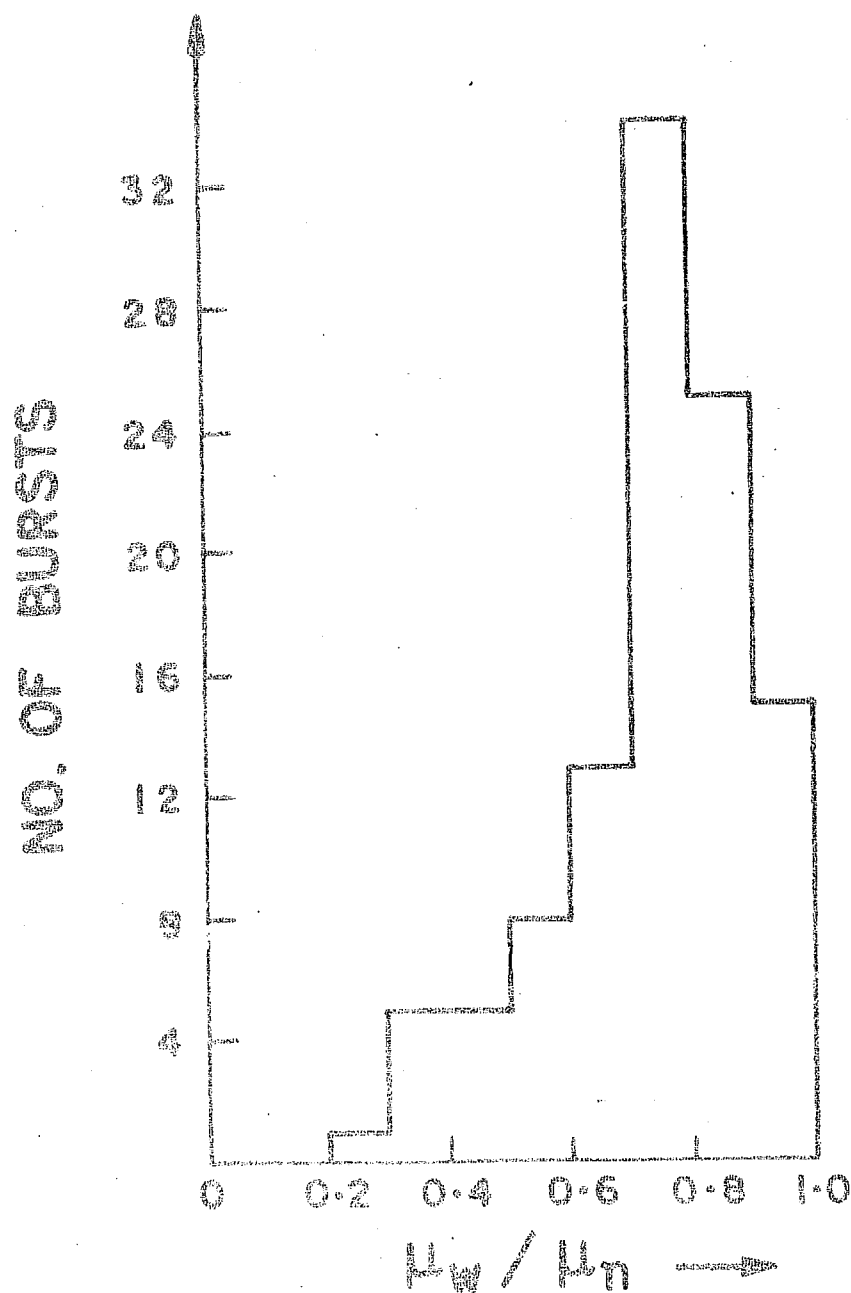


Figure 5.3 Ratio of correlation factor in wide bandwidth ( $\mu_w$ ) to the same in narrow bandwidth ( $\mu_n$ ).

Our determination of the Faraday rotation at 35 MHz is based on the following assumptions:

(1) the observed depolarization is due to the Faraday dispersion in position angles, (2) the receiver bandwidth is Gaussian in shape, (3) the polarization characteristics do not change drastically within the receiver bandwidth and during the integration time constant of the receiver.

The computed values of  $\mu_w / \mu_n$  allow  $\theta_n$  to be calculated from equation (6). These values of  $\theta_n$  are shown as histogram in Figure 5.4. The average value of

$\theta_n$  is about 0.83 radians, the extreme values being 0.35 and 1.73 radians. About 50 per cent of type III bursts have values of  $\theta_n$  between 0.4 and 1.1 radians. This grouping is significant because the decrease in the number of bursts with large  $\theta_n$  is not due to the decrease in the number of bursts with large  $m_0$  (see Figure 5.2a - c). It should be emphasized that if the number of bursts decreases as the polarization degree decreases then the number of bursts with large  $\theta_n$  should also show similar trend because a large value of  $\theta_n$  means a considerable depolarization.

From equation (1) the total amount of the Faraday rotation at 35 MHz is given by  $\Theta = 2.33 \times 10^3 \theta_n$  radians.

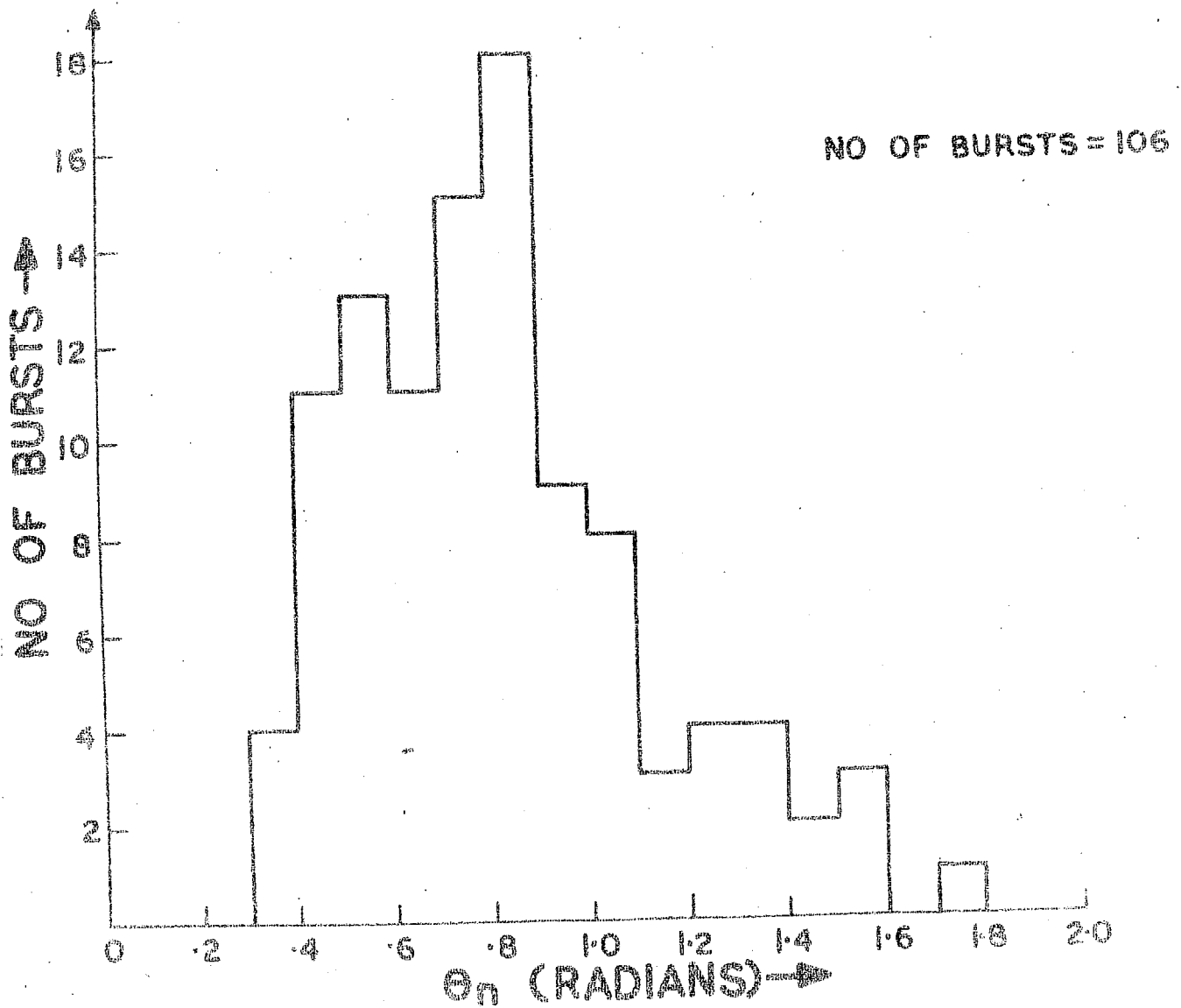


Figure 5.4 Faraday dispersion angle in narrow bandwidth.



Thus, the bursts with Faraday dispersion angle  $\theta_n$  ( $\approx 1$  rad.) shown in Figure 5.4 have suffered an amount of Faraday rotation of the order of  $2 \times 10^3$  radians, the extreme values being  $.9 \times 10^3$  and  $4 \times 10^3$  radians. It is of great interest to point out that Fokker (1971), while trying to reproduce the reported distribution of polarization degree and of axial ratio at 25 MHz (Chin et al. 1971) for the years, 1966, 1968, and 1969, from an assumed distribution of Faraday dispersion angles, obtained a value, for the Faraday rotation  $\Phi$ , of the order of  $10^5$  radians. But this value was based on the assumption that type III bursts were 100 per cent polarized at the source. This does not seem to be the case, because there are about 50 per cent bursts at 35 MHz which had a polarization degree less than 0.7 at the source. By contrast, Cohen (1959), by assuming that the source produces 100 per cent polarized radiation arrived at an upper limit on Faraday rotation at 200 MHz ( $2 \times 10^4$  radians), which is very close to the measured value at the same frequency (Akabane and Cohen 1961). This means that at higher frequencies, such as 200 MHz, the possibility, of the type III burst radiation at the source being fully polarized, is much greater than that at lower frequencies, say, at 35 or at 25 MHz. This idea, if valid, should have important consequences on the development of the theory of generation of type III bursts.

#### 5.43 AXIAL RATIO

The values of the axial ratios  $r_n$  of the polarization ellipses in the narrow bandwidth and  $r_w$  in the wide bandwidth are represented by histograms in Figures 5.5a and 5.5b respectively. From equation (7) values of the axial ratio of the polarization ellipse at the source are obtained and are shown as a histogram in Figure 5.5c. In Table 5.2, we have shown that the observed axial ratio in both the channels ranged from  $<0.05$  to about 0.55. The average value of the axial ratio was about 0.18 in the narrow bandwidth and 0.24 in the wide bandwidth channel. It can be seen from Figures 5.5a - b that there is a tendency for the number of bursts to decrease as the axial ratio (both in the wide and narrow bandwidth channels) increases from zero to 1. The sudden drop in the distribution of  $r_n$  and  $r_w$  beyond 0.25 is significant. It can be seen from Figure 5.5c that there is a significant clustering of the axial ratios (at the source) of the observed type III bursts between  $-0.15$  and  $+0.2$ . There were as many as 62 bursts, including 21 linearly polarized bursts, which had axial ratio less than 0.15. The same conclusions were reached in Chapter IV in which we have described the single bandwidth observations at 25, 35 and 74 MHz. Thus, our observations indicate that type III bursts are highly elliptically and linearly polarized

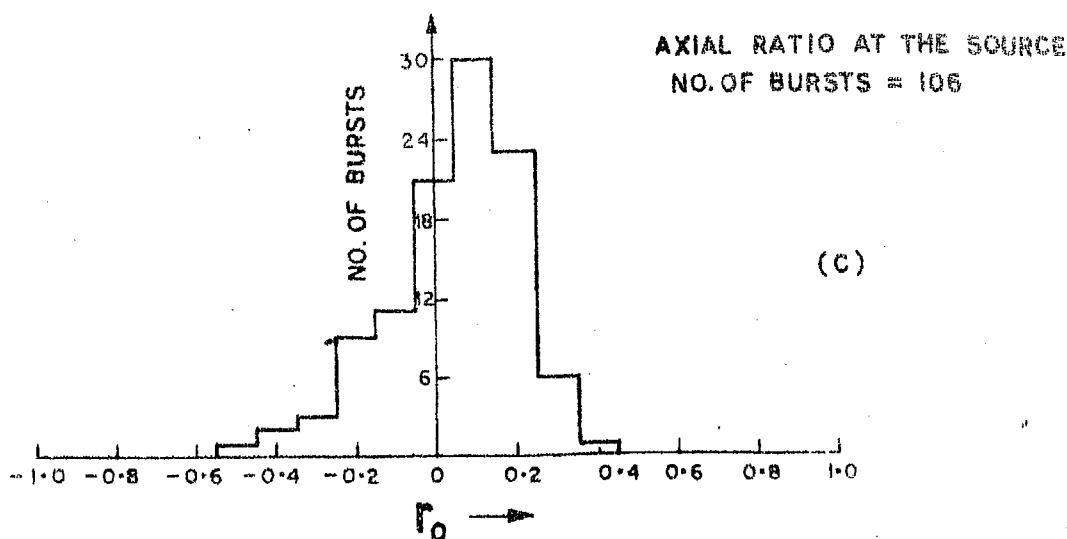
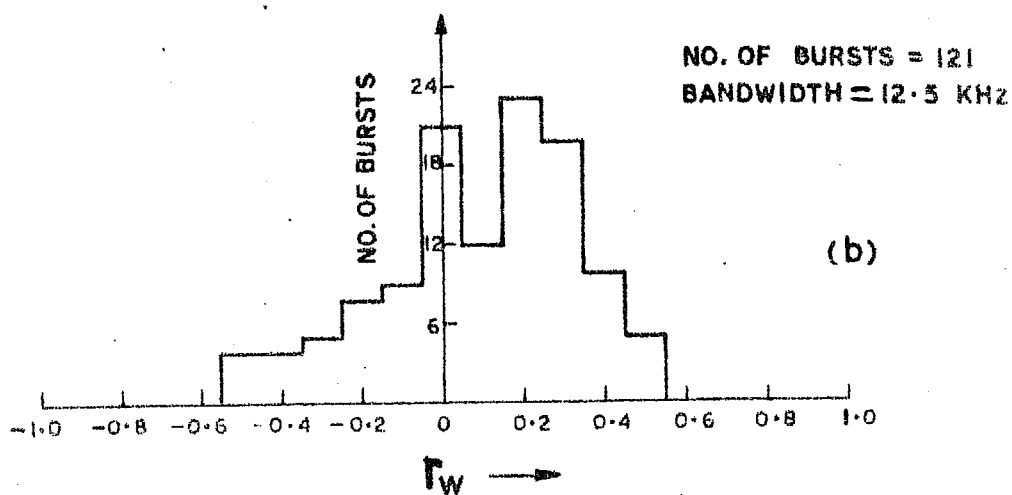
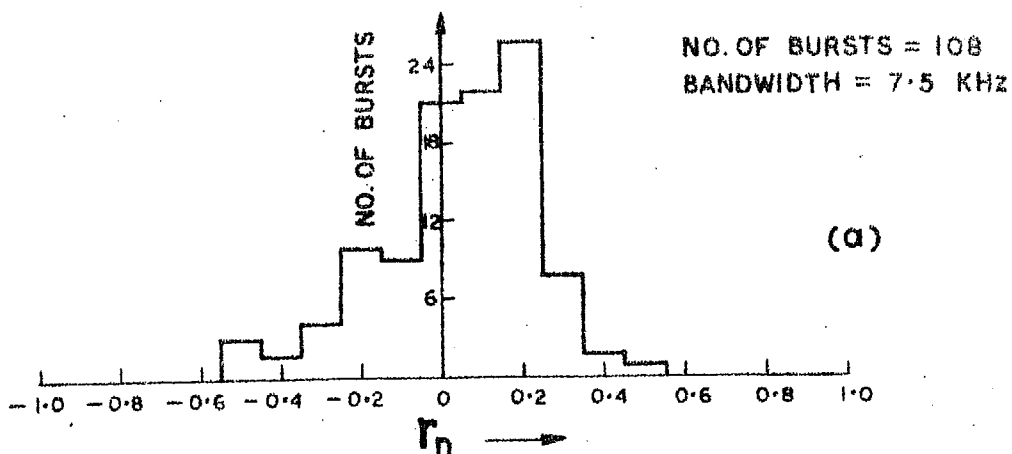


Figure 5.5 Axial ratio at 35 MHz in two bandwidths (7.5 and 12.5 KHz) and at the source.

bursts, in agreement with the narrow band observations of Chin et al.(1971) and Dodge (1972).

#### 5.44 ORIENTATION ANGLE

Figure 5.6a - b represents the distributions of the orientation angles  $\chi_n$  and  $\chi_w$  corresponding to the narrow and wide bandwidths channels respectively. It is clear from these figures that the orientations of these ellipses are not randomly distributed. The grouping in the orientation angles should be regarded significant in the sense that they represent a group of type III bursts which had orientations of the ellipses approximately the same for all the bursts of the group. This clustering of orientation angles has been reported by many authors (Cohen (1959) at 200 MHz, Bhonsle et al. (1967) at 26.3 and 22.2 MHz, Chin et al. (1969) at 25.3 MHz, Dodge (1972) at 34 MHz), and our observations (described in Chapter IV) at 25 and 35 MHz show similar trend for clustering.

#### 5.5 REPRESENTATION OF PARTIAL ELLIPTICAL POLARIZATION

A partially polarized wave can be regarded as a sum of unpolarized and polarized waves. An alternative way is to express it as a superposition of two independent fully polarized waves of intensities proportional to, say,  $C_1$  and  $C_2$ , with equal and opposite values of the axial ratio  $r$ , and perpendicular orientations (Fokker 1971).

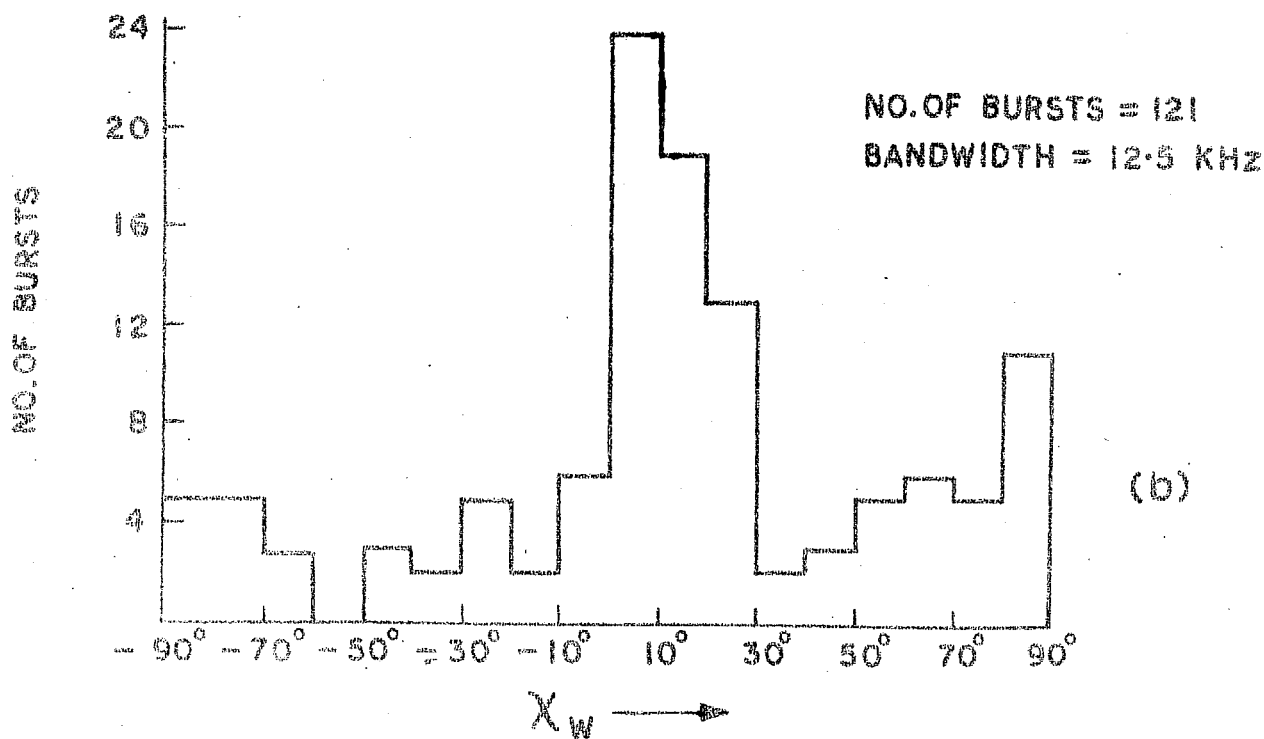
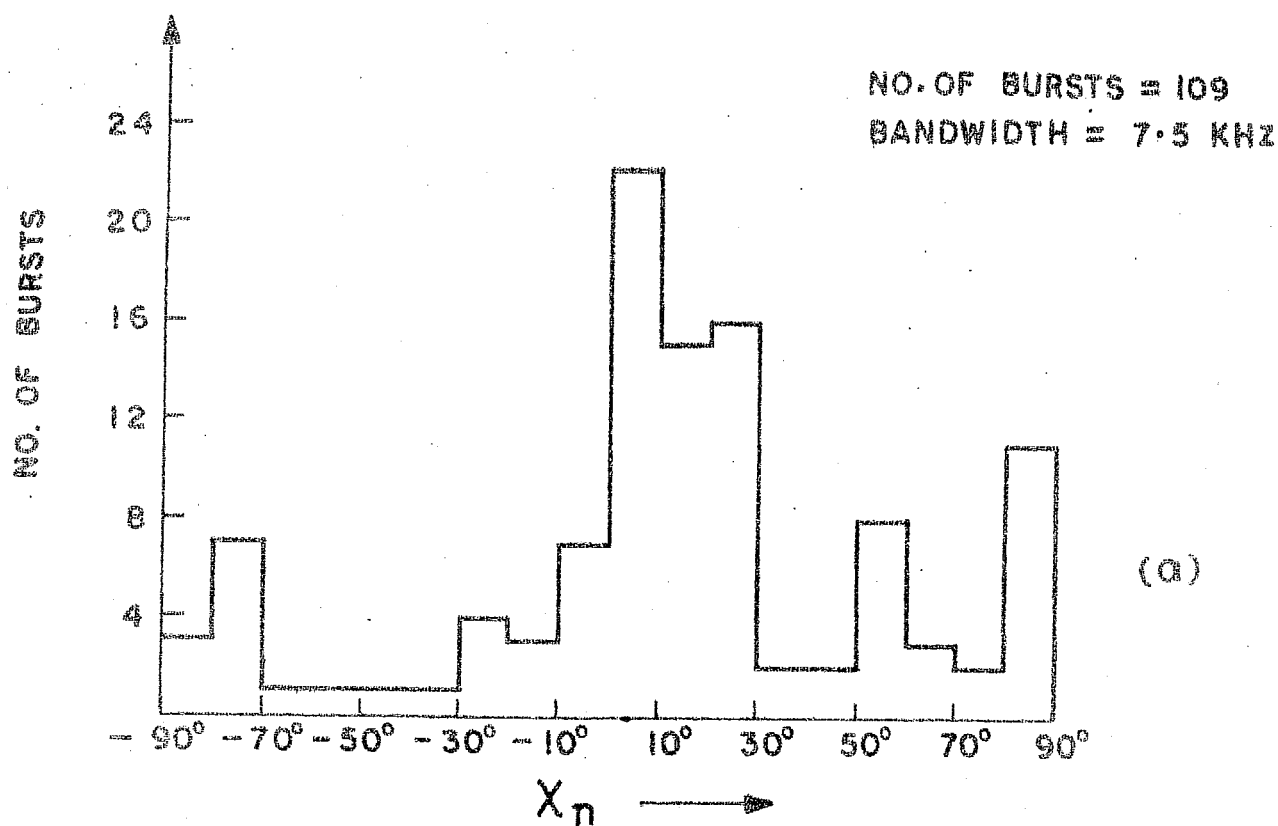


Figure 5.6 Orientation angle at 35 MHz in two bandwidths (7.5 and 12.5 KHz).

He pointed out that, for a degree of polarization greater than  $1/\sqrt{2}$ , one can always derive just as well, from the same set of Stokes parameters, a combination of two incoherent polarized signals, one circularly and the other linearly polarized. This superposition is equivalent to the superposition of an elliptically polarized signal and an unpolarized signal.

The circular polarization states can be represented in terms of Stokes parameters as

$$S_1 = \begin{bmatrix} I \\ 0 \\ 0 \\ V \end{bmatrix} \quad \text{for left circular, or} \quad \begin{bmatrix} I \\ 0 \\ 0 \\ -V \end{bmatrix} \quad \text{for right circular} \quad \dots (9)$$

$$\text{such that } I = |V|$$

Similarly, the linearly polarized state can be represented as

$$S_2 = \begin{bmatrix} I \\ Q \\ U \\ 0 \end{bmatrix} \quad \dots (10)$$

$$\text{such that } I = (U^2 + Q^2)^{1/2}$$

If the two beams are incoherent, the resultant Stokes parameters can be obtained by the scalar addition of the equations (9) and (10). Let us add equations (9) and (10) in proportion to  $C_1 : C_2$ , then

$$S = C_1 S_1 + C_2 S_2 = \begin{bmatrix} (C_1 + C_2) I \\ C_2 Q \\ C_2 U \\ \pm C_1 V \end{bmatrix} \quad \dots (11)$$

From equation (11) it can be easily shown that if such a superposition yields a polarization ellipse with the axial ratio  $r = \tan \beta$  ( $< 1$ ), then the degree of polarization  $m_f$  (Fokker 1971) is related to the axial ratio as

$$m_f^2 = \frac{(1 + \tan^2 2\beta)}{(1 + |\tan 2\beta|)^2} = \frac{C_1^2 + C_2^2}{(C_1 + C_2)^2} = m_c^2 + m_l^2 \dots \dots (12).$$

where the degree of circular polarization  $m_c = C_1/(C_1 + C_2)$ , and the degree of linear polarization,  $m_l = C_2/(C_1 + C_2)$ .

The ratio of  $C_1$  to  $C_2$  is related to the axial ratio as

$$C_1/C_2 = \tan 2\beta \dots (13)$$

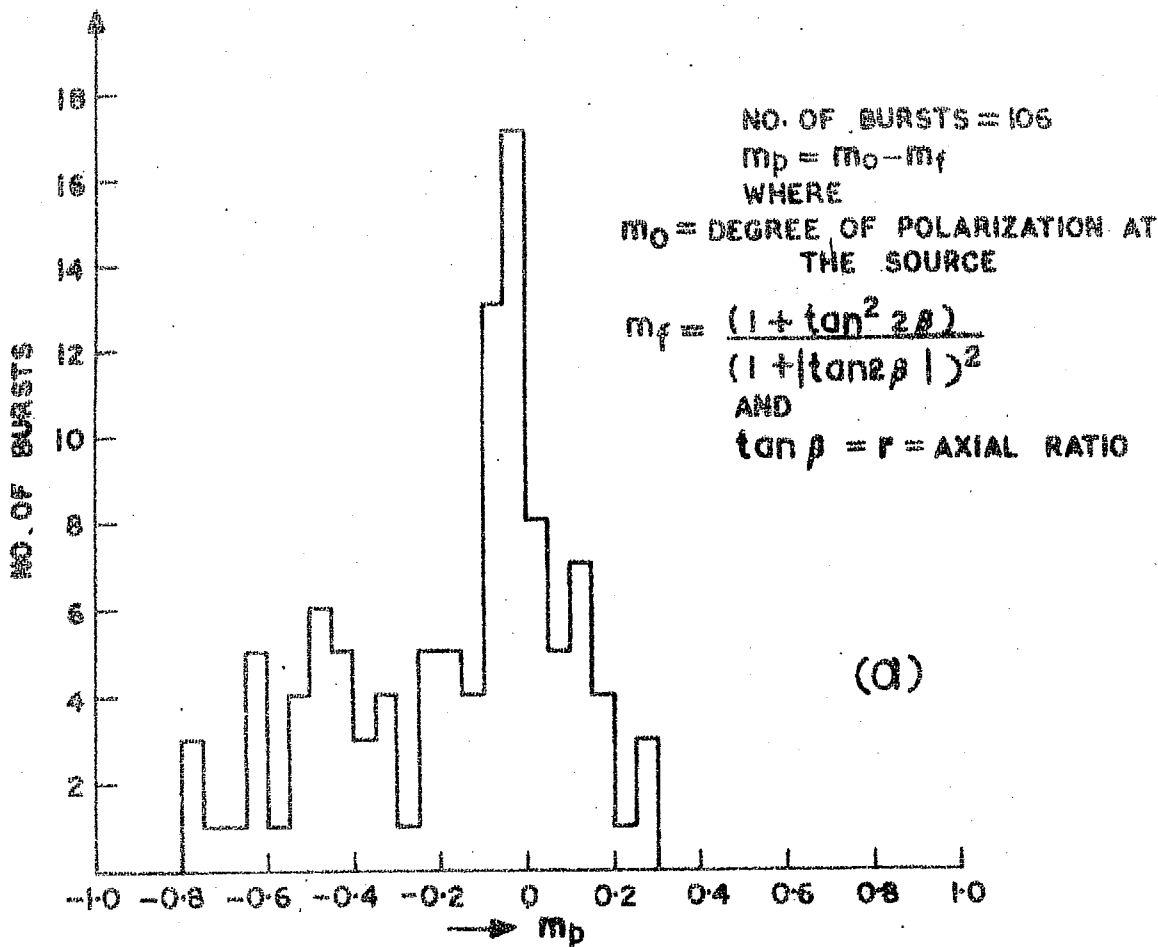
It should be emphasized that the minimum value of  $m_f$  is  $1/\sqrt{2}$ . One may, in principle, write the relation  $m_f^2 = m_c^2 + m_l^2$  for  $m_f < 1/\sqrt{2}$ ; but it is certain that the Stokes parameters representing the circular and linear components do not satisfy the additive property of Stokes parameters for  $m_f < 1/\sqrt{2}$ . In other words, it is impossible to reduce a polarization ellipse fully to a superposition of two incoherent circularly and linearly polarized signals for  $m_f < 1/\sqrt{2}$ .

It would be of interest to know whether type III burst emission can be represented in terms of a mixture of two mutually incoherent circularly and linearly polarized signals. For this, all that we have to do is to see whether relation (12) holds good in the case of type III

polarized radiation. Relation (12) can be verified only if the observed polarization degree and the axial ratios are corrected for the Faraday dispersion effect.

In Figure 5.7a, we have shown the values of  $m_p = m_o - m_f$ , as a histogram, where  $m_f$  is calculated by making use of the relation (12) and  $m_o$  is the polarization degree at the source. It is clear from Figure 5.7a that the values of  $m_p$  are not evenly distributed. The sudden cut-off beyond  $m_p = 0.3$  is because  $m_f$  ranges between 0.7 and 1. The same conclusions can be reached from the correlation diagram (Figure 5.7b) in which we have plotted the polarization degree at the source  $m_o$  against the difference between  $m_o$  and  $m_f$ . It is seen that a great majority of type III bursts have  $m_p < 0$ . This is because of the fact that, 50 per cent of type III bursts have polarization degree of less than 0.7 at the source and that  $m_f$  can never be less than  $1/\sqrt{2}$ . The very fact that there exists a correlation between  $m_p$  and  $m_o$  and that a large number of type III bursts have the observed polarization degree of less than 0.7, defeats the argument that type III radio emission can be represented in terms of a mixture of two mutually incoherent, circularly and linearly, polarized signals. However, the fact, that there are as many as 43 bursts out of 106 analyzed bursts, which have values of  $m$  less than  $\pm .1$ , cannot be ignored.





# CORRELATION DIAGRAM

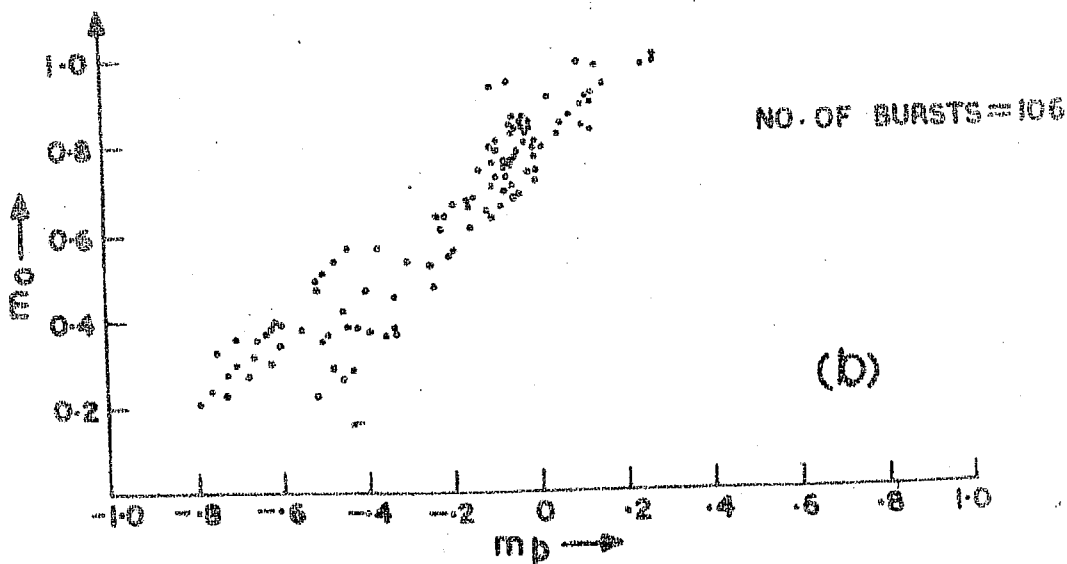


Figure 5.7 Representation of elliptically polarized type III bursts in terms of two mutually incoherent 100 per cent linearly and circularly polarized radiation.

This means that, at the very least, the representation in terms of two above-mentioned incoherent components may be possible in case of highly polarized bursts. Although there is an evidence for double sources (Labrum 1971) and multiple sources (Kai 1969a, McLean 1970) of type III bursts, the assumption that type III emission would be generated as a superposition of two incoherent components looks very artificial.

#### 5.6 INTERPRETATION OF RESULTS OF FARADAY ROTATION MEASUREMENTS

The Faraday rotation of the plane of polarization occurs in the intervening magnetoionic medium, which includes the solar corona, the interplanetary medium and the earth's ionosphere. Our estimate shows that about 10 per cent of the total Faraday rotation ( $\approx 2 \times 10^3$  radians) at 35 MHz can occur around noon in the earth's ionosphere, which is of the order of 100 radians. Contribution to the total Faraday rotation by the interplanetary medium is still less ( $\approx 10$  radians). Thus, about 85 to 90 per cent of the total Faraday rotation must occur in the vicinity of the source. It should be pointed out that the telescope-type of polarimeter, which has been used for 35 MHz observations, has a limitation in that it cannot measure the burst polarization with sufficient angular resolution. This is important because the burst source itself may have fine angular structure (Erickson 1962, Kai 1969, Wild 1970) with different polarizations

resulting in the reduction of the net degree of polarization.

Knowing the amount of Faraday rotation suffered by type III burst radiation while passing through the intervening magneto-ionic medium, one could correct for the effect of depolarization and changes in the axial ratio and talk about the polarization state at the source region provided that the following two conditions are satisfied:

- (1) Differential absorption between the ordinary and extra-ordinary modes is small between the source and the observer.
- (2) Mode coupling is weak along the entire propagation path.

By source region we mean the spatial region where electro-magnetic radiation emerges from the corona. Therefore, the polarization properties of type III burst radiation could be the resultant properties of the polarization intrinsic to the generating mechanism modified by the escape conditions (Fomichev and Chertok 1968b). We would like to emphasize that the conditions (1) and (2) mentioned above are related to the propagation characteristics outside the source region. These conditions are discussed below in detail.

5.61 DIFFERENTIAL ABSORPTION

For  $\omega \gg \omega_1$ , where  $\omega$  is the radiation frequency and  $\omega_1$  is the longitudinal component of the gyro-frequency, the differential absorption between the ordinary and extraordinary modes is proportional to  $\omega_1/\omega^3$  (Lawrence et al. 1964). This differential absorption, which changes the state of polarization of the resultant wave, decreases very rapidly with the wave frequency and has direct dependence on the electron cyclotron frequency. If one assumes that the electron cyclotron frequency at the source region and/or along the propagation path, is small compared to the wave frequency, then the resultant differential absorption through the solar corona is small (Fung and Yip 1966). The analysis by Chin et al. (1969), showed that type III bursts are associated with flares with small area. They maintained that the magnetic fields at type III sources would probably be significantly weaker than those at a type I or a type II source, under the assumption that smaller flare regions would produce weaker coronal magnetic fields. Hence, it would be reasonable to assume that the electron cyclotron frequency is much smaller than the wave frequency along the entire propagation path in the solar corona.

Assuming that the polarization characteristics of type III bursts arise due to the conditions of escape,

Fomichev and Chertok (1968b) have shown that the longitude dependence of the mean value of polarization degree can be satisfactorily explained regardless of the possible contribution of the differential absorption to the degree of polarization of type III bursts. This has been discussed in Chapter I in some detail. Thus, it seems then, that the differential absorption in the solar corona at a given frequency is negligible at all longitudes.

The differential absorption of the radio waves at 35 MHz in the ionosphere is of the order of  $10^{-2}$  db (Lawrence et al. 1964), which is very small. Thus, the change in the polarization characteristics of type III bursts, due to the effects of the differential absorption in the ionosphere, is negligible.

#### 5.62 MODE COUPLING

When a radio wave travels through a magneto-ionic medium, it splits into two different characteristic waves generally referred to as 'ordinary' and 'extraordinary' waves, which propagate independently. Each characteristic wave has a complex refractive index and a state of polarization whose values are given by the magneto-ionic theory (Ratcliffe 1959), when the magneto-ionic medium is assumed homogeneous. It is often possible to assume that the characteristic wave propagate independently in a slowly varying medium (Booker 1936). Then the features of a

single characteristic wave, including state of polarization, change as it moves from point to point in the medium. It means that there will be Faraday rotation and that the polarization rotation will reverse whenever the longitudinal component of the magnetic field changes its direction. When the medium is changing more rapidly, the simple theory no longer applies. Independence of the propagation of the characteristic waves breaks down if the magnetoionic medium is inhomogeneous. This causes the two forward modes to get tightly coupled and there will be no Faraday rotation. In this coupling region, the polarization parameters also change. Thus, it should be emphasized that it is very important to know whether the radiation has passed through a coupling region or not.

The most important cases where the coupling occurs are the following (Budden 1952):

1. Regions where the polarization of a characteristic wave varies markedly in a short distance, even though the constants of the region are slowly varying.
2. If the constants of the magnetoionic medium vary markedly in a distance small compared with one wavelength, in such a way that the polarization of a characteristic wave also varies markedly.
3. Where the electron density is very small, the refractive indices for the two characteristic modes are

very nearly equal. Here the coupling effect is cumulative.

The coupling region can exist either in the earth's ionosphere or in the solar corona. For the ionosphere, the coupling theory has been developed by Budden (1952) on the assumption that the magnetic field is constant and both the electron density and the collision frequency are variable. In the sun's atmosphere, however, the most variable parameter is the magnetic field. This case has been treated by Cohen (1960). It is shown that mode coupling occurs most effectively when the electromagnetic waves propagate in a direction transverse to the local static magnetic field (Cohen 1960). The electromagnetic waves emitted from a type III source region may meet a transverse magnetic field configuration either in the solar corona or in the earth's ionosphere.

#### 5.63 MODE COUPLING IN THE EARTH'S IONOSPHERE

The directions in the sky in which the rays from the sun pass strictly transverse to the earth's magnetic field can be found by following the method used by Chapman (1952). For Ahmedabad station (geom. lat.  $18^{\circ}\text{N}$ , long.  $0.5^{\circ}\text{W}$  geog. lat.  $23.0^{\circ}\text{N}$ , long.  $74.0^{\circ}\text{E}$ ) the fraction of the visible sky for which the rays have transverse intersections with the earth's magnetic field is of the order of 0.75 (Cohen and Dwarkin 1961). We have calculated perpendicular intersections for the rays coming from the sun with

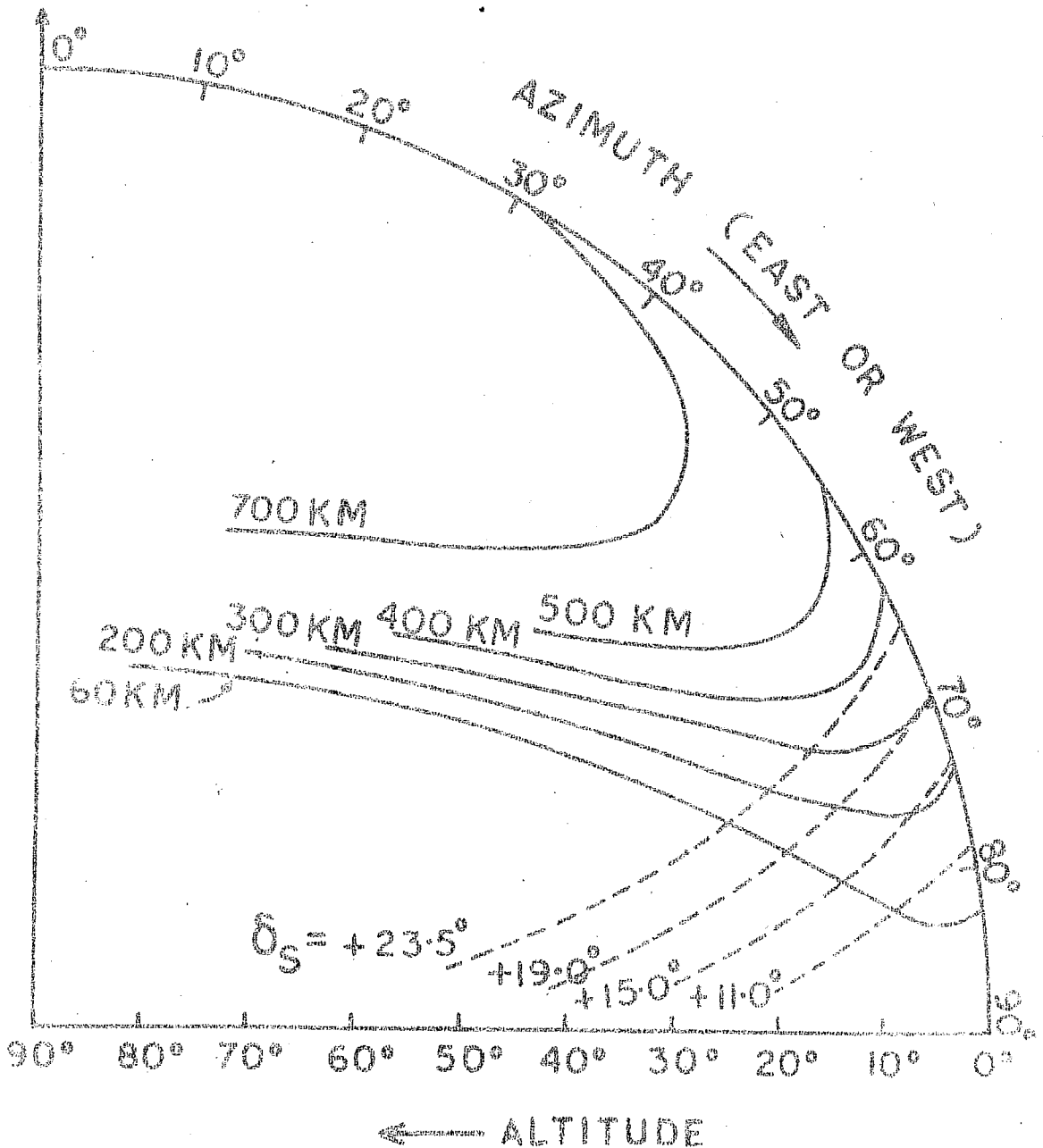
the geomagnetic field at different heights in the ionosphere. These are plotted in Figure 5.8, where the azimuth is to be measured from the magnetic north. The calculated track of the sun is translated into geomagnetic coordinate system and plotted on the same figure. Since the geomagnetic declination is only  $0.5^{\circ}\text{W}$ , the evening track of the sun in the Figure 5.8 lies very close to the morning track and, therefore, it is not plotted separately. It can be seen from Figure 5.8 that perpendicularity conditions are more favourable in the evenings and mornings than those at other times. This means that the rays from the sun will not encounter transversely the earth's magnetic field during the observation period of about two hours before and after the local noon. We have selected only those bursts for analysis which occurred during about two hours before and after the local noon (as described in Chapter IV) and, therefore, these observations were unaffected by mode coupling in the ionosphere.

#### 5.64 ESTIMATE OF THE CORONAL MAGNETIC FIELD

We make use of equation (2) to estimate the coronal magnetic field by using the measured values ( $\sim 10^4$  radians) (Akabane and Cohen 1961) and ( $10^3$  radians) (Bhonsle and Mattoo 1973) of Faraday rotation at 200 and 35 MHz respectively. For simplicity the corona is assumed spherical. We use the electron density model, of Hansen et al. (1969)



MAGNETIC  
NORTH  
POLE



- Locus of perpendicularity point for different heights of the ionosphere.
- - - - - Track of the sun at different declinations.

Figure 5.8 Calculation for sun's rays perpendicular to the earth's magnetic field for Ahmedabad station.

for the corona, which is given by

$$N(\rho) = 4 \times 10^4 + 4.32/\rho \quad \dots(14)$$

where  $\rho$  is the heliocentric altitude in solar radii. We have adopted height dependence in the inner solar corona as  $\rho^{-3}$  for  $H_{||}(\rho)$ , the component of the magnetic field along the direction of the ray. The coronal levels for 200 and 35 MHz radiations are calculated from equation (14) using  $N(\rho) = 5 \times 10^8 \text{ cm}^{-3}$  for 200 MHz and  $N(\rho) = 2 \times 10^7 \text{ cm}^{-3}$  for 35 MHz. The heliocentric altitude in solar radii from the above model turns out to be  $\rho_1 = 1.25$  for 200 MHz and  $\rho_2 = 2.0$  for 35 MHz emission levels. Let  $\Phi_1$  and  $\Phi_2$  represent the amount of the Faraday rotation at  $\nu_1 = 200$  and  $\nu_2 = 35$  MHz respectively. One can show from the equation (2) that

$$\Phi_1 \nu_1^2 - \Phi_2 \nu_2^2 = 2.36 \times 10^4 R_{\odot} \int_{\rho_1}^{\rho_2} N_1(\rho) H_{||}(\rho) d\rho \quad \dots(15)$$

where  $R_{\odot} = 7 \times 10^5 \text{ km}$ , the radius of the sun. Knowing that the Faraday rotation  $\Phi_1$  at 200 MHz is of the order of  $2 \times 10^4$  radians and at 35 MHz it is of the order of  $2 \times 10^3$  radians, and evaluating the integral in the equation (15), one can find out the value of the longitudinal component of the magnetic field at any coronal level between  $\rho_1 = 1.25$  and  $\rho_2 = 2.0$ . The value of the

magnetic field turns out to be of the order of 0.03 Gauss at  $\rho_1 = 1.25$  which is rather a low value.

Because the ray suffers the largest amount of the Faraday rotation near the plasma level, the above computations show that the measured values of the Faraday rotation give either a low value of the coronal magnetic field at the source region or else the thickness of the source region is small, which is about 1000 km at 200 MHz (Akabane and Cohen 1961). If brief, one has to then explain why the observed value of Faraday rotation is low by at least one order of magnitude at 200 MHz and two orders of magnitude at 35 MHz. One possible explanation for the observed low values of the Faraday rotation at 200 and 35 MHz is to introduce a mode coupling region, that is a transverse magnetic field configuration somewhere in the corona in the path of the radiation coming from the source region.

#### 5.65 MODE COUPLING IN THE SOLAR CORONA

The coupling region cannot be put very far from the plasma levels where the radiation originates, because then the difficulty about explaining the observed values of Faraday rotation at 200 and 35 MHz remains unexplained. In other words, it means that the radiation, immediately after emerging from the source region, due to some reasons, finds a strongly coupling region at a certain coronal level near the source region and then beyond this region, coupling

becomes weak so that both the ordinary and extraordinary modes can independently propagate and thus suffer Faraday rotation. Cohen (1960) has developed a theory for magneto-ionic mode coupling. In the quasi-longitudinal case (QL), there is a 'transitional' frequency  $\nu_t$  such that, when  $\nu \ll \nu_t$ , the modes are weakly coupled, and when  $\nu \gg \nu_t$ , there is a strong coupling. In the ionosphere and in the interplanetary and interstellar regions,  $\nu_t$  is  $\simeq 10^{12} - 10^{14}$  Hz; thus the magneto-ionic modes at radio frequencies are always weakly coupled in QL regions.

In quasi-transverse (QT) regions, the coupling can be much stronger and an estimate of  $\nu_t$  is on the order of tens of megahertz in the ionosphere and  $\simeq 10^4 - 10^6$  Hz in the interplanetary and interstellar regions. Thus we have to assume that the radiation meets a QT region but is received in QL regions to explain the observed low value of Faraday rotation. And in the QT region the transitional frequency  $\nu_t$  should be very much less than the plasma frequency of the coronal level where the source region lies. The following computations show that it may not be difficult to obtain a QT transitional frequency  $\nu_t$  of 200 MHz at  $\rho_1 = 1.25$  and of 35 MHz at  $\rho_2 = 2.0$ .

In the QT conditions, the transitional frequency is given as (Cohen 1960),

$$\nu_t^4 = 10^{17} \text{ NSH}^3 \quad \dots (16)$$

where  $\nu_t$  is in Hz,  $N$  in  $\text{cm}^{-3}$ ;  $S$ , the scale of the magnetic field, in cm, and  $H$ , the magnetic field, in Gauss. It should be pointed out that  $S$  is not the same as the scale height given by the gradient of magnetic field. Rather it is a reciprocal of the derivative of the angle between the ray and the magnetic field.

The value of  $S$  is calculated from the field due to a force-free dipole buried  $0.02R_\odot$  (Correll et al. 1956, Cohen 1959) below the photosphere. The pertinent parameters are  $\alpha$ , the angle between the dipole axis and the direction of the source;  $\theta$ , the polar angle to the earth from the source assuming that the line to the earth is in a magnetic meridian plane. We assumed that the sources at different frequencies are point sources. The positions of sources at different frequencies are indicated in Table 5.3. We considered two values of  $\alpha$ ,  $30^\circ$  and  $60^\circ$ . For calculations of  $S$  we followed the method given by Cohen (1961). In Table 5.3, we have shown the calculated values of  $S$  at 200, 74 and 35 MHz for two values of  $\alpha$ ,  $30^\circ$  and  $60^\circ$ . It is seen that  $S$  does not change much from  $\alpha = 30^\circ$  to  $\alpha = 60^\circ$ . For  $\alpha = 30^\circ$ , the estimated values of  $S$  is about  $0.36R_\odot$  for a source at  $\rho_1 = 1.25$  and  $0.82R_\odot$  for a source at  $\rho_2 = 2.0$ .

From the known values of  $\theta$ , one can compute the resulting values of  $\theta$  giving the directions of the rays

T A B L E - 5.3  
SCALE OF THE MAGNETIC FIELD AND ELECTRON  
DENSITY AT VARIOUS FREQUENCIES

Frequency in MHz	Source position from the centre of the sun, in solar radius	Electron density, (cm) <sup>-3</sup>	Angle between the dipole axis and the line joining dipole and the source	Distance of the source from the dipole axis, in solar radius	Scale of the magnetic field, in solar radius
200	1.3	5 x 10 <sup>8</sup>	30° 60°	.55 .70	.36 .46
74	1.5	6.7 x 10 <sup>7</sup>	30° 60°	.74 .97	.48 .64
35	2.0	2 x 10 <sup>7</sup>	30° 60°	1.24 1.46	.82 .97

meeting, at some level in the corona, perpendicularly to the force-free buried dipole field. The ray can be nearly perpendicular to the magnetic field at the source region itself. Thus, in the estimation of H, we have used the values of N at the source regions, that is, at the respective plasma levels of 200 and 35 MHz type III burst radiation. In Table 5.3 we have shown electron density at various coronal levels.

Substitution of the values of N, S and  $\nu_t$  in equation (16) show that at  $\varphi_1 = 1.25$  we require a magnetic field of 0.1 Gauss to obtain  $\nu_t \simeq 200$  MHz, and at  $\varphi_2 = 2.0$ , a magnetic field of  $2 \times 10^{-2}$  Gauss to get  $\nu_t \simeq 35$  MHz. These values seem to be on the order of dipole field values of the sun at the respective levels, though certainly small compared to the dipole field values, but then one can adjust the values of N to obtain the required value of  $\nu_t$  and a more reasonable value of H.

Thus, the above calculations show that reasonable values of N, S and H can be found in the solar corona so as to let the mode coupling occur at various coronal levels. It is quite important to know the extent and/or the position of the coupling regions at various coronal levels.

5.66 THE EXTENT AND/OR POSITION OF THE MODE COUPLING REGIONS

In what follows simple calculations are made to examine what should be the extent and/or positions of the mode coupling regions at various coronal levels.

We make use of equation (2) to estimate the Faraday rotation suffered by the radiation at 200, 74 and 35 MHz by using an adopted model for the electron density and the coronal magnetic field. We adopted the following coronal model.

Upto  $\vartheta = 2$ , we used Newkirk's (1961) electron density model above an active region. Beyond  $\vartheta = 2$ , we extrapolated  $(N - \vartheta)$  curve in such a way that it runs more or less parallel to the model given by Van de Hulst (1950) for the equatorial corona. The curve is connected with densities given by Blackwell (1956) for  $\vartheta > 6$ . The model of Blackwell is followed upto  $\vartheta = 16$ . Beyond  $\vartheta = 16$  we adopted the proportionality  $N \sim \vartheta^2$  (Fokker 1965b). This model is shown in Figure 5.9.

For  $H_{||}$ , the component of the magnetic field along the direction of propagation, we adopted the following models:

1. The magnetic field of 0.25 Gauss at a height of 0.25  $R_{\odot}$  above the photosphere was assumed (Fokker 1971). Two assumptions were made as regards the height dependence of  $H_{||}$  :



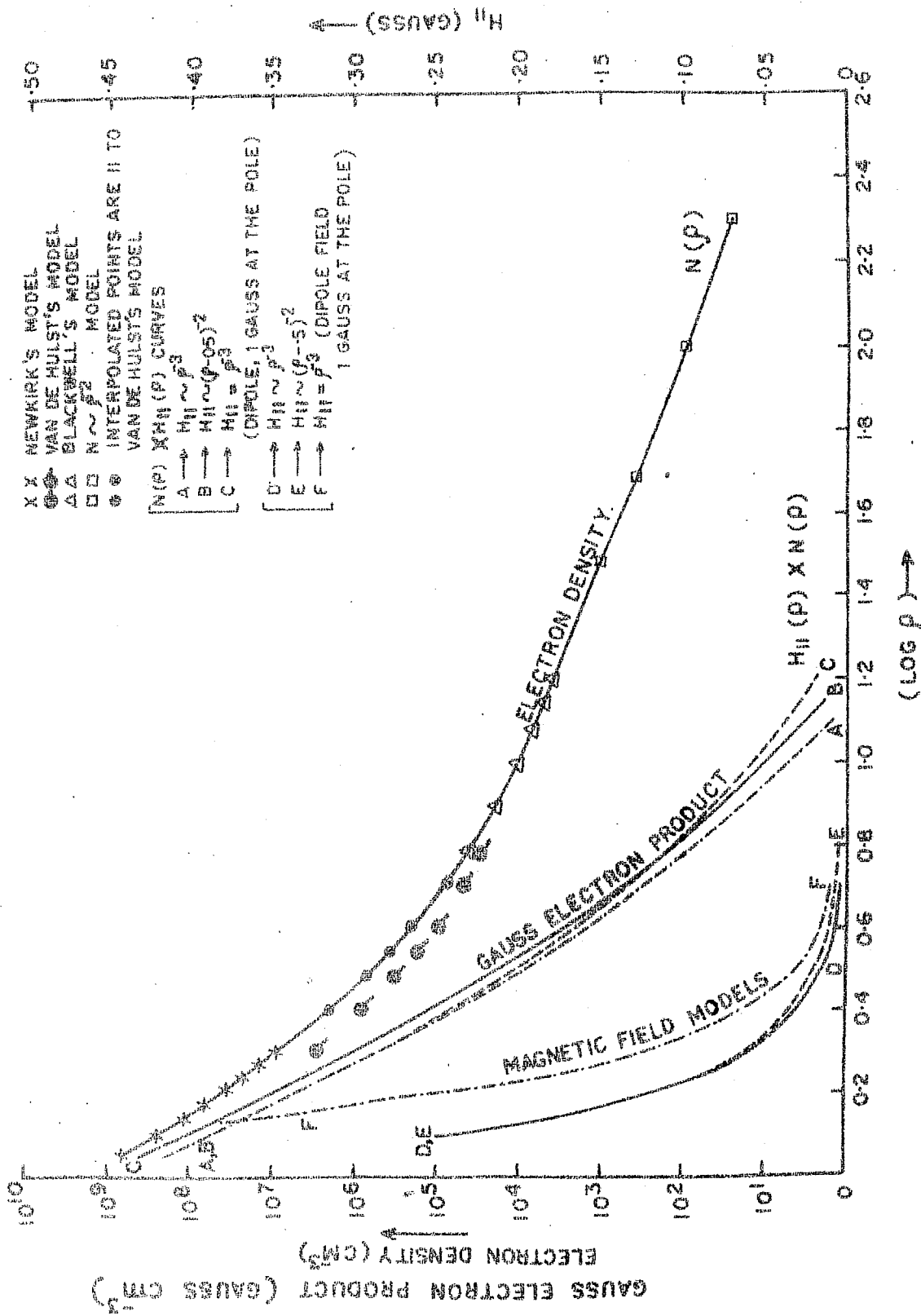


Figure 5.9 Coronal electron density and magnetic field models used for the calculation of the extent and/or the position of mode coupling regions.

a)  $H_{11} \sim \varrho^{-3}$ , shown as curve D in Figure 5.9.

b)  $H_{11} \sim (\varrho - 0.5)^{-2}$  shown as curve E in Figure 5.9.

2. The magnetic field was assumed to be of dipolar in nature due to a general magnetic field strength of 1 Gauss at the poles, that is  $H_{11} = \varrho^{-3}$  (corresponding to the curve F in Figure 5.9).

In the equation (2),  $\int N(\varrho) H_{11}(\varrho) d\varrho$  was numerically computed for a radial trajectory from various coronal levels upto  $\varrho = 200$  and the values of  $\Phi$  were obtained for three frequencies, 200, 74 and 35 MHz, by using the three different models mentioned above for the magnetic field. The values of  $\Phi$  at different frequencies are plotted as a function of heliocentric altitude in Figure 5.10. It is clear from Figure 5.10 that the estimate of  $\Phi$  is not very sensitive to the magnetic field models used here. In this figure we have indicated the positions of emission levels of three frequencies 200, 74 and 35 MHz. These position levels were calculated from Figure 5.9 by making use of the relation  $\nu_n = 9.1 \times 10^{-3} N^{\frac{1}{2}}$  where  $\nu_n$  = plasma frequency in MHz. The calculated plasma levels agree reasonably well with the reported experimental measurements as shown in Table 5.4. It should be emphasized that the agreement seems to be better at higher frequencies than at lower.

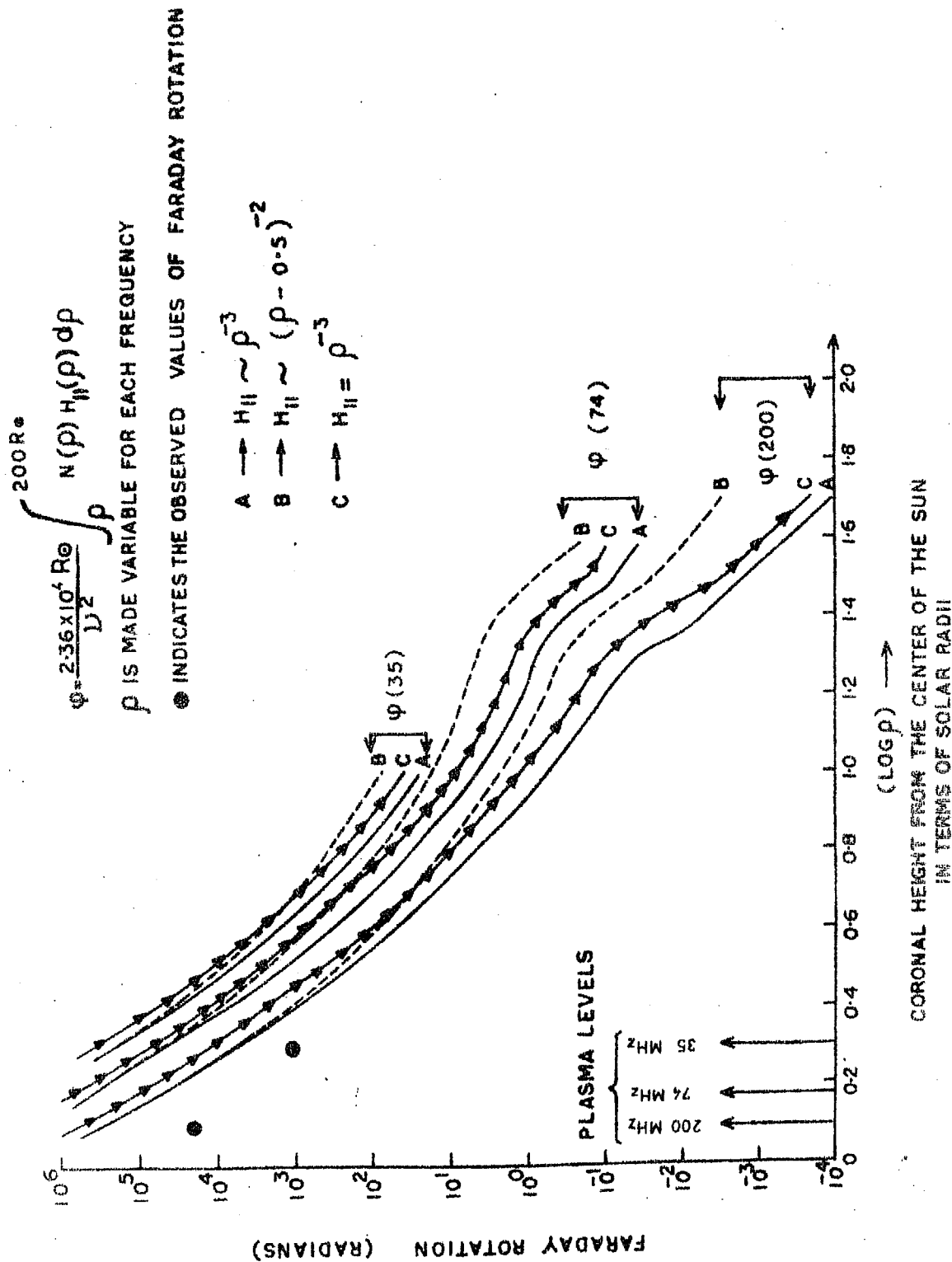


Figure 5.10 Calculated Faraday rotation as a function of the distance from the center of the sun at 35, 74 and 200 MHz

T A B L E - 5.4

COMPARISON BETWEEN THE MEASURED AND CALCULATED POSITIONS  
OF TYPE III BURSTS AT DIFFERENT FREQUENCIES

Frequency in MHz	Electron density, cm <sup>-3</sup>	Height from the centre of the sun in solar radius as derived from the model adopted	Observed height from the centre of the sun in solar radius	References
200	$5 \times 10^8$	1.25	1.25 to 1.3	1) Wild et al. (1959) 2) Morimoto and Kai (1961)
80	$6.7 \times 10^7$	1.5	1.6	Sheridan et al. (1972). They have given value at 80 MHz
35	$1.6 \times 10^7$	1.8		
25	$8 \times 10^6$	2.0		
26.3	$9 \times 10^6$	2.0	2.0 to 2.5	Erickson (1962)
41 to 12.5	$2 \times 10^7$ to $2 \times 10^6$	1.8 to 2.5	2.0 to 5.0	Warwick (1964)
19.7	$4.8 \times 10^6$	2.1	2.9	Shain and Higgins (1959)

In Table 5.5 we have shown the values of extent of QT regions required at different frequencies, if it is assumed that the radiation emerging from the source region finds QT regions just near the plasma level where Faraday rotation suffered by the radiation is the largest. These values are obtained from Figure 5.9. It is shown that for 35 MHz radiation, the coronal region from  $\theta = 2$  to  $\theta = 4.5$  should be a mode coupling region. Similarly, for 200 MHz radiation the coupling region should extend from  $\theta = 1.3$  to  $\theta = 1.75$ . The upper bounds on the magnitude of the extent of the mode coupling regions, that is  $\theta = 4.5$  for 35 MHz and  $\theta = 1.75$  for 200 MHz radiation determine the locations of the mode coupling regions in the solar corona. It should be pointed out that the measured values of Faraday rotation indicated in Figure 5.9 were used to find the extent and/or position of the mode coupling regions.

5.67 DIFFICULTIES WITH THE MODE COUPLING AS AN  
EXPLANATION FOR THE OBSERVED LOW VALUES OF  
THE FARADAY ROTATION

The QT approximation holds good over a very narrow range of angles in the vicinity of an angle of  $\pi/2$  between the magnetic field and the direction of propagation. Hence for a 35 MHz ray path, it is difficult to understand how the radial gradient of the angle, in the region where the angle between the magnetic field and the direction of propagation is  $\pi/2$ , can be so small so that the coupling

T A B L E - 5.5

THE EXTENT OF THE MODE COUPLING REGION  
AT DIFFERENT FREQUENCIES

Frequency in MHz	Source position from the center of the sun, in solar radius	Extent of the region in which mode coupling should be effective, in units of solar radius from the center of the sun
200	1.3	1.3 to $\approx$ 1.75
74	1.5	1.5 to $\approx$ 3.5
35	2.0	2.0 to $\approx$ 4.5

region, for a radial propagation path, would extend from  $\vartheta = 2 R_{\odot}$  to  $\vartheta = 4.5 R_{\odot}$ . To explain the observed low values of the Faraday rotation both at 35 and 200 MHz, we require a geometrical configuration of the coronal magnetic field and the propagation path such that the coronal regions between  $\vartheta = 1.3 R_{\odot}$  to  $\vartheta = 1.75 R_{\odot}$  and  $\vartheta = 2 R_{\odot}$  to  $\vartheta = 4.5 R_{\odot}$  should be strong mode coupling regions for 200 and 35 MHz rays respectively. Also the QL approximation should hold in the coronal regions  $\vartheta > 1.75 R_{\odot}$  and  $\vartheta > 4.5 R_{\odot}$  for 200 and 35 MHz rays respectively. This kind of a fixed geometry, which can always yield Faraday values of the order of  $10^4$  and  $10^3$  radians at 200 and 35 MHz respectively, is difficult to think of. Realizing that in the mode coupling region the independently propagating characteristic modes become coupled and that any previously acquired Faraday rotation is lost, it is not really necessary to have the mode coupling to be effective throughout the region from  $\vartheta = 1.3 R_{\odot}$  to  $\vartheta = 1.75 R_{\odot}$  and  $\vartheta = 2.0 R_{\odot}$  to  $\vartheta = 4.5 R_{\odot}$  for 200 and 35 MHz rays respectively. It is enough if we can find a "thin" mode coupling regions located at about  $1.75 R_{\odot}$  and  $4.5 R_{\odot}$  for 200 and 35 MHz respectively such that once the rays leave these mode coupling regions, the Faraday rotations suffered by 200 and 35 MHz radiations are of the right order. These regions could also serve as the "polarization limiting"

regions, that is, the regions where the polarization properties are imposed on type III burst radiation. But if the QT transitional frequency  $\nu_t$  has to continuously decrease as the heliocentric altitude increases so as to explain the observed low values of the Faraday rotation, then it is difficult to understand how 200 MHz ray starting from  $\vartheta = 1.25 R_{\odot}$  on reaching  $\vartheta = 2.0 R_{\odot}$  should always find itself in a weakly mode coupling region when the transitional frequency  $\nu_t$  at that level should be as low as 35 MHz, which implies a strong coupling region.

Dodge (1972) has examined the possibility of finding mode coupling regions in terms of tangential field discontinuities (Fokker 1969). He suggested that in the presence of localized variations in the direction and magnitude of the magnetic field, there exists a high probability of a given wave encountering a region of transverse magnetic field that would destroy all the previously acquired Faraday rotation. The important point about this explanation is that the waves could encounter transverse magnetic fields in the regions of the corona even where the average magnetic field direction is radial. Parker (1969) pointed out that many of these tangential discontinuities can correspond to Alfvén waves, some of which can propagate the entire distance from the sun to the earth, some are damped out while others may be generated in the



medium. This means that type III burst radiation can meet these tangential discontinuities any where in the interplanetary medium. It implies that the observed Faraday rotation could at times be as small as 100 radians, which is the amount of the Faraday rotation suffered by a 35 MHz ray in the earth's ionosphere. But our observations revealed that for 31 groups of bursts and 13 isolated bursts the observed Faraday rotation ranges from  $0.9 \times 10^3$  to  $4 \times 10^3$  radians. Thus we feel that it is difficult to explain the observed low values of the Faraday rotation in terms of mode coupling at the tangential discontinuities.

Summarizing these results, we have emphasized that one must find out a reasonable explanation for the discrepancy of at least two orders of magnitude between the measured and theoretically calculated values of the total Faraday rotation. To explain the observed low values of Faraday rotation both at 35 and 200 MHz, one could think of magneto-ionic mode coupling as a possible explanation because the values of electron density and magnetic field at different levels can give the right order of transitional frequencies. But the difficulty is that we cannot put the mode coupling region very far from the plasma level where type III burst radiation originates because then we fail to account for the observed low values of Faraday rotation at different frequencies. It is also shown that it is not possible

to put the coupling region very near the plasma level where type III burst radiation originates because the demands on the extent and/or position of the coupling region and on the geometry of the coronal magnetic field are very unreasonable. Further, this viewpoint is supported by the fact that the occurrence of U-type bursts at longer wavelengths seems to be rare (Sheridan et al. 1959, Stone and Fainberg 1971). This might be taken as an indication for that apparently magnetic loops which could give rise to transverse magnetic fields do not, in general, reach sufficiently high altitudes so as to pass through the levels where type III bursts at 35 MHz originate (Fokker 1970). However, it should be emphasized that for type III sources occurring near the center of the disk the observed radiation may not, generally, pass through the regions of transverse magnetic field, but in case of type III bursts occurring near the limb, the observed radiation can, in principle, meet a transverse magnetic field regions. This means that there should be a strong disk-longitude dependence of the Faraday rotation suffered by a type III burst radiation, which does not seem to be the case. In addition, for type III sources occurring near the limb, it may be the second harmonic radiation which dominates (Kundu 1965). Further, it is found that, none of the suggestions like magnetic field reversals, ducting (Dodge 1972) and mode coupling at tangential discontinuities in the magnetic

field along the propagation path (Bhonsle and Mattoo 1973), can adequately explain the observed low values of the Faraday rotation.

#### 5.68 EXPLANATION IN TERMS OF SECOND HARMONIC

Akabane and Cohen (1961) proposed that the discrepancy between the measured and theoretically expected values of the Faraday rotation could be minimized by putting the source of type III burst radiation at a greater height in the corona. If type III burst radiation is produced at the fundamental plasma frequency, as seems to be the general belief, then the source of type III burst radiation at 35 MHz has to be put at 3 to 3.5 solar radii above the photosphere, which is rather large.

The other possibility is that type III bursts might be recorded primarily in the second harmonic of the plasma frequency. This possibility makes it natural that the emission region for type III bursts occupies a comparatively higher position in the corona. This viewpoint has a strong theoretical support of Zheleznyakov and Zaitsev (1970a, b). These authors and Zaitsev et al. (1972) observationally support the idea (as discussed in Chapter I) that second harmonic emission may be more important at decametric and longer wavelengths. These authors and Haddock and Alvarez (1973) have claimed that theory of generation of type III burst radiation in terms of second harmonic can explain

many observable properties of type III bursts including the interplanetary observations of energetic electrons and radio burst at hectometer and kilometer wavelengths. (Zaitsev et al. 1972, Lin 1973). This has been discussed in greater detail in section 1.6. It follows from the above discussion that one may seriously consider the explanation, for the low values of Faraday rotation, based on the suggestion that type III emission occurs predominantly at the second harmonic of the local plasma frequency. Further it may be noted that, since the cone angle (with respect to the direction of the exciter) of emission at the second harmonic is wider than that of the fundamental (Zheleznyakov and Zaitsev 1970b, Yip 1970), the situation becomes more conducive for the mode coupling to occur at a higher position in the corona. We would like to emphasize that the idea of second harmonic generation has been invoked only for decameter and longer wavelengths because the physics of the corona seems to change beyond about 2 solar radii from center of the sun (Warwick 1965, Ellis and McCulloch 1966, 1967, de la Noë and Boischot 1972).

#### 5.7 FARADAY ROTATION AT 35 MHz AND THE EXISTENCE OF LINEAR POLARIZATION

As already indicated in Section 2.33 that many authors have reported the existence of linearly polarized type III radio bursts. Our observations at 25 and 35 MHz reported in Chapters IV and V also have revealed their

existence. Fokker (1971) pointed out that as a consequence of scattering, a spread in the position angles of the order of  $10^{-4}$  of the mean value of the Faraday rotation should completely disperse the position angles of any linear polarization originally present. Further, because of finite bandwidth of the receiver, the radiation would be received from a certain thickness of the source region, which would lead to depth depolarization within the source region. This implies that if the total Faraday rotation were indeed  $10^5$  radians or more, then it would be impossible to observe linear polarization of type III bursts.

The measured value of the Faraday rotation at 35 MHz is of the order of  $10^3$  radians (Bhonsle and Mattoo 1973). This is two orders of magnitude less than what is theoretically expected (Fokker 1971). It implies that the spread in position angles due to the scattering effects, which may cause appreciable depolarization, should be of the order of  $10^{-2}$  of the mean value of the Faraday rotation. This is two orders of magnitude greater than the Fokker's estimate of spread in the position angles due to scattering. Thus, the measured value of the Faraday rotation of the order of  $10^3$  radians at 35 MHz definitely increases the probability of occurrence of linearly polarized type III bursts. Grogard and McLean's (1973) claim for the non-existence of linear polarization in type III bursts at

80 MHz is doubted by Bhonsle and Mattoo (1973) because their instrument does not seem to have the capability of measuring the small values of differential Faraday group delay required for the Faraday rotation to be of the order of  $10^3$  radians.

## C H A P T E R - VI

### CONCLUSIONS AND SUGGESTIONS FOR FURTHER STUDY

#### 6.1 CONCLUSIONS

The polarization characteristics of type III solar radio bursts at decametric wavelengths have been studied at Ahmedabad. They render a better understanding of the generation mechanism of the radiation and the source characteristics. In addition, the Faraday rotation measurements, which formed the subject matter of this thesis, have been quite useful in understanding the role of the intervening magneto-ionic medium in modifying the polarization characteristics originally impressed at the source.

A time-sharing radio polarimeter used for the polarization studies of type III solar radio bursts was operated in the following three distinct modes: (1) single bandwidth (20 KHz) polarization measurements at 25 MHz; (2) Polarization measurements in narrow band (800 Hz) at two closely-spaced frequencies, namely 34.993 and 34.997 MHz and (3) Simultaneous measurements of polarization parameters in two bandwidths (7.5 and 12.5 KHz) for the determination of the Faraday rotation at 35 MHz. The effects of the crosstalk due to the antennas and the receiver errors due to the relative phase difference between the two cross-polarized channels and the ground reflections on the measurements of polarization parameters have been discussed in detail.

Our main results of the polarization studies of type III bursts may be summarized as follows:

(1) In agreement with the narrow band measurements by other workers, type III bursts at 25, 35 and 74 MHz are found to be highly elliptically polarized (or nearly linearly polarized) with axial ratios ranging between - 0.2 and + 0.2. Not a single type III burst at 25 and 35 MHz was observed to be circularly polarized.

(2) The average degree of polarization of type III solar radio bursts, as measured by a polarimeter at 25 MHz, with a bandwidth of 20 KHz was found to be about 30 per cent. The determination of polarization degree of type III bursts at 25 MHz at the source became possible after the measurement of Faraday rotation at 35 MHz. The polarization degree of majority of type III bursts at 25 MHz at the source was estimated to be about 70 per cent and was nearly 100 per cent in some cases. These observations are in good agreement with previous narrow band measurements.

(3) The orientation angles of polarization ellipses of bursts within a given group were found to remain constant to within  $\pm 20^\circ$  (tendency for clustering of orientation) in case of some type III groups of bursts. This has also been reported by many other authors.

(4) A detailed study of an event at 25 MHz, which occurred on July 14, 1969, revealed that the source of



radiation possibly had background as well as burst components. The background component was found to be strongly polarized and the burst component relatively weakly polarized. Our analysis indicated that the two components might have originated from two different positions in the solar corona. Such multiple sources have now been verified by two-dimensional radioheliographic observations from Culgoora, Australia.

(5) The narrow band (800 Hz) polarization measurements at two closely-spaced frequencies, 34.993 and 34.997 MHz revealed that occasionally there could be appreciable variation in the polarization characteristics of type III bursts in a band of 4 KHz. This variation is partly due to the frequency dependence of the Faraday rotation and partly intrinsic to the source.

(6) It was found that the distribution of the difference in orientations of the narrow band (800 Hz) polarization ellipses at two closely-spaced frequencies, 34.993 and 34.997 MHz was not random. Instead, we found that for many type III bursts the difference in the orientation angles at the two frequencies did not exceed  $20^{\circ}$ . This indicates that the Faraday rotation suffered by type III burst radiation at 35 MHz may not be as large as  $10^5$  radians but should be considerably less, at least by two orders of magnitude. Dodge (1972) also reached similar

conclusions from his high frequency-resolution polarization observations at 34 MHz.

(7) A few type III bursts were found to have a frequency structure of the order of a few kilohertz. Ellis and McCulloch (1966, 1967) and de la Noë and Boischot (1972) have reported similar observations.

(8) Simultaneous measurements of polarization parameters in two bandwidths (7.5 and 12.5 KHz) showed that type III burst radiation at 35 MHz suffered a Faraday rotation of the order of  $10^3$  radians after passing through the solar corona and the earth's ionosphere. This is at least two orders of magnitude less than what has been expected theoretically.

(9) Because the Faraday rotation suffered by type III burst radiation at 35 MHz is of the order of  $10^3$  radians only, it is thought that the odds against the existence of linearly polarized type III bursts are very much less than what Fokker (1971) had envisaged.

(10) It has been shown that the polarization properties are imposed on type III burst radiation at about 1.6 to 1.75  $R_{\odot}$  for 200 MHz and at about 4 to 4.5  $R_{\odot}$  for 35 MHz. This suggests that if the radiation is assumed to be radiated at the local plasma frequency, then the polarization characteristics are imposed at a relatively higher

position (compared to the position of the source of radiation) in the solar corona.

(11) Arguments have been given to account for the observed low values of the Faraday rotation both at 35 and at 200 MHz. An explanation in terms of mode coupling in the presence of the magnetic field due to sunspots and at tangential discontinuities has not been found to be entirely satisfactory. An alternative explanation that type III burst radiation may be emitted predominantly at the second harmonic of the local plasma frequency has been proposed. Theoretical and observational evidences in support of this explanation have been cited.

(12) Our observations indicated that a partially elliptically polarized type III burst radiation may not be represented in terms of two mutually incoherent 100 per cent circularly and linearly polarized signals, as has been suggested by Fokker (1971).

## 6.2 SUGGESTIONS FOR FURTHER STUDY

(1) From their observations made with an equipment which completely eliminates the errors due to reflections from the ground, Grognaud and McLean (1973) have argued against the existence of linearly polarized type III solar radio bursts at 80 MHz. However, we feel that linearly polarized type III bursts could't have been

detected by their instrument if the Faraday rotation were as low as  $10^3$  radians. This can be verified by a space-correlation-type radio polarimeter which can measure all the four Stokes parameters simultaneously at two widely separated sites. Since the ground reflection is very much dependent upon the local properties of the ground, we feel that by measuring all the four Stokes parameters simultaneously at two different sites and then taking the correlated output for the determination of polarization parameters will completely eliminate the errors due to ground reflections.

(2) For the determination of Faraday rotation at 35 MHz, the following assumptions were made, (as mentioned in Section 5.42):

The polarization characteristics of type III bursts remain constant (1) over a bandwidth of at least 50 KHz and (2) during the integration time constant of the polarimeter.

These assumption become unnecessary, if the Faraday rotation is measured from the orientation angles determined at more than two closely-spaced frequencies (a few kilohertz apart) around 35 MHz.

(3) Another important measurement would be a simultaneous determination of the amount of Faraday rotation at the fundamental and the second harmonic frequencies of

those type III radio bursts which clearly show the existence of both the harmonics. These measurements can help in deciding whether or not the explanation, for the observed low value of the Faraday rotation (suggested in this thesis) in terms of emission of type III burst radiation predominantly at the second harmonic of the local plasma frequency, is meaningful. Such measurements can also provide important clues about the other possible explanation in terms of mode coupling. Two-dimensional high-resolution position determination together with simultaneous determination of the Faraday rotation both at the fundamental and second harmonic of a type III burst can be of immense importance provided we understand a little more about the effect of scattering (this comment has been made in view of Riddle's (1972) paper).

(4) Theoretical studies of mode coupling mechanisms in the solar corona deserve more attention. In particular, one has to find out whether the tangential discontinuities can provide strong mode coupling regions so as to explain the observed low values of the Faraday rotation both at 200 and at 35 MHz. If the tangential discontinuities can provide strong mode coupling regions, then it is to be shown how these tangential discontinuities become completely ineffective in providing the mode coupling regions near the orbit of the earth. This is because our measurements indicate that in a sample of 31 groups of type III bursts and

13 isolated type III bursts, the total Faraday rotation was never as low as 100 radians, which is the amount of the Faraday rotation suffered by type III burst radiation at 35 MHz in the earth's ionosphere. In addition, it is to be investigated how the polarization characteristics can be imposed on the radiation at about 1.6 to 1.75  $R_{\odot}$  for 200 MHz and at about 4 to 4.5  $R_{\odot}$  for 35 MHz type III bursts.

(5) Very little is known about the polarization characteristics of type III solar radio bursts as a function of frequency. The available polarization observations at different frequencies belong to different periods of solar activity. The fact that polarization characteristics of type III bursts change from year to year is clearly borne out by the observations made by Chin et al. (1969, 1971). Thus, it would seem very much desirable to make simultaneous polarization observations at various frequencies covering a range of about 600 MHz to 30 MHz. Polarization observations at hectometer and kilometer wavelengths by satellite-borne radio polarimeters may also add significantly to our knowledge of type III bursts originating in the interplanetary medium. Such observations can prove to be of immense importance for the understanding of the generation mechanism of type III bursts and the propagation characteristics and other aspects of both the inner corona and the interplanetary medium.

## R E F E R E N C E S   C I T E D

- Alexander, J.K.; Malitson, H.H.; and Stone, R.G. 1969,  
Solar Phys., 8, 388.
- Alurkar, S.K.; and Bhonsle, R.V. 1969, J. Intn. Telecom.  
Engrs., 15, 255.
- Anderson, K.A.; Lin, R.P. 1966, Phys. Rev. Letters, 16, 1121.
- Akabane, K. 1958, Ann. Tokyo Astron. Obs., 6, 57.
- Akabane, K.; and Cohen, M.H. 1961, Ap. J., 133, 258.
- Aubier, M.; and Boischot, A. 1972, Astron. Astrophys., 19, 343.
- Axisa, F.; Martres, M.J.; and Soru-Escant, I. 1973, Solar  
Phys., 29, 163.
- Baldwin, D.E. 1964, Physics Letters, 12, 202.
- Bhonsle, R.V.; and McNarry, L.R. 1964a, Cand. J. Phys.,  
42, 292.
- Bhonsle, R.V.; and McNarry, L.R. 1964b, Ap. J., 139, 1312.
- Bhonsle, R.V.; Fejfar, A.; and Lusignan, B.B. 1967, Ap. J.,  
146, 595.
- Bhonsle, R.V.; and Alurkar, S.K. 1968, Information Bulletin  
of Solar Observatory, Utrecht, 24, 68.
- Bhonsle, R.V.; and Mattoo, S.K. 1973, To appear in Astron.  
Astrophys.
- Blackwell, D.E. 1956, Mon. Not. Roy. Astr. Soc., 116, 56.

- Bohm, D.; and Gross, E.P. 1949a, Phys. Rev., 75, 1851.
- Bohm, D.; and Gross, E.P. 1949b, Phys. Rev., 75, 1864.
- Boischot, A.; Lee, R.H.; and Warwick, J.W. 1960, Ap. J., 131, 161.
- Boischot, A. 1970, "Solar - Terrestrial Physics", Ed. E.R. Dyer, D. Reidel Publishing Company, Dordrecht -Holland, 87.
- Boischot, A.; de la Noë, J.; and Moller - Pedersen, B. 1970, Astron. Astrophys., 4, 159.
- Booker, H.G. 1936, Proc. Roy. Soc. London, A 155, 235.
- Budden, K.G. 1952, Proc. Roy. Soc. London, A 215, 215.
- Carmichael, H. 1964, AAS - NASA Symposium on the Physics of Solar Flares, Ed. W.N. Hess, NASA, Washington.
- Chandrasekher, S. 1955, "Radiative transfer", Oxford University Press, London, England, 24 - 35.
- Chapman, S. 1952, J. Atmos. Terr. Phys., 3, 1.
- Chin, Y.C.; Fung, P.C.W.; and Lusignan, E.B. 1969, Technical Report No. SU-SEL-69-057, Stanford Electronics Laboratories, Stanford University, Stanford, California.
- Chin, Y.C.; Fung, P.C.W.; and Lusignan, B.B. 1971, Solar Phys., 16, 135.
- Cohen, M.H. 1956, "Interpretation of radio polarization data in terms of Faraday rotation", Cornell University,



Ithaca, New York, School of Elec. Engr., Research  
Report EE. 295.

Cohen, M.H. 1958a, Proc. I.R.E., 46, 172.

Cohen, M.H. 1958b, Proc. I.R.E., 46, 183.

Cohen, M.H. 1959, Ap. J., 130, 221.

Cohen, M.H.; and Fokker A.D. 1959, "Paris Symposium on  
Radio Astronomy", 252.

Cohen, M.H. 1960, Ap. J., 131, 665.

Cohen, M.H. 1961, Ap. J., 133, 978.

Cohen, M.H.; and Dwarkin, M.L. 1961, J.G.R., 66, 411.

Correll, M.; Hazen, M.; and Bhang, J. 1956, Ap. J., 124, 597.

Covington, A.E.; and Harvey, G.A. 1961, Nature, 192, 152.

David, P.; and Voge, G. 1969, "Propagation of Waves",  
Pergamon Press.

de la Noë, J.; and Boischot, A. 1972, Astron. Astrophys.,  
20, 55.

de Groot, T. 1959, "Paris Symposium on Radio Astronomy", 45.

de Jager, C.; and Kundu, M.R. 1963, Space Research III,  
Ed. W. Priester, North - Holland Publishing Company,  
Amsterdam, 836.

de Jager, C. 1967, Solar Phys., 2, 327.

Dodge, J.C. 1972, Thesis, University of Colorado.

- Dunckel, N.; Helliwell, R.A.; and Vesecky, J. 1972, Solar Phys., 25, 197.
- Elgaroy, O. 1961, Astrophysica Norvegica, 7, 123.
- Ellis, G.R.A., and McCulloch, P.M. 1966, Nature, 211, 1070.
- Ellis, G.R.A., and McCulloch, P.M. 1967, Aust. J. Phys., 20, 583.
- Ellis, G.R.A. 1969, Aust. J. Phys., 22, 177.
- Erickson, W.C. 1962, General Dynamics/Astronautics Report ERR - AN - 233.
- Evans, L.G.; Fainberg, J.; and Stone, R.G. 1971, Solar Phys., 21, 198.
- Fainberg, J.; and Stone, R.G. 1970a, Solar Phys., 15, 222.
- Fainberg, J.; and Stone, R.G. 1970b, Solar Phys., 15, 433.
- Fainberg, J.; and Stone, R.G. 1971a, Ap. J., 164, No.3, L123.
- Fainberg, J.; and Stone, R.G. 1971b, Solar Phys., 17, 392.
- Fokker, A.D. 1965a, "Solar System Radio Astronomy", Ed. J. Aarons, Plenum Press, New York, 171.
- Fokker, A.D. 1965b, Bull. Astron. Inst. Neth., 18, 111.
- Fokker, A.D. 1970, Solar Phys., 11, 92.
- Fokker, A.D. 1971, Solar Phys., 19, 471.
- Fomichev, V.V.; and Chertok, I.M. 1968a, Soviet Astron.-AJ, 12, 21.

- Fomichev, V.V.; and Chertok, I.M. 1968b, Soviet Astron.-AJ, 12, 477.
- Fomichev, V.V.; and Chertok, I.M. 1969a, Soviet Astron.-AJ, 12, 615.
- Fomichev, V.V.; and Chertok, I.M. 1970, Soviet Astron.-AJ, 14, 261.
- Fort, B.; Picat, J.P.; Combes, M.; and Felenbok, P. 1972, Astron. Astrophys., 17, 55.
- Fung, P.C.W.; and Yip, W.K. 1966, Aust. J. Phys., 19, 759.
- Ginzburg, V.L.; and Zheleznyakov, V.V. 1958, Soviet Astron.-AJ, 2, 653.
- Ginzburg, V.L.; and Zheleznyakov, V.V. 1961, Soviet Astron.-AJ, 5, 1.
- Giovanelli, R.G. 1958, Aust. J. Phys., 11, 350.
- Goldstein, Jr., S.J. 1959, Ap. J., 130, 393.
- Gopala Rao, U.V. 1965, Aust. J. Phys., 8, 283.
- Gordon, I.M. 1968, Astrophys. Letters, 2, 49.
- Graedel, T.E. 1970, Ap. J., 160, 301.
- Grognard, R.J.M.; and McLean, D.J. 1973, Solar Phys., 29, 163.
- Haddock, F.T. 1958, Proc. I.R.E. 46, 3.
- Haddock, F.T.; and Graedel, T.E. 1970, Ap. J., 160, 293.
- Haddock, F.T.; and Alvarez, H. 1973, Solar Phys., 29, 183.

- Hanbury - Brown; Palmer, H.P.; and Thompson, A.R. 1956, Mon. Not. Roy. Astron. Soc., 115, 487.
- Handrickson, R.A., McEntire, R.W.; and Winckler, J.R. 1971, Nature, 230, 564.
- Hansen, R.J.; Garcia, C.J.; Hansen, S.F.; and Loomis, H.G. 1969, Solar Phys., 7, 417.
- Hartz, T.R. 1964, Ann. Ap., 27, 823.
- Hartz, T.R. 1969, Planet Space Sci., 17, 267.
- Harvey, G.A.; and McNarry, L.R. 1970, Solar Phys., 11, 467.
- Hatanaka, T., Suzuki, S.; and Tsuchiya, A. 1955, Proc. Japanese Acad., 31, 81.
- Hatanaka, T. 1956, Publ. Astr. Soc. Japan, 8, 73.
- Hughes, M.P.; and Harkness, R.L. 1963, Ap. J., 138, 239.
- Kai, K. 1963, Pub. Astron. Soc. Japan, 15, 195.
- Kai, K. 1969, Solar Phys., 10, 460.
- Kaplan, S.A.; and Tsyтовich, V.N. 1967, Soviet Astron.-AJ, 11, 956.
- Komesaroff, M. 1958, Aust. J. Phys., 11, 201.
- Koutchmy, S. 1971, Astron. Astrophys., 13, 79.
- Kraus, J.D. 1950, "Antennas", McGraw-Hill Book Company, 464.
- Kraus, J.D. 1966, "Radio Astronomy", McGraw-Hill Book Company, New York.

Kuckes, A.F.; and Sudan, R.N. 1969, Nature, 223, 1048.

Kuckes, A.F., and Sudan R.N. 1971, Solar Phys., 17, 194.

Kuiper, T.B. H. 1973, Thesis, University of Maryland.

Kundu, M.R. 1959, Ann.d' Astrophys., 22, 1.

Kundu, M.R. 1962, J.G.R., 62, 2695.

Kundu, M.R. 1965, "Solar Radio Astronomy", Wiley (Inter-Science), New York.

Kundu, M.R. 1970, "Physics of the Solar Corona", Ed. Macris, C.T., D. Reidel Publishing Company, Dordrecht-Holland, 287.

Kurzok, R.M. 1962, Electronics, 13, 61.

Labrum, N.R. 1971, Aust. J. Phys. 24, 193.

Lawrence, R.S.; Little, C.G.; and Chivers, H.J.A. 1964, Proc. I.E.E.E., 52, 4.

Lin, R.P.; and Anderson, K.A. 1967, Solar Phys., 1, 446.

Lin, R.P. 1970a, Solar Phys., 15, 266.

Lin, R.P. 1970b, Solar Phys., 15, 453.

Lin, R.P. 1973, NASA Symposium on high energy phenomenon on the Sun (To be published).

Little, A.G.; and Payne-Scott, R. 1952, Aust. J. Sci. Res., A4, 489.

Loughead, R.E.; Roberts, J.A.; and McCabe, M.K. 1957, Aust. J. Phys., 10, 483.

- Malville, J.M. 1961, Thesis, University of Colorado.
- Malville, J.M. 1962a, Ap. J., 135, 834.
- Malville, J.M. 1962b, Ap. J., 136, 266.
- Martres, M.J.; Pick, M.; Souru-Escant, I.; and Axisa, F.  
1972, Nature (Physical Sciences), 236, 25.
- Maxwell, A.; and Swarup, G. 1958, Nature, 188, 36.
- Maxwell, A. 1965, "The Solar Spectrum", Ed. de Jager, C.,  
D. Reidel Publishing Company, Dordrecht - Holland, 342.
- McDonald, F.B. 1973, NASA Symposium on high energy phenomena on the sun (To be published).
- McLean, D.J. 1970, Proc. Astro. Soc. Aust., 1, 315.
- McLean, D.J. 1971, Aust. J. Phys., 24, 201.
- Melrose, D.B. 1970a, Aust. J. Phys., 23, 871.
- Melrose, D.B. 1970b, Aust. J. Phys. 23, 885.
- Millman, J.; and Taub, H. 1965, McGraw-Hill Book Company.
- Morimoto, M.; and Kai, K. 1961, Publ. Astron. Soc. Japan,  
13, 294.
- Neugebauer, M.; and Snyder, C.W. 1966, "The Solar Wind",  
Ed. Mackin, R.J.; and Neugebauer, M.
- Newkirk, Jr., G. 1959, "Paris Symposium on Radio Astronomy", 149.
- Newkirk, Jr., G. 1961, Ap. J., 133, 983.
- Newkirk, Jr., G. 1967, Ann. Rev. Astron. Astrophys., 5, 213.

- Newkirk, Jr., G. 1970, IAU Symposium, 35.
- Newkirk, Jr., G.; and Dupree, R.G. 1970, Solar Phys., 15, 15.
- Newkirk, Jr., G. 1971, "Physics of the Solar Corona", 66.
- Noble, L.M., and Scarf, F.L. 1963, Ap. J., 138, 1169.
- Ohm, E.A., and Snell, W.W. 1963, Bell Syst. Tech. J., XL11, 2047.
- Parker, E.N. 1963, Ap.J., Suppl. Ser. 8, 177.
- Parker, E.N. 1969, Space Sci. Rev., 9, 325.
- Payne - Scott, R. 1949, Aust. J. Sci. Res., A2, 214.
- Payne - Scott, R.; and Little, A.G. 1951, Aust. J. Sci. Res., A4, 508.
- Payne - Scott, R.; and Little, A.G. 1952, Aust. J. Sci. Res., A5, 32.
- Ratcliffe, J.A. 1959, "The magneto-ionic theory and its applications to the ionosphere", Cambridge University Press.
- Riddle, A.C. 1972, Proc. Astron. Soc. Aust., 2, 98.
- Roberts, J.A. 1959, Aust. J. Phys., 12, 327.
- Ryle, M.; and Vonberg, D.D. 1948, Proc. Roy. Soc. London, A 193, 98.
- Sastry, Ch.V. 1972, Ap. J., 11, 47.
- Schatten, K.H. 1970, Solar Phys., 12, 484.

- Shain, C.A.; and Higgins, C.S. 1959, Aust. J. Phys., 12, 357.
- Sheridan, K.V.; Trent, G.H.; and Wild, J.P. 1959, Observatory, 79, 51.
- Sheridan, K.V., Labrum, M.R.; and Payten, W.J. 1972, Nature, 38, 115.
- Simon, P. 1962, Ann. d' Astrophys., 25, 12.
- Slysh, V.I. 1967a, Cosm. Res., 5, 759.
- Slysh, V.I. 1967b, Soviet Astron. -AJ, 11, 389.
- Smerd, S.F.; Wild, J.P.; and Sheridan, K.V. 1962, Aust. J. Phys., 15, 180.
- Smith, D.F. 1970a, Solar Phys., 15, 202.
- Smith, D.F. 1970b, Adv. Astron. Astrophys., 7, 147.
- Smith, D.F.; and Fung, P.C.W. 1971, J. Plasma Phys., 5, 1.
- Smith, D.F. 1972, Solar Phys., 23, 191.
- Steinberg, J.L.; Aubier - Giraud, M.; Leblanc, Y.; and Boischot, A. 1971, Astron. Astrophys., 10, 362.
- Steinberg, J.L. 1972, Astron. and Astrophys., 18, 382.
- Stewart, R.T. 1962, RPR - 142, Div. Radio Phys., C.S.I.R.O., Sydney, Australia.
- Stewart, R.T. 1965, Aust. J. Phys., 18, 67.
- Stewart, R.T. 1972, Proc. Astron. Soc. Aust., 2, 100.



- Stone, R.G.; and Fainberg, J. 1971, Solar Phys., 20, 106.
- Sturrock, P.A. 1963, AAS - NASA Symposium on the Physics of the Solar Flares, 357.
- Sturrock, P.A. 1965, Physics Fluids, 8, 281.
- Sturrock, P.A.; and Coppi, B.A. 1966, Ap. J., 143, 3.
- Sturrock, P.A. 1972, Solar Phys., 23, 438.
- Suzuki, S.; and Tsuchiya, A. 1958, Proc. I.R.E., 46, 190.
- Suzuki, S. 1961, Ann. Tokyo Obs., 2nd Ser., 7, 75.
- Svestka, Z. 1970, "Solar - Terrestrial Physics", Ed. E.R. Dyer, 72.
- Swarup, G.; Stone, P.H.; and Maxwell, A. 1960, Ap. J., 131, 725.
- Sweet, P.A. 1969, Ann. Rev. Astron. Astrophys., 7, 149.
- Tandenberg - Hansen, E. 1967, "Solar Activity", Bdaisdell, Waltham, Massa, Chusetts, 278.
- Thompson, A.R.; and Maxwell, A. 1962, Ap. J., 136, 546.
- Tidman, D.A.; Birmingham, T.J.; and Stainer, H.M. 1966, Ap. J., 146, 207.
- Tlamicha, A.; and Takakura, T. 1963, Nature, 200, 999.
- Tsyтовich, V.N. 1966, Soviet Astron.- AJ., 10, 419.
- Tsyтовich, V.N. 1970, "Non-linear Processes in Plasmas", Plenum, New York.
- Van de Hulst, H.C. 1950, Bull. Astr. Inst. Neth., 11, 135.

- Van Allen, J.A.; and Krimigis, S.M. 1965, J.G.R., 70, 5737.
- Van Allen, J.A. 1971, Presented at the AGU Meeting, Washington, D.C., April 13.
- Warwick, J.W. 1965, "Solar System Radio Astronomy", 131.
- Weiss, A.A.; and Sheridan, K.V. 1962, J. Phys. Soc. Japan, Supply. A-II, 17, 223.
- Weiss, A.A. 1963, Aust. J. Phys., 16, 240.
- Wilcox, J.M. 1971, "Physics of the Solar Corona", Ed. Macris, C.J., 88.
- Wild, J.P. 1950, Aust. J. Sci. Res., A3, 541.
- Wild, J.P.; and McCready, L.L. 1950, Aust. J. Sci. Res., A3, 387.
- Wild, J.P. 1952, Ap. J., 115, 206.
- Wild, J.P.; Roberts, J.A.; and Murray, J.D. 1954a, Nature, 173, 532.
- Wild, J.P., Roberts, J.A.; and Rowe, W.C. 1954b, Aust. J. Phys., 7, 439.
- Wild, J.P.; and Sheridan, K.V. 1958, Proc. I.R.E., 46, 160.
- Wild, J.P.; Sheridan, K.V.; and Neylan, A.A. 1959a, Aust. J. Phys., 12, 369.
- Wild, J.P., Sheridan, K.V.; and Trent, G.H. 1959b, "Paris Symposium on Radio Astronomy", 176.

- Wild, J.P.; Smerd, S.F.; and Weiss, A.A. 1963, Ann. Rev. Astron. Astrophys., 1, 291.
- Wild, J.P. 1963a, AAS - NASA Symposium on the Physics of Solar Flares, 161.
- Wild, J.P. 1963b, "The Solar Corona", Ed. J.W. Evans, Academic Press, New York and London, 115.
- Wild, J.P. 1969a, "Plasma Instabilities in Astrophysics", Gordon and Beach, New York.
- Wild, J.P. 1970, Proc. Astron. Soc. Aust., 1, 365.
- Wild, J.P.; and Smerd, S.F. 1972, Ann. Rev. Astron. Astrophys., 10, 159.
- Yip, W.K. 1970, Planet Space Sci., 18, 867.
- Zaitsev, V.V.; Mityakov, N.A.; and Rapoport, V.O. 1972, Solar Phys., 24, 444.
- Zheleznyakov, V.V.; and Zlotnik, E. Ya. 1964, Soviet Astron. -AJ, 7, 485.
- Zheleznyakov, V.V.; and Zaitsev, V.V. 1970a, Soviet Astron. - AJ, 14, 47.
- Zheleznyakov, V.V.; and Zaitsev, V.V. 1970b, Soviet Astron. -AJ, 14, 250.

PREPRINT

CR-73-0

DETERMINATION OF FARADAY ROTATION OCCURRING  
BETWEEN THE BURST-SOURCE IN THE  
SOLAR CORONA AND THE EARTH\*

R.V. Bhonsle and S.K. Mattoo  
~~Physical Research Laboratory~~

**PHYSICAL RESEARCH LABORATORY**

**AHMEDABAD-380009, INDIA.**

PREPRINT

CR-73-04

DETERMINATION OF FARADAY ROTATION OCCURRING  
BETWEEN THE BURST-SOURCE IN THE  
SOLAR CORONA AND THE EARTH\*

R.V. Bhonsle and S.K. Mattoo  
Physical Research Laboratory  
Ahmedabad-380009, India.

SUMMARY

The total Faraday rotation suffered by type III solar radio bursts, as measured by means of the two bandwidth (7.5 and 12.5 KHz) time-sharing polarimeter at 35 MHz, has been found to be of the order of  $10^3$  radians. It is suggested that such low values of the Faraday rotation can be qualitatively explained on the basis of generation of type III bursts primarily at the second harmonic of the local plasma frequency.

KEY WORDS: Polarimeter - Stokes' parameters -  
Type III bursts - Faraday rotation -  
Solar corona.

---

\*To appear in Astronomy and Astrophysics, a European Journal.

## 1. Introduction

A time-sharing radio polarimeter operating at 35 MHz has been set up at the Physical Research Laboratory, Ahmedabad, India, in 1972 for the determination of Faraday rotation suffered by the polarized component of solar radio bursts. The time-sharing scheme used in the design of this polarimeter is similar to that of Suzuki and Tsuchiya (1958) and Bhonsle and McNarry (1964 a) at 200 MHz and 74 MHz respectively. The polarimeter outputs are recorded on 8-channel chart recorder directly in terms of four Stokes' parameters simultaneously in the two bandwidths, namely, 7.5 and 12.5 KHz, with a time constant of one second. Since errors in the measurement of polarization parameters can arise due to non-zero cross-talk between the two antennas and reflections from ground and local objects, a particular care has been taken in the design of a cross-polarized Yagi antenna system used for this polarimeter. The measured antenna cross-talk is about -32 db, which means that the error in the measurement of polarization parameters will not be more than 6 per cent. The antenna system has a half-power beam width of about  $40^\circ \times 40^\circ$ . The front-to-back ratio of the antenna system has been measured to be about 22 db. In order to avoid unwanted radiation from the source after ground reflection, the polarimeter is operated only for  $\pm 2$  hours around the local noon. The performance of the polarimeter was further

tested using galactic radio noise as an extended unpolarized source and by transmitting a 35 MHz linearly polarized signal from the height of about 300 feet vertically above the antenna by means of a tethered balloon. All these tests indicated that errors in the measurement of polarization parameters do not exceed  $\pm 10\%$ .

## 2. Results

Figure 1 shows the 35 MHz polarimeter recording made with a bandwidth of 12.5 KHz, of a group of spectral type III solar radio bursts, which occurred between 0425 and 0440 UT on August 1, 1972. The occurrence of this group of type III bursts was confirmed by our solar radio spectroscope as well as by the Culgoora solar radio observatory. We have reduced the two bandwidth (7.5 and 12.5 KHz) polarization data at the peak intensities of type III solar radio bursts at 35 MHz in terms of the degree of polarization, axial ratio and orientation angle of the polarization ellipse. The total Faraday rotation suffered by the plane of polarization of solar burst radiation at 35 MHz has been calculated by applying the theory of Faraday dispersion developed by Akabane and Cohen (1961).

Table I summarizes the two-bandwidth measurements of polarization parameters required for the calculation of

total Faraday rotation of the plane of polarization of type III solar radio bursts shown in Figure 1. It can be seen from Table I that the total Faraday rotation has a mean value of  $1.8 \times 10^3$  radians with extreme values lying between  $0.9 \times 10^3$  and  $3.3 \times 10^3$  radians.

### 3. Discussion

Akabane and Cohen (1961) measured the Faraday rotation of type III solar bursts at 200 MHz using the two-bandwidth (10 and 22 KHz) analogue correlation-type polarimeter. They obtained a value for the Faraday rotation of the order of  $10^4$  radians which is at least one order of magnitude smaller than the Hatanaka's (1956) computed value. Dodge (1972) attempted to measure the Faraday rotation within 3 KHz bandwidth at 34 MHz. But he gave only an upper limit on the total Faraday rotation to be of the order of  $1.75 \times 10^3$  radians. This is in good agreement with our measured mean value of  $1.8 \times 10^3$  radians at 35 MHz.

Thus it is clear, that our experimentally measured value of the Faraday rotation at 35 MHz and that of Akabane and Cohen at 200 MHz and its upper limit as given by Dodge at 34 MHz have been lower than the corresponding theoretically calculated values.

It should be pointed out that about 10% of the total Faraday rotation at 35 MHz can occur in the earth's



ionosphere, that is, of the order of 100 radians. Contribution to the total Faraday rotation by the interplanetary magneto-ionic plasma is much less than that due to the earth's ionosphere. Thus, about 85 to 90% of the total Faraday rotation must occur near the source. If one calculates the total Faraday rotation, taking into account the polar magnetic field of the sun to be 1 gauss (ignoring the magnetic field due to sunspots), it turns out to be of the order of  $10^5$  radians. Therefore, one must find out a reasonable explanation for the discrepancy of at least two orders of magnitude between the measured and theoretically calculated values of the total Faraday rotation. It is found that, none of the suggestions like the magnetic field reversals, ducting and mode coupling at tangential discontinuities in the magnetic field along the propagation path, can adequately explain the observed low values of the Faraday rotation. Dodge (1972) favours the idea of mode coupling at the tangential discontinuities at higher levels in the solar corona as being responsible for the low values of the Faraday rotation. If this were so, then one should observe, at least for some type III bursts, the total Faraday rotation as low as a few hundred radians due to the earth's ionosphere alone, because such discontinuities have been observed near the orbit of the earth by the space-crafts (Parker 1969). From the analysis

of 35 groups of type III bursts during 1972 we have not observed the total Faraday rotation less than  $0.9 \times 10^3$  radians. This makes it difficult to explain the low values of the Faraday rotation in terms of mode-coupling at the tangential discontinuities. If one assumes that type III bursts are generated primarily at the second harmonic of the local plasma frequency then it would naturally place the source at comparatively greater height in the solar corona, where both the magnetic field and electron density are lower by an appropriate factor. This appears to explain our observed values of Faraday rotation of the order of  $10^3$  radians. There is a strong theoretical support to the idea that, at decameter and longer wavelengths, type III emission may be primarily generated at the second harmonic of the local plasma frequency (Zheleznyakov and Zaitsev 1970 a, b; Zaitsev et al. 1972). Zaitsev et al. (1972) and Haddock and Alvarez (1973) substantiate this theory from the analysis of space-craft measurements of type III bursts. We would like to emphasize that the idea of second harmonic generation has been invoked only for decameter and longer wavelengths because the physics of the solar corona seems to change beyond about 2 solar radii from the center of the sun (Warwick 1965; Ellis and McCulloch 1966, 1967; de la Noë and Boischot 1972).

Many workers have reported the occurrence of strong linear polarization in type III bursts (Akabane and Cohen 1961; Bhonsle and McNarry 1964 b, Chin et al. 1971, Dodge 1972). Our unpublished narrow-band polarization data of type III bursts at 25 and 35 MHz also confirms the occurrence of linear polarization. Fokker (1971) pointed out that the occurrence of linear polarization in type III bursts is inconsistent in the presence of scattering effects in the solar corona. Further, because of finite bandwidth of the receiver, the radiation would be received from a certain thickness of the source region. This would lead to depth depolarization within the source region. If the total Faraday rotation were indeed  $10^5$  radians or more, then it would be impossible to observe linear polarization of type III bursts. But in view of the measured Faraday rotation of the order of  $10^3$  radians at 35 MHz and an upper limit of about  $5 \times 10^3$  radians at 74 MHz calculated from the data of Bhonsle and McNarry (1964 b), the situation as regards the occurrence of linear polarization is not all that unfavourable. Grogard and McLean (1973) have claimed the non-existence of linear polarization in type III bursts at 80 MHz. However, it must be pointed out that their instrument does not seem to have the capability of measuring the small values of differential Faraday group delay required for the Faraday rotation to be of the order of  $10^3$  radians.

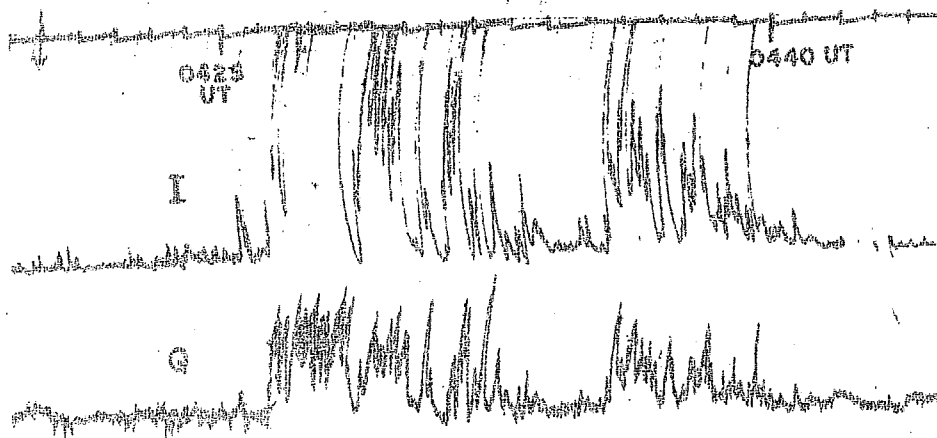
### Acknowledgment

The authors wish to express their sincere thanks to Prof. K.R. Ramanathan for his keen interest in the work and to Dr. S.K. Alurkar for critically reading the manuscript. Shri Sohan Lal assisted in developing the electronics for the polarimeter. Solar radio astronomy programme at the Physical Research Laboratory receives financial support from the Department of Space, Government of India.

### REFERENCES

1. Akabane, K.; Cohen M.H. 1961, Ap. J. 133, 258.
2. Bhonsle, R.V.; McNarry, L.R. 1964 a, Canadian J. Phys. 42, 292.
3. Bhonsle, R.V.; McNarry, L.R. 1964 b, Ap.J. 139, 1312.
4. Chin, Y.C.; Fung, P.C.W.; Lusignan, B.B. 1971, Solar Phys. 16, 135.
5. de la Noë, J.; Boischot, A. 1972, Astron. Astrophys. 20, 55.
6. Dodge, J.C. 1972, Thesis, University of Colorado.
7. Ellis, G.R.A.; McCulloch, P.M. 1966, Nature, 211, 1070.
8. Ellis, G.R.A.; McCulloch, P.M. 1967, Aust. J. Phys. 20, 583.

9. Fokker, A.D. 1971, Solar Phys. 19, 471.
10. Grogard, R.J.M.; McLean, D.J. 1973, Solar Phys. 29, 149.
11. Haddock, F.T.; Alvarez, H. 1973, Solar Phys. 29, 183.
12. Hatanaka, T. 1956, Publ. Astr. Soc. Japan 8, 73.
13. Parker, E.N. 1969, Space Science Reviews 9, 325.
14. Warwick, J.W. 1965, Solar System Radio Astronomy,  
Ed. J. Aarons, Plenum Press, New York, 131.
15. Zaitsev, V.V.; Mityakov, N.A.; Rapoport, V.O. 1972,  
Solar Phys. 24, 444.
16. Zheleznyakov, V.V.; Zaitsev, V.V. 1970 a, Soviet  
Astron. -AJ, 14, 47.
17. Zheleznyakov, V.V.; Zaitsev, V.V. 1970 b, Soviet  
Astron. -AJ, 14, 250.



POLARIMETER RECORD OF TYPE III SOLAR BURSTS  
 FREQ. 35 MHz, BANDWIDTH 12.5 KHz  
 DATE: 1 AUG. '72 AHMEDABAD

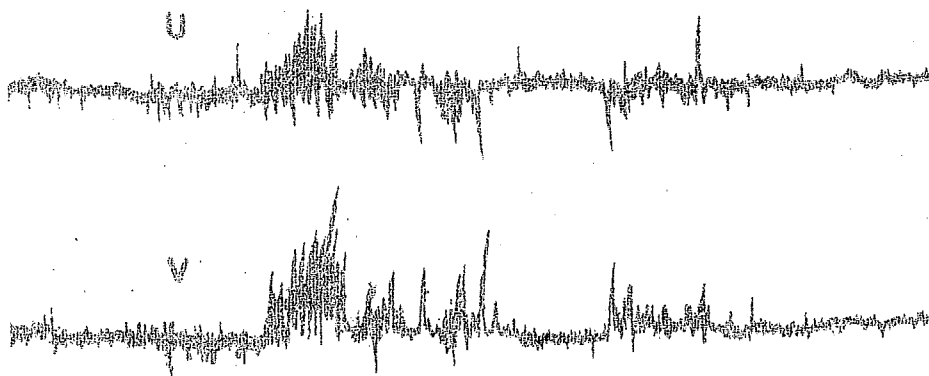


Figure 1. Polarimeter record on 1st August, 1972 of a group of type III solar radio bursts at 35 MHz in a bandwidth of 12.5 KHz.

Table 1. Summary of the Faraday rotation data (1st August, 1972)

Time (U.T.)	$m_n$	$r_n$	$m_w$	$r_w$	$\mu_n$	$\mu_w$	$\mu_w/\mu_n$	$\theta_n$ (radians) ( $\times 10^3$ )	$\phi$ (radians) ( $\times 10^3$ )
0425	30.0	0.55	0.13	0.39	0.09	0.54	0.39	0.72	0.86
0428	45.0	0.70	0.10	0.53	0.17	0.69	0.50	0.73	0.85
0429	15.0	OFF SCALE	0.37	0.19	0.19				
0430	0.0	OFF SCALE	0.45	0.17	0.17				
0431	45.0	0.90	0.07	0.21	0.21	0.90	0.63	0.69	0.91
0431	15.0	0.88	0.15	0.38	0.38	0.87	0.35	0.40	1.44
0432	30.0	OFF SCALE	0.36	0.27	0.27				
0432	0.0	0.83	0.08	0.22	0.22	0.82	0.76	0.93	0.41
0432	30.0	0.88	0.12	0.26	0.26	0.87	0.68	0.77	0.76
0433	0.0	0.92	0.0	0.19	0.19	0.92	0.76	0.83	0.65
0433	15.0	0.73	0.13	0.13	0.13	0.72	0.68	0.93	0.39
0433	30.0	0.77	0.12	0.14	0.14	0.76	0.45	0.60	1.08
0436	15.0	0.62	0.16	0.20	0.20	0.60	0.46	0.76	0.79
0436	30.0	0.56	0.14	0.22	0.22	0.54	0.48	0.38	0.53
0437	45.0	0.62	0.18	0.29	0.29	0.60	0.47	0.79	0.73
0437	15.0	0.65	0.14	0.20	0.20	0.64	0.41	0.64	1.01
0438	0.0	0.62	0.16	0.28	0.28	0.61	0.43	0.71	0.87
0439	30.0	0.65	0.16	0.30	0.30	0.64	0.45	0.71	0.88
0439	0.0	0.56	0.12	0.19	0.19	0.55	0.44	0.80	0.70
0440	30.0	0.74	0.10	0.10	0.10	0.74	0.51	0.70	0.90
0440	45.0	0.69	0.12	0.12	0.12	0.68	0.49	0.72	0.87

\* Symbols used

U.T. = Universal time

$m_n, m_w$  = degree of polarization at 7.5 and 12.5 KHz respectively

$r_n, r_w$  = axial ratio at 7.5 and 12.5 KHz respectively

$\mu_n, \mu_w$  = degree of coherence between R & L components at 7.5 and 12.5 KHz respectively

$\theta_n$  = the Faraday dispersion angle in 7.5 KHz bandwidth, radians

$\phi$  = the Faraday rotation, radians